Citrobacter rodentium infection in mice to dissect host pathogen relationship in the gut

Submitted in fulfilment of the requirements of the Degree of Doctor of Philosophy

By

Taneem Salwa

Centre for Immunology & Infectious Diseases

Blizzard Institute for Cell and Molecular Sciences

Barts and the London School of Medicine and Dentistry

4 Newark Street

London

E1 2AT

October 2016

Declaration

The work presented in this thesis is my own.

Taneem Salwa

Abstract

Citrobacter rodentium is a gut pathogen, which infects the distal colon of mice. It has many similarities to human *Enteropathogenic* and *Enterohemorrhagic E.coli* in terms of mechanisms of pathogenicity and methods of transmission. Like many other gram negative bacteria, *C. rodentium* has developed a complex and highly specialised protein secretion system, known as type three (T3SS), to deliver bacterial proteins into eukaryotic cells. By injecting effector proteins into host cell cytoplasm, the pathogens are able to modulate host cellular functions to facilitate their own survival and replication.

There is growing evidence that Attaching Effacing (AE) pathogens can inject effector proteins into gut epithelial cells, which dampen pro-inflammatory responses. There is also evidence that *EPEC, Yersinia* and *Shigella* can inject effectors into immune cells and also modulate their function. The objective of this work was to visualise and identify the host cells targeted for type III secretion by *C. rodentium*, and consequently determine the effect on host immune responses. The method chosen to detect cells targeted for effector protein delivery was the β-lactamase reporter system, where cells loaded with the fluorogenic substrate CCF2-AM emit a green FRET signal upon excitation by UV light, but emit a blue signal when cleaved by β-lactamase.

By creating reporter strain of *C.rodentium* expressing fusion proteins between NleD effector and β-lactamase, I was able to show that *C.rodentium* is capable of injecting NleD in a wide variety of murine cell lines including Swiss 3T3 fibroblasts, J774 macrophages, CMT93 epithelial cells and BW715 T cells in a dose and time dependent manner *in vitro*. In addition, I found that *C.rodentium* has the ability to inject proteins into the cytoplasm of immune cells isolated from mouse lymphoid tissues including the spleen, mesenteric lymph nodes and Peyer's patches. Detailed analysis of the types of cells injected with effectors in vitro showed that NleD- injected cells represented B cells, dendritic cells and T cells.

After inoculation of mice with the reporter strain of *CitropACYCnleD*, the plasmid encoded reporter fusion remained stable throughout infection and was able to inject cells *in vitro* after passage through the mouse gut. Unfortunately under the conditions described in this study, we were unable to visualise any gut cells targeted for protein delivery by *C. rodentium in vivo*, thus highlighting the complex nature of the host

pathogen relationships in the gut. Although there is a need to develop better strategies to visualise effector translocation *in vivo*, our study has demonstrated, for the first time, the ability of *C. rodentium* to target immune cells for effector injection *in vitro*.

Acknowledgements

First and foremost, I would like to thank Allah, the most gracious, most merciful for enabling me to complete this task.

I would like to express my gratitude to my supervisors Professor Tom Macdonald and Dr. Olivier Marches for their guidance, time and patience throughout my PhD. Without their immense knowledge and expertise, I couldn't have done this PhD.

I wish to acknowledge the financial support of the Collaborative Awards in Science and Engineering (CASE) studentship by Biotechnology and Biological Sciences Research Council (BBSRC) for funding my research and Barts and the London School of Medicine and Dentistry at Queen Mary University, for giving me the opportunity to do a PhD.

I'm incredibly grateful to Professor Joy Hinson and Dr Paul Allens for their crucial support, sincere advice and amazing positivity during the most difficult part of my PhD. We need more people like you in this world.

Thank you to Professor Dan Pennington, Professor Lucinda Hall and Dr. Andy Stagg for your stimulating lectures and discussions, you never fail to inspire me and teach me something new.

I would also like to thank my viva examiners Dr. Abigail Clements and Dr. Mark Travis for allowing my viva to be a positive experience and giving me amazing comments and suggestions.

Special thanks to all the staff and colleagues at the Centre for Immunology and Infectious Diseases (CIID) including Aijay, Suzanne, Nadia, Alison, Anna, Paolo, Juliet, Jhon, Fernanda, Joanna, Ahmed, Joe, Sandra and Naseem, for all your help in the lab, suggestions, discussions, chats, coffees, food and laughter… you have made it a great pleasure for me to come to work everyday and given me many wonderful memories to cherish.

I'm truly indebted to my beloved parents, words cannot express the love, prayers, inspiration, encouragement, comfort and hope you have given me to make me who I am today. I couldn't have done it without Naju, Jubair vai, Musab, Umair and Aisha, you are the greatest uncle and aunt my son could ever wish for. Im truly grateful to Heeba vabi and Nazrul Uncle for your wonderful advice and enthusiasm when I needed it most. Many thanks to my mother in law, Mohsina apu, Khadiza apu, Rayyan, Shuborna, and all my brother in laws for being part of this incredible journey. To my long suffering husband, we did it…its finally over! To my little Muadh, thank you for always reminding me that no matter what, being a mummy is always the best job in the world!

Lastly, I would like to dedicate this thesis to my late father in law who has been an invaluable source of inspiration and hope throughout my PhD, but sadly passed away before my final submission. Your prayers, wisdom and love gave me the strength to be where I am today. Words cannot express the emptiness we feel without you, may Allah reward you the highest and reunite us again in paradise.

Contents

List of Figures

List of Tables

List of Abbreviations

AE	Attaching Effacing
AID	Activation-induced cytidine deaminase
AMP	Antimicrobial peptides
Amp	Ampicillin
APC	Antigen presenting cells
APRIL	Proliferation inducing ligand
Arp	Actin related protein
ASC	Apoptosis speck-like protein
BAFF	B cell activating factor
CMF	Calcium and magnesium free
CCF2/4	7-hydroxycoumarine-3-carboxamide cephalosporin flourescin 2/4
CFU	Colony forming unit
Cm	Chloroamphenicol
CLP	Common lymphoid progenitor
CP	Cryptopatches
C.rodentium	Citrobacter rodentium
CSR	Class switch recombination
Cya	Adenylate cyclase
DC	Dendritic cells
dH_2O	Distilled water
DMEM	Dulbecco's modified eagle medium

dNTP	deoxynucleotide triphosphate
DPBS	Dulbecco's phosphate buffered saline
DSS	Dextran sulphate sodium
EAF	E.coli adherence factor
E.coli	*Escherichia coli*
EHEC	Enterohammorhagic *Escherichia coli*
EPEC	Enteropathogenic *Escherichia coli*
Esc	*Escherichia* secretion (component)
Esp	*Escherichia* secretion protein
FAE	Follicle associated epithelium
FcRn	Neonatal Fc receptors
Foxp3	Forkhead box P3
FRET	Fluorescence resonance energy transfer
(fw)	Forward
g	g-force
GAP	Goblet cell associated antigen passage
GALT	Gut associated lymphoid tissue
HBSS	Hanks balanced salt solution
IBD	Inflammatory Bowel Diseases
IEC	Intestinal epithelial cells
IFN	Interferon gamma
IgA	Immunoglobulin A
IgM	Immunoglobulin G

ILC	Innate lymphoid cells
ILF	Isolated lymphoid follicles
IM	Inner membrane
iNOS	Nitric oxide synthase
ILF	Isolated lymphoid follicles
IPTG	Isopropyl β-D-1-thiogalactopyranoside
Kan	Kanamycine
λ	Lambda
LB	Luria-Bertani
LEE	Locus of enterocyte effacement
LP	Lamina propia
LTβR	Lymphotoxin beta receptor
LTi	Lymphoid tissue inducer cells
M cells	Microfold cells
MAdCAM-1	Mucosal vascular addressin cell adhesion molecule 1
MAMP	Microbe associated molecular pattern
MAPK	Mitogen activated protein kinases
min	Minute(s)
MLN	Mesenteric Lymph node
MOI	Mutiplicity of infection
MyD88	Myeloid differentiation primary response gene 88
NET	Neutrophil extracellular trap
NFκB	Nuclear factor kappa B

Nal	Nalidixic acid
Nle	Non locus of enterocyte effacement
NLR	NOD like receptors
NLRP3	NOD like receptor family pyrin domain
NOD	Nucleotide binding oligomerization domain
NWASP	N-Wiskott-Alderich syndrome protein
OD_{600}	Optical density at 600 nm
O/N	Overnight
OM	Outer membrane
PBS	Phosphate buffered saline
PCR	Polymerase chain reaction
p.i.	Post inoculation
pIgA	Polymeric immunoglobulin A
pIgR	Polymeric immunoglobulin receptor
PP	Peyer's patches
PRR	Pattern recognition receptors
RAG	Recombination-activating genes
RANK	Receptor activator of nuclear factor κ B
RANKL	RANK ligand
REG III	Regenerating islet-derived protein III
RELMß	Resistin-like molecule ß
RET	Receptor tyrosine kinase
(rv)	Reverse

Rpm	Rounds per minute
RORyt	RAR related orphan receptor gamma t
SFB	Segmented filamentous bacteria
SILT	Solitary intestinal lymphoid tissue
TAE	Tris-acetate-EDTA
TACI	Transmembrane activiator and CAML interactor
TED	Transepithelial dendrites
TEM-1	Gene encoding β-lactamase enzyme
Tet	Tetracycline
TFF3	Trefoil factor 3
Th	T helper
TI	T cell independent
Tir	Translocated intimin receptor
TLR	Toll like receptors
TMCH	Tranmissible murine crypt hyperplasia
TNFα	Tumor necrosis factor α
Treg	T regulatory
T3SS	Type three secretion system
VCAM-1	Vascular cell adhesion molecule 1

Chapter 1: General Introduction

1.1 Intestinal immune system

- 1.1.1 Intestinal epithelial cells
- 1.1.2 Goblet cells
- 1.1.3 Paneth cells
- 1.1.4 Neutrophils
- 1.1.5 Microbial recognition by intestinal cells
  - 1.1.5.1 TLR
  - 1.1.5.2 NLR
- 1.1.6 Gut associated lymphoid tissue
  - 1.1.6.1 Peyer's patches
  - 1.1.6.2 Cryptopatches and isolated lymphoid follicles
  - 1.1.6.3 Antigen uptake by intestinal cells
    - 1.1.6.3.1 M cells
    - 1.1.6.3.2 Epithelial cells
    - 1.1.6.3.3 Dendritic cells
  - 1.1.6.4 Antigen presentation and lymphocyte migration in the GALT

1.2 *Citrobacter rodentium*

- 1.2.1 Course of infection
- 1.2.2 Transmissible murine crypt hyperplasia
- 1.2.3 Host immune response to *C. rodentium* infection in mice
  - 1.2.3.1 Pattern recognition receptor mediated response
  - 1.2.3.2 Innate lymphoid cells
  - 1.2.3.3 Th17 cells
  - 1.2.3.4 Adaptive immune cells

1.3 Enteropathogens

- 1.3.1 Attaching Effacing pathogens
- 1.3.2 Adherence
- 1.3.3 Assembly of the T3SS injectisome
- 1.3.4 Signal transduction and intimate attachment
- 1.3.5 Pedestal formation
- 1.3.6 Locus of enterocyte effacement (LEE)
- 1.3.7 Non-LEE encoded genes

1.3.8 Effector targeting of host defences

1.3.8.1 Apoptosis

1.3.8.2 Phagocytosis

1.3.8.3 Inflammation

1.4 Concluding remarks

1.5 Objectives

1. General Introduction

1.1 Intestinal immune system

The human gastrointestinal tract, with an approximate surface area of 400m^2, is the largest mucosal surface of the body. It is organised into millions of crypts and villi and is lined by a continuous row of intestinal epithelial cells, forming an epithelial barrier that separates the outside world from the internal host environment. The primary function of the gastrointestinal tract is the digestion of food and absorption of nutrients and water. However, the large surface area also makes the gastrointestinal tract particularly vulnerable to pathogens present in food and drinking water, which can damage the intestinal wall. In order to maintain barrier functions while enabling nutrient uptake, the gastrointestinal tract has developed an extensive network of organised gut associated lymphoid tissue (GALT) to protect against infectious microorganisms, such as pathogenic *Escherichia coli (E. coli)* and *Citrobacter rodentium.* Additionally, in the modern world, excessive immune responses to food and the microflora are responsible for hypersensitive conditions such as Coeliac disease and Crohn's disease. The intestinal epithelial barrier is thus at a crossroad between defence and nutrition (reviewed in MacDonald et al., 2011; Brandtzaeg, 2013; Peterson & Artis 2014).

1.1.1 Intestinal epithelial cells

The epithelial barrier (Fig. 1.1) is composed mainly of a single, continuous row of intestinal epithelial cells (IEC) (reviewed in Rescigno 2011a). IECs are polarised with a basolateral surface facing the lamina propria and an apical surface facing the intestinal lumen. Each IEC is columnar, 30μm thick, and covered with a microvillus brush border containing glycocalyx on the apical surface. Through various intimate associations between the epithelial cells – including tight junctions, adherens junctions and desmosomes – the intestinal epithelium forms a physical barrier against food and microorganisms in the gut lumen and prevents the uncontrolled entry of foreign antigens.

Tight junctions are protein complexes, which form belt-like contacts between adjacent epithelial cells and seal the paracellular space (Turner et al 2009). They are made up of the transmembrane proteins claudin and occludin, as well as the peripheral membrane proteins zonula occludin1, which establish a diffusion barrier

between the apical and basolateral domains of the epithelium. This prevents the influx of luminal contents into the lamina propria (LP). In addition, tight junctions are associated with cytoplasmic actin and myosin networks that regulate intestinal permeability. The adherens junctions, made up of cadherin transmembrane proteins, 'glue' the epithelial cells together. Loss of adherens junctions results in cell-cell and cell-matrix contact disruption, ineffective epithelial cell polarisation, and apoptosis (Hermiston et al., 1995). Desmosomes are intracellular junctions that hold the epithelial sheet together. Desmosomes form extracellular bonds that are anchored at the cell surface to the intermediate filament-based cytoskeleton. Tight junctions, adherens junctions, and desmosomes thus work together to maintain the epithelial barrier integrity. Any defects in these structures can lead to an increase in epithelial permeability and an altered composition of the microbiota, known as dysbiosis, resulting in inflammatory disorders, such as inflammatory bowel disease (IBD) (Peterson & Artis, 2014).

Intestinal epithelial cells undergo continuous renewal from stem cell progenitors residing near the base of the intestinal crypts (Fig. 1.1) (Potten et al., 1997). As these cells migrate toward the tip of the crypts, they differentiate into one of four cell lineages (Yen and Wright, 2006). Although the majority of IECs lining the gut lumen are (1) absorptive epithelial cells (enterocytes), the epithelium also contains secretory epithelial cells, including (2) goblet cells, (3) Paneth cells, and (4) enterochromaffin cells (Peterson & Artis 2014).

1.1.2 Goblet cells

Overlaying the gut epithelium is a thick layer of mucus (Fig.1.1), produced by goblet cells, which provides the first line of defence against luminal microbes (reviewed in McGuckin 2011). Mucus is a complex fluid rich in mucin glycoproteins and antimicrobial molecules. It varies in thickness between 150μm in the stomach, 300μm in the small intestine, and 700μm in the large intestine (Atuma et al., 2001). The thickness of the mucus layer depends on the presence of the microbiota, where goblet cells constitute 10% of IECs in the upper small intestine compared to 25% in the distal colon (Rescigno et al., 2011a; Mowat and Agace, 2014). The small intestine is covered by a single layer of mucus (Johansson et al., 2011), in contrast to the large intestine, which is coated by two mucus barriers consisting of a thin, dense,

inner layer – that is attached to the epithelial surface and impermeable to bacteria – and a thicker outer layer which contains bacteria (Johansson et al., 2011). The resulting mucucs layer forms a highly charged gel that physically separates luminal bacteria from the epithelial cell surface and is also composed of mucin glycoproteins that is directly toxic to many bacteria. In addition, the mucus layer provides an attachment site to antimicrobial peptides (AMP) and IgA antibodies (discussed later), which further strengthens the barrier properties (Mowat and Agace, 2014).

Defects in mucus production have been linked with increased infiltration of commensal bacteria into the LP and an increased susceptibility to colitis and colon cancer. For example, mice lacking mucin-specific genes developed spontaneous colitis (Heazlewood et al., 2008) and mice deficient in mucin 1 are more susceptible to infection with *Helicobacter pylori* and *Campylobacter jejuni* (McGuckin et al., 2007; McAuley et al., 2007). In addition, mice deficient in the mucin 2 gene show a reduced inner mucus layer, resulting in the direct contact of epithelial cells with the microbiota, (Hansson and Johansson, 2010) leading to inflammation, spontaneous colitis (Van der Sluis et al., 2006), and intestinal tumours (Velcich et al., 2002). The importance of mucus is further shown in Winnie mice, which have a missense mutation in the mucin 2 gene, display increased epithelial permeability, and develop an ulcerative colitis-like inflammation (Heazlewood et al., 2008). Taken together, these studies demonstrate the important role of mucus in the protection of the host against gut microorganisms.

Cross-linking of mucin with trefoil factor 3 (TFF3) provides additional structural integrity to the mucus barrier (Peterson & Artis, 2014). Also secreted by goblet cells, TFF3 is upregulated around areas of epithelial cell damage and has been suggested to play a role in promoting epithelial cell migration and resistance to apoptosis, both of which are important for wound healing and intestinal repair (Wright et al., 1997; Peterson & Artis, 2014). TFF3-deficient mice show impaired mucosal healing that can lead to severe dextran sulphate sodium (DSS) induced colitis and death (Podolsky et al., 2009). Conversely, the addition of TFF3 has been effective in treating colonic injury in both *in vitro* and *in vivo* models of colitis (Kindon et al., 1995; Mashimo et al., 1996).

Resistin-like molecule-ß (RELMß) is another product secreted by goblet cells that further reinforces the intestinal barrier functions. It plays an important role in

promoting mucin 2 secretion and in the regulation of macrophage and T cell responses during inflammation (Peterson & Artis, 2014). RELMß was also shown to provide protection against parasitic helminths that reside in the intestinal lumen by directly inhibiting parasite chemotaxis and the ability of the worms to feed on host tissue (Herbert et al., 2009; Peterson & Artis, 2014).

Recently, 2-photon time lapse imaging was used to demonstrate an important role for goblet cells in delivering luminal antigens to dendritic cells (DCs) in the LP (McDole et al., 2012). In addition to the trans-epithelial dendrite (TED) formation by DCs (discussed later), this new source of luminal antigens for small intestinal DCs is known as a 'goblet cell-associated antigen passage' (GAP). According to the study by McDole et al. (2012), GAP formation occurred either through stable contacts with DCs, which slowly collected antigens over several minutes, or when DCs actively probed GAPs and captured antigen clumps. The luminal antigens were captured preferentially by the tolerogenic CD103+DCs, which promoted the development of regulatory T cells. Such findings suggest that goblet cells, through the GAP mechanism, play an important role in promoting intestinal immune homeostasis (McDole et al., 2012).

1.1.3 Paneth cells

The secretion of antimicrobial peptides (AMPs) by Paneth cells strengthens the regulation of a physical barrier in the intestine**.** Paneth cells are found in the small intestine and, unlike the rest of the IECs, migrate downward toward the base of the crypts after differentiating from stem cells (Fig.1.1) (Mowat and Agace, 2014). These cells are specialised to secrete a wide variety of AMPs, including defensins, lysozymes, cathelicidins, and regenerating islet-derived protein (REG) III lectins (McGuckin et al., 2011; Peterson & Artis et al., 2014).

These AMPS display antimicrobial activity against bacteria, fungi, and viruses. For example, cathelicidins and pore forming defensins target bacterial surface membranes, while C-type lectins target gram-positive cell wall peptidoglycans (Gallo and Hooper, 2012; Mukherjee et al., 2014). Knockout mice that are deficient in active defensins display an impaired ability to clear *Escherichia coli* (*E.coli*) infection and show an increased susceptibility to *Salmonella typhimurium* (*S.typhimurium*) infection following oral inoculation of mice with these pathogens

(Wilson et al., 1999). In addition, transgenic mice over-expressing α defensins show increased resistance to *S. typhimurium* infection (Salzman et al., 2003).

As well as providing resistance to invading pathogens, AMPs also play a role in shaping the microbiota composition. For instance, in comparison to wildtype mice, mice deficient in α-defensins display a completely altered microbiota, while mice over-expressing α-defensins show reduced colonisation by segmented filamentous bacteria (Salzman et al., 2010), which have been implicated in the protection of mice from *C. rodentium* infection (Ivanov and Littman, 2010). Furthermore, REGIIIγ produced by both Paneth cells and enterocytes have recently been shown to mediate host-microbial segregation in the gut. Similar to mucin 2 function in the colon, REGIIIγ helps to exclude bacteria from the epithelial surface of the small intestine, and interactions between REGIIIγ and mucins lead to increased antimicrobial activity at the epithelial surfaces (Vaishnava et al., 2011). In short, the combined effects of IEC-secreted products reinforce the epithelial barrier functions by limiting the diversity and quantity of bacteria that can access the epithelial surface and interact with the underlying mucosal lymphoid tissues (Peterson & Artis et al., 2014).

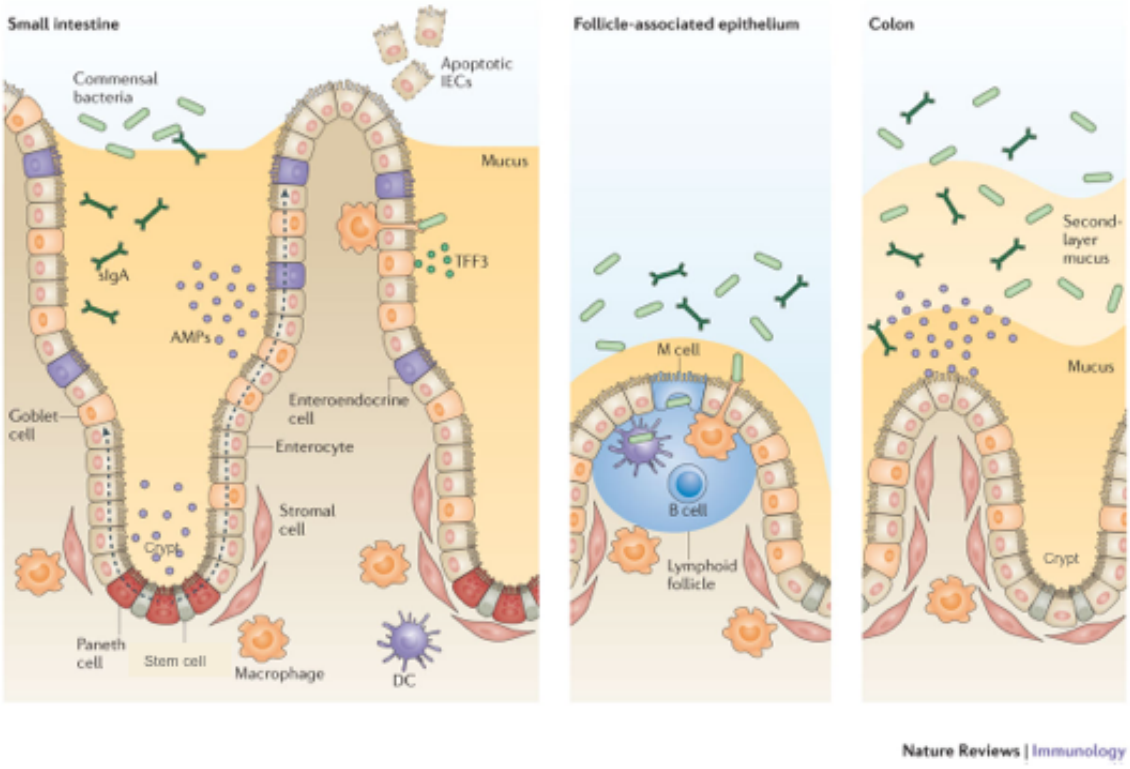

Figure 1.1: The intestinal epithelial cell barrier. The renewal of the epithelial cell layer is controlled by the intestinal epithelial stem cells, residing in the crypts, where differentiated IECs migrate up the crypt-villus axis. To exclude bacteria from the epithelial cell surface, goblet cells secrete mucus while Paneth cells secrete antimicrobial proteins (AMPs). Epithelial cells further contribute to this barrier function through transcytosis and luminal release of secretory IgA (SIgA). Luminal antigens and live bacteria are transported across the epithelial barrier by M cells, goblet cells, and intestine-resident macrophages (discussed later). (Taken from Peterson & Artis, 2014).

1.1.5 Microbial recognition by intestinal cells

To maintain barrier functions and immune homeostasis, intestinal epithelial cells and immune cells are able to sense the presence of microbes and respond accordingly. This is done through the expression of pattern recognition receptors (PRR), which recognise microbe associated molecular patterns (MAMPs). Members of the toll-like receptor (TLR) and the nucleotide-binding oligomerisation domain (NOD)-like receptor (NLR) families mediate the recognition of microbial ligands or signals associated with enteropathogens (reviewed by Lavelle et al., 2010; Kawai & Akira, 2011). PRR recognition can lead to the activation of downstream signalling cascades, including that of nuclear factor kappa B (NFκB), activator protein 1, and mitogen-activated protein (MAP) kinases (Fig.1.2a) . These pathways promote the production of antimicrobial peptides and proinflammatory cytokines, which are important for antigen presentation and for inducing the proliferation of effector immune cell populations (Fig.1.2b). However, in addition to their role in initiating highly inflammatory cascades, the abundance of symbiotic commensals in the intestine make it necessary for the intestinal cells to maintain a state of epithelial homeostasis and immune tolerance upon microbial recognition of commensal bacteria (Lavelle et al., 2010; Petrson & Artis, 2014).

1.1.5.1 Toll-like receptor (TLR)

The number of TLRs identified so far total to 10 in humans and 13 in mice (Abreu, 2010). TLR1,2,4, 5 and 6 are expressed on the cell surface (Fig.1.2) and mainly recognise microbial membrane components such as bacterial lipoproteins, peptidoglycans, lipopolysaccharides (LPS) and flagellin. In contrast, TLR3,7, 8 and 9 are associated with intracellular vesicles (Fig.1.2) that recognise DNA and RNA from bacteria, virus, fungi and parasites (Abreu, 2010).

TLR signalling through the myeloid differentiation factor (MyD)-88 adapter protein, is essential for driving resistance responses against enteric bacterial pathogens, partly by the production of antimicrobial peptides and lectins. Following infection of mice with *Listeria monocytogenes*, MyD88 signalling was shown to promote the production of microbicidal lectin RegIII by Paneth cells that can directly suppress the growth of *L. monocytogenes* (Brandl et al., 2007). Similarly, TLR2 signalling was shown to regulate the expression of RegIIIβ, without which animals were more

susceptible to infection with *Yersinia pesudotuberculosis* (Dessein et al., 2009). Similarly, mice deficient in TLR9 have decreased expression of α-defensin in the small intestine (Lee et al., 2006) while antibiotic treatment of mice decreased the expression of antimicrobial peptides (Brandl et al., 2008). Likewise, MyD88 signalling was required for the control of pathogenic bacteria in a model of enterocolitis induced by *S. typhimurium* (Keestra et al., 2011).

The importance of TLR mediated MyD88 signalling in the control of bacterial growth can be seen clearly in the *C. rodentium* model of mice infection. MyD88-/- mice infected with *C. rodentium* carried a bacterial burden up to 100-fold higher than wild type mice (Lebeis et al., 2007; Gibson et al., 2008b). As well as resulting in an abrogated production of TNFα and IL6 from macrophages, these MyD88-/-mice displayed an inability to recruit neutrophils and macrophages to the site of infection, which suggests that the control of bacterial burdens is related to the host inflammatory response. These mice were also unable to promote the proliferation and turnover of crypt epithelial cells, leading to bacterial invasion of colonic crypts (Gibson et al., 2008b). Moreover, MyD88-/- mice had defects in the MyD88-dependent production of iNOS, which can contribute to the direct killing of *C. rodentium* (Vallance et al., 2004). Therefore, TLR-mediated MyD88 signalling proved essential in providing resistance against *C. rodentium* infection through direct killing, recruitment of phagocytes to the site of infection, and removal of infected epithelial cells (Bergstrom et al., 2012).

As well as promoting resistance to invading pathogens, TLR activity is also associated with host responses that limit intestinal tissue damage. These TLRs drive processes that protect the host from pathogen-associated injury during bacterial infection. For example, mice deficient in MyD88 not only carried greater bacterial burden during *C. rodentium* infection but also suffered from severe necrosis in the colonic tissue (Lebeis et al., 2007; Bergstrom et al., 2012). In addition, studies in knockout mice show that, in the absence of TLR-mediated NFκB activation, epithelial cells undergo apoptosis, increased epithelial permeability, and translocation of microorganisms across the epithelium, which lead to the development of chronic intestinal inflammation (Nenci et al., 2007). TLR signalling

is therefore crucial in the maintenance of intestinal homeostasis, especially during gut infections.

TLR-mediated protection from epithelial cell injury was also reported in mice with chemically-induced colitis. In the absence of TLR2 mediated expression of TFF3 by goblet cells and IECs, mice displayed an increase in apoptosis and susceptibility to DSS-induced colitis. Similar effects were seen in wild-type mice induced with colitis following treatment with antibiotics. Mice that are deficient in; MyD88 adapter protein, TLR4 (which recognises bacterial LPS), TLR5 (which recognises flagellin) and TLR2 (which recognises bacterial glycolipids) also displayed increased susceptibility to DSS colitis (Rakoff-Nahoum et al., 2004; Fukata et al., 2005; Vijay-Kumar et al., 2007b; Araki et al., 2005). Conversely, the administration of flagellin (Vijay-Kumar et al., 2008), TLR2 ligand (Cario et al., 2007), TLR3 ligand (Vijay-Kumar et al., 2007a), and TLR9 ligand (Rachmilewitz et al., 2004) in DSS induced mice conferred protection against DSS-induced injury by decreasing apoptosis, dampening proinflammatory cytokines, and increasing epithelial cell proliferation. Such data establish the role of TLR signalling in the maintenance of epithelial cell proliferation and repair of colitis-damaged gut.

TLR signalling in response to bacterial antigens is also associated with expression of tight junction proteins by epithelial cells. In a model epithelium, TLR2 activation led to the reorganisation of tight junction associated proteins (Cario et al., 2004), which provided protection against colitis induced by *C. rodentium* (Gibson et al., 2008a). Similarly, treatment of IEC with TLR2 ligands resulted in a decrease in epithelial cell apoptosis and enhanced tight junction function through reorganisation of tight junction associated proteins in mice with DSS-induced colitis (Cario et al., 2007). Thus, TLR signalling can contribute to minimising intestinal damage by tightening the barrier formed by the epithelial cells.

TLR signalling in IECs can enable antibody class switching to IgA since TLR activation of human IECs induces the secretion of a B cell stimulating factor known as proliferation-inducing ligand (APRIL) (He et al., 2007). APRIL binds to transmembrane activator TACI on B cells to induce plasma cell survival and class switching (Castigli et al., 2005). In mice where TLR4 is constitutively expressed, there is a higher number of IgA-producing plasma cells in the LP, higher expression of APRIL in the epithelium, and increased IgA in the faeces relative to control mice

(Shang et al., 2008). Therefore, TLR signalling in the epithelium is necessary for inducing IgA responses in the intestine.

Despite the protective role of TLR signalling, contradictory evidence indicates a pathogenic role for TLRs in the development of inflammatory disorders. Evidence from genome-wide association studies suggests that TLR4 polymorphisms may be associated with Crohn's disease and ulcerative colitis (Franchimont et al., 2004). In addition, studies of epithelial cells show higher expression of TLR4 in IBD patients than in control individuals (Cario and Podolsky et al., 2000). However, it is difficult to conclude whether this is a cause or an effect of IBD, since the presence of proinflammatory cytokines such as IFNγ and TNFα can also induce the transcription of TLR4 (Suzuki & Podolsky et al., 2003; Vamadevan et al., 2010). Even so, additional studies confirm that TLR4 expression by epithelial cells was responsible for neoplasia seen in mice induced with carcinogen azoxymethane and DSS (Fukata et al., 2009), where mice deficient in TLR4 were protected from neoplasia (Fukata et al., 2007). This is supported by further studies in mice lacking MyD88, which did not develop colitis after *Helicobacter hepaticus* infection (Asquith 2010), and in mice lacking a negative regulator of NFκB, which showed elevated levels of inflammatory cytokines and reduced barrier permeability (Zhou et al., 2009). Not only do such findings reveal a 'darker side' to TLR signalling – despite its well-established role in providing protection in the intestinal mucosa – but also highlights the complexity of TLR-induced effects in the mucosa.

The complexity of TLR-induced effects is further demonstrated by the co-activation of TLR2 and TLR4 signalling during *C. rodentium* infection in mice (Khan et al., 2006; Gibson et al., 2008a). Although TLR2 and TLR4 signalling can have different effects during a *C.rodentium* infection, they can also cooperate to provide host defence. Mice deficient in TLR4 displayed a delay in *C. rodentium* colonisation, with a marked reduction in bacterial burden in the first week of infection, followed by an impaired host response that included a reduced expression of chemokines and limited tissue infiltration of phagocytes. Although *C. rodentium* was eventually able to colonise and cause inflammation in the absence of TLR4, these mice suffered little tissue damage and were able to clear the infection. This suggests that TLR4 is responsible for much of the mucosal damage that occurs during a bacterial infection. However, it has also been suggested that this pro-inflammatory role may actually

promote *C. rodentium* colonisation, perhaps by helping to remove competing commensals during the initial stages of an infection (Lupp et al., 2007).

In contrast, TLR2-deficient mice are highly susceptible to *C. rodentium* infection. These mice displayed severe ulceration in the colon, which led to rapid weight loss and high mortality within the first two weeks of infection (Gibson et al., 2008a). The colonisation of *C. rodentium* in TLR2 deficient mice is the same as wild-type mice, indicating that bacterial burden does not account for the severe disease pathogenesis. Instead, TLR2 deficient mice displayed a reduced production of IL-6, which resulted in exaggerated epithelial cell apoptosis during infection. The presence of further defects in the epithelial barrier in addition to the abnormal distribution of tight junction proteins in the absence of TLR2, suggest that TLR2 signalling promotes intestinal homeostasis and protection of the epithelium following pathogen-induced injury (Bergstrom et al., 2012).

Mice deficient in TLR 2 and TLR 4 (TLR2/4) show increased barrier dysfunction but little damage during *C. rodentium* infection. When reconstituted with TLR2-deficient – but not TLR4-deficient – bone marrow, the TLR2/4-deficient mice developed severe mucosal ulcerations (Gibson et al., 2010). It was further found that TLR2 signalling leads to the production of IL-11 by sub-epithelial mesenchymal cells. IL-11 is a cytoprotective cytokine that exerts its functions in colonic crypt epithelial cells and has been suggested to promote epithelial cell health and proliferation (Pickert et al., 2009). Taken together, these studies suggest that, during *C. rodentium* infection, TLR4 activation is responsible for pathogen-associated mucosal damage, while TLR2 activation results in the protection of the intestine from the TLR4 driven damage (Bergstrom et al., 2012).

Finally, TLR signalling enables the epithelium to distinguish between harmless microflora and harmful pathogens. Inoculation of MyD88 deficient mice with *E. coli* K-12 resulted in an increased translocation of live bacteria into the spleen, indicating that TLR signalling is required to restrict the presence of microbiota in the lumen (Slack et al., 2009). In addition, the polarised nature of the intestinal epithelium enables spatial segregation of the PRRs. For example, TLR5 is expressed on the basolateral surface of the epithelial cells and is only activated when bacteria breach the epithelial barrier and invade the lamina propia. Similarly, the intracellular location of TLR3, 8, and 9 in the endosomal organelles ensures that only pathogenic

bacteria which enter and invade the epithelial cells are recognised, rather than bacteria residing on the apical surface (Kayama & Takeda, 2012). Furthermore, apical exposure of IECs to TLR9 ligands resulted in an inhibitory effect on the proinflammatory pathway, while the basolateral exposure of IECs to the same ligand resulted in the activation and translocation of NFκB (Fig.1.2a), demonstrating the existence of a differential response to microbial signals based on anatomical location (Peterson & Artis, 2014).

1.1.5.2 NOD-like receptors (NLR)

The NLR family of PRRs are primarily cytosolic and recognise intracellular MAMPs present in the cell cytosol (Kumar et al., 2009). NOD1 and NOD2 are well-characterised NLR receptors that recognise components of the bacterial peptidoglycan. NOD1 is expressed by all adult cells and is upregulated in IECs in response to IFNγ (Inohara et al., 1999). In contrast, NOD 2 expression – restricted to leukocytes, DCs, and epithelial cells – is upregulated upon receiving stimuli from LPS, TNFα, and IFNγ (Rosenstiel et al., 2003). Activated ligands for both NOD1 and NOD2 enter cells by endocytosis via clathrin-coated pits (Lee et al., 2009).

Like TLR signalling, NOD signalling drives the downstream activation of MAPK and NFκB pathways, which upregulate the expression of proinflammatory cytokines and defensins responsible for antibacterial effects (Lavelle et al., 2010). Mice with NOD2 deficiency display abnormally large PP with increased numbers of M cells and CD4 T cells, resulting in the increased translocation of bacteria and yeast across the PP which leads to elevated levels of inflammatory cytokines TNFα, IFNγ, IL12, and IL4 in the LP (Barreau et al., 2007). Furthermore, NOD2-deficient mice are more susceptible to oral infection with *Listeria monocytogenes*, and have reduced cryptidin production by Paneth cells (Kobayashi et al., 2005) compared to NOD1 deficient mice, which are highly susceptible to *Helicobacter pylori* infection (Viala et al., 2004).

Genome-wide studies have revealed strong associations between NOD2 gene mutations and Crohn's disease (Ogura et al., 2001). NOD2 mutations result in the inability to sense components of the bacterial peptidoglycan (Inohara et al., 2003), leading to a decrease in peptidoglycan-induced NFκB activity and impaired bacterial clearance (Netea et al., 2005). *In vitro* studies using epithelial cell lines expressing

mutations in the NOD2 gene, show impaired signalling in response to peptidoglycan from *S. typhimurium*, thereby indicating the role of NOD2 in the protection against intracellular bacteria (Hisamatsu et al., 2003).

In the inflammatory disorder known as 'Blau syndrome', a NOD2 gain-of-function mutation causes constitutive activity of NOD2, which results in enhanced NFκB activation, increased apoptosis, and secretion of IL1B (Maeda et al., 2005). In addition, it was found that NOD2 mutations in Paneth cells resulted in the reduction of human defensin 5 and 6 levels (Grimm and Pavli, 2004) and that an α-defensin deficiency in Paneth cells contributed to the development of ileal Crohn's disease (Wehkamp et al., 2005). Taken together, these studies establish a link between NOD2 mutations and Crohns disease susceptibility.

NOD1 and NOD2 have also been implicated in the host defence to *C. rodentium*, despite the fact that it is an extracellular pathogen. In a recent study, a greater bacterial burden was observed in mice deficient in NOD2 compared to wild-type mice infected with *C. rodentium* (Kim et al., 2011). It was proposed that NOD2-dependent production of CCL2 led to the recruitment of CD11c+ inflammatory monocytes to promote *C. rodentium* killing at the site of infection. However, mice deficient in NOD1/2 displayed more severe colitis in response to *C. rodentium* infection, which was associated with a higher bacterial load in the spleen (Geddes et al., 2011). According to the study, NOD1 and NOD2 play an important role in the protection against pathogen-induced damage by limiting pathogen translocation across the epithelium and promoting mucosal integrity. The protective effects of NOD1/2 are due to the early production of IL17A by a unique population of innate lymphocyte TH17 cells (Geddes et al., 2011). These cells presumably produce IL22 and RegIIIγ, which are protective molecules in this model (discussed later) (Zheng et al., 2008). Collectively, these studies implicate NOD signalling in promoting resistance to infection through chemokine production and inflammatory cell recruitment, as well as promoting tolerance through activation of novel TH17 cell responses.

Other members of the NLR family, including NLRP3 and NLRP4, are involved in inflammasome formation (Ting et al., 2008). Inflammasomes are cytoplasmic multi-protein complexes containing the apoptosis speck-like protein (ASC) adapter molecule, which control the recruitment and activation of caspase-1 required for the

maturation of proinflammatory cytokines IL1β and IL18 (Fig. 1.2a) (Bryant and Fitzgerald, 2009). NLR4 inflammasome formation occurs in response to the presence of flagellin, delivered by *Salmonella* type three secretion systems (T3SS, discussed later) into the cytosol of macrophages, resulting in the secretion of IL1β by these macrophages (Franchi et al., 2006). In addition, the activation of NLRP3 inflammasome formation in response to stimuli from ATP, pore-forming toxins, uric acid (Ting et al., 2008), and TLR agonists (Sharp et al., 2009) has been shown to induce innate immune responses. ATP, produced in high concentrations by commensal bacteria (Atarashi et al., 2008), is able to induce NLRP3 inflammasomes to activate cytokines that in turn induce the differentiation of TH17 cells in the LP (Lavelle et al., 2010). TH17 cells have been implicated in the protection against bacterial pathogens such as *C. rodentium* (Mangan et al., 2006). Mice deficient in NLRP3 or Caspase 1 are more susceptible to DSS colitis and colitis-associated cancer. The increased susceptibility can be reduced by the addition of IL18, which suggests that part of the protective role of NLRP3 is mediated by IL18 (Zaki et al., 2010; Allen et al., 2010). In addition, mutations in the NLRP3 gene have been associated with susceptibility to other inflammatory disorders, demonstrating the requirement for bacterial recognition by NLR-mediated inflammasome formation to prevent autoimmune responses (Petrilli et al., 2007).

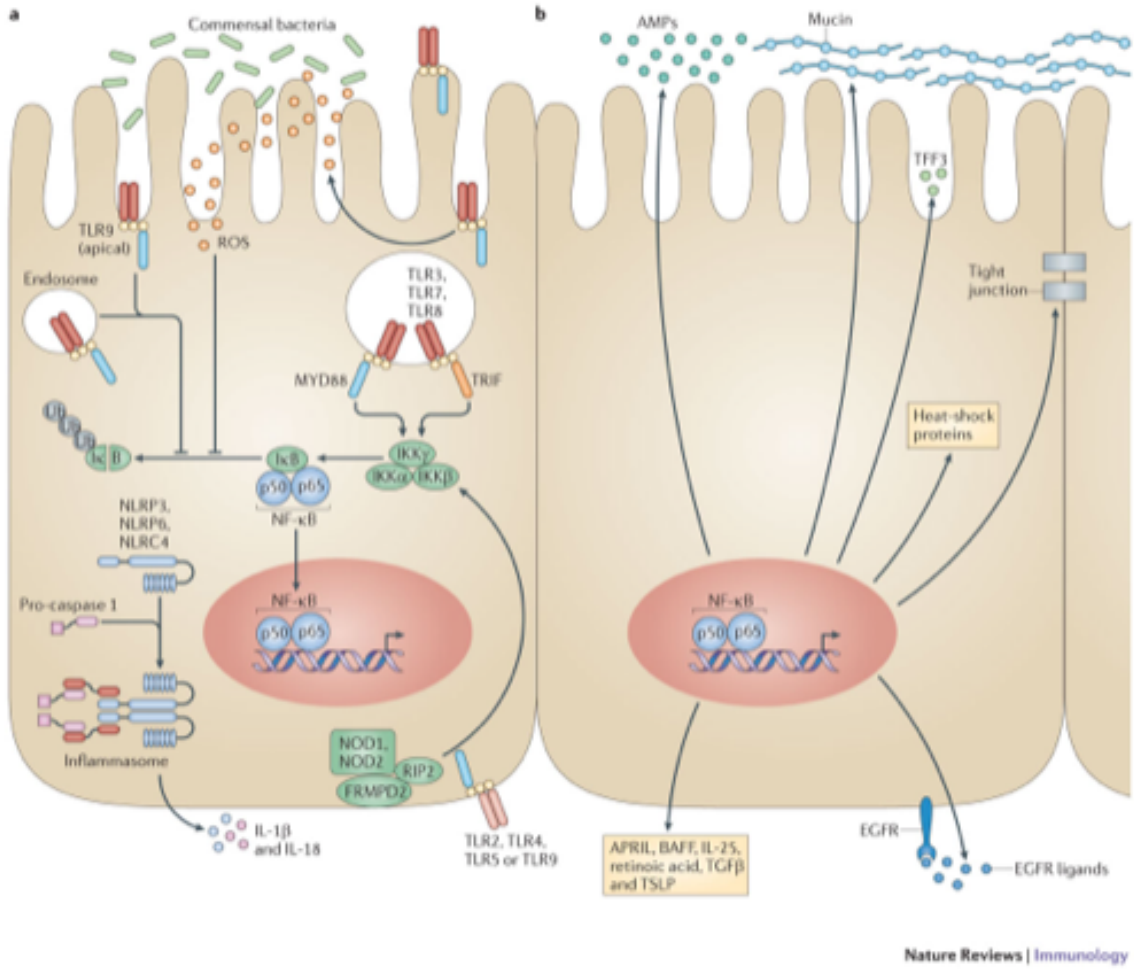

Figure 1.2: Microbial recognition by intestinal epithelial cells. (A) Intestinal epithelial cells express TLRs, which recruit MyD88 signalling adaptor proteins to signal molecules via the NFκB and MAPK pathway. IECs also express NOD1 and NOD2, which activate NFκB and MAPK, as well as other NLRs including NLRP3 that form inflammasome complexes with pro-caspase 1 for the cleavage and activation of IL-1β and IL18. (B) Microbial recognition by epithelial cells also promote barrier function (increased mucin and AMP production), cell survival and repair and immunoregulatory responses. (Taken from Peterson and Artis, 2014).

1.1.6 Gut-associated lymphoid tissue

The gut-associated lymphoid tissue (GALT) is the inductive site of mucosal immune responses. GALTs sample antigens directly from the mucosal surface across the follicle-associated epithelium (FAE) and therefore do not require the afferent lymphatic supply of antigens (Brandtzaeg, 2010). The FAE forms the interface between the GALT and the gut lumen and contains specialised 'microfold' (M) cells which are able to transport bacteria and antigens to the underlying lymphoid tissue. This leads to the activation of a systemic immune response, including specific T cell responses that lead either to the generation of immunoglobulin A (IgA) or to immune cell tolerance. Studies show that mice which do not have M cells, or antigen sampling by M cells, have reduced antigen-specific T cell responses in the Peyer's patches following oral inoculation with *S. typhimurium* (Mabott et al., 2013). GALT comprises the Peyer's patches in the small bowel, isolated lymphoid follicles (ILF) in the colon and small intestine, and cryptopatches in mice and the appendix (Brandtzaeg 2011). The GALT contains up to 70% of the body's immune cells, making it the largest lymphoid organ in the body (reviewed in Jung et al., 2010).

1.1.6.1 Peyer's patches

The most well characterised GALT tissues are the macroscopically visible Peyer's patches (PPs). PPs are lymphoid aggregates made up of 5 to 25 individual follicles. They are oval in shape and distributed irregularly along the anti-mesenteric side of the small intestine. In the distal ileum, however, there are about 300 PPs in an adult (Jung et al., 2010).

In humans, PP development occurs during gestation and rapidly progresses after birth when the gut is exposed to commensal bacteria and antigens. Peyer's patch numbers steadily increase through puberty, peak between the ages of 15 and 25, and then decline later in life (Jung et al., 2010). The embryonic steps of PP development have been studied extensively in mice, in which PP development is initiated by the expression of vascular cell adhesion molecule 1 (VCAM-1) on stromal cells (Jung et al., 2010; Pavert & Mebius 2010). Located on the anti-mesenteric side of the small intestine, distinct clusters of VCAM-1+ stromal cells express receptor tyrosine kinase (RET) ligands. RET ligands are encountered by RET+CD11c+ cells, which – following RET-dependent signalling – recruit haematopoietic cells. This initiates haematopoietic cell clustering which contains VCAM-1+ stromal cells,

RET+CD11c+ cells, and lymphoid tissue inducer (LTi) cells. Mice lacking RET, are unable to initiate haematopoietic cell clustering (Veiga-Fernandes et al., 2007).

RET-dependent signalling also leads to the expression of lymphotoxins by CD11c+ cells, which interact with the lymphotoxin-ß receptor (LTßR) expressed by the VCAM-1+ stromal cells. This produces IL7 and homeostatic chemokines CXCL13 and leads to further expression of surface lymphotoxin by LTi cells, resulting in the growth of PP (Yoshida et al., 2002). LTi cells are derived from common lymphoid progenitors, which are found in the foetal liver and give rise to all cells of the lymphoid lineage, including T cells, B cells, DCs, NK cells, and LTi cells (Mebius et al., 2001). The generation of LTi cells from common lymphoid progenitors require the expression of retinoic acid receptor-related orphan receptor-γt (RORγt) transcription factor (Eberl & Littman 2003). RORγt-deficient mice lacking LTi cells fail to develop PP, as well as lymph nodes and isolated lymphoid follicles (Eberl et al., 2004; Eberl et al., 2007). In contrast, very few CD11c+ cells are found in the developing lymph nodes (Van de Pavert et al., 2009) where the induction of lymphotoxin is fulfilled by receptor activator of nuclear factor κ B (RANK) signalling, a member of the tumour necrosis factor family (Kim et al., 2000).

The PP contains numerous B cell lymphoid follicles, which are surrounded by smaller T cell areas. The presence of germinal centres on all PP structures is indicative of the continual immune stimulation that occurs in response to luminal antigens (Mowat & Agace 2014). Other macroscopic structures that also contain M cells are the caecal patches and colonic patches, distributed throughout the colon and the rectum (Owen et al., 1991). Recent studies suggest that the intestinal microbiota play a crucial role in the generation of IgA-producing plasma cells in the PP and caecal patches. While PPs seem to be the main source of IgA plasmablasts that are targeted to the small intestine, it is suggested that caecal patches may be the major site for IgA-producing plasma cells that migrate to the colon (Masahata et al., 2014; Mowat & Agace, 2014).

1.1.6.2 Cryptopatches and isolated lymphoid follicles

The GALT also contains smaller lymphoid aggregates that can only be detected microscopically. These include the smaller cryptopatches (CPs) in mice and the more mature isolated lymphoid follicles (ILFs) (reviewed in Mowat & Agace, 2014). An ILF is a single B cell follicle, which has the capacity to develop a germinal centre following maturation (Knoop et al., 2011). ILFs are composed mainly of B cells surrounded by LTi or LTi-like cells, DCs, and stromal cells (Pearson et al., 2012). Like the PPs, ILFs are also covered by FAE-containing M cells, and therefore serve as an inductive site for IgA synthesis; however, unlike PPs, ILFs have no clear T cell zones and have been implicated as important sites for T cell-independent IgA class switching in mice. A single ILF can occupy the space of an entire villus, whereas CPs are smaller and found deep within the crypt LP. An adult mouse contains approximately 100-200 ILF in the small intestine and 50 in the colon. In comparison, 1500 CPs are found in the small intestine and 150 in the colon (Hamada et al., 2002; Taylor & Williams, 2005; Knoop et al., 2011).

Cryptopatches, which are yet to be identified in humans, develop postnatally within the first two weeks of life. They are present in germ-free mice and RAG-/- knockout mice lacking T and B cells. Cryptopatches contain DCs, common lymphoid progenitor cells and LTi-like cells (Pearson et al., 2012). In contrast, ILFs are absent in germ-free mice and in the foetus, and develop following re-colonization of mice gut with commensal bacteria. Hence, the development of ILFs in the small intestine requires stimulation from commensal microbiota. Such findings have led to the suggestion that the CP and ILF, rather than representing distinct types of intestinal lymphoid tissue, are two extremes on a continuum of solitary intestinal lymphoid tissue (SILT), whereby activated cryptopatches can develop into larger B cell follicles to form ILFs, which increase in size depending on the presence of microflora in the gut lumen (Pabst et al., 2006; Knoop et al., 2011; Eberl et al., 2010). Indeed, it was recently shown, in a human-mouse chimeric model, that mouse cryptopatches can initiate human GALT genesis in which the resulting GALT structures first contain T cells, B cells, DCs, and macrophages, and secondly can initiate IgA production (Nochi et al., 2013).

1.1.6.3 Antigen uptake by intestinal cells

Antigen uptake into the GALT is the first step required for the induction of the mucosal immune response. This can occur through several pathways involving M cells (direct and indirect mechanisms), epithelial cells, and DCs.

1.1.6.3.1 M cells

Within the FAE of GALT structures are specialised transcytotic epithelial cells known as microfold cells (M cells). M cells sample antigens directly from the gut lumen and transport them into the subepithelial dome region containing T cells, B cells, DCs, and macrophages (Neutra et al., 2001). Direct antigen uptake by an M cell occurs by various mechanisms, including phagocytosis, endocytosis, and macropinocytosis. Phagocytosis of whole bacteria can induce membrane ruffling and cytoskeletal rearrangements to form pseudopodia-like structures on the apical surface of the M cell (Borghesi, 1996). M cells also contain microfolds – instead of microvilli – on the apical surface that are rich in clathrin-coated pits, which mediate endocytosis of viruses and other particles (Acheson and Luccoili, 2004). Alternatively, non-adherent particles are internalised by fluid-phase endocytosis, known as macropinocytosis (Gebert & Bartels, 1995; Jung et al., 2010). In the small intestine, antigens are taken up by M cells in the FAE of the PP and ILF, whereas in the colon, the same antigen transport mechanism occur in the colonic ILF and caecal patches (Mowat & Agace 2014).

Indirect antigen uptake through M cells in the FAE can also occur in the form of secretory immunoglobulin A (IgA) complexes. Secretory IgA complexes may consist of secretory IgA bound to soluble antigens, as well as secretory IgA-coated bacteria. Although the exact mechanism of secretory IgA-complex internalisation by M cells remain unknown, it is speculated that IgA binding to an antigen may induce conformational changes in the IgA complex that enable it to bind preferentially to M cells rather than to free secretory IgA (Schulz & Pabst, 2013).

After internalisation, the particulate material is released into the M cell intraepithelial pockets. These are distinct subdomains in the M cell formed from deeply invaginated basolateral membrane (Neutra et al., 1996). Within these pockets, antigen-presenting cells – including B cells, macrophages, and DCs – internalise, process, and present the luminal antigens to naïve CD4+ T lymphocytes (Kraehenbuhl & Neutra, 2000).

1.1.6.3.2 Epithelial cells

Antigen uptake can also occur in absorptive enterocytes lining the villous epithelium (Schulz & Pabst, 2013). Epithelial cells express neonatal Fc receptors (FcRn), which bind to IgG-antigen complexes for transport across the epithelium to underlying DCs. The FcRn expression is restricted to the neonatal period in mice, unlike in humans, who express it throughout life (Yoshida et al., 2004). Transgenic expression of the FcRn in mice promotes bidirectional transport of IgG across the epithelium and into the lumen, as well as the IgG-dependent sampling of luminal antigens across the epithelium (Yoshida et al, 2006). This bidirectional FcRn transport not only helps to sample the gut commensal microflora, but also inhibits colonisation of pathogenic bacteria by IgG secretion. This has been shown in mice infected with pathogenic bacteria including *C. rodentium* (Yoshida et al., 2006) or *H. pylori* (Ben Suleiman et al., 2012).

1.1.6.3.3 Dendritic cells

An alternative means of antigen entry is mediated by intestinal dendritic cells (DCs). These DCs are found in close association with the gut epithelium, as well as in the lamina propia. Rescigno et al (2001) first showed the *in vitro* uptake of non-pathogenic *E. coli* and *S. typhimurium* by DCs through a monolayer of epithelial Caco-2 cells. These DCs were shown to extend dendrites in a paracellular manner between the epithelial cells by the formation of tight junction complexes, which did not disrupt the integrity of the epithelial barrier. These cells were subsequently shown to express the chemokine receptor CX_3CR_1 (Neiss et al., 2005). Upon oral administration of fluorescent *E. coli* or non-invasive *S. typhymurium* to CX_3CR_1-deficient mice, there was an absence of transepithelial protrusions and reduced bacterial translocation to the MLN (Niess et al., 2005). Taken together, these studies confirm that CX_3CR_1+ cells express tight junction proteins which enable them to extend 'trans-epithelial dendrites' (TEDs) through the epithelial barrier to sample bacterial antigens in the gut lumen (Rescigno et al., 2001; Niess et al., 2005; Vallon-Eberhard et al., 2006).

TED formation by CX_3CR_1+ cells is dependent on the presence of microbial products and TLR signalling in epithelial cells (Chieppa et al, 2006), since challenging mice with pathogenic bacteria or TLR ligands increased the number of

TEDs (Niess et al., 2005; Chieppa et al., 2006). In addition, DCs from germ-free mice, MyD88-deficient animals, and mice treated with antibiotics exhibit reduced numbers of TED processes (Niess et al., 2005; Niess & Adler, 2010). CD103+ DCs, another subset of DCs, have also been implicated in the capture of luminal antigens, upregulated expression of maturation markers, and migration to secondary lymphoid organs (Jaensson et al., 2008). This alternative route of antigen entry has important physiological relevance because the DCs, which are migratory cells, can transport pathogens/antigens directly to the MLN and spleen for induction of the systemic immune response.

1.1.6.4 Antigen presentation and lymphocyte migration in the GALT

Following entry into the GALT, antigens are processed by antigen presenting cells (APCs) located below the dome of the epithelium. These APCs then move to T cell areas or B cell follicles where they can interact with naïve lymphocytes. APC interaction with naïve CD4+ T cells generate T helper (Th) cell responses that lead to the activation of B cells within germinal centres of GALT follicles (Brandtzaeg, 2009). In the follicles, B cells undergo immunoglobulin class switching from expression of IgM to IgA in the presence of TGFβ, IL10, microbial signals, and other cellular signals from DCs and T cells (Cerutti et al., 2008). Mice with reduced bacterial colonisation display PPs with smaller and fewer germinal centres, while a lack of the TLR-associated adapter protein MyD88 results in an altered IgA response (Fagarasan et al., 2010; Chorny et al., 2012).

The primed lymphocytes exit the PP and enter the mesenteric lymph node (MLN) through the draining lymphatics, where they may undergo further differentiation. The cells then migrate to the bloodstream through the thoracic duct before homing back to the LP to carry out effector functions (Brandtzaeg, 2011). Lymphocytes primed in the GALT lose expression of L-selectin and specifically upregulate the expression of gut-homing markers. The interaction of the gut-homing receptors α4ß7 integrin and chemokines CCR9, with their corresponding ligands MAdCAM-1 and CCL25, respectively, facilitate lymphocyte migration to the LP (Mora, 2008). The addressin MAdCAM-1 and CCL25 are found on endothelial cells of the tissue post venules of the small and large bowel, while the gut-homing molecules α4ß7 and CCR9 are imprinted on activated T and B cells by gut-associated DCs (Mora, 2008; Cassani et al., 2012).

Gut-associated DCs express high levels of retinaldehyde dehydrogenase enzymes that enable them to metabolise retinoic acid from vitamin A (retinol) in the diet (Iwata et al., 2004). Vitamin A is essential for lymphocyte homing to the intestine, as retinoic acid upregulates the expression of gut-homing receptors (α4ß7 and CCR9) on lymphocytes while suppressing the expression of skin-homing markers (L-selectin) on lymphocytes (Iwata et al., 2004). As well as lymphocyte homing, vitamin A enhances B cell class switch recombination (CSR) (Mora et al., 2006; Cerutti and Rescigno, 2008) and has been implicated in the modulation of Foxp3+ regulatory T cell (Treg) and Th17 cell differentiation (Kang et al., 2007; Wang et al., 2010). Studies using vitamin A depleted mice demonstrate a reduction in the level of free retinol and retinyl esters, an absence of T cells and IgA secreting plasma cells in the small intestine, and an inability to induce gut tropic effector T cells (O'Byrne et al., 2005; Iwata et al., 2004; Mora et al., 2006; Hall et al., 2011).

Activated effector lymphocytes primed in the GALT and expressing gut-homing markers enter the LP and epithelium effector sites. Here, they generate protective immune responses including cytotoxic T lymphocytes, cytokine secreting T helper (Th) cells, and mature B cells (plasma cells) that produce secretory IgA. These effector responses can lead to tolerance of food and commensals or rejection of pathogenic microbes, depending on the initial antigen encountered by the APCs in the GALT inductive sites. Adaptive mucosal immune responses result from T cell help, by either Th1 or Th2 cells, which support the development of IgA-producing plasma cells (McGhee & Fujihashi, 2012; Castro-Sanchez & Martin-Villa, 2013).

1.2 *Citrobacter rodentium*

C. rodentium infection in mice has been used extensively to study host mucosal immune response to enteric pathogens. Mice infected with *C. rodentium* display colonic inflammation (hyperplasia) accompanied by a Th1 immune response, making this model particularly relevant for the *in vivo* study of host inflammatory responses. In addition, since *C. rodentium* infection is limited to the intestinal mucosa, it is also used to model important human intestinal diseases such as Crohn's disease, ulcerative colitis, and colon tumorigenesis. *C. rodentium* is host-adapted to laboratory mice, such that both the pathogen and the host can be genetically manipulated. Furthermore, the ability to quantify bacterial burden during *C. rodentium* infection, and the availability of the completed *C. rodentium* genome sequence, makes *C. rodentium* an ideal model system to study host-pathogen relationship in the gut.

C. rodentium, a natural pathogen of mice, infects the distal colon and causes transmissible murine crypt hyperplasia (TMCH). *C. rodentium* is transmitted by the faecal-oral route, and disease severity varies depending on mice strain, age, genetic background, and the composition of the mice intestinal microbiota (Barthold et al, 1978; Vallance et al, 2003; Collins et al, 2014). Infection of highly susceptible mice, such as young, inbred, genetically modified or C3H mice, can lead to severe inflammation and death. In contrast, resistant mice, including Balb/c, adult, or immunocompetent mice, display a self-limiting disease with minimal inflammation and tissue damage upon *C. rodentium* infection (Barthold et al, 1978; Mundy et al, 2005; Vallance et al, 2003; Collins et al, 2014). Although *C. rodentium* is non-invasive and colonises the surface of gut epithelial cells (Fig. 1.5), it can spread to systemic sites including the blood, spleen, and liver in mice in which the protective immune response is impaired (Collins et al, 2014). For infection studies, mice are usually orally gavaged with laboratory cultured *C. rodentium* whereby the course of infection can be monitored mainly through quantification of bacteria in the faecal shedding.

1.2.1 Course of infection

Following the oral gavage of mice with *C.rodentium*, bacteria colonise the caecum during the first day of infection and progress to the distal colon by day 2-3 post inoculation (p.i). Bacterial colonisation of the caecal patch, which is the largest

lymphoid structure in the caecum, is thought to facilitate the establishment of disease, as it is the site where bacteria adapt to the gastrointestinal environment and switch on virulence genes (Wiles et al, 2004; Wiles et al, 2006; Collins et al, 2013). Following bacterial colonisation of the distal colon and rectum, there is a peak of infection, during which bacterial shedding can release hyperinfectious bacteria into the environment and disease can be transmitted to uninfected mice via the faecal-oral route (Wiles et al, 2005; Bishop et al, 2007). Increased growth of *C. rodentium* in the colon leads to a reduction in the overall diversity of commensal microbiota (Lupp et al, 2007; Collins et al, 2014). Bacteria begin to clear from the caecum and the colon after the second week of infection, until complete clearance is seen at 3-4 weeks p.i (Wiles et al, 2004; Wiles et al, 2006; Collins et al, 2014).

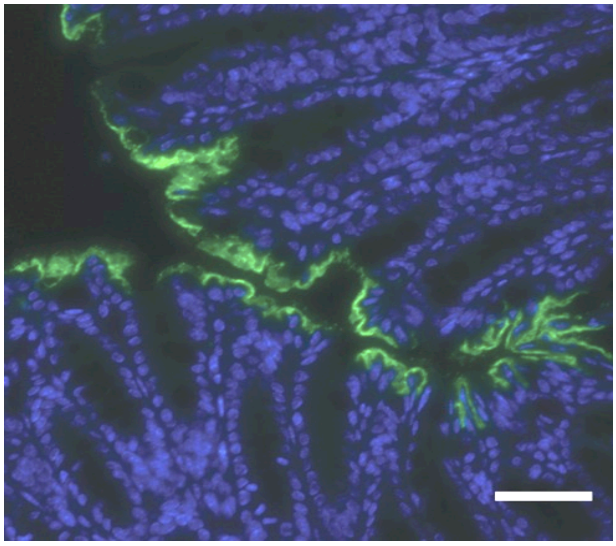

Figure 1.3 : *C. rodentium* colonisation of mouse intestinal epithelial cells (IEC) *in vivo*. Immunofluorescent staining of mouse colonic tissue at day 6 p.i using *C. rodentium*-specific anti-Tir antibody (green) and DAPI (blue) as a counterstain for host cell nuclei. Magnification (40x), scale bar (50um). Taken from Law et al. (2013).

1.2.2 Transmissible murine crypt hyperplasia (TMCH)

The main pathological feature of *C. rodentium* infection is transmissible murine crypt hyperplasia (TMCH) (reviewed in Collins et al, 2014). TMCH is characterised by the elongation of colonic crypts and thickening of the mucosa (Fig 1.6). This occurs due to the induction of excessive intestinal epithelial repair processes, which include epithelial cell proliferation, epithelial cell turnover, and shedding of infected epithelial cells into the gut lumen (Luperchio and Schauer, 2001; Mundy et al, 2005; Bergstrom et al, 2012; Collins et al, 2014). Epithelial cell proliferation is triggered by the activation of specific signalling pathways in response to bacterial attachment to epithelial cells (Higgins et al, 1999; Collins et al, 2014). For example, the activation of host TLR4 and TLR2 in response to *C. rodentium* infection was shown to contribute to MyD88 signalling and the downstream activation of NFκB pathway required for the proliferative response of crypt epithelial cells (Lebeis et al, 2007; Khan et al, 2006; Gibson et al, 2008b; Collins et al, 2014). TMCH is also triggered by the loss of epithelial barrier integrity and the translocation of bacteria into the LP (Gibson et al, 2010).

Although the initiation of TMCH does not depend on T or B cells, as indicated by the presence of TMCH in RAG-/- knockout mice, adaptive immunity is required for bacterial clearance and the resolution of TMCH (Vallance et al, 2003; Collins et al, 2014). TMCH may be beneficial for *C. rodentium* infection as it provides increased surface area for bacterial adherence and enables reduction of commensal microbiota, resulting in a competitive advantage for *C. rodentium* colonisation. In addition, TMCH enhances the transmission of bacteria to other hosts through increased shedding of epithelial cells and *C. rodentium* into the gut lumen (Higgins et al, 1999). However, increased epithelial cell shedding in TMCH can also contribute to host resistance, because it can facilitate the removal of infected cells and enhance bacterial clearance (Bergstrom et al, 2012).

Another pathological feature of *C. rodentium* infection is goblet cell depletion in the colon of infected mice (Fig. 1.6) (Luperchio & Schauer, 2001). Although goblet cells are abundant in the colon and secrete Mucin 2, which has been shown to provide protection against *C. rodentium* (McGuckin et al, 2011; Bergstrom et al, 2010), the reduction in goblet cell numbers during *C. rodentium* infection can also be beneficial to the host (Chan et al, 2013). In a recent study by Chan et al (2013), *C. rodentium*

was observed to preferentially localise within crypts that were non-hyperplastic and contained numerous goblet cells, compared to hyperplastic, goblet cell-depleted crypts, which were protected from infection. In addition, goblet cell depletion appeared to be driven by IFNγ production from CD4+T cells, as mice lacking CD4+T cells did not exhibit goblet cell depletion (Bergstrom et al, 2008; Chan et al, 2013). This suggests that goblet cell depletion is a protective host response against *C. rodentium* whereby the reduction in goblet cell numbers may reduce the surface area for bacterial attachment and limit *C. rodentium* colonisation of the colonic crypts.

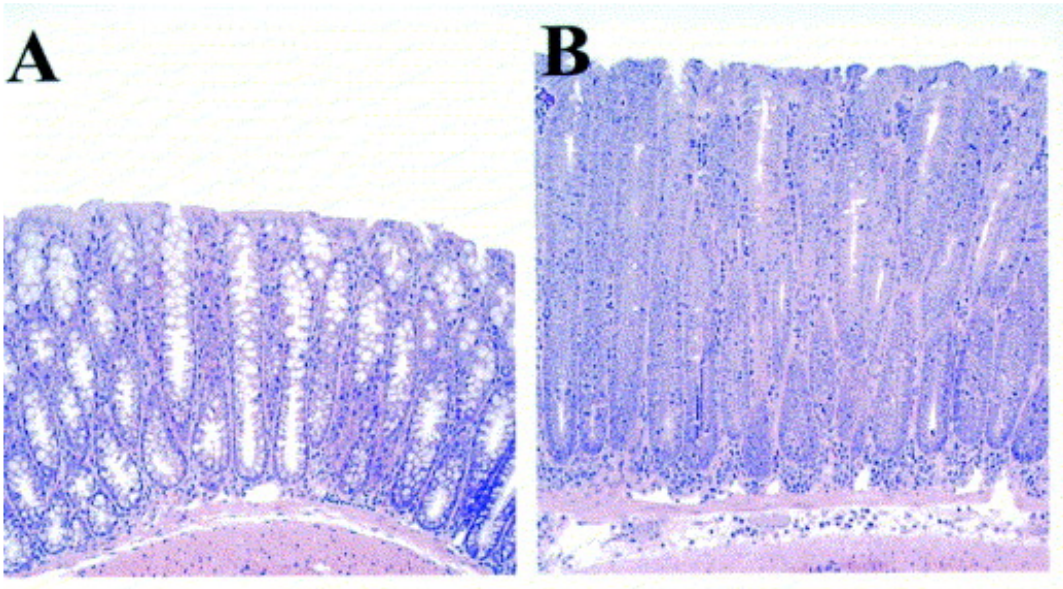

Figure 1.4: H &E stained colonic sections from *C. rodentium* infected mice. (A) Normal colonic architecture from uninfected mice (B) colon showing crypt hyperplasia, goblet cell depletion, and mild inflammation from 31-day old Swiss-Webster mice infected with *C. rodentium*. Taken from Luperchio and Schauer (2001).

1.2.3 Host immune response to *C. rodentium* infection in mice

The requirement for both innate and adaptive immunity for the clearance of *C. rodentium* (Appendix A) has been widely demonstrated in various genetically modified mice lacking specific components of the immune system (Appendix B). Due to space restrictions, I will be focusing on the role of pattern recognition receptors, innate lymphoid cells, and adaptive immunity in the resolution of *C. rodentium*-mediated disease (Fig. 1.7).

1.2.3.1 Pattern recognition receptor signalling

C. rodentium and its pathogen-associated molecular patterns (PAMPS)—including lipopolysaccharides (LPS), peptidoglycans, and the T3SS—are recognised by MyD88-dependent TLR signalling (Gobert 2005; Collins et al, 2014), which has been shown to be essential for host defences against *C. rodentium* (Fig. 1.7a). Mice deficient in MyD88 are unable to control *C. rodentium* growth in colonic tissue, fail to recruit neutrophils and macrophages to the site of infection, unable to produce iNOS that contribute to the direct killing of *C. rodentium*, and unable to promote epithelial cell turnover and repair (Vallance et al, 2004; Lebeis et al, 2007; Gibson et al, 2008b; Bergstrom et al, 2012). The main contributors to MyD88-mediated signalling during *C. rodentium* infection are TLR2 and TLR4 (Fig.1.7a), which have been shown to control the production of proinflammatory cytokines TNFα, IL6 and keratinocyte chemoattractant (KC) as well as the upregulation of iNOS (Gibson et al, 2008a; Lebeis et al, 2007; Bergstrom et al, 2012; Collins et al, 2014). Although *C. rodentium* is extracellular, the intracellular Nod-like receptors NOD1 and NOD2 have also been implicated in triggering innate host responses to *C. rodentium* (Fig. 1.7) (Geddes et al, 2011). Mice deficient in NOD1 and NOD2 display high systemic loads of *C. rodentium* throughout the course of infection (Kim et al, 2011; Geddes et al, 2011). This is because NOD2 signalling results in the production of monocyte chemotactic protein 1 (MCP1) or CCL2, which is involved in the recruitment of CD11c+ inflammatory monocytes to the site of infection for bacterial killing (Kim et al, 2011; Geddes et al, 2011). NOD1 and NOD2 signalling also provide protection against pathogen-induced damage by stimulating the production of IL17 by innate lymphoid cells (Geddes et al, 2011).

1.2.3.2 Innate lymphoid cells

The group 3 innate lymphoid cells (ILC3s), which are induced early during *C. rodentium* infection, belong to a newly identified group of innate lymphoid cells that produce T helper cell-associated cytokines but do not express a T cell receptor (Walker et al, 2013). These cells develop as a result of bacterial imprinting by the intestinal microbiota (Geddes et al, 2011). ILC3s are important producers of IL17 and IL22 cytokines, which are both essential in the control of *C. rodentium* infection (Fig. 1.7b) (Collins et al, 2014).

ILC3s are an important source of IL-22 production in the gut (Ahlfors et al, 2014). During the early stages of *C. rodentium* infection, IL22 is upregulated and provides protection by regulating the secretion of antimicrobial proteins (RegIII) from epithelial cells (Zheng et al, 2008). IL22 also maintains epithelial barrier integrity and prevents the dissemination of bacteria (Ahlfors et al, 2014). The fact that IL22 is produced from an innate cell source emerged from studies using RAG1-/- KO mice, in which IL22 maintained the epithelial barrier integrity and contained *C. rodentium* infection despite the absence of T and B lymphocytes (Vallance et al, 2002). However, these mice eventually died as a result of chronic inflammation. Furthermore, mice lacking the ILC3 subset failed to contain *C. rodentium* infection in the gut, and, like IL22-/- mice, exhibited an increased infiltration of inflammatory cells and mucosal hyperplasia (Zheng et al, 2008; Lee et al, 2012; Walker et al, 2013). ILC3s therefore provide a rapid source of IL22 to strengthen the epithelial barrier in response to *C. rodentium*.

The IL22 response to *C. rodentium* is dependent on a lymphotoxin pathway, since in the absence of lymphotoxin signalling, mice succumb to infection (Tumanov et al, 2011). Lymphotoxin, expressed by the RORγt transcription factor, propagates a signal through the lymphotoxin receptor (LTβR) present on DCs, macrophages, and epithelial cells. This induces the production of IL23, which binds to and activates the IL23R on ILCs to produce IL22. IL22 signals via IL22R on intestinal epithelial cells to drive the expression of antibacterial proteins (RegIIIγ and RegIIIβ) and promote epithelial barrier integrity and epithelial cell generation. IL-22-dependent RegIIIγ secretion is crucial for protection against *C. rodentium*, as exogenously added RegIIIγ rescues IL-22-deficient mice from fatal infection (Zheng et al, 2008). In the later stages of *C. rodentium* infection, however, CD4+T cells (Th17) function as the

main source of IL22 that is dependent on IL6 (Basu et al, 2012). The production of IL22 from both ILC3s and Th17 cells is therefore required to provide complete protection against *C. rodentium* infection (Basu et al, 2012; Collins et al, 2014).

1.2.3.3 Th17 cell response:

Citrobacter rodentium induces a potent Th17 cell response, which is stronger than a IFNγ mediated Th1 response one week after oral inoculation of mice (Mangan et al, 2006). During the peak of infection (Day 8 p.i), a higher frequency of colonic CD4+T cells express IL17 in comparison to a smaller fraction of cells expressing IFNγ (Mangan et al, 2006). Although host protection was previously associated with IFNγ mediated Th1 dependent IgG response (Simmons et al, 2003), the expression of IL17 and IL22 cytokines by Th17 cells appear to play an important role in controlling the severity of gut pathology and *C. rodentium* infection (Collins et al, 2014). In particular, IL17 promotes the recruitment of neutrophils and other effector cells to the site of infection while IL22 activates epithelial cell defenses through the expression of antimicrobial peptides and mucus production (Chen et al, 2014; Wang et al, 2014). Deficiencies in any of the Th17 cell effector molecules or the IL17 receptors including IL17A, IL17F, IL17RA or IL17RE, result in the reduction of neutrophil recruitment and expression of genes encoding antimicrobial peptides which in turn leads to the increase in bacterial burden, mucosal ulceration, bacterial dissemination and early mortality following *C. rodentium* infection (Geddes et al, 2011; Song et al, 2011; Collins et al, 2014).

During infection of mice with *C. rodentium*, the CD4+Th17 cell subset was observed to increase in the PP but not in the MLN (Li et al, 2014). Further studies revealed that IL6 is required for the differentiation of Th17 cells in the PP, since treatment with anti-IL6 neutralizing antibodies reduced the Th17 cell subset, resulting in increased susceptibility of mice to *C. rodentium* infection (Li et al, 2014). In addition to IL6, TGFβ contributes to the development of Th17 cells (Mangan et al, 2006). By actively suppressing the production of IFNγ (a potent inhibitor of Th17 development) TGFβ inhibits Th1 immune responses and promotes Th17 cell development. In the presence of IL23, TGFβ induces further suppression of IFNγ+ cells and increases the fractions of Th17+ cells. Mice deficient in IL23 failed to clear the high bacterial load and succumbed to infection (Mangan et al, 2006).

Furthermore, the generation of a Th17 cell response is influenced by the intestinal microbiota, since germ free mice have substantially fewer IL17 producing CD4+ T helper cells than specific pathogen free mice (Ivanov et al, 2008). Faecal microbiota transplantation (FMT) and cohousing studies reveal that mice that have higher Th17 cell numbers, have higher levels of SFB in their microbiota, and the introduction of SFB into germ free mice or Th17 cell deficient mice induce the appearance of IL17 and IL22 producing CD4+T helper cells in the lamina propia. SFB mediated Th17 response is correlated with increased expression of genes associated with inflammation and anti microbial defenses resulting in enhanced resistance against *C. rodentium* (Ivanov et al, 2009). SFB typically adhere tightly to the epithelium in the ileum where they have been suggested to induce the production of serum amyloid A that act on lamina propia DCs to promote Th17 cell differentiation. SFB colonized mice that have been infected with *C. rodentium*, display reduced colon mucosal thickness, a decrease in bacterial titre recovered from the colon wall and an overall reduction in the growth and colonization of *C. rodentium* in mouse distal colon (Ivanov et al, 2009; Ivanov & Littman, 2010).

Recent studies suggest that adhesion of SFB to the intestinal epithelial cells is critical in the induction of a Th17 response (Atarashi et al, 2015). Similarly, strong adhesion of *C. rodentium* to intact epithelial cells was shown to stimulate the production of reactive oxygen species, which lead to the induction of a potent Th17 response. Mice colonised with *C. rodentium* lacking intimin, a protein essential for epithelial cell adhesion, were unable to adhere to epithelial cells resulting in a weak Th17 cell response (Atarashi et al, 2015).

Moreover the development of the Th17 cell response is associated with *C. rodentium*-induced apoptosis of IECs (Torchinsky et al, 2009, Collins et al, 2014). The phagocytosis of infected apoptotic IECs by innate immune cells, such as DCs, trigger the release of cytokines IL6 and TGFβ, which play an important role in the differentiation and proliferation of Th17 cells. Blocking apoptosis of IECs during *C. rodentium* infection impairs the development of the Th17 cell response in the lamina propia (Torchinsky et al, 2009). Phagocytosis of apoptotic cells in the absence of microbial signals induce the differentiation of regulatory T cells that are important for controlling autoimmunity. Effector Th17 cells produce IL17, IL10 and IL22

which are important for the clearance of *C. rodentium* as well as repair of the infection-damaged intestinal epithelium (Torchinsky et al, 2009).

1.2.3.4 Adaptive immune cells

Mice infected with *C. rodentium* elicit a T helper 1 (Th1) cell response, characterised by a large infiltrate of CD4+T cells in the LP and an increased production of IL12, TNFα, and IFNγ in the colonic tissue (Higgins et al, 1999). Many of the effector functions of CD4+T cells are mediated by IFNγ, as mice lacking CD4+T cells or IFNγ have increased susceptibilities to *C. rodentium* infection (Simmons et al, 2003; Bry & Brenner, 2004; Shiomi et al, 2010). IFNγ, amongst other functions, stimulates the activation of antigen-specific T helper cells that lead to the subsequent increase in B cell production of antigen-specific IgG (Shiomi et al, 2010). Mice lacking B cells show similar pathology and mortality in response to *C. rodentium* infection as mice lacking CD4+T cells. The administration of immune sera from wildtype mice that have recovered from infection protects B cell-deficient mice and CD4+T cell-deficient mice from systemic infection and mortality (Simmons et al, 2003; Maaser et al, 2004; Bry et al, 2006; Belzer et al, 2011). Passive immunization with serum IgG is sufficient to protect CD4-deficient mice from fatal infection, while mice lacking secretory IgA, secretory IgM, or proteins required for their transport into the lumen (pIgR or J chain) clear *C. rodentium* normally (Bry and Brenner, 2004; Maaser et al, 2004; Uren et al, 2005).

Although the mechanism of IgG entry into the gut lumen is unclear, studies suggest that FcRn-mediated epithelial transport may play a role (Bry et al, 2006; Spiekermann et al, 2002). Infection of C57Bl/6 mice with *C. rodentium,* generates high numbers of IgG2c and IgG2b, which enter the intestinal lumen (Bry et al, 2006) and bind to neutrophil Fcγ receptors for pathogen opsonization. These antigen-associated IgG complexes can further activate the complement system since complement protein C3b and IgG isotypes were found coating the surface of *C. rodentium* bacteria shed in mice stool (Belzer et al, 2011). This suggests that *C. rodentium* opsonization with IgG and/or C3 molecules may enhance the uptake and killing of *C. rodentium* by neutrophils, while the activation of the complement cascade can have direct antimicrobial effects, including bacterial lysis and neutralisation of bacterial adhesins (Belzer et al, 2011).

Collectively, these studies show a dynamic interplay between components of the innate and adaptive immune system to initiate a well-coordinated host response against *C. rodentium* infection. Therefore, *C. rodentium* serves as an ideal model for the study of host-pathogen relationship in the gut. In addition, since *C. rodentium* possesses a type 3 secretion system (T3SS) and shares many of its virulence genes and disease strategies with pathogenic *E. coli*, it is also an excellent small-animal *in vivo* model to study the virulence mechanisms of T3SS-containing enteropathogens.

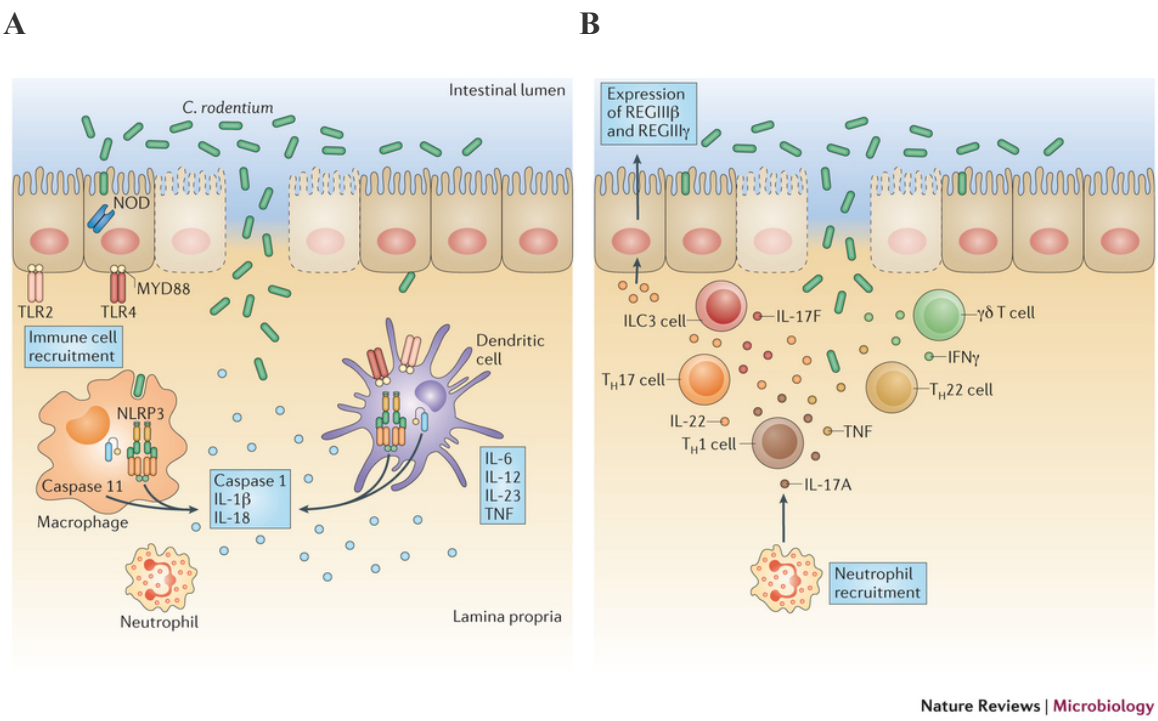

Figure 1.5: Immune response to *C. rodentium* infection. *C. rodentium* infection in mice triggers host inflammation through the recognition of lipopolysaccharide (LPS), the type III secretion system (T3SS), and peptidoglycans by host TLRs. **(A)** *C. rodentium* recognition by host TLR2, TLR4, and NOD proteins initiates MYD88 signalling, which results in the activation of NFκB and the production of the proinflammatory cytokines IL-6, IL-12, IL-23, and TNF by innate immune cells, including dendritic cells, macrophages, and neutrophils. *C. rodentium* also induces IL-1β and IL-18 production by macrophages and dendritic cells via the caspase 1-dependent NLRP3 inflammasome. **(B)** *C. rodentium* infection induces T_H1 and $T_H17$cell responses, which drives host resistance to *C. rodentium* infection through the production of IL-17A (which recruits neutrophils) and IL-22 (which upregulates the expression of antimicrobial peptides, RegIIIβ and RegIIIγ in colonocytes). In the caecum, group 3 innate lymphoid cells (ILC3s), induced early during infection in a NOD-dependent manner, are an important source of IL-17 and IL-22 and contribute to the clearance of *C. rodentium* infection. Taken from Collins et al. (2014).

1.3 Enteropathogens

Enteropathogens are specific gram-negative bacteria that have acquired sophisticated strategies to breach the intestinal barrier, exploit the mucosa to replicate and disseminate, and cause intestinal disease (reviewed in Sansonetti & Santo, 2007; Coburn et al, 2007). Many successful enteropathogens possess a specialized macromolecular export apparatus known as a type three secretion system (T3SS) to inject virulence proteins (effectors) directly into the cytoplasm of host cells (Cornelis 2006; Coburn et al, 2007; Erhardt et al, 2010). Inside host cells, effectors target subcellular structures and components of the host cell machinery including tight junctions, cytoskeletal proteins, microtubules, mitochondria, Golgi, nucleus, and plasma membranes to regulate actin dynamics, subvert endocytic trafficking, block phagocytosis, modulate apoptotic pathways, and manipulate host inflammatory responses (Dean et al, 2011). Subversion of host cellular processes by the T3SS effectors enable the non-invasive enteropathogens to successfully attach to and colonise host intestinal epithelial cells while facilitating invasive enteropathogens to invade intestinal epithelial cells, survive intracellularly and disseminate to deeper tissues (reviewed in Reis & Horn, 2010; Raymond et al, 2013).

The T3SS is the most complicated secretion system in bacteria (Cornelis et al, 2006; Coburn et al, 2007). It is made up of approximately 25 proteins and delivers over 20 effectors to the host target cell (Cornelis 2010). The T3SS enables bacteria to transport proteins directly across the bacterial cell wall and the eukaryotic cellular membranes (Pugsley, 1993; Galan et al, 1999; Coburn et al, 2007). It differs from other bacterial secretion systems because it requires host cell contact for activation of the T3SS pathway and the presence of chaperone proteins for effector translocation (Cornelis 2006). The T3SS apparatus is highly conserved among the different pathogens and shares a strong homology to components of the flagellar system (Blocker et al, 2003; Erhardt et al, 2010). Although the presence of the flagellar system in both gram-positive and gram-negative bacteria suggests that all T3SS may have evolved from the flagellum (Hueck 1998; Macnab 2004), phylogenetic studies indicate that the flagellum and the injectisome are both ancient and may share a common ancestor instead (Gophna et al, 2003; Cornelis 2006). The T3SS is present in over 25 species of gram-negative bacteria, including the causative agents of pneumonia (*Pseudomonas*), plague (*Yersinia*), typhoid fever (*Salmonella*), dysentery

(*Shigella*) and bloody diarrhoea (*E. coli*) (Dean et al, 2011). Due to space limitations, the focus here will be on the attaching effacing pathogens comprising of *EPEC, EHEC, and C. rodentium* for the purposes of this thesis.

1.3.1 Attaching Effacing Pathogens

Enteropathogenic *E. coli* (EPEC), enteroheamorrhagic *E.coli* (EHEC), and *Citrobacter rodentium* are gram-negative, non-invasive, extracellular bacteria that belong to the attaching and effacing (AE) group of pathogens. These enteropathogens are characterised by their ability to create AE lesions on mucosal surfaces of the host gastrointestinal tract (Fig. 1.9a -1.9b). Bacterial translocation of effectors into the host cell subverts host cytoskeletal pathways that lead to the formation of pedestal-like structures. These are raised surfaces of electron-dense material consisting mostly of polymerised actin filaments that protrude into the lumen on which the bacteria reside (Fig.1.9c – Fig.1.9d). Pedestal formation facilitates increased bacterial adherence (attachment) and the loss or destruction of the microvilli brush border (effacement) on the surface of enterocytes (Nataro & Kaper 1998; Wales et al, 2005; Clements et al, 2012; Lai et al, 2013).

EPEC is a major cause of infectious diarrhoea in children worldwide, producing significant morbidity and mortality in developing countries. EPEC is transmitted by human carriers through the faecal-oral route, weaning fluids, and contaminated surfaces (Nataro & Kaper, 1998). The ingestion of contaminated food and water has been responsible for causing rare outbreaks amongst adults (Croxen et al, 2013). EPEC colonises the small bowel, resulting in diarrhoea accompanied by fever, vomiting, and dehydration in children under 2 years of age (reviewed in Nataro & Kaper, 1998; Croxen et al, 2013). EPEC is classified into “typical” and “atypical” subtypes based on the presence of an *E. coli* adherence factor (EAF) plasmid (Croxen et al, 2013). Humans are the only known reservoir for typical EPEC, while atypical EPEC has been isolated from human and animal sources, including dogs, rabbits, monkeys, and sheep (Swennes et al, 2012). The strain E2348/69 is a prototype of EPEC and is used widely in the laboratory to model AE pathogenesis.

EHEC is a subset of Shiga toxin-producing *E. coli* (STEC) associated with haemorrhagic colitis (HC) and the fatal haemolytic-uremic syndrome (HUS) (Nataro & Kaper, 1998). EHEC colonizes the large bowel in humans and can cause mild to

bloody diarrhoea in both adults and children. It often causes outbreaks of severe gastroenteritis in developed countries, commonly by the EHEC serotype O157:H7 in contaminated food and water. Disease transmission usually occurs through the faecal-oral route and the infectious dose is very low. Cattle are widely known to be major reservoirs for EHEC because exposure to their faecal matter is an important source of human illness. EHEC virulence factors include Shiga toxin (also known as Vero toxin) and hemolysin, a pore-forming toxin that lyses erythrocytes (Croxen et al, 2013).

C. rodentium is the only known AE lesion-forming pathogen to infect mice. The LEE of *C. rodentium* also shows striking similarity to that of EPEC and EHEC (Fig. 1.8) (Deng et al, 2001) and is required to produce AE lesions in mouse intestinal cells (Schauer & Falkow 1993). Although *C. rodentium* infection results in colonic inflammation and hyperplasia (Barthold et al, 1978) rather than causing obvious diarrhoea, as is the case with EPEC and EHEC, mouse infection with *C. rodentium* has greatly improved our understanding of AE pathogenesis and virulence mechanisms *in vivo*. Attaching and effacing pathogenesis occurs in a sequential process, which in this thesis is described in 4 stages: adherence, assembly of the T3SS injectisome, signal transduction and intimate attachment, and pedestal formation.

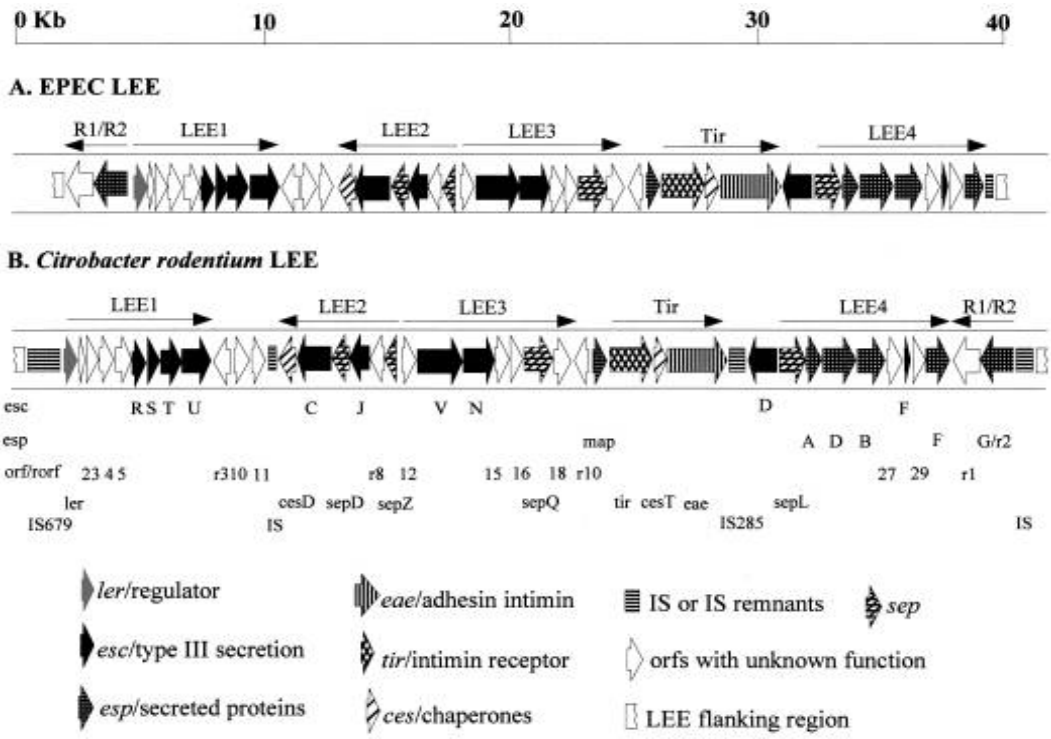

Figure 1.6: Virulence genes in *EPEC* and *C. rodentium.* Taken from Deng et al. (2001). The organisation of virulence genes between the AE pathogens are very similar. The LEE core region for both EPEC and *C. rodentium* is 36kb and contain 41 open reading frames (ORFs) that are organised into 5 operons (LEE 1-5). The core region of *C. rodentium* LEE is 98% identical to that of EPEC.

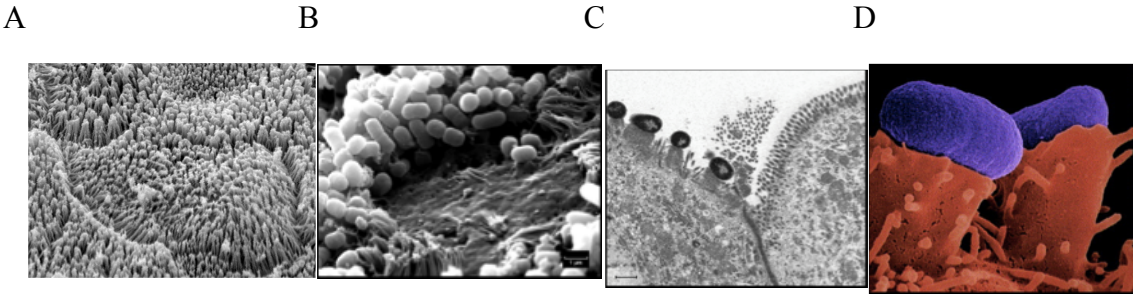

Figure 1.7: Attaching effacing lesion and pedestal formation in AE pathogens. (A) Uninfected intestinal surface showing normal microvilli. (B) EPEC infected intestinal cell surface showing loss of microvilli. Taken from (www.staff.ncl.ac.uk/p.dean/body_index.html). (C) Transmission electron micrograph (TEM) showing A/E lesions induced by EHEC in the colon of a calf where the microvillus effacement and the raised electron-dense pedestals are clearly visible. Taken from Stevens and Frankel (2014). (D) Scanning electron microscope image of EPEC (purple) sitting on top of a pedestal (orange). Image originally published in Rosenshine et al. (1996).

1.3.2 Adherence

The first stage in the AE lesion process involves the non-intimate adhesion of EPEC to host enterocytes in the small bowel. This is mediated by bundle-forming pili (BFP) encoded by the *E.coli* adherence factor (EAF) plasmid present in typical EPEC (Giron et al, 1991; Trabulsi et al, 2002). Bundle-forming pili (BFP), synthesised in response to bacterial contact with host cells, are rope-like filaments that can interact with receptors on the microvilli of host enterocytes (Hyland et al, 2008). Bundle-forming pilli also interact with other EPEC bacteria to produce localised adherence and form characteristic EPEC microcolonies. There is evidence that *E. coli* common pilus may also act in combination with the BFP to stabilize EPEC attachment to host cells (Saldana et al, 2009). Following BFP production, adhesion of typical EPEC to the epithelial cells activates the assembly of the T3SS. Atypical EPEC strains, however, do not possess the EAF plasmid and so do not produce BFP. Instead they form loose clusters of bacteria in a localised adherence-like pattern that is slower to establish than localised adherence. In addition, EPEC encodes a lymphocyte inhibitory factor, a surface protein required for epithelial cell adherence *in vitro* and intestinal colonisation of mice by *C. rodentium in vivo* (Badea et al, 2003; Klapproth et al, 2005). Lymphocyte inhibitory factor, more commonly found in typical rather than atypical EPEC, has been identified as the largest effector to be secreted by T3 pathogens (Vieira et al, 2010). Although the initial attachment of EHEC to enterocytes in the colon is not well-defined, recent work has identified a role for haemorrhagic *coli* pilli, flagella, and the *E. coli* common pilli in the adherence of EHEC to host cells (Xicohtencatl-Cortes et al, 2009; Erdem et al, 2007; Rendon et al, 2007). The initial attachment of AE pathogens with host epithelial cells initiates the assembly of the T3SS injectisome.

1.3.3 Assembly of the T3SS injectisome

The T3SS injectisome is a supermolecular complex that is made up of the basal body, needle, and pore complex (Fig.1.10) (Sekiya et al, 2001; Cornellis 2006). The basal body of the injectisome spans the inner and outer membranes of the bacteria and is composed of scaffolding proteins, an export apparatus, and an ATPase complex. The needle extends from the basal body to the extracellular environment, and the needle tip is connected to the host cell by the pore complex in the host cell membrane. The complete injectisome, when docked onto a host cell, allows the

translocation of proteins directly from the bacteria to the host cell cytosol (Dewoody et al, 2013; Monjaras Feria et al, 2012)

Assembly of the injectisome is a sequential, tightly regulated process (Cornelis, 2006; Deane et al, 2010). In AE pathogens, basal body formation begins with the oligomerisation of EscC secretin, which forms a ring in the bacterial outer membrane (OM), followed by assembly of an inner membrane (IM) ring using proteins EscD and EscJ (Diepold et al, 2010; Gauthier & Finlay, 2003). Together these proteins create a scaffold anchored within the peptidoglycan, which serves as a base for the assembly of the remaining injectisome components.

The export apparatus is localised in a patch of membrane within the inner membrane ring. This is made up of the integral membrane proteins EscR, EscS, EscT, EscU, and EscV, and its assembly is independent of the scaffolding proteins (Moraes, 2008; Wagner et al, 2010). The formation of the EscN ATPase occurs on the cytosolic face of the basal body (Andrade et al, 2007). This energizes the secretion process and also functions as a docking site for the chaperone-effector complexes present in the bacterium prior to secretion (Gauthier & Finlay 2003; Zarivach et al, 2007; Feria et al, 2012). The joining of the scaffold with the export apparatus and the ATPase complex completes the basal body formation, which is then capable of exporting secretion substrates. The protein substrates are secreted in 3 stages: early substrates (inner rods and needle subunits), middle substrates (translocators), and late substrates (effectors) (Deane et al, 2010; Buttner et al, 2012). This is summarised in Table 1.1.

Upon completion of the basal body, the "early" substrates, necessary for needle assembly, are exported (Table 1.1). One of the first proteins to be translocated is the EscI protein, which polymerises to form the periplasmic inner rod of the T3SS basal complex (Sal-Man et al, 2012). Secreted through the inner rod are the EscF subunits, which polymerise to form the extracellular needle to an approximate length of 50 nm (Diepold et al, 2012; Wilson et al, 2001). Regulation of the needle length is carried out by "ruler" proteins, which are known as YscP in *Yersinia*, Spa32 in *Shigella*, InvJ in *Salmonella*, and, more recently, EscP in *E. coli* (Journet et al, 2003; Feria et al, 2012). Mutations in these genes result in the production of abnormally long needles and the inability of the T3SS to secrete "middle" and "late" substrates (Journet et al, 2003; Feria et al, 2012).

When the needle reaches full length, a substrate specificity switch is triggered, which arrests needle export. The substrate specificity switch is mediated by the interaction of EscP with EscU of the export apparatus, resulting in the autocleavage of EscU (Minamino et al, 2005). The substrate specificity switch also enables the secretion of the middle and late substrates (Thomassin et al, 2011; Feria et al, 2012). The middle substrates refer to proteins that make up the pore complex, while the late substrates refer to the effectors (Dewoody et al, 2013).

During the initiation of the pore complex, a long helical homopolymeric filament—generated by the polymerisation of EspA subunits—extends the needle, projecting from the bacteria to the intestinal cell surface (Knutton et al, 1998). Through this EspA filament, translocators EspB and EspD travel to and form a translocation pore in the enterocyte membrane (Munera 2010). The translocation pore creates an opening in the host cell membrane and promotes the entry of late substrates (effectors) (Table 1.1) into the host cell cytosol. To initiate the secretion of effectors, contact with host cell is required (Forsberg et al, 1991).

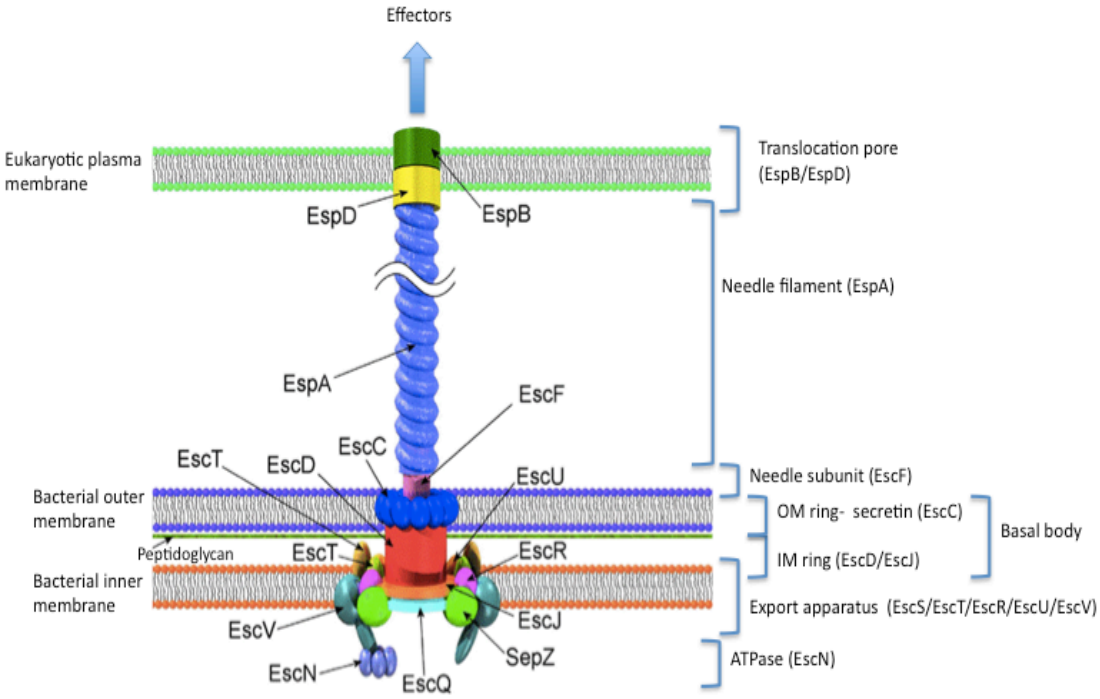

Figure 1.8: The T3SS injectisome. A schematic representation of the T3SS encoded within the LEE of AE pathogens. The T3SS effectors leave bacteria through the export apparatus, travel through the needle filament and enter the host cell cytoplasm through the translocation pore in the eukaryotic plasma membrane. Adapted from Pallen et al. (2005).

Table 1.1: LEE encoded Type III components in AE pathogens. Adapted from Deane et al. (2010).

Early substrates:	
Needle subunit	EscF
Inner rod subunit	EscI
Ruler protein	EscP
Substrate specificity switch	EscU
Middle substrates:	
Needle filament	EspA
Pore	EspD, EspB
Secretion apparatus components:	
Outer membrane ring (OM)	EscC
Inner membrane ring (IM)	EscD, EscJ
Export apparatus	EscR, EscS, EscT, EscU, EscV
ATPase	EscN
ATPase-associated protein	EscL, Orf4, EscQ
Regulator/gatekeeper	SepL
Chaperones	CesT (Tir), EspA (CesA), EscG, EscE
Late substrates (Effectors)	LEE encoded Tir, Map, EspB, EspF, EspG, EspH, EzpZ, and non-LEE encoded effectors.

1.3.4 Signal transduction and intimate attachment

Upon completion of the T3SS injectisome, one of the first effectors to be injected into host cells is the translocated intimin receptor (Tir) (Kenny et al, 1996). Following entry into host cells, Tir proteins insert themselves back into the apical membrane of host epithelial cells, where they act as receptors to interact with their own bacterial intimin (Fig.1.11). The N- and C-termini of the Tir protein are cytosolic, while the central portion, known as the intimin binding domain, forms a hairpin loop on the external surface of the host cell (Kenny et al, 1999; Luo et al, 2000). This hairpin loop binds bacterial intimin with high affinity, enabling an intimate attachment between the bacteria and the mammalian host cell (Devinney et al, 1999; Ross and Miller, 2007).

Intimin, encoded by the eae gene, is a 94-kDa protein that is found in all strains capable of inducing AE histopathology (Nataro & Kaper, 1998). Intimin binding causes Tir clustering inside the host cell, where host kinases phosphorylate Tir tyrosine (Y474) residues located within the C terminus (Kenny et al, 1997; Lai et al, 2013). Tir phosphorylation recruits Nck host adapter proteins that activate actin nucleation promoting factors such as N-Wiskott-Aldrich syndrome protein (N-WASP). This, in turn, activates the actin-related protein (Arp) 2/3 complex required for actin polymerization and pedestal formation (Gruenheid et al, 2001; Campellone et al, 2002; Miki & Takenawa, 2003).

Unlike EPEC, EHEC Tir is not tyrosine phosphorylated by the host cell, and the pedestal formation is Nck-independent (Fig.1.11). This type of actin assembly is promoted by another translocated EHEC effector, EspFU, also known as Tir cytoskeleton-coupling protein (TccP) (Campellone et al, 2004; Garmendia et al, 2004). EspFU is linked to Tir by host insulin receptor tyrosine kinase substrate (IRTKS) and interacts with N-WASP to activate the Arp2/3 complex for actin assembly (Weiss et al, 2009; Vingadassalom et al, 2009). Although Tir is essential for the formation of A/E lesions and bacterial colonisation of host gut surfaces *in vivo* (Deng et al, 2003; Vlisidou et al, 2006), the phosphorylation of Tir is dispensable for A/E lesion formation *ex vivo*, as a Tir phosphorylation mutant can still recruit N-WASP independently of Nck, activate the Arp 2/3 complex, form pedestals, and generate AE lesions (Schuller et al, 2007).

1.3.5 Pedestal formation

The Arp 2/3 complex contains two ATP-binding subunits (Arp2 and Arp3) that closely resemble an actin monomer and serve as the nucleation site for new actin filaments (Fig.1.11). The Arp 2/3 complex binds to the sides of existing ("mother") filaments and initiates growth of a new ("daughter") filament at a distinctive 70-degree angle from the mother filament through ATP hydrolysis. This generates the build-up of densely branched filamentous actin (F-actin) networks directly beneath where the bacteria is attached to the host cell (Campellone & Welch, 2010; Veltman & Insall, 2010; Smith et al, 2013). The growth of actin filaments pushes the cell membrane upward, and the bacterium becomes perched on a pedestal-like structure which may stand up to 10μm away from the epithelial cell surface (Kaper et al, 1998; Wales et al, 2004). These actin pedestal structures, which can act as localised signalling centres to coordinate bacterial modulation of host cell functions, are important virulence factors required for efficient colonisation of the host (Munera et al, 2012; Lai et al, 2013).

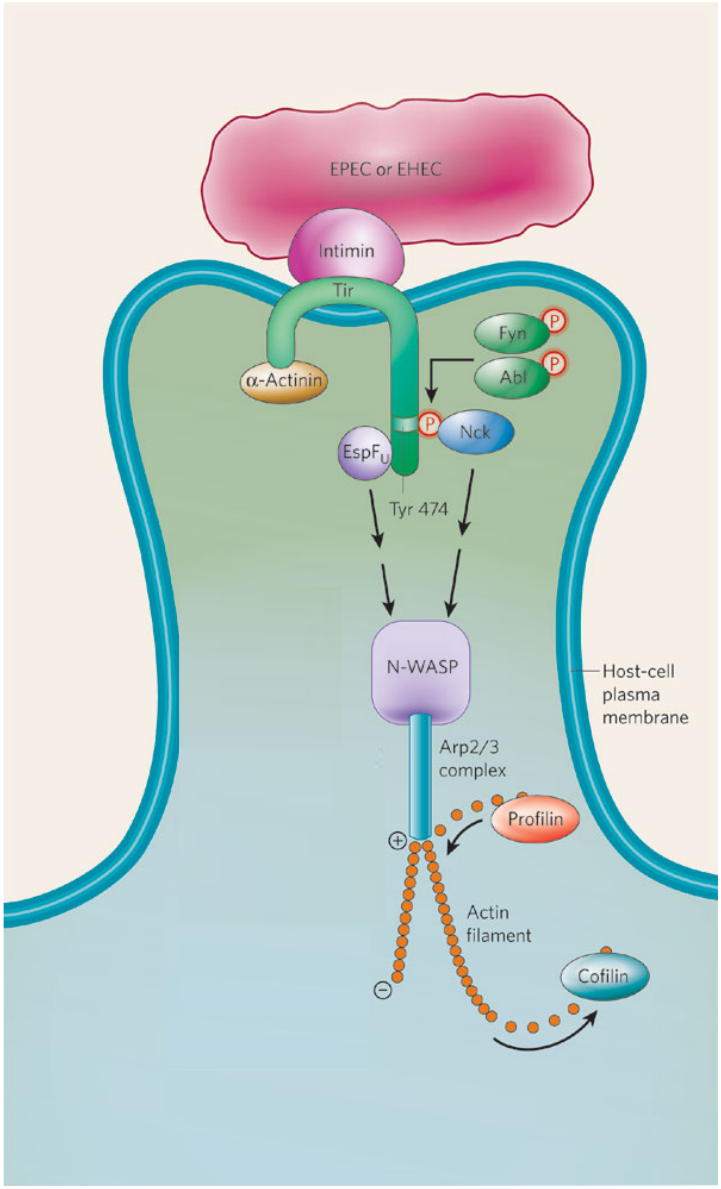

Figure 1.9: Molecular mechanisms of pedestal formation. In EPEC infection, the intimin receptor (Tir) translocates into the host cell and inserts itself into the host-cell plasma membrane. Tir interacts with intimin on the bacterial surface, firmly anchoring the bacterium to the host cell. The carboxy terminus of EPEC Tir becomes phosphorylated on the tyrosine residue at position 474, resulting in host adaptor protein Nck being recruited and binding directly to Tir. In EHEC infection, the tyrosine-phosphorylation event is fulfilled by the EHEC effector EspF$_u$, so Nck is not required. Subsequently, N-WASP and the Arp2/3 complex are recruited downstream of the Tir-interacting protein (Nck or EspF$_u$), leading to the generation of actin filaments beneath the attached bacteria and the formation of the pedestal structure. It has been demonstrated that the tight junction-associated protein ZO1 localises to the distal portion of the actin filaments of the EPEC pedestal. In addition, the actin-disassembly protein cofilin has been shown to localise to pedestals and, presumably, together with the actin-assembly protein profilin, regulates the actin-filament dynamics in pedestals. Taken from (Bhavsar et al. 2007).

1.3.6 Locus of Enterocyte Effacement (LEE)

The genes responsible for AE lesion formation are encoded on a 35.4kb pathogenicity island known as a LEE (Fig. 1.12) (reviewed in Schmidt 2010). The LEE sequence is different from the rest of the chromosomal DNA because it has a lower GC content (38%) than that of chromosomal DNA (50.8%) and has been associated with the ability to induce diarrheal disease (McDaniel et al, 1995). It is present in all AE pathogens and absent from non-pathogenic *E. coli*, for which transfer of the LEE into an avirulent strain, such as *E. coli k12* or commensal *E.coli*, is sufficient to confer the AE phenotype on the recipient (McDaniel & Kaper, 1997).

EPEC LEE contains approximately 41 open reading frames (ORFs) organised into 5 operons termed LEE 1-5 (Fig. 1.12). Together, LEE encodes the structural components of the T3SS apparatus, the effector proteins, chaperone proteins, and LEE regulator proteins (Sal-man et al, 2012b). The LEE genes encoding the structural proteins of the T3SS are highly conserved among all AE pathogens and is thought to have been acquired by horizontal gene transfer (Deng et al, 2001; Muller et al, 2009). The genes encoding the effector proteins, however, show substantial variability and may have been obtained by distinct genetic events (Castillo et al, 2005). In addition, the LEE is inserted into different chromosomal loci amongst the different AE pathogens, which suggests that the LEE may have been acquired more than once during bacterial evolution (Schmidt 2010). The role of LEE-encoded effector proteins in AE pathogens is summarised in Table 1.2.

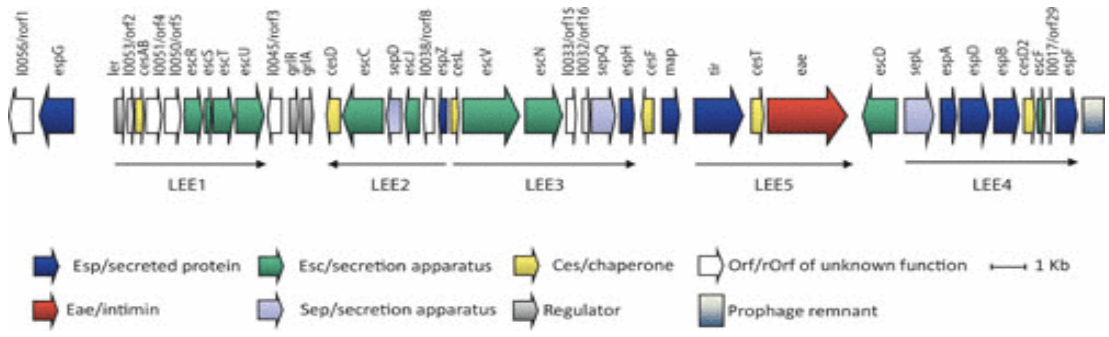

Figure 1.10: Genetic organisation of LEE genes in AE pathogens. LEE pathogenicity island of pathogenic *E. coli*. Taken from Stevens and Frankel (2014).

Table 1.2: Common LEE encoded effectors in AE pathogens and their role in host cells.

Effector	Role	Reference
Tir	Receptor for intimin. Nucleates and polymerises actin filaments. Involved in attaching effacing lesions. Regulates the functions of other effectors including Map, EspF and EspG. Inhibits NFκB activation. Initiates a strong host antibody response. Promotes T3 translocation and host cell binding.	Kenny et al, 1997 Garmendia et al, 2004 Ruchaud-Sparagano et al, 2011 Gavilanes-Parra et al, 2013 Battle et al, 2014
Map	Mediates tight junction disruption and microvilli effacement. Alters mitochondrial morphology and function. Interacts with Tir to activate processes that contribute to formation of membrane filopodia. Map expression contributes to the maintenance of EPEC colonisation.	Kenny & Jepson, 2000 Jepson et al, 2003 Papatheodorou et al, 2006 Molloy 2012 Nguyen et al, 2014
EspB (eaeB)	Component of the pore-forming translocator, essential for effector translocation into host cell. Promotes actin bundling, involved in microvilli effacement and inhibits macrophage phagocytosis. Oral immunisation with EspB induces specific mucosal and systemic antibody responses, implicating its use as an oral vaccine.	Donnenberg et al, 1993 Hamada et al, 2010, Hamaguchi et al, 2013 Ahmed et al, 2014
EspF	Mediates F-actin filament aggregation to form AE lesions and induce pedestal formation. Induces mitochondria-targeted apoptosis, inhibits macrophage phagocytosis, disrupts tight junctions and limits bacterial translocation through M cells. Stimulates the cleavage and loss of epidermal growth factor receptor in host epithelial cells resulting in host cell death later in infection.	McNamara & Donnenberg, 1998, Tahoun et al, 2011; Zhao et al, 2013 Maddocks et al, 2013 Roxas et al, 2014
EspG	Plays a minor role in epithelial barrier dysfunction. Interacts with tubulin to disrupt microtubule formation. Causes actin stress fibre formation. Localises to Golgi apparatus and disrupts protein secretion. Disrupts recycling endosome function and cell surface receptor levels during infection.	Elliot et al 2001 Selyunin et al, 2011 Clements et al, 2011 Clements et al, 2014 Glotfelty et al, 2014
EspH	Necessary for actin pedestal formation and elongation. Promotes recruitment of N-WASP and the Arp2/3 complex to the bacterial attachment site. Induces focal adhesion disassembly, triggers cell detachment, induces apoptosis and cytotoxicity. Inhibits macrophage phagocytosis.	Tu et al 2003; Wong et al, 2012a Wong et al, 2012b
EspZ	Blocks protein translocation of effectors (Tir, Map, EspF) following a secondary infection. Inhibits host cell apoptosis by localising to host mitochondria. Inhibits epidermal growth factor receptor cleavage and loss, which contributes to the survival of host cells early in infection.	Kanack et al 2005; Berger et al, 2012; Roxas et al, 2012 Shames et al, 2011 Roxas et al, 2014

1.3.7 Non–LEE encoded (Nle) effectors

The T3SS translocated proteins, which are not encoded by the LEE genes, are known as non-LEE encoded (Nle) effectors. First described in *C. rodentium,* Nle proteins are a topic of recent research (Deng et al, 2004; 2010). The Nle genes are carried on mobile genetic elements that are surrounded by phage-related and transposase-like genes. They are clustered in to six pathogenicity islands scattered throughout the genome (Fig. 1.13) (Dean et al, 2009). Like LEE, Nle pathogenicity islands have a low GC content and are thought to have been acquired through horizontal gene transfer. Unlike LEE encoded effectors, which are well conserved among AE pathogens, the Nle effectors vary. For instance, all AE pathogens contain over 40 LEE genes, while rabbit EPEC contains an additional 40 Nle effectors in comparison to EPEC/69 which contains an additional 21 Nle genes (Iguchi et al, 2009). The role of Nle effectors common to all AE pathogens is summarised in Table 1.3.

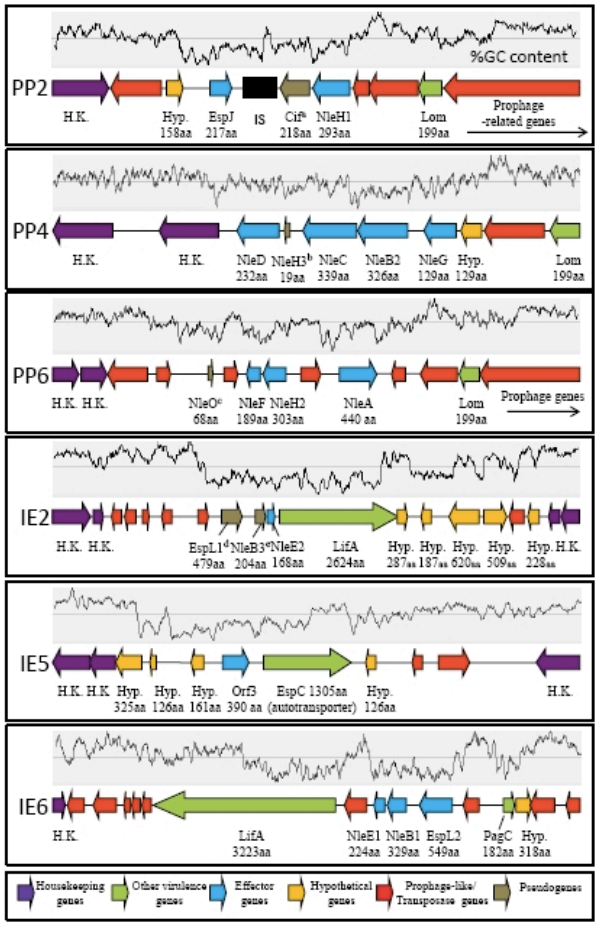

Figure 1.11: Genetic organisation of Non-LEE encoded genes in AE pathogens. Non-LEE pathogenicity islands of EPEC. Taken from Dean and Kenny (2009).

Table 1.3: Common Nle effectors in AE pathogens and their roles in host cells.

Effector	Role	Reference
NleA/ EspI	Disrupts tight junction and impairs cellular secretion. Mediates proteolytic cleavage and inactivation of host proteins during infection.	Gruenheid et al, 2004; Mundy et al, 2004; Thanabalasuriar et al, 2011 Weiss et al, 2014
NleB	Suppresses NFκB activation and antagonises death receptor induced apoptosis of infected cells. *C.rodentium* lacking NleB is unable to colonise mice.	Deng et al, 2004; Kelly et al, 2006; Gao et al, 2013; Pearson et al, 2013
NleC	Targets and cleaves NFκB transcription factors to dampen the host inflammatory response. Antagonises repression of IL-8 secretion. No role identified *in vivo*.	Deng et al, 2004; Marches et al, 2005; Sham et al,2011; Pearson et al, 2011 Turco & Sousa, 2014 Li et al, 2014
NleD	Inhibits NFκB activation. Contributes to bacterial inhibition of IL-8 *in vitro*. Displays pro-apoptotic activity. Plays a role in colonization of calves. Inhibits cytokines that regulate IEC tight junction proteins that are necessary to maintain barrier function and enhances TNFα production to promote barrier disruption.	Marches et al, 2005, Baruch et al, 2011 Long et al, 2014
NleE	Shuts off nuclear translocation of NFκB following translocation into intestinal DCs. This inhibits expression of proinflammatory cytokines. Can also bind to and interact with molecules involved in the DNA repair processes.	Wickham et al, 2007; Vossenkaemper et al, 2010; Nadler et al, 2010; Newton et al, 2010. Yao et al, 2014
NleF	Binds to and inhibits catalytic activity of host caspases, preventing apoptosis of cells *in vitro*. Slows down intracellular trafficking of proteins from the endoplasmic reticulum to the Golgi. Contributes to bacterial colonisation *in vivo*. Induces the NFκB mediated proinflammatory pathway and IL-8 expression early during EPEC infection.	Dean, 2011; Blasche et al, 2013; Olsen et al, 2013; Pallett et al, 2014
NleG/ NleI	NleG homologues make up the largest family of T3 effectors delivered by pathogenic *E. coli*. Inhibits apoptosis.	Deng et al, 2004; Tobe et al, 2006; Wu et al, 2010 Li et al., 2006b
NleH1 NleH2	Blocks apoptosis and has a role in post-translational regulation of effectors required for active secretion of effectors through the T3SS. NleH1 and NleH2 have high sequence similarity but are expressed differentially. NleH2 resembles the structure of protein kinases and NleH1 inhibits NFκB signalling. NleH deletion reduces *C. rodentium* colonisation and mice mortality, which can be reversed after complementation with NleH1. *C. rodentium* expressing EHEC NleH1 and NleH2 is hypervirulent in mice.	Garcia-Angulo et al, 2008; Gao et al, 2009 Hemarajani et al, 2010 Pham et al, 2012 Holmes et al, 2012 Halavaty et al, 2014 Feuerbacher & Hardwidge, 2014 Grishin et al, 2014
EspJ	Blocks phagocytosis of opsonised bacteria. Contributes to bacterial clearance in mice.	Dahan et al, 2005; Marches et al, 2008; Kurushima et al, 2010
EspL	Enhances F-actin bundling activity and formation of micro-colonies.	Dean & Kenny, 2009
EspO	Interacts with integrin linked kinase to reinforce host cell adherence to the basement membrane.	Dean & kenny, 2009 Deng et al, 2010

1.3.8 Effector targeting host defences

Like many disease-causing bacteria, a key feature of the virulence of AE pathogens is their ability to deliver effector proteins into eukaryotic cells via the T3SS. These T3SS effectors are virulence proteins that mimic eukaryotic proteins in structure and function. An important feature of bacterial effectors is their modular architecture, which comprises domains that have subversive functions inside the eukaryotic cell (Dean et al, 2011). These subversive functions include, the regulation of actin dynamics (previously discussed), inhibition of phagocytosis, modulation of the apoptotic pathway, and subversion of host inflammatory responses (Fig. 1.14) (reviewed in Vossenkamper et al, 2011; Wong et al, 2011; Clements et al, 2012; Raymond et al, 2013). By manipulating host cellular processes and protective mechanisms, these pathogens are able to facilitate their own survival and subsequently colonise, infect, and disseminate to additional hosts.

1.3.8.1 Apoptosis

One of the protective mechanisms of the gut mucosa is the removal of damaged or infected cells through programmed cell death, or apoptosis. Apoptosis is triggered by cell stress that stimulates pro-apoptotic signalling pathways, which activates caspase proteases and causes mitochondrial dysfunction. Apoptotic cells undergo characteristic changes in cell morphology, including chromatin condensation, nuclear fragmentation, cell rounding, and plasma membrane blebbing to eventually form apoptotic bodies that are engulfed by phagocytes (reviewed in Galluzzi et al, 2014).

The host apoptotic defence mechanisms can be averted by AE pathogens (Fig. 1.14), which, like other gram-negative bacteria, use T3S effectors to promote their own colonisation. The effector NleH, for example, is able to block apoptosis in infected epithelial cells by directly interacting with Bax inhibitor I, which is an anti-apoptotic protein (Hemrajani et al, 2010; 2008). The role of NleH to protect cells from the activation of the pro-death pathway is complemented by NleD, which suppresses the transcription factors required for activation of the pro-apoptotic proteins (Baruch et al, 2011). More recently, two additional effectors, NleF (Blasche et al, 2013) and NleB (Pearson et al, 2013), were shown to inhibit apoptosis by specifically binding to and inhibiting caspase activity and antagonising death receptor-induced apoptosis of infected cells, respectively.

Other anti-apoptotic effectors protect host cells from death by promoting cell survival mechanisms. This includes preventing epithelial cell detachment by stabilising intestinal cell adhesions to the extracellular matrix. For example, EspO binds to host integrin-linked kinase, while EspZ interacts with host protein CD98, both of which lead to increased cell adhesion and survival (Kim et al, 2009; Shames et al, 2010). Infection of cell monolayers with an EPEC mutant lacking EspZ resulted in strong cytotoxicity (Shames et al, 2010), while infection of mice with *C. rodentium* mutants lacking EspZ led to severe attenuation and reduced colonisation by *C. rodentium* (Deng et al, 2004). In summary, the combined activities of the anti-apoptotic effectors may stabilise the epithelium during bacterial colonisation and reduce the cytotoxic effects of bacterial infection, which in turn may promote sustained colonisation by these pathogens (Shames et al, 2010).

The anti-apoptotic activities of AE pathogens are antagonised by the translocation of pro-apoptotic effectors such as EspF and Cif (Fig. 1.14) (Raymond et al, 2013). EspF is targeted to the mitochondria, where it induces mitochondrial lysis and is involved in degradation of anti-apoptotic proteins that leads to an increase in caspase cleavage (Nougayrede & Donnenberg, 2004). In contrast, Cif acts mainly as a bacterial cyclomodulin and arrests cell cycle by stabilising cell cycle inhibitory proteins, thereby inducing a delayed form of apoptosis (Samba-Louaka et al, 2009). Other pro-apoptotic effectors include Map and EspH, which trigger mitochondrial dysfunction and induce caspase cleavage, respectively (Wong et al, 2011; Raymond et al, 2013)

1.3.8.2 Phagocytosis

Phagocytosis is the process by which a cell engulfs solid particles, including microorganisms or dead cells from the extracellular space. Once internalised, the engulfed particles are contained within a phagosome, which then fuses with the lysosomes for degradation. This leads to the clearance of the microorganism and initiation of adaptive immune responses. Professional phagocytes include neutrophils, macrophages, and dendritic cells, which can recognise bacteria directly or indirectly through recognition of antibody-coated bacteria and bacteria coated with complement receptors (Underhill & Goodridge, 2012).

Although there is no direct evidence that AE pathogens target professional phagocytes for effector translocation *in vivo*, recent data suggest that these pathogens

have the ability to paralyse the general phagocytic mechanism (Fig. 1.14). For example, the effector EspB targets myosin function, which is required for phagosome closure during phagocytosis of non-opsonised bacteria (Cox et al, 2002). An EPEC expressing EspB lacking the myosin-binding domain is unable to inhibit its own uptake by phagocytosis (Iizumi et al, 2007). EspF is another effector known for inhibiting the phagocytosis and translocation of bacteria through macrophages and an M-cell co-culture system, respectively (Quitard et al, 2006; Martinez-Argudo et al, 2007; Tahoun et al, 2011). EPEC lacking EspF and a functional T3SS are phagocytosed by macrophages and translocated through M cells (Quitard et al, 2006; Marches et al., 2008). Additionally, EspJ was recently shown to prevent phagocytosis of both IgG and complementary opsonized particles, although it could not prevent phagocytosis of non-opsonised bacteria (Marches et al., 2008). EspH is another newly characterised anti-phagocytic effector, without which EPEC loses its ability to inhibit both opsonized and non-opsonized phagocytosis (Dong et al, 2010; Marches et al, 2008).

By targeting multiple pathways for bacterial uptake, anti-phagocytic effectors cooperate to exclude AE pathogens from the intracellular environment of the professional phagocytes (Wong et al, 2011). As a result, these pathogens not only escape phagocyte killing but also prevent the generation of MHC peptides for antigen presentation by antigen presenting cells, which is necessary for the activation of adaptive immune responses. Although AE pathogens are unlikely to encounter professional phagocytes during their colonisation of epithelial cell surface, neutrophils were shown to be necessary for bacterial clearance in a *C. rodentium* model of mice infection (Spehlmann et al, 2011). In addition AE pathogens are known to preferentially adhere to the FAE of the gut, which contains M cells surrounded by professional phagocytes and antigen presenting cells. Such findings suggest that bacteria may interact with phagocytes at some point during infection.

1.3.8.3 Inflammation

The inflammatory response is initiated when host PRRs recognize PAMPs on the surfaces of microorganisms. This initiates host inflammatory cascades, including NFκB and MAPK pathways, which lead to the production of cytokines involved in the host inflammatory response. Central to the initiation of inflammation is the

transcription factor NFκB, which exists as inactive dimers bound to an inhibitor of NFκB (IκB) in the host cell cytoplasm. With the phosphorylation and degradation of IκB by the cell proteosome, NFκB is released and allowed to translocate to the nucleus, where it initiates the transcription of many proinflammatory cytokines, including IL8 (reviewed in Newton & Dixit, 2012).

Infection of host cells with AE pathogens results in the induction of an inflammatory cell response, mainly through the host recognition of bacterial flagella (Schuller et al, 2009). In addition, the translocation of EspT effector was shown to trigger the expression of proinflammatory genes (Raymond et al, 2011). However, in the presence of increasing bacterial burden, the production of proinflammatory cytokines such as IL8 is reduced, indicating that these pathogens have the ability to dampen host inflammatory responses in a type 3-dependent manner (Fig. 1.14) (Wong et al, 2011).

NleB, for example, was shown to inhibit the activation of NFκB in epithelial cell lines *in vitro* (Newton et al, 2010) and play an important role in the bacterial colonisation of mice (Kelly et al, 2006). Mice infected with *C. rodentium* containing a deletion in the *nleB* gene displayed reduced crypt hyperplasia and reduced colonisation of the gastrointestinal tract (Kelly et al, 2006). Similarly, NleE was also shown to inhibit NFκB subunits and cause a decrease in the expression and production of IL8 (Nadler et al, 2010; Newton et al, 2010; Vossenkamper et al, 2010). Although this was reported in epithelial cells by a number of studies, Vossenkamper et al (2010) was the first to show this in immune cells (dendritic cells). Both NleB and NleE were able to suppress the inflammatory pathway by inhibiting Ikb degradation and hence the nuclear translocation of NFκB subunits (Newton et al, 2010). Additionally, NleC and NleD were reported to downregulate the inflammatory responses by targeting NFκB subunits and MAPK proteins. NleC can cleave more than one NFκB subunit and block the subsequent production of IL8 following infection (Marches et al, 2005; Baruch et al, 2011; Pearson et al, 2011), while NleD specifically degrades MAPK proteins and contributes to the overall inhibition of IL8 secretion by infected cells.

The absence of genes encoding NleC, NleE, or NleD in a single EPEC mutant does not affect colonization of EPEC in calf, lamb, or mouse animal models (Marches et

al, 2005; Kelly et al, 2006), nor does it result in increased production of IL8 in the host (Baruch et al, 2011; Pearson 2011). However, infection with an EPEC NleEC double mutant (in comparison to a single mutant), nleBEC triple mutant (in comparison to a double mutant) or nleBECD quadruple mutant (in comparison to a triple mutant) results in significantly higher IL8 production (Baruch et al, 2011; Pearson et al, 2011). This demonstrates the functional redundancy of these effectors, which seem to work together simultaneously and contribute to the overall anti-inflammatory activities of the AE pathogens.

NleH effectors seem to have an uncertain role in the inflammatory responses, as NleH1 was shown to block the nuclear translocation of NFκB subunits, while NleH2 induced the expression of proteins required for the nuclear translocation of NFκB (Gao et al, 2009; Wan et al, 2011). However, the role of NleH in promoting colonization and modulating the host inflammatory response was clearly demonstrated in mice during subsequent studies. Mice infection with EPEC mutants lacking NleH1 and NleH2 led to a decrease in bacterial colonisation and an increase in the infiltration of neutrophils and keratinocyte cell levels (a mice homologue of IL8), in comparison to mice infection using wildtype EPEC (Royan et al, 2010). Lastly, Tir, most well-known for its role in pedestal formation, was also shown to inhibit host inflammatory responses and cytokine production in infected cells, since deletion of Tir enhanced the activation of MAPK proteins during EPEC infection (Yan et al, 2012).

By inhibiting proinflammatory responses, these AE pathogens effectively reduce the secretion of cytokines and chemokines that facilitate leukocyte extravasation from the circulation to the affected site. Leukocytes, mainly neutrophils and macrophages, are able to kill bacteria directly or secrete antimicrobial factors (Newton & Dixit, 2012). Therefore, by preventing the recruitment of these cells during infection, AE pathogens are able to subvert innate immune responses that may allow prolonged survival in the host gut (Vossenkamper et al, 2011).

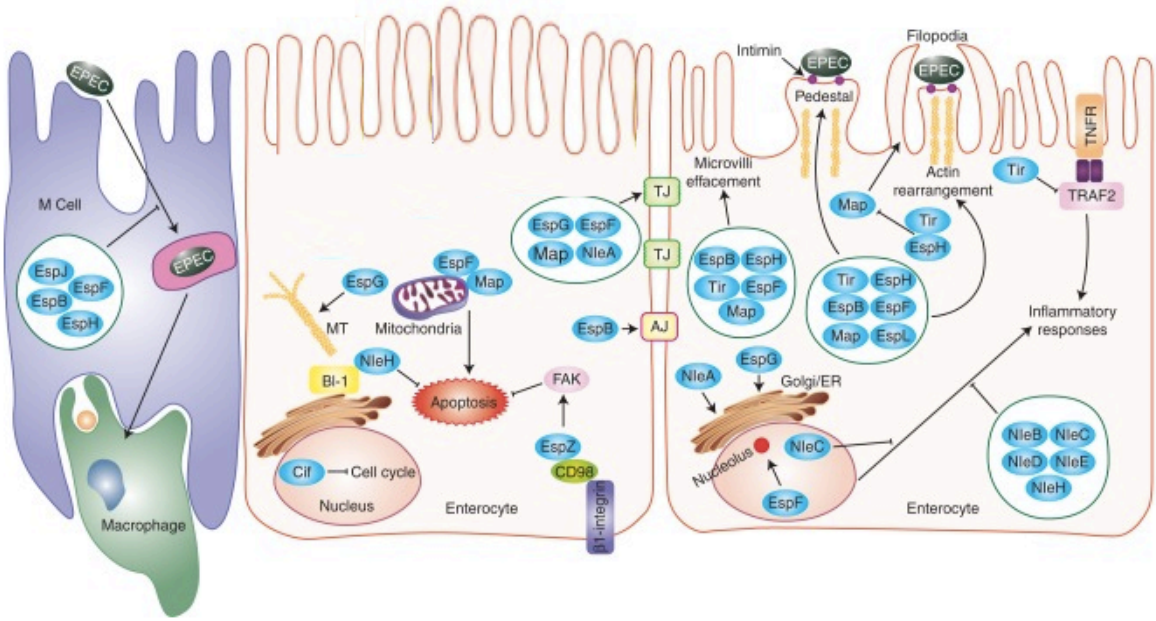

Figure 1.12: Common T3SS effectors of AE pathogens and their targets within host cells. Effectors from AE pathogens target sub- cellular structures and organelles in the host cell including TJ (tight junction), AJ (adherens junction), ER (endoplasmic reticulum), MT (microtubules), FAK (focal adhesion kinase), BI-I (BAX inhibitor-1), TNFR (tumour necrosis factor receptor), TRAF2 (TNF-associated factor 2). The figure depicts the multifunctional nature of the effectors and their overlapping functions, adapted from Law et al. (2013).

Table 1.4: Host cells targeted for effector injection and subsequent cellular modulation by AE pathogens (summarized).

Effector	Target cell	Host modulation
Tir	Epithelial cells	Modulates actin cytoskeleton, blocks MAPK signaling, inhibits NFκB activation
Map	Epithelial cells	Modulates actin cytoskeleton
Cif	Epithelial cells	Blocks cell cycle
EspZ	Epithelial cells	Prevents cell detachment
NleB	Epithelial cells	Inhibits NFκB activation, blocks apoptosis of infected cells
NleC	Epithelial cells	Inhibits NFκB activation, induces IL8 secretion
NleD	Epithelial cells	Delays apoptosis, inhibits MAPK pathway, inhibits IL8 production
NleF	Epithelial cells	Delays or inhibits apoptosis and disrupts intracellular trafficking
NleH	Epithelial cells	Blocks apoptosis, inhibits NFκB activation
NleE	Epithelial cells, Dendritic cells	Inhibits activation of NFκB and production of inflammatory cytokines
EspT	Epithelial cells, macrophages	Modulates actin cytoskeleton, induces production of IL8 and IL1b
EspF	M cells, macrophages	Inhibits M cell uptake of bacteria and prevents phagocytosis in macrophages
EspB	Macrophages	Prevents phagocytosis of bacteria
EspJ	Macrophages	Blocks FcyR and CR3 opsonophagocytosis
EspH	Macrophages	Inhibits FcyR opsonophagocytosis, induces apoptosis

1.4 Concluding remarks

By injecting effectors into host cells, AE pathogens not only (1) alter the host cytoskeleton for secure attachment to epithelial cells, but also dampen the host immune responses by (2) preventing their uptake by phagocytes, (3) inhibiting apoptosis, and (4) suppressing proinflammatory signalling pathways. The ability to antagonise and subvert host immune responses is a central feature of many enteropathogens. Despite the variation in bacterial morphology and infection strategies, T3SS-containing pathogens including EPEC, EHEC, *Citrobacter, Salmonella, Shigella*, and *Yersinia* show a high degree of homology between the effectors they translocate

Although these translocated effectors often act in concert with each other, their functions can sometimes seem contradictory. The apparent contradiction can be resolved if effector injection occurs at different time points during bacterial pathogenesis according to the specific survival needs of and/or virulence strategy required by the pathogen at that time. Attaching effacing bacteria, for example, initially inject effectors such as EspT into host cells, which trigger host innate inflammatory responses including the release of proinflammatory cytokines IL-8 and IL-1β following the activation of the NFκB pathway. However, the resulting proinflammatory responses are unlikely to kill the AE pathogens, and instead may disrupt and remove the competing commensal microbiota (Lupp et al, 2007). This may give the AE pathogens a survival advantage over the commensal bacteria, enabling them to colonise the host gastrointestinal tract. Subsequently, the AE pathogens inject anti-inflammatory effectors that suppress different components of the NFκB and MAPK pathway, inhibiting host inflammatory responses against themselves. Bacterial anti-inflammatory effectors therefore limit the effectiveness of the host resistance mechanisms directed against the AE pathogens to facilitate their own survival.

A similar phenomenon is seen in invasive *Salmonella*, where the injection of proteins occurs in two stages. During the initial stage of infection, *S. enterica* injects effectors using the *Salmonella* pathogenicity island 1 (SPI-1) to facilitate its invasion of the intestinal epithelial cells (Coburn et al, 2007). This results in host macrophages migrating to the site of infection and engulfing bacteria in an attempt to destroy it through the production of reactive oxygen species such as nitrogen oxides (Swindle

& Metclife, 2007). However, the intracellular environment of the macrophage induces the expression of a second wave of effector injection from *Salmonella* pathogenicity island 2 (SPI-2) that enables the bacteria to create protected vacuoles termed *Salmonella* containing vacuoles (SCVs) within which *Salmonella* can grow and multiply (McGourty et al, 2012). Similarly, the inhibition of apoptosis in epithelial cells (AvrA from SPI-1) may be beneficial for promoting sustained colonisation of *Salmonella* initially, while the subsequent induction of pyroptosis in macrophages (SipB from SPI-2) may facilitate dissemination of *Salmonella* (Stavrinides et al, 2008; Raymond et al 2013). Thus, although the immune responses initiated by SPI-1 effectors are very different from those initiated by SPI-2, both are employed by *Salmonella* to facilitate its survival and spread in the host epithelium. Due to this, it is believed that the interactions between the T3S effectors and their host cells may have resulted in the co-evolution of survival strategies by both the pathogen and the host.

In summary**,** the manipulation of host immune responses by AE pathogens has not been reported until recently. Perhaps this is due to the non-invasive nature of these pathogens, which, unlike their invasive counterparts, colonise the surface of the epithelial cells and are thought not to encounter immune cells. However, recent reports of the ability of AE pathogens to inhibit apoptosis, prevent phagocytosis, and suppress host inflammatory pathways in a type three-dependent manner has shed new light on the possibility that immune cells may be targeted for effector translocation by these pathogens.

Since AE pathogens colonise the surface of lymphoid structures (described in detail in chapter 5), such as the PP and the caecal patches, there is a possibility that these pathogens may exploit the M cell gateway to enter the subepithelial dome, where they may encounter professional APCs and other immune cells. In addition, subepithelial DCs send processes through the epithelium and into the gut lumen, during which the DCs may have some contact with luminal pathogens. Furthermore, intraepithelial T lymphocytes residing between the epithelial cells are another population of immune cells that may be encountered by these AE pathogens. Innate cells such as neutrophils, monocytes, and macrophages may be exposed to these gut pathogens during the leukocyte extravasation process as a result of inflammation occurring in response to bacterial infection. Additionally, the disruption of tight

junctions and the loss of barrier properties in the gut epithelium during AE infection may result in a "leaky gut", enabling increased translocation of bacteria through the epithelial barrier and resulting in increased interaction between bacteria and immune cells. Following interaction with bacteria, these immune cells may be targeted for effector injection. The injected immune cells may subsequently drain to the MLN and spleen, where they may be impaired from generating protective immune responses.

To gain more insight into the consequences of bacterial effector injection on host immune cells, it would be interesting to visualise which host cells are being targeted for effector delivery and at which stage of the infection these cells are being targeted. Several different reporter systems have been previously utilised to detect the translocation of effector proteins inside eukaryotic cells. One of the first reporter systems developed was adenylate cyclase (CyaA) toxin of *Bordetella pertussis* (reviewed in Dautin et al, 2004). Sory and Cornelis (1994) created translational fusions of Yops (*Yersinia* outer membrane proteins) with the calmodulin-dependent catalytic domain of CyaA to study the *Yersinia enterocolitica* T3S pathway. CyaA is able to convert cellular ATP to cyclic AMP (cAMP) in the presence of the eukaryotic protein calmodulin, which is not produced in bacteria. So by monitoring cyclic AMP (cAMP) accumulation in eukaryotic cells, they were able to detect the translocation of Yops into host cells. Although extensively used, this reporter system has some drawbacks. The CyaA assay is time consuming and some pathogenic bacteria produce toxins that can synthesize cAMP, such as ExoY toxin from *Pseudomonas aeruginosa*, leading to an increase in cellular cAMP that could mask the increase of cAMP converted by the CyaA fusion.

Another method to detect the translocation of effector proteins inside eukaryotic cells involves the use of a phosphorylatable Elk tag (Day et al, 2003). The translocation of an ELK-tagged effector protein into a eukaryotic cell results in host cell protein kinase-dependant phosphorylation of the ELK tag, which can be subsequently detected by Western blotting with phosphospecific Elk antibodies. The ELK tag has been utilized to study the injection of T3S effector proteins by *Yersinia pestis* (Day et al, 2003), *Yersinia pseudotuberculosis* (Rosenzweig et al, 2005), and *Salmonella enterica* (Day et al, 2003). This system is specific since it relies on cellular processes to detect proteins that are specifically injected into the host cells. However, the Elk

tag needs to be artificially directed to the host nucleus for phosphorylation through fusion with a nuclear localization signal from a simian virus 40 antigen, and this is a major limitation for the study of many effectors which are naturally targeted to other compartments of the host cell, such as the mitochondria (Map), the plasma membrane (Tir), or the Golgi apparatus (NleA).

Lee et al. (1998) developed an alternative strategy based on cell fractionation that selectively solubilised the eukaryotic plasma membrane with digitonin to measure Yop targeting during *Yersinia* infections of HeLa cells by immunoblotting. Neomycin phosphotransferase (NPT) fusions to Yops using the fractionation assay further enabled the presence of Yop-NPT fusions in the cytosol of HeLa cells to be visualised with anti-NPT staining and immunofluorescence confocal laser microscopy. However, the requirement for disruption of the eukaryotic cell is a major limitation of this strategy.

In contrast, recent studies have demonstrated the use of a novel fluorescence-based reporter system involving the TEM-1 β-lactamase enzyme (Described in detail in chapter 4) (Charpentier & Oswald, 2004). TEM-1 β-lactamase lacks a leader peptide sequence for export, which means it can only enter host cells if fused to a secreted protein such as a translocated effector protein. Studies have shown that fusing this enzyme to the ends of T3 effectors did not affect their activity (Charpentier & Oswald, 2004). Following translocation of the fusion proteins into host cells, TEM-1 β-lactamase activity can be measured directly by the addition of the fluorescent substrate CCF2-AM. In the presence of TEM-1 β-lactamase enzyme, the CCF2-AM substrate molecule is cleaved, causing the host cell to appear blue under UV illumination, whereas in the absence of the enzyme the CCF2-AM substrate remains intact, causing the host cell to appear green. The major advantage of this reporter system is its use of the CCF2-AM fluorescent substrates, which enables the analysis of effector translocation in live cells without disruption of the host cell. Therefore, the TEM-1 β-lactamase reporter system was chosen to be used in this study to enable the visualisation of effector translocation into mouse cells by *Citrobacter rodentium*.

1.5 Objectives

In this study, the TEM-1 β-lactamase reporter system will be utilised to visualise host intestinal cells targeted for protein translocation by *C. rodentium*.

The aims of this study are to:

- generate a reporter *C. rodentium* strain that encodes a fusion protein between an effector and TEM-1 β-lactamase (Chapter 3);
- visualise effector translocation into murine cell lines and primary immune cells *in vitro* using TEM-1 β-lactamase translocation assay (Chapter 4); and
- visualise effector translocation into murine cells *in vivo* using TEM-1 β-lactamase translocation assay (Chapter 5)

Chapter 2: Materials and Methods

2.1 Bacteria

2.1.1 Bacterial strains

2.1.2 Bacterial media & growth conditions

2.2 Molecular cloning

2.2.1 Polymerase chain reaction (PCR)

2.2.2 DpnI digestion

2.2.3 PCR purification

2.2.4 Gel purification

2.2.5 DNA gel extraction

2.2.6 Plasmid preparation

2.2.7 DNA restriction digestion

2.2.8 Dephosphorylation

2.2.9 Ligation

2.2.10 Transformation (Heat chock)

2.2.11 DNA sequencing

2.3 TOPO TA cloning

2.4 CloneJET PCR cloning

2.5 Lambda (λ) Red mediated recombination

2.5.1 Electrocompetent cells

2.5.2 Electroporation

2.6 Mammalian cell culture

2.6.1 Mammalian cell lines

2.6.2 Growing & harvesting cells

2.6.3 Isolation of intestinal cells

2.6.3.1 Spleen and MLN

2.6.3.2 PP

2.6.3.3 Colonic epithelial cells

2.6.4 Cell count

2.6.5 Microscopy

2.2.2 Flow cytometry

2. Materials and Methods

2.1 Bacteria

2.1.1 Bacterial strains

Formerly known as *Citrobacter freundii* biotype 4280 (ATCC 51459) (Barthold et al, 1976), ICC169 *Citrobacter rodentium* is a nalidixic acid resistant derivative of strain ICC168 and was kindly provided by Dr. S. Wiles for this study (Division of Cell and Molecular Biology, Imperial College, London). The strain *Citro* pKD46, containing a λ Red expression system, was used for the homologous recombination of linear DNA into *C. rodentium* chromosome. TOP10 chemically competent *E. coli* cells (Invitrogen, UK) was used for the routine propagation of cloning plasmids.

Table 2.1: Strains and plasmids used in this study

Strain name	**Strain description**	**Reference**
Citrobacter rodentium (ICC169)	Wild type *C. rodentium*, Nal^r	Wiles et al., 2004
Citro pKD46	ICC169 encoding the λ-red expression system, Nal^r, Amp^r	This study
Citro pCX*nleD*	ICC169 containing pCXnleD plasmid, Nal^r,Tet^r	This study
Citro ΔescN	ICC169 containing escN deletion, Nal^r, kan^r	This study
Citro ΔescNpCXnleD	ICC169 containing escN deletion and pCXnleD plasmid, Nal^r,Tet^r, kan^r	This study
Citro pACYCnleD	ICC169 containing pACYCnleD plasmid, Nal^r, Cm^r	This study
Citro ΔescNpACYCnleD	ICC169 containing escN deletion and pACYCnleD plasmid, Nal^r, Cm^r, Kan^r	This study
Top 10 *E. coli* cells	Chemically competent *E. coli* cells for plasmid propagation, Amp^r	Invitrogen
Plasmid name	**Plasmid description**	**Reference**
pKD46	Plasmid encoding the λ-red expression system, Amp^r	Dr. Marches
pCX340	Expression vector encodingTEM-1, Tet^r	Charpentier & Oswald, 2004
pSB315	Expression vector encoding Kan^r	Dr. Marches
pCR2.1 TOPO	Expression vector for TA cloning, Amp^r , Kan^r	Invitrogen
pCX315	pCX340 plasmid encoding Kan^r, Tet^r	This study
pCX315nleD	pCX315 plasmid encoding NleD. Tet^r , Kan^r	This study
pCXnleD	pCX340 plasmid encoding NleD. Tet^r	This study
pACYC184	Expression vector, Cm^r , Tet^r	Dr. Marches
pICC440	pACYC184 containing 5' and 3' regions of *xylE*. Cm^r Tet^r	Girard et al., 2009
pICC442	pICC440 encoding nleDTEM-1 fusion constructs, Cm^r , Tet^r	This study
pACYCnleD	pACYC184 encoding nleDTEM-1 fusion constructs, Cm^r , Tet^r	This study

2.1.2 Bacterial media & growth conditions

All bacteria were grown aerobically in solid agar or liquid broth in Luria-Bertani (LB) medium. The solid agar was prepared by dissolving 35g of Lennox LB agar powder (15g/L Agar, 10g/LTryptone, 5g/L Yeast extract, 5g/L NaCl from Sigma-Alderich, uk) in 1 litre of distilled water and autoclaved. Antibiotics were added to the liquid agar as required (Listed in table 2.2) and poured into standard 90mm x 15mm triple vent petri dishes (Sterillin). The liquid broth was prepared by autoclaving 25g of Miller LB broth powder (tryptone, yeast extract and sodium chloride from Sigma-Alderich, uk) dissolved in 1 litre of distilled water. For growth on solid medium, agar plates containing the appropriate antibiotics were streaked with freshly isolated colonies, frozen beads (-80C) or overnight broth cultures and incubated in a static incubator at 37˚C overnight. For liquid cultures, 3ml LB broth containing 3µl of the corresponding antibiotic was inoculated with a freshly isolated colony or a frozen bead and grown in a 37°C orbital shaker at 200 rpm overnight. For long-term storage of bacterial cells in -80°C, 750 µl of an overnight liquid culture was added to a cryovial containing cryobeads and vigorously mixed. The liquid was then decanted and the cryovial containing bacteria-coated-cryobeads stored in -80°C.

Table 2.2: Antibiotics used for the selective growth of bacteria

Antibiotic	**Final concentration (µg/ml)**	**Source**
Nalidixic Acid (NA)	30	Sigma-Aldrich, UK
Ampicillin (Amp)	100	
Tetracycline (Tet)	12.5	
Kanamycin (Kan)	50	
Chloramphenicol (Cm)	25	

2.2 Molecular cloning

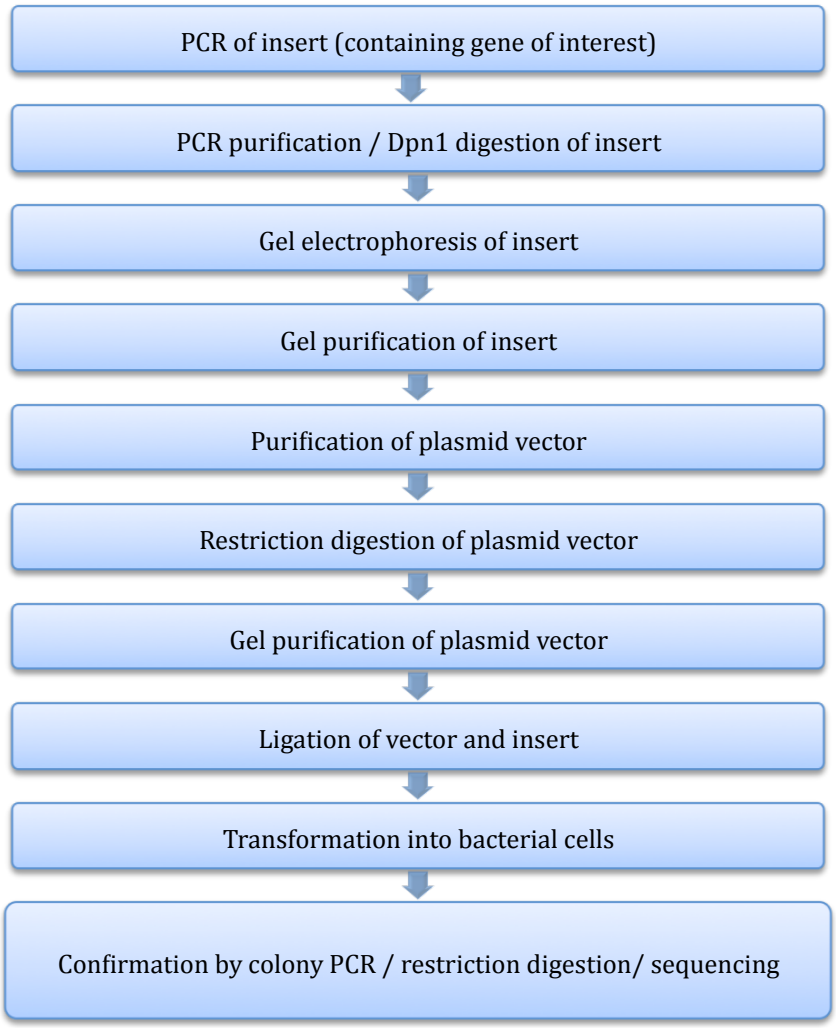

Figure 2.1: Overview of molecular cloning used in this study.

2.2.1 Polymerase chain reaction (PCR)

To amplify the gene of interest, PCR was carried out using the correct primer pairs (listed in Table 2.4). Primers were designed using the DNAssist software, synthesised by Eurofins Genomics and supplied at a concentration of 100µm. A typical PCR reaction mix (Table 2.3) contained 0.75µl of the DNA template (genomic or plasmid DNA), 5µl of 10X Taq buffer (NEB), 5 µl of dNTP mix (5mM/µl per dNTP, NEB), 5 µl of each primer (10Þm/µl), 0.3µl of Taq polymerase (NEB) in 50µl total volume (made up by 28.95µl dH_2O). A typical PCR programme comprised of an initial denaturation at 97°C for 3 min, 30 cycles of 45seconds at 94°C, 45 seconds at 58-75 °C, 2 minutes at 72 °C in each cycle and a final extension at 72°C for 10 minutes. Annealing temperatures varied according to the primer sets (typically between 58-75°C). Colony PCR was carried out using the same PCR programme but with a smaller reaction volume (25µl) and a single bacterial colony. A typical thermocycling programme used in this study is shown below.

Initial denaturation	97°C	3 minutes
Denaturation	94 °C	45 seconds
Annealing temperature (Tm)	58 -75 °C	45 seconds
Extension	72 °C	2 minutes
Final extension	72 °C	10 minutes
Hold	4 °C	until use

30x cycle

Table 2.3: Reaction components for PCR

Component	Volume (µl) to add in a single reaction mix		Final concentration
	Normal PCR	Colony PCR	
Total	50	25	
dH2O	28.95	14.35	
dNTP (5mM/µl)	5	2.5	0.5mM
ThermoPol Buffer (10x)	5	2.5	1x
Primer (fw) 10pM/µl	5	2.5	1pM/µl
Primer (rv) 10pM/µl	5	2.5	1pM/µl
Template DNA	0.75	colony	
Taq polymerase	0.3	0.15	

Table 2.4: Primers used in this study

Gene or DNA region amplified	Primer names	Nucleotide sequence 5'-3' (restriction sites shown in bold)
TEM-1 in pCX340	pCX340(fw)	TCAGGCAACTATGGATGAACG
	pCX340(rv)	GAGCTGACTGGGTTGAAGGCT
	pCX340endTEM(fw)	TCAGGCAACTATGGATGAACG
	pCX340endTEM(rv)	GAGCTGACTGGGTTGAAGGCT
Kn315 (Kanamycine^R) in pSB315	Kn315(fw)	ATGCGCTTCTCGCAAGCAGCGGTG
	Kn315 (rv)	GAAAAGTTGCTTATACTACAA
	Xba1-kn315(fw)	GC**TCTAGA**CACGTTGTGTCTCAAAATCT
	Sal1-kn315(rv)	AGC**GTCGAC**GAATTCCCCGGATCCGTCGA
Effector-TEMkn315 in *C.rodentium*	Tir-TEMkn315(fw)	CAGGGAGCGCTGCGAATGCCGCTACAACACCGGG AGTTGAACGTTTCGTCGGAAGCTTGGGTACCTCCG CGGAG
	Tir-TEMkn315(rv)	GAAACATTGACATACTCCCCCTCCCCCCCAACAAA ATACCCATTATATATGTCGACCTGCAGATTAGAAA AAC
	nleD-TEMkn315(fw)	ACAATACAGTGACTCAGGGATTCCAGCGGAAAAA ACTGCATCCGTTACTTCACCCAGAAACGCTGGTGA AAG
	nleD-TEM kn315(rv)	AGCGATTTTTCATCCATATATGCAGATGAGTCCTC ATATAAGCAACGTAGGTCGACCTGCAGATTAGAA AAACT
nleD in *C. rodentium*	Nde1-NleD(fw)	GAATAA**CATATG**CGCCCTACATCCCTT
	EcoRI- NleD(rv)	C**GAAATTC**TCAAGTAACGGATGCAGTTTTTTC
nleDTEM in pCXnleD	NleD-rbs-EcoRV(fw)	ACC**GATATC**AAGAAGGAGATATACCATGCGCCCT ACATCCCTTAACCTGACATTA
	BamH1-stop-TEM1(rv)	CGC**GGATCC**TTACCAATGCTTAATCAGTGAGGCA CCTATCTCA
escN in *C. rodentium*	escNFRT (fw)	ATGATTTCAGAGCATAATTCTATGTTGGAAAGATA CCCACGTATCCAGAATGTGTAGGCTGGAGCTGCTT CG
	escNFRT (rv)	TCAGGCAACCACTTTGAATAGATTTTCAATCGTTT TTTCATAACTACTGACATATGAATATCCTCCTTAG
	B171DescN(fw)	CGTCATTCTGACCGCTTTAG
Kanamycine^R in pKD4	K1 (fw)	AGGCTATTCGGCTATGACTG
	K2 (rv)	AATCGGGAGCGGCGATACCGT
xylE in pICC440 and pICC442	pACYCtc(fw)	CATCCTCGGCACCGTCACCCTGGA
	pACYCtc(rv)	GTGATGTCGGCGCGATATAGGCGCCA
	XmnI-C-XylE(fw)	CCC**GAACTGTTTC**CCGTCTTTCAGCAGTTTGTCG
	AseI-N-XylE (rv)	CCC**ATTAAT**ACGCAGTACACCAGCAGCTG
Insert region in pCR2.1TOPO	M13 (fw)	GTAAAACGACGGCCAGT
	M13 (rv)	CAGGAAACAGCTATGAC.
	T7	TAATACGACTCACTATAGGG
Insert region in pJET1.2	pJET1.2 (fw)	CGACTCACTATAGGGAGAGCGGC
	pJET1.2 (rv)	AAGAACATCGATTTTCCATGGCAG

2.2.2 DpnI digestion

Following the completion of PCR cycle, any remaining template plasmid was removed by DpnI digestion. Dpn1 cleaves off and removes methylated sites which are only present in the template plasmid and not in the PCR product. For Dpn1 digestion, 2µl of Dpn1 (NEB) was added to a 50µl reaction and incubated at 37°C for 1 hour (Table 2.5). The PCR products were then separated on an agarose gel, gel purified and stored at -20°C until use.

Table 2.5: Reaction components for Dpn1 digestion

Component	**Volume (µl)**	
PCR product	200	Incubate for 1 hour at 37°C
Dpn1 buffer	25	
Dpn1	1	
H2O	24	
Total	250	

2.2.3 PCR purification

Purification of the PCR products was carried out using a commercially available QIAquick PCR purification kit (Qiagen) according to the manufacturers instructions. To bind the DNA, Buffer PB was added to the PCR reaction and passed through a QIAquick column by centrifugation at 16000 x g for 1 minute using a bench top centrifuge (Heraeus Fresco 17, Thermoscientific). To wash the DNA, 0.75ml buffer PE, which contains ethanol, was added to the QIAquick column and centrifuged at 16000 x g for 1 minute. The residual wash buffer was subsequently removed by quick centrifugation, before eluting the DNA using 50 µl of dH2O. The resulting purified PCR product was kept on ice until further use, including the electroporation of PCR products into bacterial cells.

2.2.4 Gel electrophoresis:

DNA was analysed by electrophoresis in 0.7% agarose gels. This was made by dissolving 700mg molecular biology grade agarose powder (Melford labs) into 100ml of 1x Tris-acetate-EDTA (TAE) and melting it. The TAE buffer was made using 242g Tris base, 57.1 ml glacial acetic acid and 100 ml 0.5 M EDTA (pH 8.0) per litre of distilled water and diluted 1 in 50 for working concentration. Once the

agar had cooled but not set, 5µl of ethidium bromide (100ng/ml from VWR) was added. The agar was then poured into pre-made moulds containing combs of the required size (Biorad) and once set, submerged in to TAE buffer in a Biorad electrophoresis tank. DNA samples were mixed with DNA loading buffer (6x blue loading dye: 0.25% bromophenol blue, 0.25% xylene cyanol FF, 30% glycerol in dH2O, from NEB) of which, 5µl was added to each well. To determine the size and quantity of the DNA bands, -2 log kb DNA ladder (NEB) was added to the left most lane. Gels were typically run at 100 volts for 45 minutes. DNA bands were visualised using a UV-transluminator and analysed using the GeneSnap software.

2.2.5 DNA Gel extraction

DNA extraction was carried out using a gel extraction kit (Qiagen) according to the manufacturer's instruction. In summary, a slice of the agarose gel containing the DNA band was cut out using a sterilised scalpel under UV light. The gel pieces were dissolved in buffer QG and incubated in a 50°C water bath for approximately 10 minutes. Once the gel dissolved, it was pipetted into the spin columns and centrifuged at 16000 x g for 1 minute. The spin column containing the bound DNA was then washed with 1ml buffer QG to remove any residual agarose. The DNA was further washed with buffer PE, which contained ethanol to remove the salt. With 20µl of distilled water, the DNA was eluted out from the column and stored at 4°C or -20°C depending on its subsequent use.

2.2.6 Plasmid preparation

Plasmid DNA was obtained from bacterial cells using the commercially available miniprep kits following the manufacturer's instructions (Qiagen). Three ml of overnight cultures were centrifuged at 3000 x g for 10 minutes at 4°C. The resulting palette was resuspended in 250µl of buffer P1. A further 250µl of buffer P2 was added to the sample and thoroughly mixed before incubating at room temperature for 5 minutes. For neutralisation, 350µl of buffer N3 was added and thoroughly mixed. The resulting solution was centrifuged at 16000 x g for 10mins after which the supernatant was put into the spin column for a further 1 minute spin in the centrifuge. The plasmid DNA was washed with 70 µl of buffer PE and eluted with 50µl of distilled water.

2.2.7 DNA restriction digestion

Restriction digestion of plasmid DNA was completed using 10µl of DNA (approx. 0.5-1 µg), 5µl of 10X buffer and 1µl of each restriction enzyme in a final reaction volume of 50µl (made up by dH_2O). Samples were incubated in a 37 ^oC water bath for 2 hours and the resulting degests were confirmed by gel eletrophoresis. Restriction enzymes are listed in Table 2.7.

Table 2.6: Reaction components for Restriction digestion

Component	**Volume (µl)**		
DNA	10 (0.5 – 1 µg)	3	Incubate@ 37°C 2hours
10X buffer	5	2	
Restriction enzyme I	1	0.5	
Restriction enzyme II	1	0.5	
dH_2O	33	14	
Total	50	20	

Table 2.7: Enzymes used for restriction digestion

Enzyme	**Buffer used**	**Source**
Xba1	Buffer 4	NEB, UK
Sal1	Buffer 3	
Nde1	Buffer 4	
EcoRI	EcoRI buffer	
BamHI	Buffer 2	

2.2.8 Dephosphorylation

Following restriction digestion, the open plasmids were dephosphorylated by alkaline phosphatase to remove any phosphate groups from the 5'end of the cut DNA to prevent self-ligation. Dephosphorylation was only necessary in the case where plasmids were digested by a single enzyme or by two enzymes with compatible ends. For dephosphorylation, 50µl of digested plasmid was mixed with 1µl of alkaline phosphatase in 5µl of phosphate buffer and incubated at 37˚C for 1 hour. Enzyme activity was subsequently stopped by heat inactivation at 65˚C.

Table 2.8: Reaction components for dephosphorylation

Component	Volume	
Digested plasmid	50µl	Incubated for 1 hour at 37˚C and heat inactivated for 5 minutes at 65˚C prior to Ligation.
Antarctic phosphate buffer	5 µl	
Antarctic alkaline phosphatase	1µl	
Total	56 µl	

2.2.9 Ligation:

In a 20µl reaction volume, insert and vector were added at a quantitative ratio of 3:1, 1µl of T4 DNA ligase, 2µl of buffer (10x) and the required volume of distilled water (Table 2.9). The ligation mixture was left at 16°C overnight and heat inactivated at 65°C for 5 minutes to remove any remaining enzyme activity before transformation.

Table 2.9: Reaction components for Ligation

Component	Volume (µl)	
Insert	9 (3:1)	Leave O/N at 16°C and heat inactivated at 65°C for 5 minutes prior to transformation.
Vector	3 (1:3)	
T4 DNA ligase	1	
10x buffer	2	
Water	5	
Total	20	

2.2.10 Heat shock transformation

A vial of chemically competent TOP 10 cells was transformed with 5µl of ligated plasmids before leaving on ice for 30 minutes. The cells were subsequently heat shocked in a water bath at 42°C for 45 seconds and transferred back onto ice for 5 minutes. The cells were mixed with 600µl of super optimal broth with catabolite repression (SOC: 20g/L tryptone, 5g/L yeast extract, 4.8g/L $MgSO_4$, 3.6g/L dextrose, 0.5g/L NaCl, 0.186g/L KCl, Invitrogen), transferred to a 15ml falcon tube and grown in agitation at 37°C for 1 hour. The transformed cells were plated onto LB agar containing the appropriate antibiotic and incubated overnight at 37°C.

2.2.11 DNA sequencing

Plasmid DNA was extracted using the miniprep kits (Qiagen) as described above. The sequence of the insert DNA within the plasmid constructs were confirmed by automated DNA sequencing by MWG Eurofins (www.ecom.mwgdna.com). Sequencing reactions contained 2µl of primers (15 pmol/µl) and 8µl of purified plasmid template DNA (50-100ng/µl) in a final volume of 17 µl (made up with dH_2O). All sequencing reactions were pre-mixed in a 1.5ml eppendorf tube, labelled with a MWG Eurofins barcode label and sent to MWG Eurofins for the value read services. Sequencing results were sent back by email and viewed using the DNAssist software. Sequence data were analysed by performing sequence alignments with theoretical sequences. The complete sequence of the *C. rodentium* genome is available online at the Sanger Institute: www.sanger.ac.uk/resources/downloads/bacteria/citrobacter-rodentium.html.

2.3 TOPO TA Cloning

TOPO TA cloning® is a commercially available kit that enable the subcloning of PCR products containing the gene of interest, directly in to a plasmid vector without the need for restriction enzymes or DNA ligase. The TOPO TA cloning process is based on the Topoisomerase I mediated ligation of the PCR product containing adenine (A) overhangs with the TOPO vector containing thymin (T) overhangs. The adenine overhangs are created by amplifying the PCR product with Taq DNA polymerase, which lacks 3' to 5' proofreading activity and attaches on adenine at the 3' end of the PCR product. The supplied vector pCR2.1-TOPO is found linerized containing a single 3' thymin overhang and a covalently bound topoisomerase at each linear end. When the 5' end of the PCR product attach to the 3' end of the vector, the complementary base pairs adenine and thymine hybridize, and ligate in the presence of topoisomersae enzyme. The hydroxyl group of the PCR product then attacks the phosphotyrosyl bond between the vector DNA and the topoisomerase enzymes, thus releasing the enzyme and resulting in a sealed vector containing the insert.

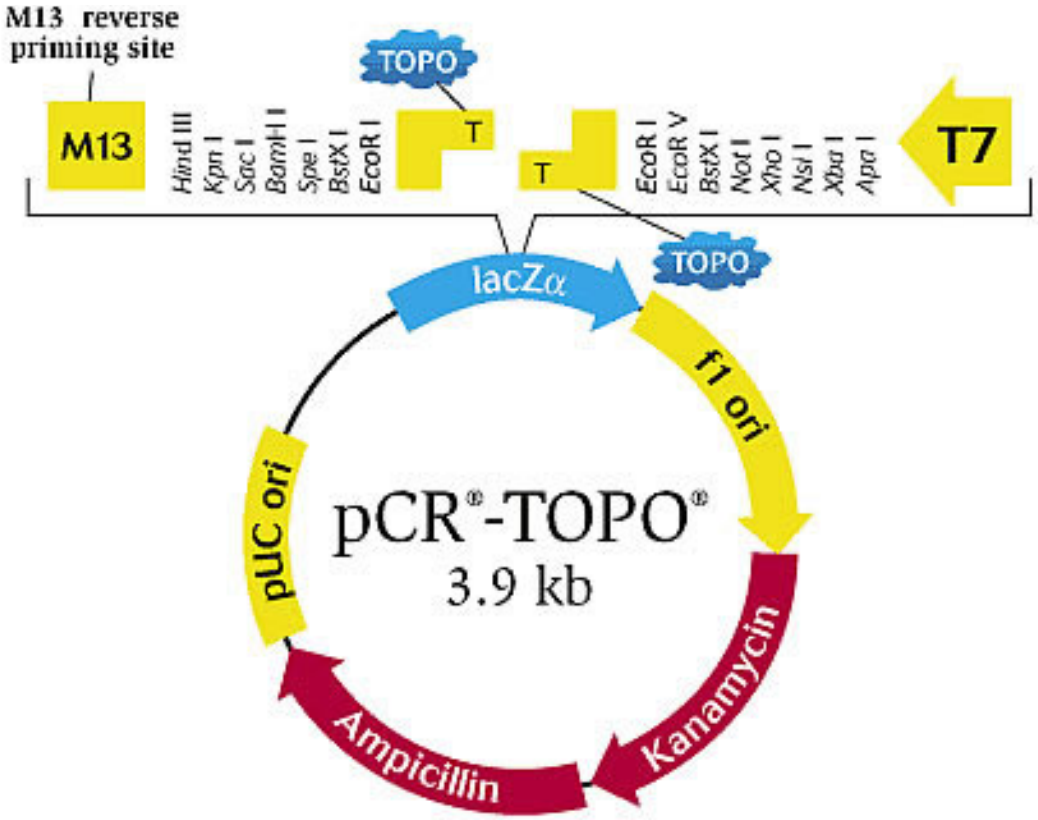

Figure 2.2: The pCR2.1 TOPO cloning vector.

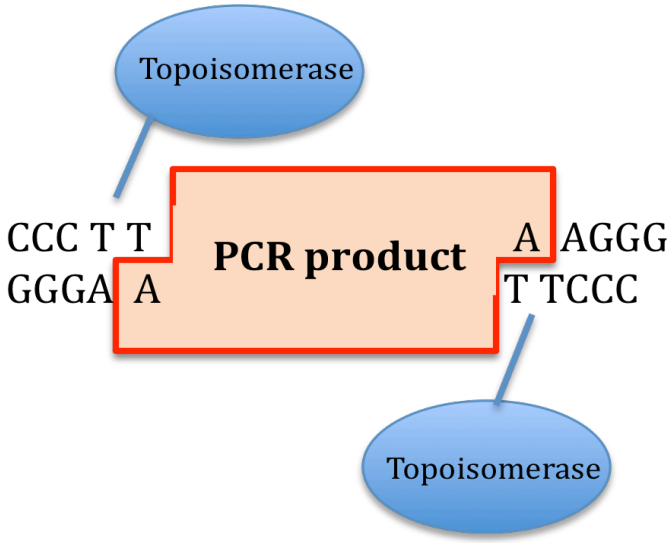

Figure 2.1: Topoisomerase I enzyme. The insertion of a PCR product into a TOPO vector containing topoisomerase I enzyme

Table 2.10: Reaction components for TA PCR

Component	**Volume (µl)**
Total	50
dH2O	28.95
5mM/µl dNTP	5
10x ThermoPol Buffer	5
10pM/µl Primer (fw)	5
10pM/µl Primer (rv)	5
Template DNA	10-100ng
Taq polymerase	1

The TOPO cloning reaction was performed using 4µl of the PCR products, 1µl of salt solution (200mM NaCl and 10mM $MgCl_2$) and 1µl of TOPO vector, and incubated for 5mins at room temperature. The resulting pCR2.1-TOPO plasmid containing the insert was then transformed into chemically competent *E.coli* cells and plated onto ampicillin and x-gal containing plates at 37^0C overnight. Positive transformants (white) were confirmed by colony PCR, restriction analysis and sequencing.

Table 2.11: Reaction components for TOPO cloning

Component	**Volume (µl)**	
PCR product	4	Incubate for 5 minutes at room temperature
Salt solution	1 (200mM NaCl and 10mM $MgCl_2$)	
TOPO vector	1	
Total	6	

For selection of positive transformants, the pCR2.1-TOPO vector contains ampicillin and kanamycin resistant markers. Additionally, the vector contains lacZα gene for blue / white screening. In the presence of pCR2.1-TOPO without the insert, *E.coli* cells carrying the lacZ deletion mutant (lacZΔM15) express an intact lacZα gene, which produces a functional ß-galactosidase enzyme. This enzyme can cleave x-gal, which is a chromogenic analogue of lactose, to form a blue colour. However, in cells where the plasmid contains an insert, the lacZα gene is disrupted, resulting in a non-functional ß-galactosidase enzyme that is incapable of cleaving x-gal, thereby producing white colonies. Therefore, the presence of white colonies on x-gal plates can indicate successful insertion of the gene of interest into the pCR2.1-TOPO vector.

2.4 CloneJET PCR Cloning

An alternative method of sub-cloning required the use of a pJET1.2/Blunt cloning vector (Thermoscientific). This cloning strategy is based on the expression of a lethal restriction enzyme by the pJET1.2/Blunt cloning vector. The ligation of a DNA insert into the cloning site of the pJET1.2/Blunt vector, disrupts the expression of this lethal gene, enabling the cells containing only the insert to grow and replicate. In contrast, the PJET1.2/Blunt cloning vector that does not contain a DNA insert, circularizes to express the lethal restriction enzyme, eco47IR, which kills its host (*E. coli*) after protein synthesis. This results in the positive selection of the transformant cells while reducing the time required for colony screening and additional cost associated with blue/white screening.

2.5 Lambda (λ) Red mediated recombination

In order to generate a chromosomally encoded gene disruption or gene fusion in the *C. rodentium* genome, linear DNA was generated by PCR amplification. In the case of a chromosomally encoded gene fusion between an effector and the TEM-1 reporter, the PCR product was generated through the PCR amplification of the plasmid region containing TEM-1 and the kanamycine resistance gene using primers that have homology sequences to the *C. rodentium* effector gene. In the case of an *escN* deletion mutant, the PCR product was generated by PCR amplifying a kanamycine resistance gene using primers that contained homology extensions to the *escN* gene sequence. The primers used are listed in Table 2.4. The resulting PCR product was then PCR purified, quantified in the Nanodrop and kept on ice until electroporation.

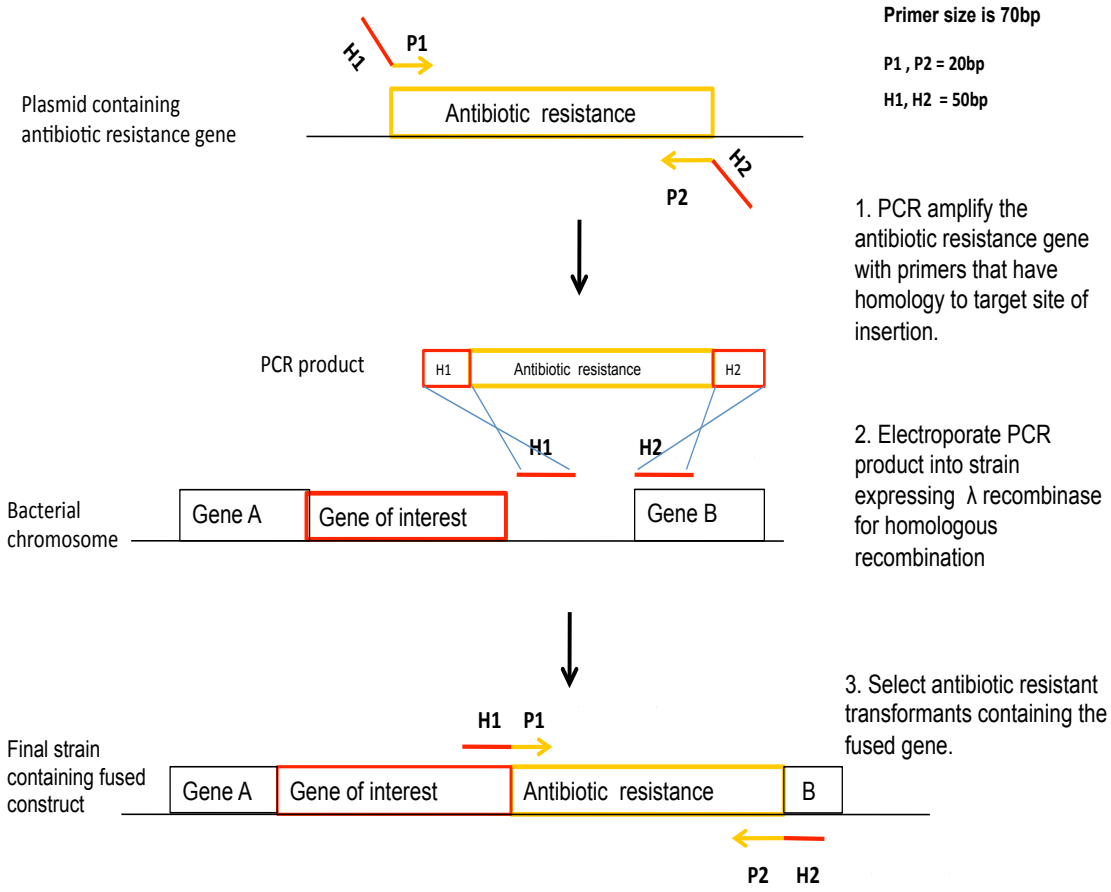

Figure 2.4: Overveiw of the λ Red recombination system. The use of λ Red recombinase mediated homologous recombination for the disruption or fusion of chromosomal genes in *C. rodentium*.

2.5.1 Electrocompetent cells

Electrocompetent cells were prepared by growing an overnight culture of *Citro* pKD46 at 30˚C with antibiotics and agitation. In the following morning, 500µl of overnight culture was diluted in fresh 50ml LB broth containing 50µl of ampicillin and grown in 200 rpm agitation at 30 ˚C until bacterial cells had reached OD_{600} 0.3-0.4. At this point, 50µl of L-Arabinose (1mM) was added to the *Citro* pKD46 cells before putting back in the shaker for the bacterial cells to reach mid-log phase (OD_{600} 0.6- 0.7) for approximately 2-2 ½ hours in total.

The culture was then chilled on ice for 15 mins before being divided into 50ml falcon tubes. The cells were then spun at 3000 x g for 15 minutes in a pre-cooled centrifuge. The supernatant was discarded and the pellet was washed by gently resuspending with 50ml sterile, ice-cold 15% (v/v) glycerol water. The pellets were washed twice more and after the final wash, bacterial cells were resuspended with 200µl sterile cold glycerol water and transferred to a 1ml eppendorf tube. The cells were centrifuged again for 5 mins, resuspended into 80µl of cold glycerol water and kept on ice until electroporation.

2.5.2 Electroporation

For electroporation, 80 µl of electrocompetent cells were pipetted into pre-cooled 2mm gap cuvettes. 8-10µg of purified PCR product was added to the cuvette and mixed with the electrocompetent cells. The cuvettes were dried and the cells shocked in the electroporator with a pre-set programme (OHMS: 200, Voltage: 2.50 kV, capacitance: 25). Immediately after electroporation, 700µl of SOC medium was added to the cuvette and the electroporated cells were transferred to a 15ml falcon tube and incubated with agitation (225rpm) at 37˚C for 1 ½ -2 hours. The cells were then spread across agar plates containing the appropriate antibiotic and incubated overnight at 37˚C.

2.6 Mammalian cell culture

2.6.1 Mammalian cell lines

In this study, the following murine cell lines were used: Swiss 3T3 fibroblasts, CMT93 Colonic epithelial cells, J774 macrophages and BW5157 T cells (summarised in Table 2.12)

Table 2.12: Cell lines used in this study

Cell line	Cell line description	Growth media	Source
Swiss3T3	Mice fibroblasts (adherent)	Complete DMEM	Dr O. Marches
CMT93	Mice colonic epithelial cells (adherent)	Complete DMEM (supplemented with 25 mM Hepes)	Dr V. MacDonald
J774	Mice macrophages / monocyte (adherent)	Complete DMEM	Dr O. Marches
BW5147	Mice T cells (non- adherent)	Complete DMEM (supplemented with 0.05mM 2-Mercaptoethanol)	Dr D. Pennington

2.6.2 Growing & harvesting cells

All cells were cultured in Dulbecco's Modified Eagle Medium (DMEM) high glucose, GlutaMAX^{TM} supplemented with 10% Foetal calf serum (FCS) and 1% penicillin-streptomycin (100 U/ml penicillin and 100 μg/ml streptomycin) (all from GIBCO/Invitrogen, UK). The complete media was further supplemented with either 25mM Hepes for culturing CMT93 Colonic epithelial cells or 0.05mM 2-Mercaptoethanol for culturing T cells (all from GIBCO/ Invitrogen, UK). The complete medium was filter sterilised using 500ml vacuum filter system and a cellulose nitrate filter membrane with a pore size of 0.22um (Corning), prior to use. All cell lines were grown in 75cm^2 flasks placed in 5% CO_2 incubators at 37°C.

When a cell density of greater than 70% to 80% confluency was reached, cells were subcultured. Briefly, the media was aspirated and the adherent cells were washed twice with Dulbeccos phosphate buffered saline (DPBS). To detach cells from the flasks, Swiss 3T3 cells were incubated with Trypsin-EDTA at 37°C for 5 minutes, CMT93 cells were incubated in DPBS at 37°C for 15 minutes and macrophages were detached using a cell scraper in DPBS, followed by strong shaking or tapping of the

flask. Pre-warmed media was then added (to inactivate the trypsin) and cell clumps were disrupted with gentle pipetting. Cells were spun at approximately 300 x g using a swing out rotor centrifuge (Jouan CR412) for 5 minutes and subsequently resuspended in fresh, pre-warmed media. The cells were then distributed into fresh 75 cm^2 flasks (with a dilution of 1 in 9) for subculturing. For cells in suspension, an aliquote of confluent cells were pippeted into fresh flasks containing pre-warmed media at an approximate dilution of 1 in 20 for subculturing.

For frozen storage, cells were harvested at 300 x g following cell detachment. Cell palletes were resuspended at a density of 3 x 10^6 cells per ml in 5% DMSO in foetal bovine serum in polypropylene vials. Vials were frozen for 12-24 hours inside styrofoam racks before permanent storage in the -80°C freezer. Cells were recovered by rapid thawing at 37°C and mixing with 10 to 15 ml of fresh pre-warmed complete medium.

2.6.3 Isolation of intestinal cells

All lymphoid organs were harvested from female Balb/c mice and placed in 10ml ice-cold complete medium (RPMI 1640 GlutaMAX™ supplemented with 10% heat inactivated filter sterilised fetal calf serum (FCS), 1% penicillin-streptomycin (100U/ml penicillin and 100μg/ml streptomycin) and 25μg/ml gentamycin (all from GIBCO/Invitrogen, UK).

2.6.3.1 Spleen and mesenteric lymph node (MLN) cells

Single cell suspensions were prepared from the spleen or MLN by gentle compression between the frosted ends of two glass slides in ice cold RPMI media and the resulting cell suspension homogenised by repeatedly passing through a 10ml pipette. After allowing the debris to settle by leaving the cell suspension on ice for 5 mins, the supernatant was passed through a sterile 100μm cell strainer (VWR, UK). Cells were subsequently washed by centrifugation at 300 x g for 5 minutes at 4°C in calcium and magnesium free (CMF) HBSS (GIBCO/Invitrogen). After the final wash, cells were re-suspended in 1-2 ml of complete medium and viable cell counts were performed using trypan blue in the haemocytometer. The cells were then diluted to 2x10^5 - 6x10^5 cells/ml or 1x10^6 cells/ml depending on subsequent experiment and kept on ice until use.

2.6.3.2 Peyer's patch (PP) cells

The small intestine was placed in a petri dish containing ice-cold complete medium. The PP were removed from the small intestine, transferred into calcium and magnesium free (CMF) HBSS solution containing 2mM EDTA (GIBCO/Invitrogen) and incubated on a magnetic stirrer for 30 minutes in 37°C. The resulting supernatant, containing the epithelial cells were discarded. The PP were then teased apart with tweezers and digested in collagenase (2mg/ml) for 30 minutes in a 37°C cell shaker. The resulting cell suspension was poured through a sterile 100µm cell strainer, washed using CMF HBSS and resuspended in 1ml of complete medium for performing viable cell counts (described below).

2.6.3.3 Colonic epithelial cells

The colons of infected mice were collected in 50ml tubes containing RPMI on ice. The whole colon was washed by flushing with ice cold PBS using an oral gavage needle. The colons were placed onto pre wet (ice cold PBS) paper towels and the debris from fat, blood vessels and the mesentery removed using fine tweezers. The colon was cut into smaller pieces, put individually on to parafilm, and cut longitudinally. Once each piece was opened and the lumen exposed, the epithelium was gently scrapped off the intestine using a scalpel. The epithelium was rinsed off the scalpel into a100ml beaker containing RPMI supplemented with 10% Newborn calf serum (NCS) at 37°C. The beaker was topped up to 50ml and 8mg of Dithioerythritol (DTE) added to a final concentration of 1mM (Sigma). Each beaker was covered with foil and placed on a magnetic stirrer for 40 minutes at room temperature. The contents of the beaker were then collected into a 50ml falcon tubes and spun at 300 x g for 5 minutes at room temperature. The supernatant was discarded and the pellets were resuspended in 10ml RPMI 10% NCS. After vortexing the tubes at maximum speed for 3 minutes, 40ml of RPMI 10% NCS was added and poured through nylon wool columns to remove mucus and large debris. The nylon wool columns were prepared using 0.7g of nylon wool, separated into fine strands and pushed into a 50ml syringe barrel, wrapped in foil and autoclaved. The columns were set up using clamps to hold the syringe, an infusion tube with fitted clamp to modulate the column flow and sterile 50 ml falcon tubes to collect the eluate. The columns were equilibrated with RPMI containing added Hepes (0.5mg/50ml at a final concentration of 38mM). The epithelial cell suspension was

run through the columns by gravity flow and the columns washed with a further 50ml RPMI 10% NCS. The column eluate was spun at 300 x g for 5 minutes and resuspended in CMF HBSS for CCF4 staining.

2.6.4 Cell count

All viable cell counts were performed using 1 in 20 dilution of cells in 0.4% tryphan blue (Sigma-Alderich), a haemocytometer cell counting chamber (Hausser Bright-line 3100) and a phase contrast microscope.

2.6.5 Microscopy

Live cells were viewed using Leica DM5000B Epi-fluorescence microscope with the DAPI filter set (340-380 nm excitation and 425 nm long pass emission). Images were taken using DFC490 digital colour camera using the Leica Application Suite V3 (LAS) software. All microscopy work was carried out in the Blizzard Advanced Light Microscopy core facility (BALM).

2.6.6 Flow cytometry

Cells were analysed using the BD FACS Canto II machine with BD FACSDiva v6.1.3 software located in the Flow cytometry core facility at the Blizzard Institute of Cell and Molecular Sciences (BICMS).

2.6.7 Cell characterization

Cell characterization by flow cytometry was performed to identify various immune cell populations present in the spleen. Single cell suspensions of splenocytes were washed and resuspended into 100µl of FACS buffer (0.5% BSA, 0.05% NaN_3 and sterile PBS) containing up to $5x10^7$ cells in round bottom FACS tubes. The cells were stained with various anti-mouse antibodies (all from BD eBioscience) conjugated to different flurochrome, including anti-mouse CD3e PE Cy7 (1µg/test), CD19 PerCP-Cy5.5 (0.25/test) or CD11c APC (0.25µg/test) and incubated on ice for 15 minutes in the dark. After staining, cells were washed and resuspended into 300µl of ice-cold FACS buffer for analysis in the flow cytometer. Fluorochrome compensations were performed to prevent spectral overlap.

2.6.8 Cell stimulation assay

Single cell suspensions were prepared from the spleen, MLN and PP as outlined above. Aliquots of $2x10^5$ to $7x10^5$ viable cells were cultured in 1 ml of complete medium in a 12 well plate. Cells in duplicate plates were stimulated by the addition of 5μg/ml of concanavalin A (ConA) and cultured at 37°C for 72 hours in the $C0_2$ incubator. Stimulation was confirmed using visual inspection, such as the increase in cell size and presence of cell clumps. After 72 hours, cells were harvested, infected with *C. rodentium* and stained with CCF4-AM substrate.

2.7 β-lactamase translocation assay

The β-lactamase translocation assay, which utilizes translational fusions to TEM-1 was recently developed to study effector translocation into host cells (Charpentier & Oswald, 2004). Fusing a T3SS effector gene with the TEM-1 β-lactamase reporter gene generates a translational fusion protein that can be detected by the addition of the fluorescent substrate CCF4-AM. Eukaryotic cells containing TEM-1 are able to cleave CCF4-AM and appear blue under UV light, while cells lacking TEM-1 are not able to cleave CCF4-AM and appear green. To detect the translocation of NleD-TEM-1 fusion protiens in this study, mice cells were infected with *Citro* pACYCnleD expressing a gene fusion between the NleD effector and the TEM-1 β-lactamase enzyme, and incubated with CCF4-AM substrate. The β-lactamase substrate CCF4 is more soluble than CCF2 in aqueous solutions and has therefore been preferred over CCF2. β-lactamase enzyme activity in mouse cells was detected using fluorescence microscopy or flow cytometry. The translocaion assays, originally described in EPEC (Charpentier & Oswald, 2004), were adapted for use in *C. rodentium* according to the advice of Dr. O. Marches.

2.7.1. Day before the assay

To prepare the bacterial inoculum, 3 ml LB broth (supplemented with 1mg/ml chloroamphenicol) was inoculated with a single colony of *Citro pACYCnleD* and grown in a 37°C shaker at 200 rpm. After 8 hours, the resulting bacterial culture was diluted 1:100 in the interaction media (25mM Hepes modified DMEM with glutamax and 10% FCS) and transferred into a 6 well plate (Corning). The plates were incubated static at 37°C in a 5% CO_2 incubator overnight (for activation).

To prepare the mouse cell lines, adherent cells were seeded at an approximate density of $4x10^4$ cells into each well of an 8-well LabTek chamber slide (Sigma-Alderich) containing 500µl DMEM, while non-adherent cells were seeded at an approximate density of $8x10^4$ cells / ml. All cells were incubated at 37°C in 5% CO_2 overnight.

2.7.2 Day of the assay

Adherent cells in the LabTek were washed twice with pre warmed DPBS and replaced with 500µl of the bacterial suspension. The bacterial suspension was prepared from overnight cultures by washing with DPBS (centrifuging at 3000 x g for 5 minutes) and resuspending in the interaction media. 1 in 10 dilution was made by diluting 50µl of overnight bacterial culture into 450µl of pre-warm interaction media to prepare a 500 µl bacterial inoculum. The infected cells were incubated in a static incubator with 5%CO_2 and 37°C for 6 hours. After infection, bacteria were removed by washing cells three times in calcium and magnesium free (CMF) HBSS. After the final wash, cells were resuspended in 200µl of HBSS to which 40µl of freshly prepared CCF4-AM solution was added at a concentration of 1mM per well according to the CCF4-AM substrate loading kit (Invitrogen). The cells were incubated in the dark, at room temperature for 60 minutes and then washed three times in HBSS. After the final wash, the plastic chamber partitions were removed from the LabTek slide and excess HBSS removed using Whatman 3 mm filter paper. The wells were covered with $2cm^2$ glass coverslips and ready for observation by fluorescence microscopy.

Non-adherent cells were washed in HBSS by centrifugation at 300 x g for 5 minutes, resuspended in the interaction media and distributed into a 12 well plate at an approximate density of $5x10^5$ cells per well. The bacterial inoculum was made by diluting the overnight cultures in 1:10, 1:100 or 1:1000 in the interaction media. 100µl of the diluted bacterial culture was added to the 900µl cell suspension and mixed by gentle pipetting. The infected cell suspensions were incubated in a static incubator with 5%CO_2 and 37°C for 6 hours. After infection, bacteria were removed and the cells were washed in HBSS. After the final wash, cells were resuspended in 400µl of HBSS in a 24 well plate to which 80µl of freshly prepared CCF4-AM solution was added at a concentration of 1mM per well according to the CCF4-AM

substrate loading kit (Invitrogen). After an hour long incubation in the dark at room temperature, cells were washed three times in HBSS, resuspended into 1ml of DPBS and transferred to FACS tubes for immediate FACS analysis.

For the time course assay, approximately 10^5 T cells were infected with approximately 10^8 *Citro* pACYCnleD (MOI=1000 or 10^3) for 6, 4, 2 and 1 hour. The cells were subsequently stained and analysed by flow cytometry.

To investigate the multiplicity of infection (MOI), overnight cultures of bacteria were washed and resuspended in the interaction media at various dilutions including 1:10, 1:100, 1:1000, 1:10000 and 1:100000. Bacteria from the various dilutions were pipetted in to each well containing ~10^5 cells/ml. Retrospective plating confirmed the number of bacteria per cell.

Table 2.13: The multiplicity of infection (MOI). All values are approximate.

Bacterial dilution of overnight culture	**Bacterial count per well**	**T cell count per well**	**MOI**
1:10	10^{10}	10^5	10^5
1:100	10^9	10^5	10^4
1:1000	10^8	10^5	10^3
1:10 000	10^7	10^5	10^2
1:100 000	10^8	10^5	10^1

2.7.3 β-lactamase translocation assay in vivo

Single cell suspensions were prepared from the spleen, MLN and PP of infected mice, washed and resuspended in HBSS. 400µl of each cell suspension was distributed in a 24 well plate with an approximate density of ~ 10^6 cells per well. For substrate staining, 80µl of freshly prepared CCF4-AM solution (1mM) was added to each well according to the manufacturers instructions from the CCF4-AM substrate loading kit (Invitrogen). Following an hour long incubation in the dark at room temperature, cells were washed three times in HBSS, resuspended into 1ml of DPBS and transferred to FACS tubes for immediate FACS analysis.

2.8 Mouse infection studies

2.8.1 Mice

Five to seven week old, female, specific pathogen free (SPF) Balb/c mice were purchased from Charles River Laboratories (Scotland, UK). They were housed in groups of 5-6 mice in closed, ventilated cages with sterile bedding and free access to commercial food and water in the biological sciences unit (BSU). Following transportation to the BSU, the mice were left to acclimatize for a period of 10 days before the commencement of any mice experiments. Independent infection experiments were performed at least twice using a minimum of five mice per group. All procedures were performed in accordance with the Animals in Scientific Procedures Act and United Kingdom home office regulations.

2.8.2 Bacterial inoculum for mice infection

The day before infection, 50ml of LB broth containing nalidixic acid (100µg/ml) and/or chloramphenicol (50µg/ml) were inoculated with freshly isolated *C. rodentium* and grown overnight in a 37°C shaker (200 rpm). On the day of infection, bacterial cultures were harvested by centrifugation at 3000 x g for 10 minutes followed by washing to remove any antibiotics in the media and resuspension in 5ml of sterile PBS (Sigma-Alderich) to prepare a 10x concentrated bacterial inoculum, which was kept on ice until use.

2.8.3 Oral inoculation of mice

Individual mice were orally gavaged with 200µl of 10x concentrated *C.rodentium* by a gavage needle. Retrospective plating confirmed that ~$2x10^9$ to ~$6x10^9$ colony forming units (cfu) of *C. rodentium* were received by each mice. The tails of each mouse was colour coded to enable the infection to be followed in each individual animal. Mice were regularly monitored over a period of 8-12 days post inoculation by measuring body weight and bacterial burden (recovering viable CFU counts from mice stool samples). At the end of the infection experiment, mice were killed by terminal anaesthesia (CO_2 gas) or by cervical dislocation. The distal colon was removed and snap frozen in liquid nitrogen for subsequent Haematoxylin and Eosin

staining. The spleen, MLN and PP were collected for preparing single cell suspensions, which were analysed for β-lactamase activity.

2.8.4 Retrospective plating

Infection in individual mice was monitored by retrospective plating of viable bacteria from stool samples. Faecal pellets were collected in eppendorf tubes, weighed and added to sterile PBS at a concentration of 100mg/ml. The pellets were mashed using a 1ml pipette tip and vortexed before separating the debris by a quick centrifugation at 200 x g. The resulting supernatant containing the bacterial suspension was serially diluted in PBS and plated onto LB agar containing nalidixic acid. The plates were air dried and incubated at 37°C overnight. The number of bacteria shed per gram of stool was determined by viable count of CFU present on the plates, using the following formula: CFU/g of stool = CFU on plate / dilution factor.

2.8.5 Hematoxylin and Eosine (H&E)

Frozen colonic tissues were mounted in OCT (Agar Scientific Ltd, UK) on dry ice using plastic moulds and fast freeze spray. Five micrometer (μm) sections of tissue were cut on a cryostat (OTF5000, Bright Instruments Ltd, UK) and mounted on polysine slides (VWR, UK). The slides were air dried for 30mins at room temperature and fixed in 100% acetone for 20 minutes before drying again for another hour. The slides were then dipped in Meyer's haematoxylin (Sigma-Alderich Ltd, UK) for 30 seconds, quickly rinsed in tap water before dipping into acid alcohol and washing again in tap water for 5 minutes to develop the blue stain. The slides were subsequently placed in 1% eosin yellow solution (VWR, UK) for 5 minutes, quickly rinsed in tap water, dipped into acid alcohol and washed again in tap water for 1minute. The sections were then dehydrated using an ethanol gradient (70%, 90%, 95% and 2x 100%) with 2 minutes in each concentration. Finally, the sections were cleared in Histo-clear (VWR) for 5 minutes in the fume hood and mounted on cover glass using DPX mountant before drying them overnight at room temperature. The hematoxylin and the eosine stained tissue sections were viewed under an inverted, phase contrast microscope where the length of the colonic crypts were measured using a calliberated graticule placed on the eye piece of the microscope. An average of 10 to 25 measurments were recorded for each tissue section and the data expressed as colonic crypt length in μm.

2.8.6 Data analysis

Data shown in a scatterplot or barchart were expressed as the mean+SEM values of several independent experiments / individual mice (indicated by error bars). All data analyses were performed using Graphpad prism version 4 software for Windows (GraphPad Software, California, USA).

Chapter 3: Construction of a reporter *C. rodentium* strain encoding a fusion between the effector and the β-lactamase gene

3: Construction of a reporter *C. rodentium* strain encoding a fusion between the effector and the β-lactamase gene

3.1 Introduction

The purpose of this study was to create a reporter *C. rodentium* expressing a chromosomally encoded fusion protein between a T3SS effector and the ß-lactamase reporter enzyme (TEM-1). To do so, the Datsenko and Wanner (2000) strategy of λ Red recombination-mediated gene replacement was used. Previous gene replacement methods for disrupting or inserting a chromosomal gene in bacteria required the construction of various plasmids and suicide vectors in multiple cloning steps prior to the recombination of plasmid DNA into the bacterial chromosome (Metcalf et al, 1996; Kato et al, 1998). Datsenko and Wanner (2001), however, developed a λ Red recombination system that directly creates a chromosomal gene replacement in *E.coli* using linear DNA in a single step. The use of linear DNA to disrupt chromosomal genes and insert foreign DNA was first demonstrated in *Saccharomyces cerevisiae* and *Candida albicans* (Rothstein, 1991). The linear DNA was generated through polymerase chain reaction (PCR) amplification of a selectable gene marker with flanking DNA regions homologous to the chromosomal target site. Mitotic recombination, a highly efficient homologous recombination process in yeast, then created a chromosomal gene disruption through the insertion of the marker gene at the flanking site (Rothestein, 1991).

In bacteria, however, homologous recombination using PCR fragments is ineffective due to the presence of intracellular exonucleases. Exonuclease V (Exo V), for example, belonging to the bacterial RecBCD recombination complex, degrades linear DNA, including PCR products transformed into bacterial cells (Lorenz & Wackernagel, 1994). To overcome this problem, many studies used mutants of the RecBCD recombination complex and conditions that inhibit ExoV nuclease activity, but these resulted in inefficient homologous recombination between the chromosome and the PCR fragments (Dabert & Smith, 1997; Toro et al., 1998).

The discrepancy was finally solved when extensive studies led to the exploitation of the homologous recombinase genes from bacteriophage λ. Bacteriophage λ possesses the Red system, which greatly enhances homologous recombination of linear DNA

with chromosomal DNA in bacteria (Murphy et al, 1998). The Red system consists of three proteins, Gam, Bet and Exo, which are synthesised from the genes *γ, ß,* and *exo* clustered in a single operon. The Gam protein binds to the bacterial RecBCD recombination complex, inhibits its exonuclease activity, and prevents host degradation of linear DNA. This enables Exo and Bet proteins to have access to the ends of the linear DNA, where Exo digests the 5'-end of the double-stranded DNA to single-stranded DNA and Bet binds to the single-stranded DNA to promote strand annealing to complimentary DNA. By doing so, the Red enzymes induce a 'hyper-rec' state in *E. coli*, wherein recombination events between the chromosome and linear DNA with shared sequences occur at high frequencies (reviewed in Poteete 2001 & 2006 and in Madyagol et al, 2011).

Use of the λ Red system for *in vivo* genetic engineering was revolutionised in 2000 by three independent studies, which demonstrated DNA recombination of PCR products flanked by short (35-50bp) homologous sequences (Datsenko & Wanner, 2000) or by long (1000bp) homologous sequences, in the presence of the Red system expressed either from the lac promoter (Murphy et al, 2000) or a defective λ prophage with a thermosensitive repressor (Yu et al, 2000) in *E. coli.*

The strategy developed by Datsenko and Wanner (2000) for chromosomal gene replacement is rapid and highly efficient (outlined in Figure 3.1.1). It involves the expression of the λ Red enzymes on a low copy plasmid where *γ, ß,* and *exo* are placed under the control of the P_{araB} promoter and induced with arabinose (Fig. 3.1.2). The linear DNA is generated through the PCR amplification of an antibiotic resistance marker using primers that contain 36 base pairs flanking regions homologous to the sequence of the desired insertion site. Electroporation of the resulting PCR products into *E. coli* cells, following arabinose induction, enables Red-mediated homologous recombination to occur between the PCR products and the *E. coli* chromosome at the flanking regions. Following selection, the resistance marker, flanked by FLP recognition target (FRT) sites, can be eliminated by the expression of FLP recombinase from a helper plasmid directly acting on the FRT sites. The λ Red expression plasmid and FLP helper plasmid, containing the temperature sensitive replicon maintained at 30°C, are eliminated by growth at 37˚C. Using this method, mutants can be created within a week, which is a short timeframe compared to the month-long procedure required for the creation of the same mutant

using traditional plasmid-based methods. In addition, the use of primers with short flanking regions homologous to the chromosomal insertion site allows flexibility in designing and choosing the specific chromosomal location (Datsenko & Wanner, 2000; Madyagol et al, 2011).

Since its inception, the λ Red-mediated gene replacement method has been used extensively for the mutational analysis of genes belonging to several different *E. coli* pathotypes, including enteropathogenic *E. coli (EPEC),* enteropathogenic *E. coli (EHEC),* enteroaggregative *E. coli (EAEC),* uropathogenic *E. coli (UPEC)*, and enterotoxigenic *E. coli (ETEC)* (Murphy & Campellone 2003; Savage et al, 2006; Lee et al, 2009). In addition, it has been an indispensable tool in the creation of the Keio collection, which is a set of *E. coli* K-12 mutants containing precisely defined single gene deletions in all non-essential genes (Baba et al, 2006). Moreover, the λ Red-mediated gene replacement method has been widely used to study other gram-negative bacteria including *Salmonella* (Uzzau et al, 2001; Hussaaeiny & Hensel 2005; Yu et al, 2011), *Shigella* (Ranallo et al, 2006; Bhagwat et al, 2012), and *Yersinia* (Derbise 2003; Sun et al, 2008).

Therefore, we used the Datsenko and Wanner (2000) strategy of λ Red recombination-mediated gene replacement to create a gene fusion between the T3SS effector and a ß-lactamase reporter gene (TEM-1) in *C. rodentium* (Fig 3.1.3). However, since the aim of this study was to create a reporter *C. rodentium* encoding a gene fusion rather than a gene replacement, the use of FRT sites and the expression of FLP recombinase was not necessary.

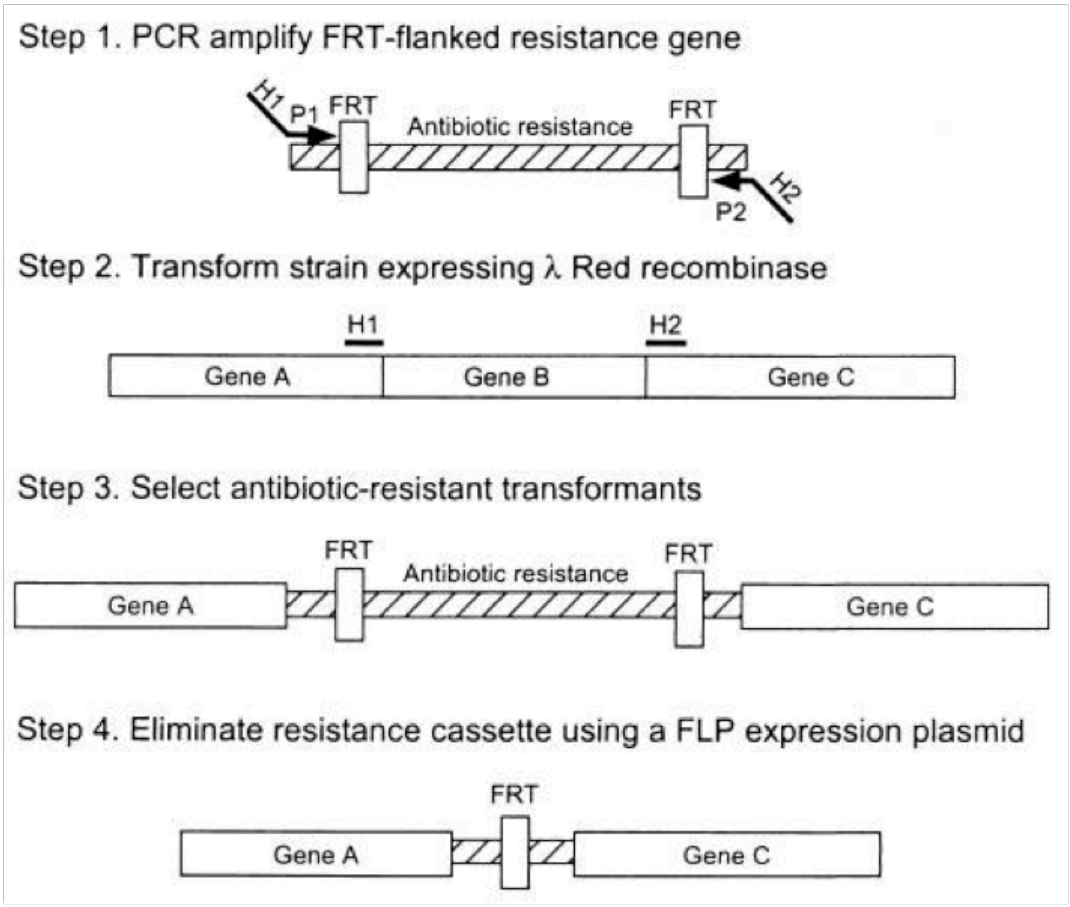

Figure 3.1.1: The Datsenko and Wanner (2000) strategy of gene replacement. The antibiotic resistance gene is amplified using primers that contain primer binding sites (P1 and P2) and homology extensions (H1 and H2). P1 and P2 bind to the antibiotic resistance gene, while H1 and H2 are homologous to the chromosomal insertion site. Homologous recombination occurs at the H1 and H2 regions, resulting in the replacement of gene B with the antibiotic resistance marker in the bacterial chromosome. FLP recombinase acting on the FRT sites can subsequently eliminate the antibiotic resistance marker. Taken from Datsenko and Wanner (2004).

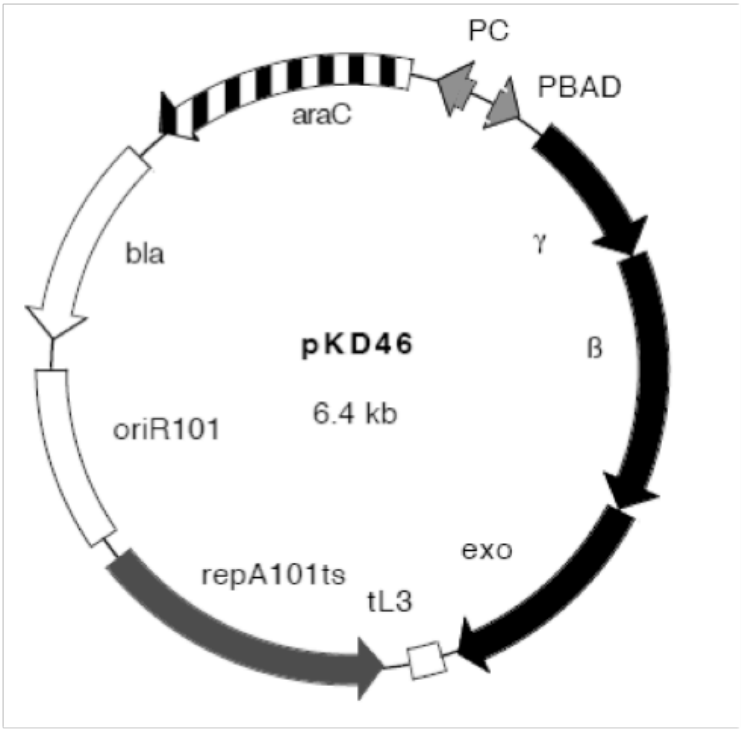

Figure 3.1.2 Plasmid map of pKD46. Described by Datsenko and Wanner (2004), pKD46 plasmid encodes the λ Red genes *(γ, β,* and *exo*) from the araBAD promoter. The temperature-sensitive replicon is maintained at 30°C and cured at 37°C. Image taken from imagekb.com

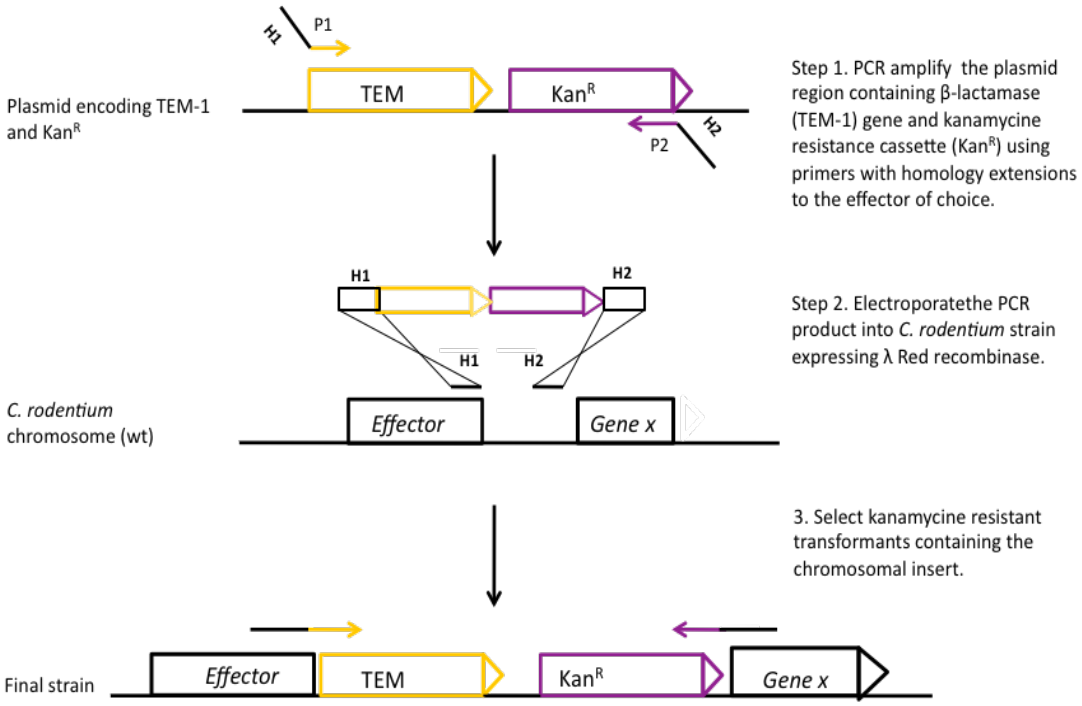

Figure 3.1.3: Chromosomal gene fusion strategy. The plasmid region containing TEM-1 and the kanamycin resistance gene is amplified by primers that have primer binding sites (P1 and P2) and homology extensions (H1 and H2). Homologous recombination occurs at the H1 and H2 regions, resulting in the chromosomal insertion of TEM-1 and the kanamycin resistance gene into the *C. rodentium* chromosome. The insertion of TEM-1 next to a bacterial effector results in effector-TEM-1 gene fusion.

3.2 Results

The aim of this chapter was to generate a reporter strain of *C. rodentium* expressing a chromosomally encoded gene fusion between a T3SS effector and the ß-lactamase reporter (TEM-1) using the Datsenko and Wanner (2000) strategy for gene replacement. As a negative control, the *Citro ΔescN* mutant strain containing a chromosomal gene disruption in the *escN* locus was also generated. Although the *ß-lactamase (blaM*) gene encodes the TEM-1 protein, for simplicity, the terms TEM-1 or TEM will be used to refer to both the gene and the protein throughout the rest of this thesis. In addition, the figures in this chapter will be incorporated within the results section for the reader's convenience.

3.2.1 Construction of a *Citro ΔescN* mutant

Previous research has shown that *Escherichia* secretion component N (EscN) in *E. coli* is homologous to the extensively studied *Yersinia* secretion component N (YscN) in *Yersinia* and Invasion C (InvC) in *Salmonella*. These cytoplasmic proteins show high similarity to proton-translocating ATPases in bacterial cells (Hueck 1998), which interact with membrane-bound components of the T3SS to provide energy for the assembly of the T3 apparatus and secretion of its effectors (Fan et al, 1996). Mutations in these genes result in the inability of bacteria to catalyse ATP hydrolysis (Eichelberg et al, 1994) and energise the type 3-mediated translocation of proteins (Woestyn et al, 1994). Consequently, the use of *YscN* and *EscN* deletion mutants as negative controls enabled the study of T3SS-mediated translocation of effectors in *Yersinia* (Marketon et al, 2005; Koberle et al, 2009) and *EPEC* (Ritchie & Waldor 2005, Vossenkaemper et al, 2010), respectively. Therefore, a *ΔescN* deletion mutant of *C. rodentium* was used as a negative control in this study.

The *ΔescN* deletion mutant was constructed by desrupting the *C. rodentium escN* gene with a kanamycin resistance cassette (*kn315)*. To do so, the *kn315* gene was amplified by PCR from pKD4 plasmid using primers escNFRT (fw) and escNFRT (rv) containing flanking DNA homologous to the *escN* gene (Fig. 3.2.1 A). The PCR product was then purified and electroporated into electrocompetent *Citro* pKD46 cells expressing the λ Red recombinase genes. The resulting mutants were selected on kanamycin plates and verified through colony PCR (Fig 3.2.1 B-C).

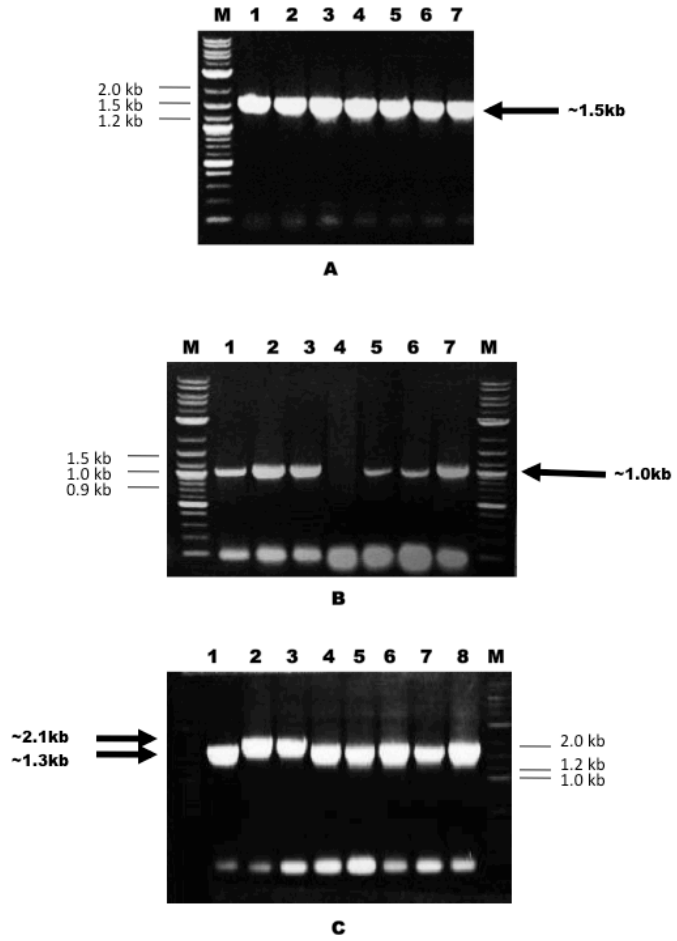

Figure 3.2.1: Construction of the Citro *ΔescN* deletion mutant. (A) Gel electrophoresis showing PCR amplification of the kanamycin resistant gene (0.792kb) from the pKD4 plasmid using primers escN-FRT (fw) and escN-FRT (rv). The primers contain extension homologies to the *escN* gene in *C. rodentium,* thus resulting in a PCR product with a band size of ~1.5kb in total. (B) Colony PCR of transformants using primers K1 (fw) and B171DescN(rv) that amplifies a ~1kb region comprising partly of the kanamycin resistance gene and partly of the *escN* gene, thus confirming the construction of the *ΔescN* deletion mutant . (C) Colony PCR of transformants using primers B171 (fw) and B171DescN (rv) resulting in a band size of 1.3kb (intact escN gene) or 2.1kb (disrupted escN gene with kanamycin insert) for verification of the *ΔescN* deletion mutant. Marker sizes are indicated next to the marker and band sizes are indicated by arrow heads.

3.2.2 Construction of a chromosomally encoded gene fusion

The translocated intimin receptor (Tir) is one of the first effectors to be delivered into host cells by the bacterial T3SS. It is essential for the attachment of bacteria to intestinal epithelial cells (Marches et al, 2000) and for bacterial colonisation of the host gut *in vivo* (Deng et al, 2003). Tir is encoded in the locus of enterocyte effacement (LEE) and expressed when AE pathogens come into close contact with a host cell (Knutton et al, 1997). Upon translocation into the host cell cytoplasm, Tir is inserted into the plasma membrane in a hairpin loop topology, exposing an extracellular loop that interacts with the bacterial surface protein Intimin and an intracellular domain that interacts with host cytoskeletal proteins. Intimin binding to Tir facilitates tight attachment to host epithelial cells, which leads to the formation of actin-rich pedestals and the characteristic attaching and effacing (AE) lesions (Kenny et al, 1997; Frankel et al, 2001; Goosney et al, 2000; Pelegrin et al, 2014). Since Tir is essential for AE pathogenesis, we aimed to create translational fusions to TEM-1 in order to investigate the host cells targeted for Tir translocation by *C. rodentium*.

3.2.2.1 Construction of plasmid pCX315 encoding TEM-1 and an antibiotic resistant marker

To generate translational fusions of Tir with TEM-1, the plasmid pCX315 was first created using the plasmid pCX340. Plasmid pCX340, a β-lactamase TEM-1 fusion cloning plasmid, was previously constructed by Charpentier and Oswald (2004) to create translational fusions with EPEC effectors. It was designed to carry the ß-lactamase (*blaM)* gene encoding TEM-1, P*trc* promoter upstream of *blaM*, tetracycline resistance gene and a multiple cloning site (containing unique restriction sites NdeI, KpnI, and EcoRI) upstream of *blaM* (Fig. 3.2.2). Consequently, the plasmid pCX340 encodes the β-lactamase TEM-1 enzyme under an isopropyl-ß-$_{D}$-thiogalactopyranoside (IPTG) inducible promoter. In addition, the presence of a multiple cloning site enables the cloning of effector genes with *blaM* to generate Effector-TEM fusion proteins (Charpentier & Oswald, 2004).

To construct the pCX315 plasmid, a kanamycin resistance cassette (*kn315*) was inserted downstream of *TEM-1* in the pCX340 plasmid (Fig. 3.2.3). The *kn315* gene (968bp) was amplified by PCR from plasmid pSB315 (provided by Dr O. Marches) using the primers XbaI-kn315 (fw) and Sal1-kn315 (rv). The primers were designed

to contain the restriction sites Xba1 and Sal1 to enable the insertion of *kn315* into the Xba1/Sal1 site located downstream of *TEM-1* in the pCX340 plasmid. The resulting PCR product was cut using the Xba1 and Sal1 restriction enzymes and ligated into the cut pCX340 plasmid vector (Fig. 3.2.4). The transformed bacterial strains were grown on plates containing kanamycin. Despite several attempts, however, we did not manage to isolate any kanamycin-resistant transformants containing the pCX315 plasmid.

Since we were unable to clone the *kn315* gene directly into pCX340 through the restriction digestion of linear DNA (PCR product containing kn315), we decided to subclone the kn315 gene into a plasmid because restriction digestion works better in circular DNA. Consequently, kn315 was subcloned into the TOPO TA cloning vector (3.9kb) to generate the plasmid pCR2.1TOPOkn315 (~4.9kb). TOPO TA cloning uses Toposiomerase I enzyme to directly insert PCR products (containing A overhangs) into the TOPO vector (containing T overhangs), without the need for restriction enzymes or DNA ligase (described in Chapter 2). In addition, the TOPO cloning reaction occurs in 5 minutes with up to 95% of transformants containing the cloned insert, which can be analysed through blue/white screening (on x-gal containing plates), restriction digestion, PCR analysis and sequencing (using the M13 forward and reverse primers). For these reasons, we hoped that TA sub-cloning would improve the efficiency of kn315 cloning into pCX340. Following verification (by PCR analysis, EcoR1 restriction digestion, and sequencing), the plasmid pCR2.1TOPOkn315 was digested with XbaI and Sal1 restrciton enzymes and ligated into the digested pCX340 vector (Fig 3.2.4). This generated the pCX315 plasmid containing a kn315 insertion downstream of TEM-1. The plasmid construct was then confirmed using restriction digestion (Fig 3.2.5) and sequence analysis.

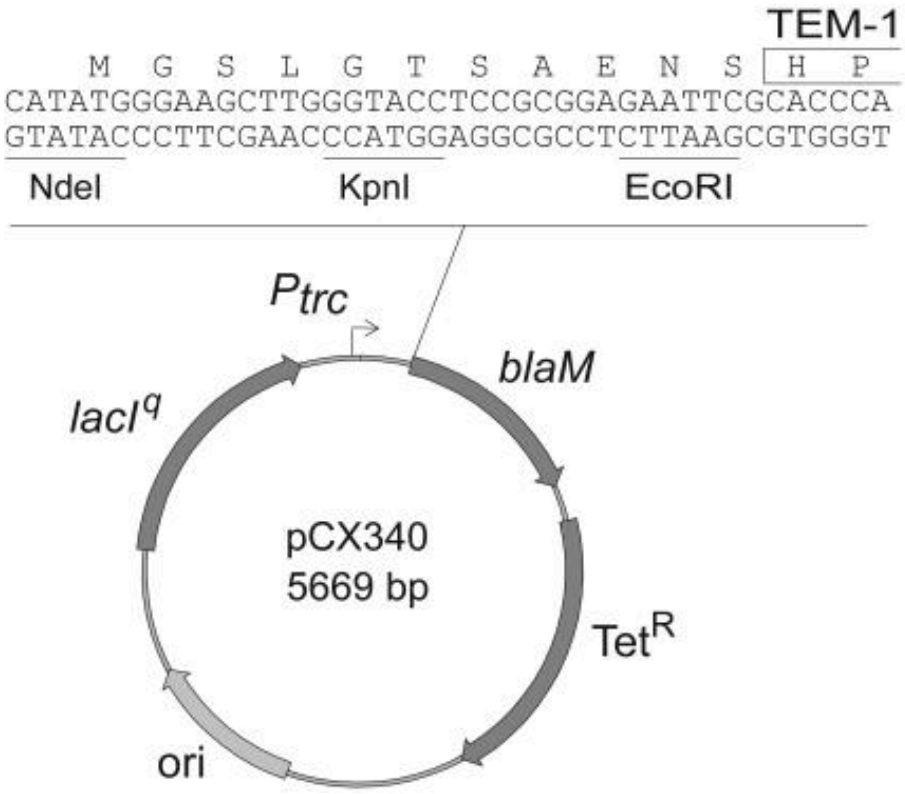

Figure 3.2.2: Map of the pCX340 cloning vector. The pCX340 plasmid carries the *blaM* gene encoding the ß-lactamase TEM-1 enzyme. The presence of the multiple cloning sites upstream of TEM-1 enables the creation of translation fusion proteins with bacterial effectors. Taken from Charpentier and Oswald (2004).

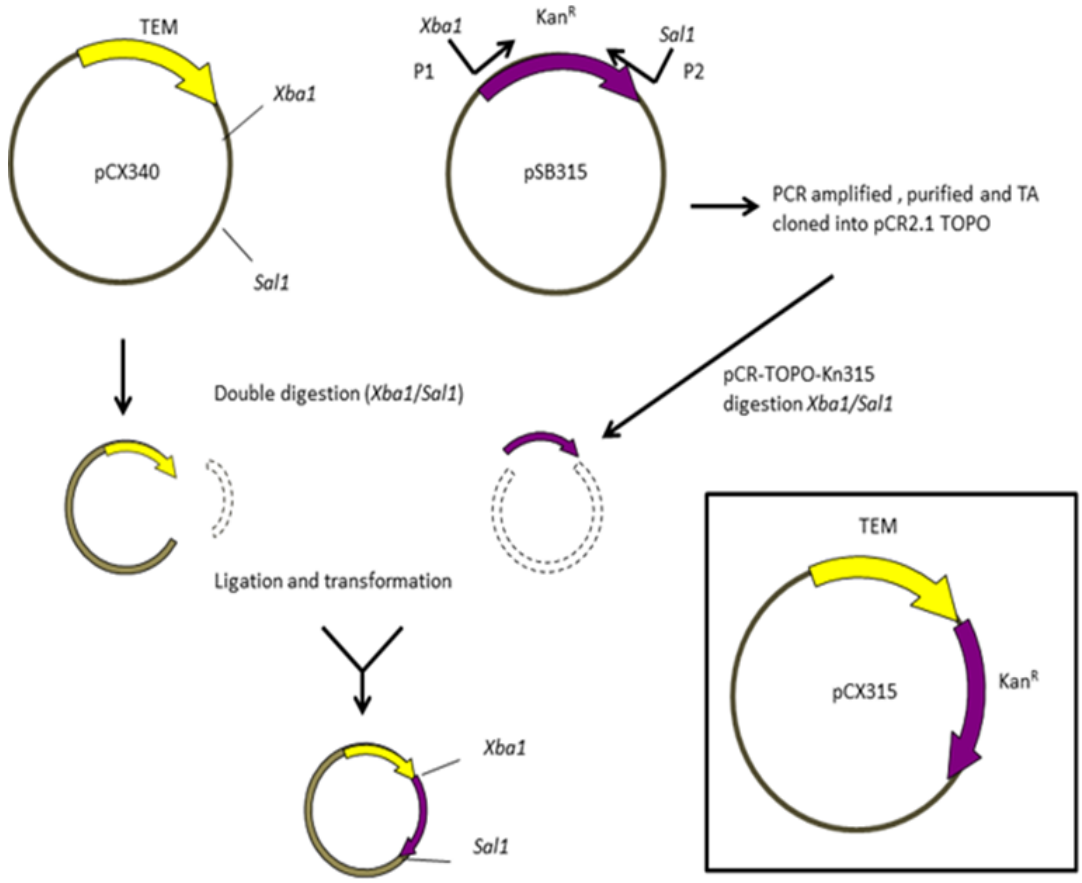

Figure 3.2.3 Overview of pCX315 plasmid construction. The *kn315* antibiotic resistance cassette was PCR-amplified from pSB315 using primers that contain the restriction sites Xba1 and Sal1. The PCR product was TA-cloned, cut using Xba1 and Sal1 restriction enzymes, and ligated into pCX340 to generate the pCX315 plasmid.

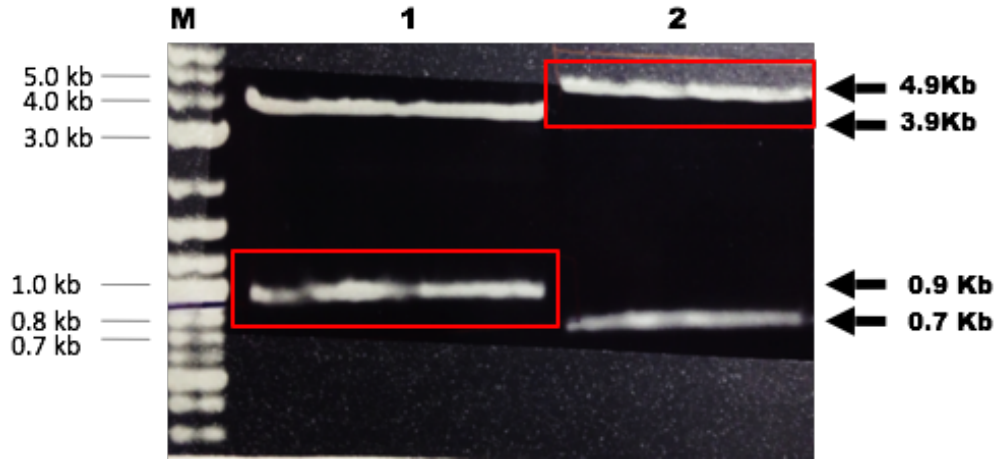

Figure 3.2.4: Cloning of pCX315 plasmid. Sal1 and XbaI restriction digestion of pCR2.1TOPOkn315 (produce DNA fragments 3.9 kb and 9.68 kb) in lane 1 and pCX340 (produce DNA fragments 4.914 kb and 0.755 kb) in lane 2. The 0.968 kb insert was used for ligation into the 4.914 kb cut vector.

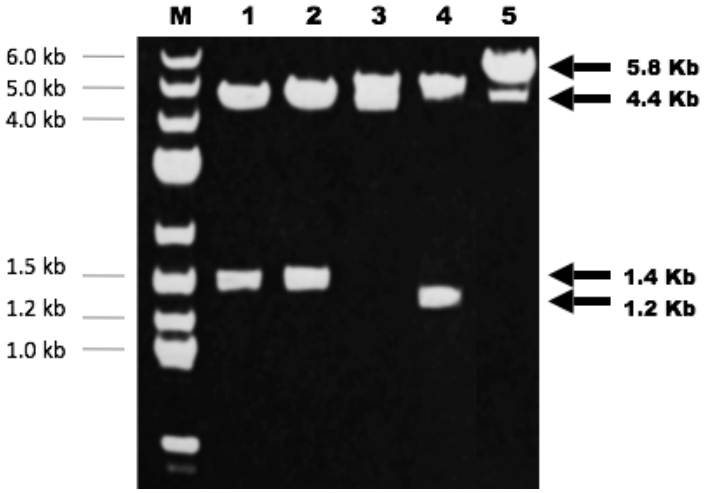

Figure 3.2.5: Verification of pCX315 plasmid. HindIII restriction digestion of pCX315 (lane 1-2) and pCX340 (lane 4). Two HindIII restriction sites are located at 4.402 kb and 1.267 kb sites in the pCX340 plasmid, and at 4.402 kb and 1.480 kb in the pCX315 plasmid just outside the insert (kn315) fragment. Undigested plasmid pCX315 (5.882 kb) is shown for comparison (lane 5).

3.2.2.2 Homologous recombination with *tir*

To generate the PCR product required for λ-Red mediated homologous recombination, the plasmid construct containing the TEMkn315 region was amplified by PCR using pCX315 and primers with flanking regions homologous to the chromosomal insertion site adjacent to *tir*. The 5' end of the *Citro* tirTEMkn315 (fw) primer contained 50bp sequences homologous to 3' end of *tir*, while the 5' end of the *Citro* tirTEMkn315 (rv) primer contained 50bp sequences homologous to the non-coding sequences directly after the end of *tir.* The primers were designed to ensure that the *effector-TEM* gene fusion, through homologous recombination at the flanking sites, occurred with minimum disruption to the *C. rodentium* LEE genes (Fig. 3.2.6).

The resulting PCR product (Fig. 3.2.7) was purified and electroporated into the *C. rodentium* strain expressing the λ-Red recombinase system (*Citro* pKD46). In theory, this process of homologous recombination should create a chromosomally encoded fusion between *tir* and TEMkn315, resulting in the expression of *tir* from its native promoter in the *C. rodentium* chromosome. However, despite many attempts to electroporate the TEMkn315 DNA fragment into *C. rodentium*, including the use of longer homology extensions in the PCR primers and increasing the concentration of the insert DNA, we were unable to isolate any positive transformants, as verified by PCR analysis (Fig. 3.2.8).

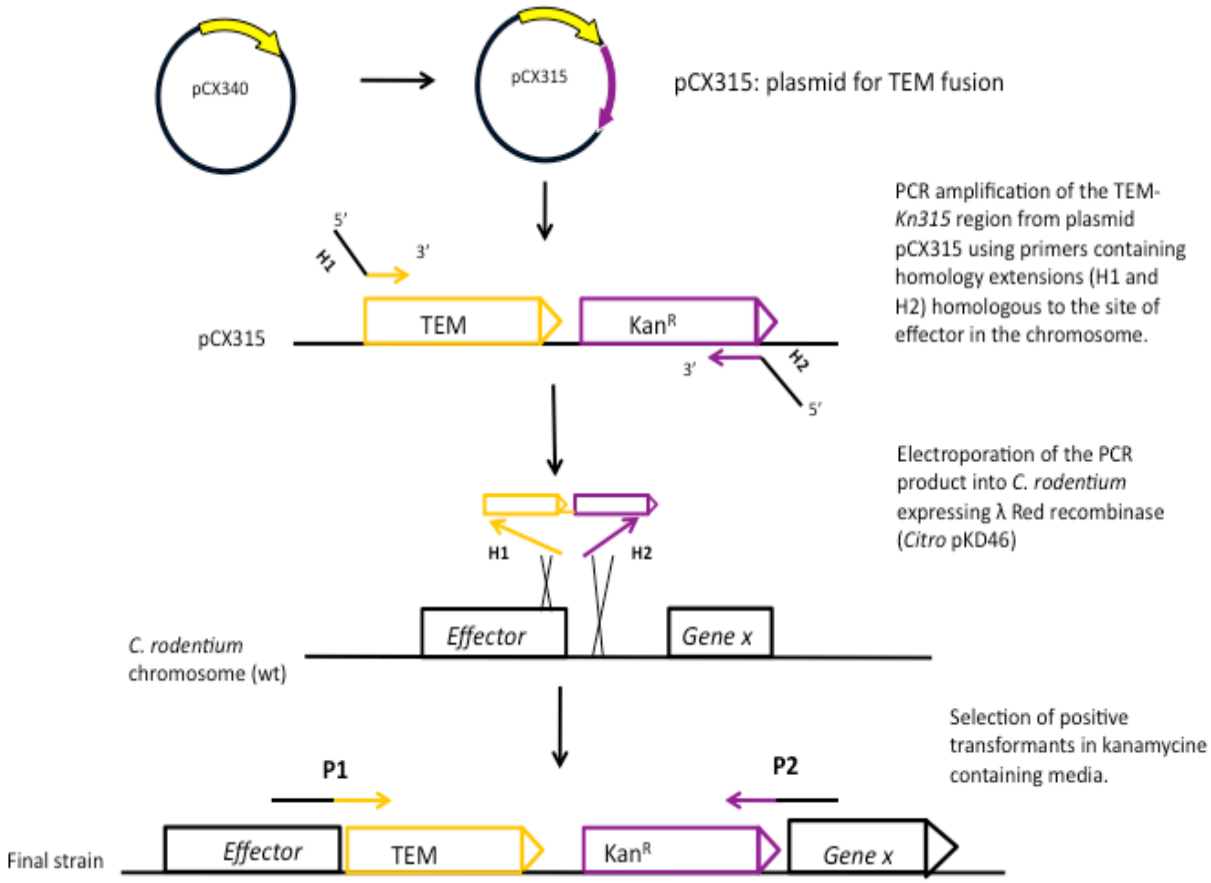

Figure 3.2.6 Overview of a chromosomally encoded effector fusion using pCX315. To construct a chromosomal effector fusion with TEM-1, the TEMkn315 region from the pCX315 was PCR-amplified using primers with flanking DNA homologous to the chromosomal effector site. The resulting PCR product was electroporated into a λ Red recombinase expressing *C. rodentium* strain and selected on kanamycin-containing media.

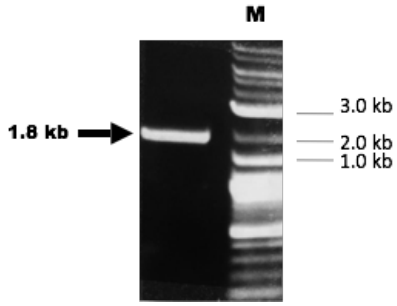

Figure 3.2.7: PCR product (TirTEMkn315) for homologous recombination. PCR amplification of the TEMkn315 region (1.850 kb) from pCX315 plasmid using primers TirTEMkn315 (fw) and TirTEMkn315 (rv).

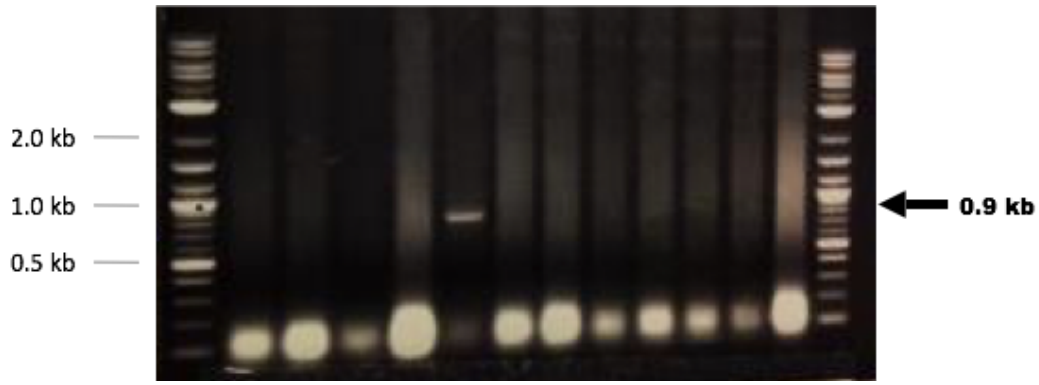

Figure 3.2.8: Verification of the chromosomally encoded TirTEMkn315 fusion. Colony PCR using primers pCX340 (fw) and pCX340 (rv) of overnight cultures grown from the electroporation of TEM-kn315 into *Citro* pKD46. The presence of a 1.045 kb band size would indicate that successful homologous recombination had taken place. Therefore, the absence of this band confirms our inability to generate the strain *Citro* TirTEMkn315.

3.2.2.3 Homologous recombination with *nled*

Facilitated by the *C. rodentium* genome sequence (www.sanger.ac.uk) bioinformatics analysis comparing the AE pathogens revealed the presence of many novel and putative effectors in *C. rodentium.* Additional studies using proteomics and genetic screens have determined that some of these potential effectors are translocated into host cells by the LEE-encoded TTSS, but not encoded within the LEE (Gruenheid et al, 2004; Deng et al, 2004; Marches et al, 2005; Li et al, 2006; Garcia-Angulo et al, 2008).

The non-LEE-encoded D (*nleD*) gene, present in pathogenicity islands (PAIs) outside the LEE (Deng et al, 2004), was shown to encode NleD, which is highly translocated into HeLa cells (Marches et al, 2005) through the LEE-encoded T3SS (Deng et al, 2010). Although a signature-tagged mutagenesis screen showed NleD to be essential for the colonisation of the bovine gut by EHEC (Dziva et al, 2004), the role of NleD in virulence has not been established in mouse or lamb infection models. For example, the deletion of NleD had no effect on EHEC colonisation of calves or lambs (Marches et al, 2005) or on *C. rodentium* colonisation of mice (Kelly et al, 2006). The *nleD* gene exists as two copies in the *C. rodentium* genome (Kelly et al, 2006); this may be advantageous in the creation of chromosomal gene fusions. If, for example, the translational fusion with TEM-1 resulted in a gene disruption, it would not affect the overall phenotype of *C. rodentium* due to gene redundancy whereby the intact second copy of the chromosomal *nleD* would compensate. As a result, the NleD effector was chosen for the creation of translational fusion protiens with TEM-1.

To create a translational fusion with TEM-1, the TEMkn315 construct was PCR-amplified from pCX315 using primers *Citro* nleDTEMKn315 (fw) and *Citro* nleDTEMKn315 (rv). The resulting PCR product (1850bp) contained the TEMkn315 construct with flanking regions homologous to the *nleD* gene. However, upon electroporation of the PCR product into λ-Red recombinase-expressing *C. rodentium*, we were unable to isolate any positive transformants in which homologous recombination had taken place (Fig. 3.2.9).

Despite PCR amplification of the TEMkn315 construct under optimized conditions and verification of its size through gel electrophoresis as well as removal of residual impurities through PCR purification via QIAquick column (Qiagen), the resulting

PCR product did not undergo homologous recombination at the chromosomal target site. Since recombineering did not occur at the *tir* or the *nleD* site of the *C. rodentium* chromosome, it may have been useful to analyze the TEMkn315 PCR product by DNA sequencing. In an attempt to further identify the source of the problem, electroporation experiments using control PCR products such as a kanamycin resistance cassette would be very useful. To do so, the kanamycin resistance cassette would be PCR amplified using primers containing flanking regions homologous to the *nleD* gene. This would generate a PCR product that is suitable to undergo homologous recombination at the chromosomal *nleD* site as well as enable the selection of positive transformants on kanamycin containing plates following electroporation into electrocompetent *C. rodentium* cells. Since the control PCR product would be the same as the TEMkn315 PCR product but without the TEM region, the use of such control experiments would help to identify if the source of the problem was associated with the pCX315 plasmid or the TEM gene. Due to time constraints however, we decided to explore alternative strategies to generate chromosomally encoded fusions.

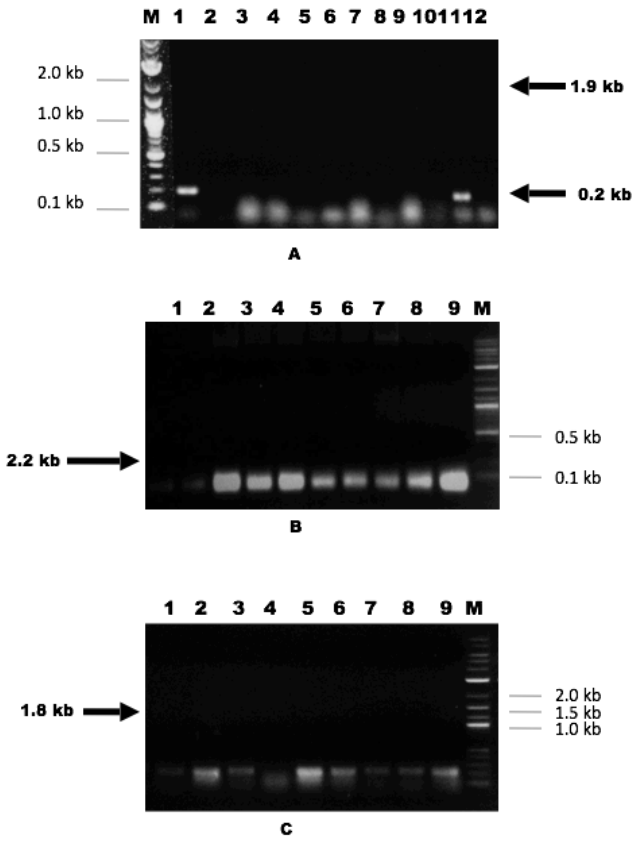

Figure 3.2.9. Verification of the nleDTEMkn315 chromosomally encoded fusion. Colony PCR of overnight *C. rodentium* cultures (electroporated with TEMkn315) using primers (A) pCX340endTEM (fw) and pCX340endTEM (rv), (B) pCX340endTEM(fw) and Kn315 (rv), and (C) nleDTEMkn315 (fw) and nleDTEMkn315 (rv). No bands were observed.

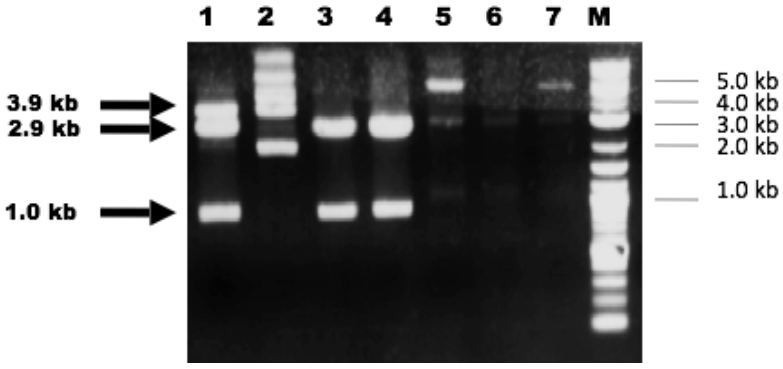

Figure 3.2.10: Cloning using pJETkn315. BglII restriction digestion of pJETkn315 resulting in 2.928 kb and 1.063 kb DNA fragments (lane 2-4). Undigested pJETkn315 plasmid with a band size of 3.991 kb (lane 5) is shown for comparison. Although the TEM-kn315 was successfully cloned into the pJET cloning vector, subsequent PCR amplification of this region resulted in a PCR product that did not undergo homologous recombination.

3.2.2.4 The *xylE* locus

An alternative strategy to generate a chromosomally encoded fusion was explored using the *xylE* locus. A housekeeping gene expressed in most bacterial cells, *xylE* encodes the XylE protein, which is involved in xylose transport in *E. coli* K12 but is not essential for bacterial survival. In previous studies, the *xylE* locus was manipulated to insert a gene of interest into the *C. rodentium* chromosome, such that the disruption of the *xylE* gene did not change bacterial virulence. For example, the disruption of the *xylE* gene to insert an antibiotic resistance cassette and a LUX transposon reporter gene into the *xylE* locus caused no effect on the virulence of *C. rodentium* (Wiles et al, 2004).

Similarly, Girard et al (2009) created a chromosomally encoded insertion of TccP (a T3SS effector also known as $EspF_U$) in the *xylE* locus of *C. rodentium*. This was done by sequentially cloning the 5' and 3' ends of the *xylE* gene into the AseI and XmnI sites of the pACYC184 plasmid, thus generating the plasmid pICC440 from which the cloning of *tccP* into the EcoRV/BamHI sites produced the plasmid pICC441. PCR amplification of the pICC441 plasmid construct—containing *5' xylE*, the tetracycline promoter *tccP*, the chloroamphenicol resistance cassette, and *3' xylE*—was subsequently used for homologous recombination of *tccP* into the *xylE* locus (Girard et al, 2009). Using this strategy, we wanted to create a chromosomally encoded *effector-TEM* fusion in the *xylE* locus (Fig. 3.2.11). One advantage of this strategy is the increased efficiency of homologous recombination, due to the presence of longer homology extensions (150 bp) compared to the 50 bp homologies used in the previous strategy with plasmid pCX315. In addition, the creation of the gene fusion in the *xylE* locus should ensure that the *effector-TEM* fusion is encoded chromosomally without disrupting the organisation of effector genes in their native sites, thereby having no effect on the overall growth and virulence of *C. rodentium.*

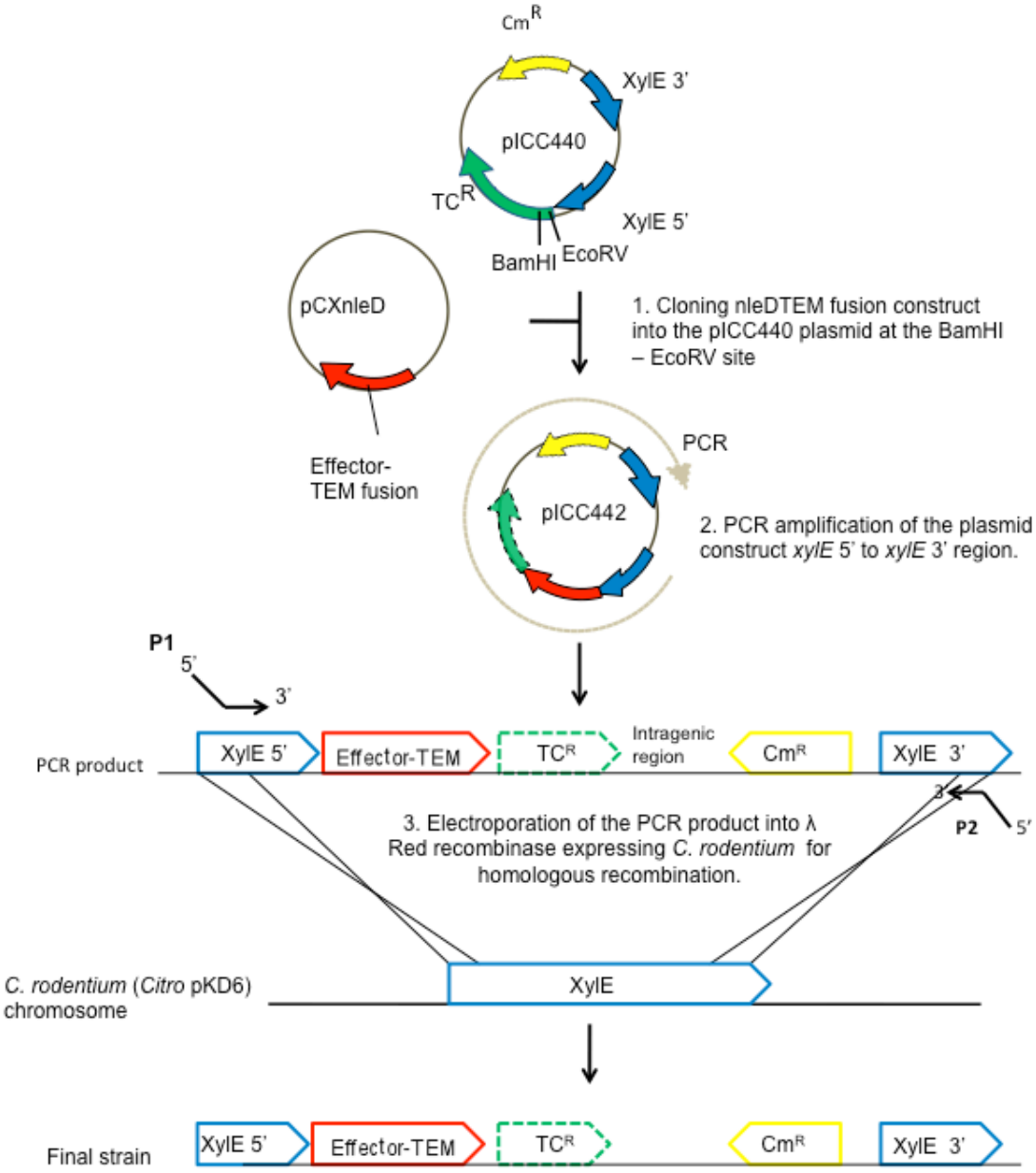

Figure 3.2.11 Overveiw of the chromosomally encoded nleDTEM fusion at the xylE locus. To construct a gene insertion within the *xylE* locus, the pICC442 plasmid was first created by cloning the *nleDTEM* gene fusion at the BamHI and EcoRV site of the pICC440 plasmid. The resulting pICC442 plasmid was subsequently PCR amplified from the xylE5' to xylE3' region containing the *nleDTEM* gene fusion, and electroporated into λ Red recombinase-expressing *C. rodentium*. Homologous recombination between the PCR product and the bacterial chromosome should result in the disruption of the *xylE* gene and insertion of the *nleDTEM* fusion construct into the *C. rodentium* chromosome.

3.2.2.5 Construction of pCXnleD

To create the *nleDTEM* gene fusion, we needed to clone the *nleD* gene into the pCX340 plasmid containing TEM-1 (Fig. 3.2.12). This was done by PCR-amplifying a 776bp fragment containing the *nleD* gene from *C. rodentium* genomic DNA using the primer pair nleDNdeI (fw) and nleDEcoRI (rv). The primers contained homology extensions to the restriction sites NdeI and EcoRI, which are located within the multiple cloning site (MCS) upstream of *TEM-1* in the pCX340 plasmid. The PCR product was then purified and TA cloned into the TOPO cloning vector to generate the plasmid pCR2.1nleD. The pCR2.1nleD plasmid, following confirmation by colony PCR and sequence analysis, was digested with NdeI and EcoRI restriction enzymes and ligated into the cut pCX340 (Fig. 3.2.13). The resulting pCXnleD plasmid, containing the *nleDTEM* construct (1505bp), was electroporated into *C. rodentium* to generate the strain *Citro* pCXnleD*,* which was verified by colony PCR and DNA sequence analysis (Fig. 3.2.14).

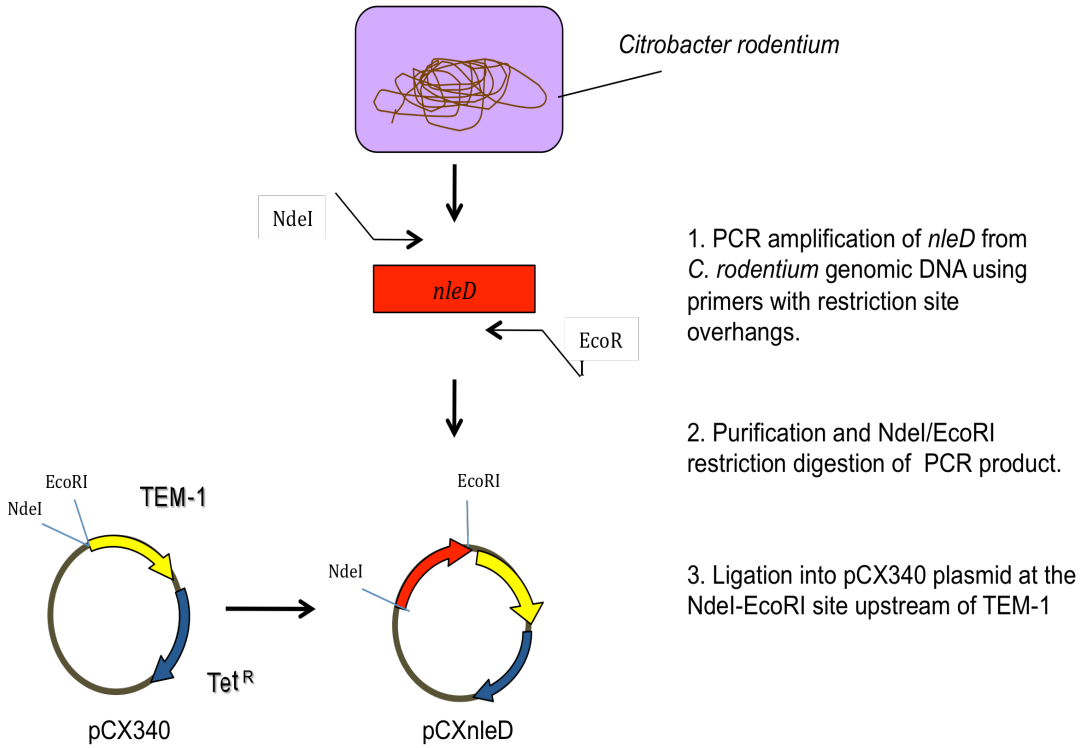

Figure 3.2.12. Overview of pCXnleD plasmid construction. To create a gene fusion between the effector and TEM-1, the *nleD* gene was PCR amplified using primers containing restriction site overhangs. The resulting PCR product was digested using restriction enzymes NdeI and EcoRI, and ligated into the pCX340 plasmid upstream of TEM-1, generating the plasmid pCXnleD.

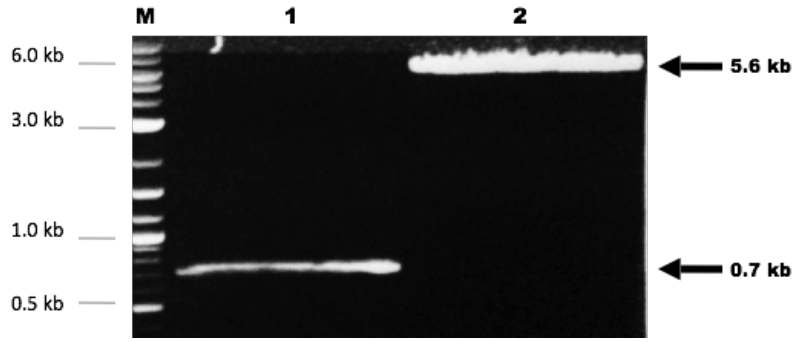

Figure 3.2.13 Construction of plasmid pCXnleD. EcoR1 and Nde1 restriction digestion of NleD insert (lane 1) and pCX340 vector (lane 2).

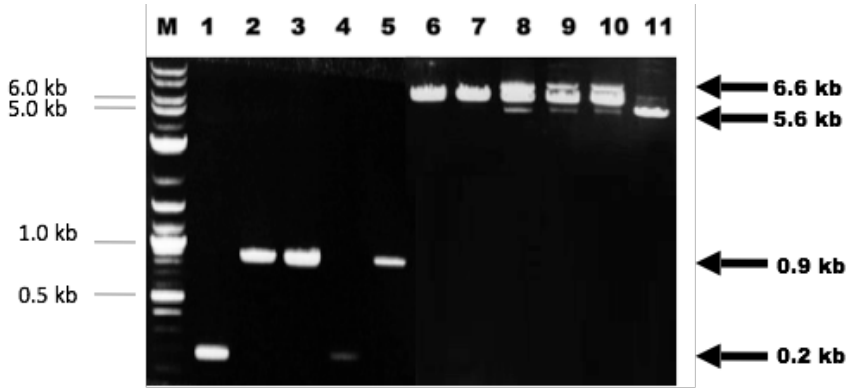

Figure 3.2.14 Verification of pCXnleD. Colony PCR using primers 94 (fw) and 95 (rv) to confirm the insertion of nleD into pCXnleD (lane 2-5) and its absence in pCX340 (lane 1). Primers 94 and 95 are located just outside the nleD insert in pCXnleD, and hence the resulting PCR products would have a fragment size of 0.9 kb in pCXnleD and 0.2 kb in pCX340. EcoRl digestion confirms the presence of pCXnleD (6-10) and pCX340 (11).

3.2.2.6 Construction of pICC140

To construct plasmid pICC442, the *nledTEM* gene fusion was cloned from plasmid pCXnleD and into plasmid pICC440 containing the 3' and 5' ends of the *xylE* gene. This was done by PCR-amplifying the *nleDTEM* region from pCXnleD using the primers EcoRV-rbs-nleD (fw) and BamHI-stopTEM (rv). The PCR product was TA-cloned, (Fig. 3.2.15), cut using EcoRV/BamHI restriction enzymes, and ligated into the EcoRV/BamHI sites located between the 3' and 5' ends of the *xylE* gene (Fig. 3.2.16). Subsequent PCR of the plasmid pICC442 using the primers aseI-N-xylE (fw) and xmnI-C-xylE (rv) produced a PCR construct (5.527kb) containing 5' *xylE, nleDTEM*, the chloramphenicol resistance cassette, and 3' *xylE*. However, several difficulties were encountered in obtaining the PCR product. For example, PCR amplification produced a strong band at 1kb and a very weak band at the required 5.5kb size (Fig. 3.2.17 - 3.2.18). One possible reason for this that the efficiency of the Taq polymerase enzyme is reduced when it amplifies DNA fragments larger than 4kb. The 5.5kb PCR product may have been produced at the right size, purified, and electroporated into *C. rodentium* for homologous recombination at the *xylE* locus; but no colonies were observed the following day (Fig. 3.2.21). Consequently, PCR optimisation experiments were carried out using different polymerase enzymes (PFU, phusion and deepvent), different PCR conditions, and various thermocycler programmes, including the use of a Tm gradient (Fig 3.2.17-1.2.21). Eventually this strategy was discontinued due to time constraints.

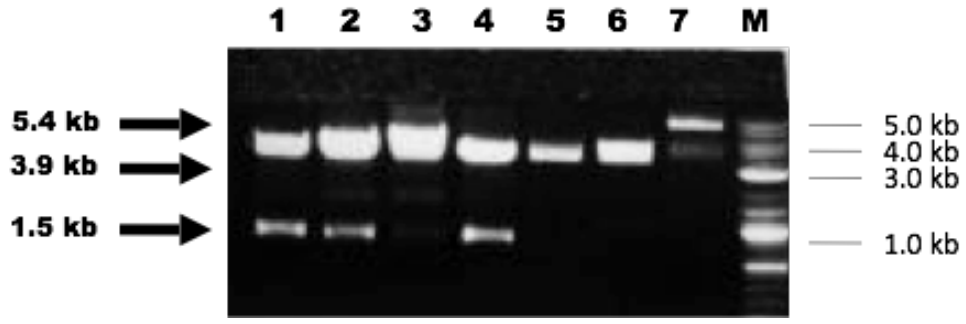

Figure 3.2.15 Verification of plasmid pCR2.1TOPOnleDTEM. EcoRI restriction digestion of pCR2.1TOPOnleDTEM (lane 1-5) and pCR2.1TOPO empty vector (lane 6). Undigested pCR2.1TOPOnleDTEM (lane 7) is shown for comparison. The EcoRI restriction sites are located on either side of the insert region in the TOPO vector.

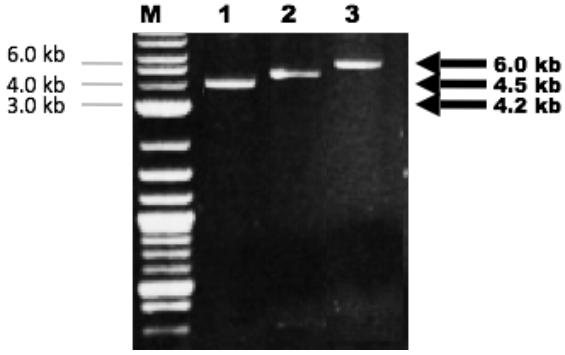

Figure 3.2.16 Construction of plasmid pICC442 in various stages. Gel electrophoresis of plasmid pACYC184 (1), pICC440 (2) and pICC442 (3).

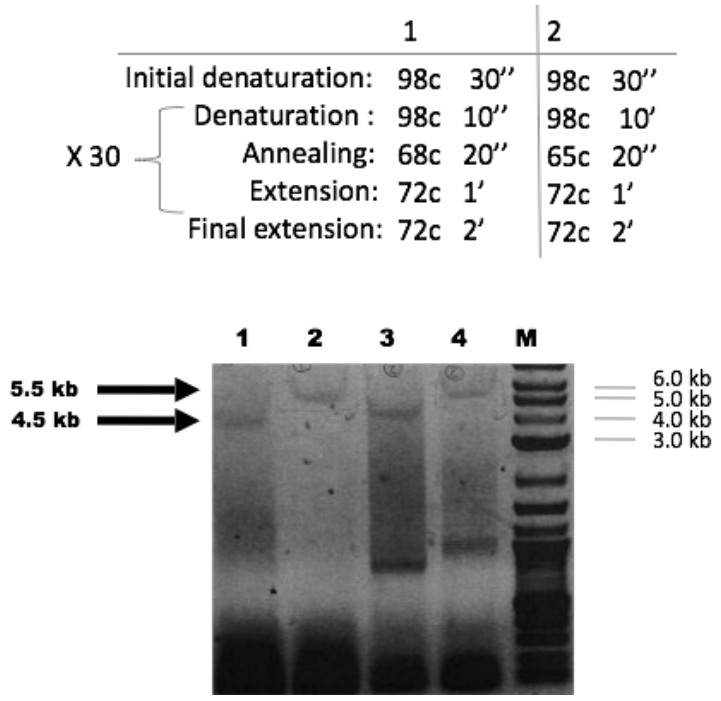

Figure 3.2.17 PCR optimisation I. PCR amplification of pICC440 (lane 1) and pICC442 (lane 2) using PCR programme 1, as well as pICC440 (lane 3) and pICC442 (lane 4) using PCR programme 2. The primer pair XmnI-C-xylE (fw) and AseI-N-xylE (rv) was used.

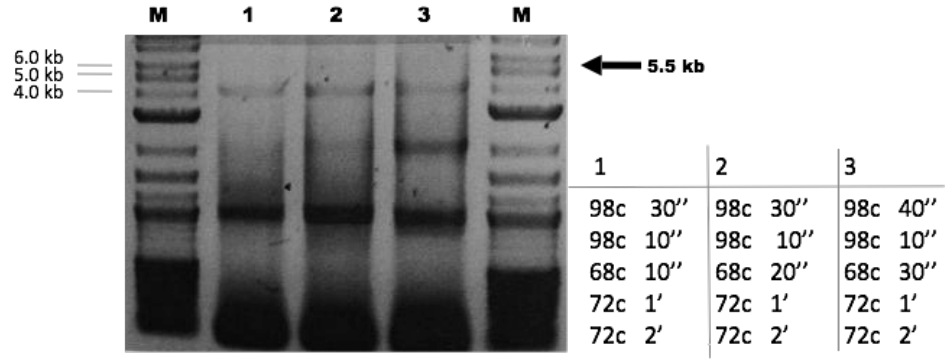

Figure 3.2.18 PCR optimisation II. PCR amplification of pICC442 using the above primers XmnI-C-xylE (fw) and AseI-N-xylE (rv) under various PCR programmes.

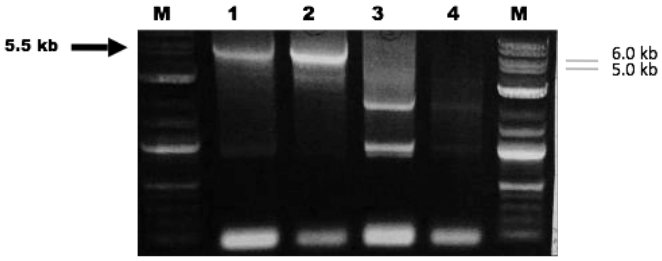

1	2	3	4
98c 10''	98c 10''	98c 30''	98c 30''
98c 10''	98c 10''	98c 10''	98c 10''
68c 20''	75c 20''	68c 20''	81c 20''
74c 2'	74c 2'	72c 2'	72c 2'
74c 3'	74c 3'	72c 3'	72c 3'

Figure 3.2.19 PCR optimisation III. PCR amplification of pICC442 using primers XmnI-C-xylE (fw) and AseI-N-xylE (rv) under various different PCR programmes.

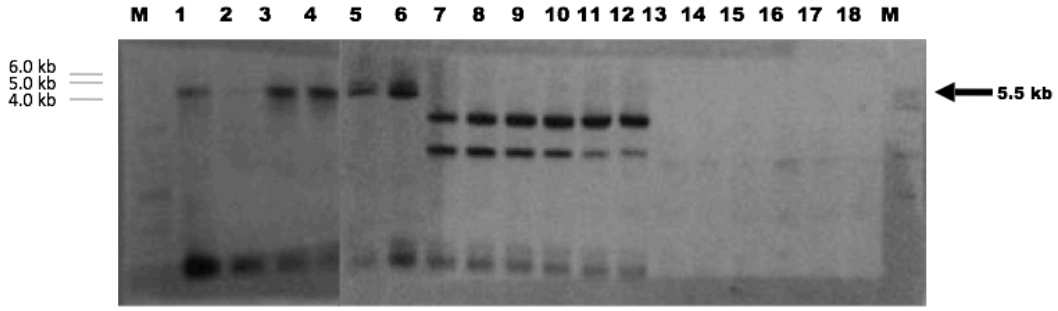

	Tm gradient					
Polymerase	61.3	63.1	64.6	66.6	68.3	69.2
Taq	1	2	3	4	5	6
Phusion	7	8	9	10	11	12
Deepvent	13	14	15	16	17	18

94c 2'
95c 20''
65c 30'' Δ10c
72c 2'
72c 3'

Figure 3.2.20 PCR optimisation IV. PCR amplification of pICC442 using primers XmnI-C-xylE (fw) and AseI-N-xylE (rv) with various polymerases including Taq (lane 1-6), Phusion (lane 7-12) and Deepvent (lane 13-18) under a Tm (annealing temperature) gradient.

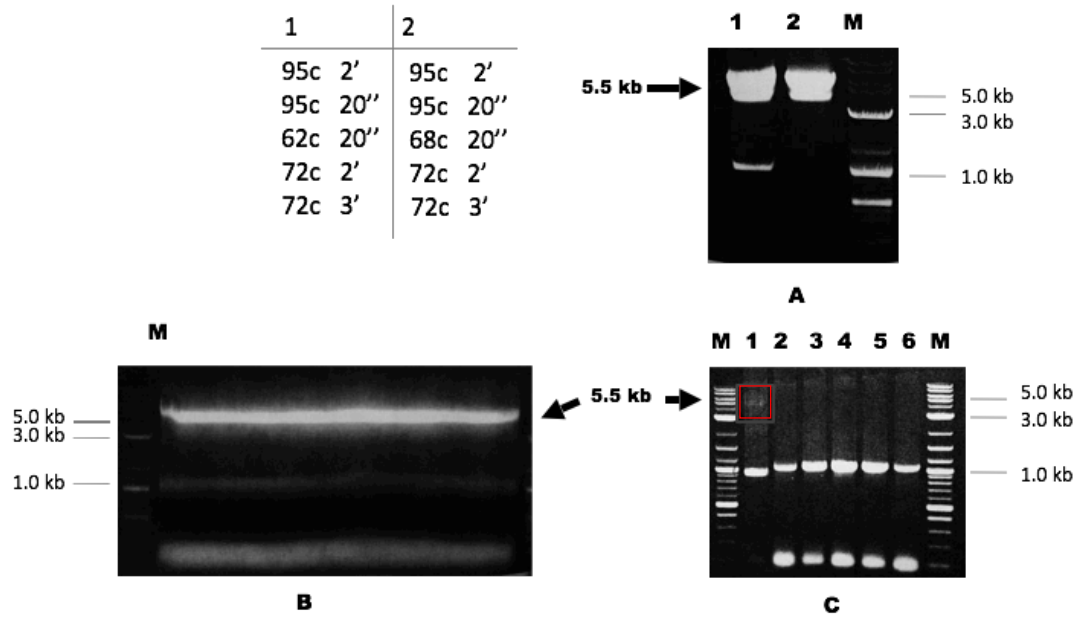

Figure 3.2.21 Generating PCR product (5'xylE-nleDTEM-3'xylE) for homologous recombination. (A) PCR product (5.572kb) from the amplification of pICC442 using the primer pair XmnI-C-xylE (fw) and AseI-N-xylE (rv) under two different thermocycler programmes. (B) PCR product (pooled from 10 tubes for increased concentration of DNA) using the same PCR conditions as (2) from (A) prior to electroporation. (C) Colony PCR of transformed *C. rodentium* to verify the chromosomal insertion of 5'xylE-nleDTEM-3'xylE following homologous recombination in *C. rodentium*.

3.2.3 Construction of a plasmid encoded reporter fusion

Having tried and failed with several cloning strategies to generate a chromosomally encoded fusion, we decided to construct the *nleDTEM* gene fusion on a plasmid. Although we had previously generated the pCXnleD plasmid encoding the NleDTEM fusion protein, we needed to use a more stable plasmid suitable for *in vivo* studies in mice. The pACYC184 plasmid has been used previously for *in vivo* studies involving *C. rodentium* (Mundy et al, 2003; Mundy et al, 2004; Kelly et al, 2006). The plasmid pACYC184 (Fig 3.2.22) is an *E. coli* cloning vector that contains a p15 origin of replication, has a low copy number at about 15 copies per cell, and carries a gene encoding resistance to tetracycline (Tc^R) and another encoding resistance to chloramphenicol (Cm^R) (www.neb.com).

To clone the *nleDTEM* gene fusion into plasmid pACYC184 (3.2.23), a 1.5kb region containing the *nleDTEM* construct was amplified by PCR from plasmid pCXnleD using the primers Ecorv-rbs-nleD (fw) and BamHI-stop-TEM (rv). The PCR product was TA-cloned into pCR2.1TOPO, digested, and ligated into pACYC184 at the EcoRV/BamHI site (Fig 3.2.24). The resulting pACYCnleD plasmid construct (5.579kb) was verified and transformed into *C. rodentium* to generate the strain *Citro* pACYCnleD. Overnight colonies were selected on chloroamphenicol plates and confirmed by colony PCR (Fig. 3.2.25).

To ensure plasmid transformations occur with efficiency, various control experiments can be useful. For instance, the transformation of uncut plasmid vectors into competent cells can enable the verification of competent cell viability and the antibiotic resistance of the plasmid, provided that the corresponding antibiotic is used in the agar media. Additionally, the transformation of cut plasmids without an insert can help to determine the amount of background due to undigested plasmid, since efficient restriction digestion should produce only digested plasmids that cannot circularize and grow into colonies. A third control experiment could include the transformation of a cut plasmid vector that has undergone ligation reaction to determine if the plasmid can re-ligate in the absence of the insert. In the case where a single restriction enzyme has been used, the ends of the vector DNA should be compatible and easily joined during the ligation reaction resulting in the growth of bacterial colonies. In the case where vector has undergone double digestion with two

restriction enzymes, two incompatible ends would be generated that are unable to re-ligate and produce colonies. The use of such control experiments would have greatly improved the reliability of the plasmid transformations carried out in this study and may have provided good insight into where things have gone wrong in case plasmid transformation experiments failed.

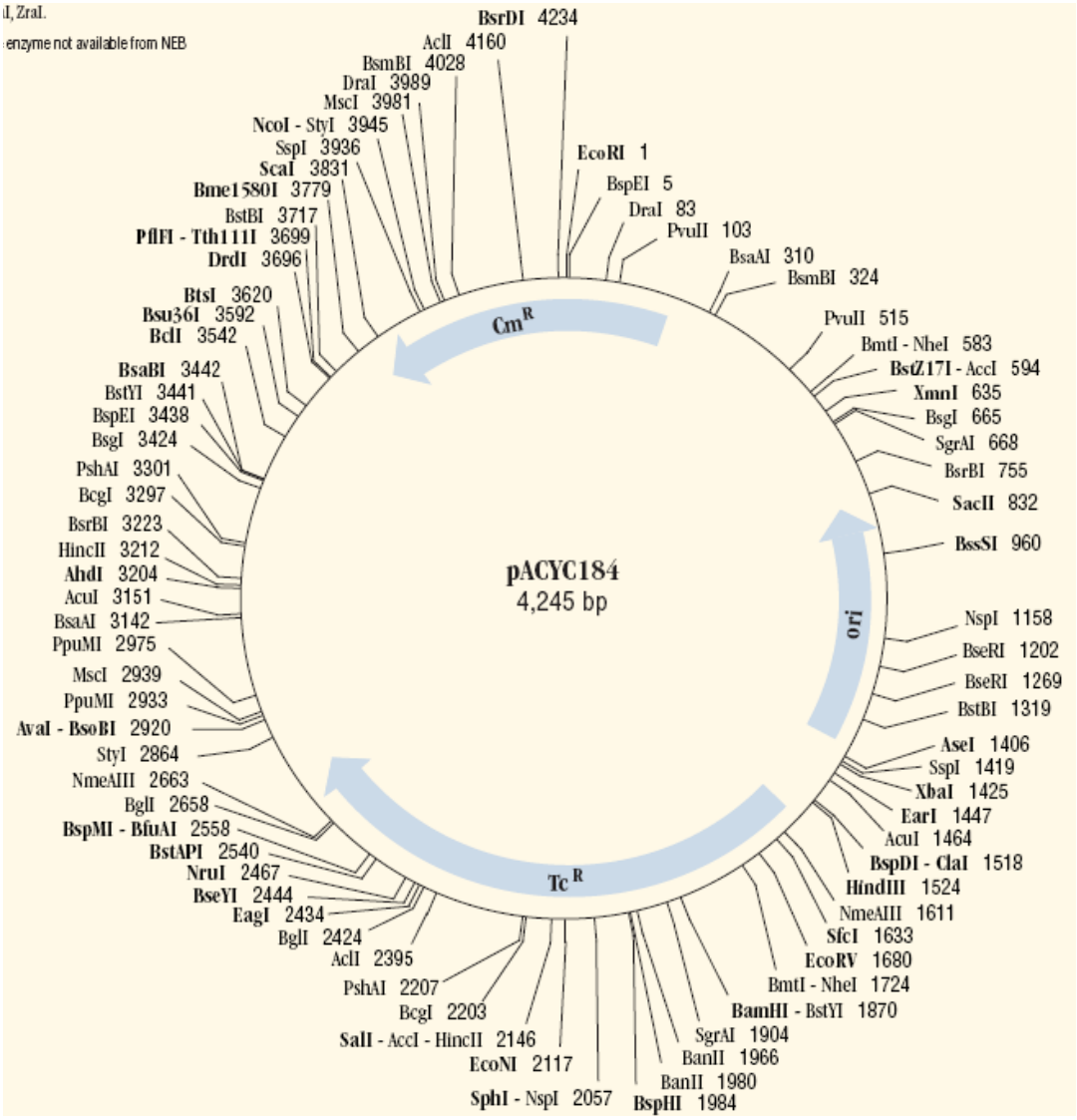

Figure 3.2.22 Map of the pACYC184 plasmid. This is a low-copy plasmid encoding resistance to chloroamphenicol and tetracycline. The presence of numerous restriction sites enables the cloning of a gene of interest into the desired location in the pACYC184 plasmid. Taken from www.neb.com.

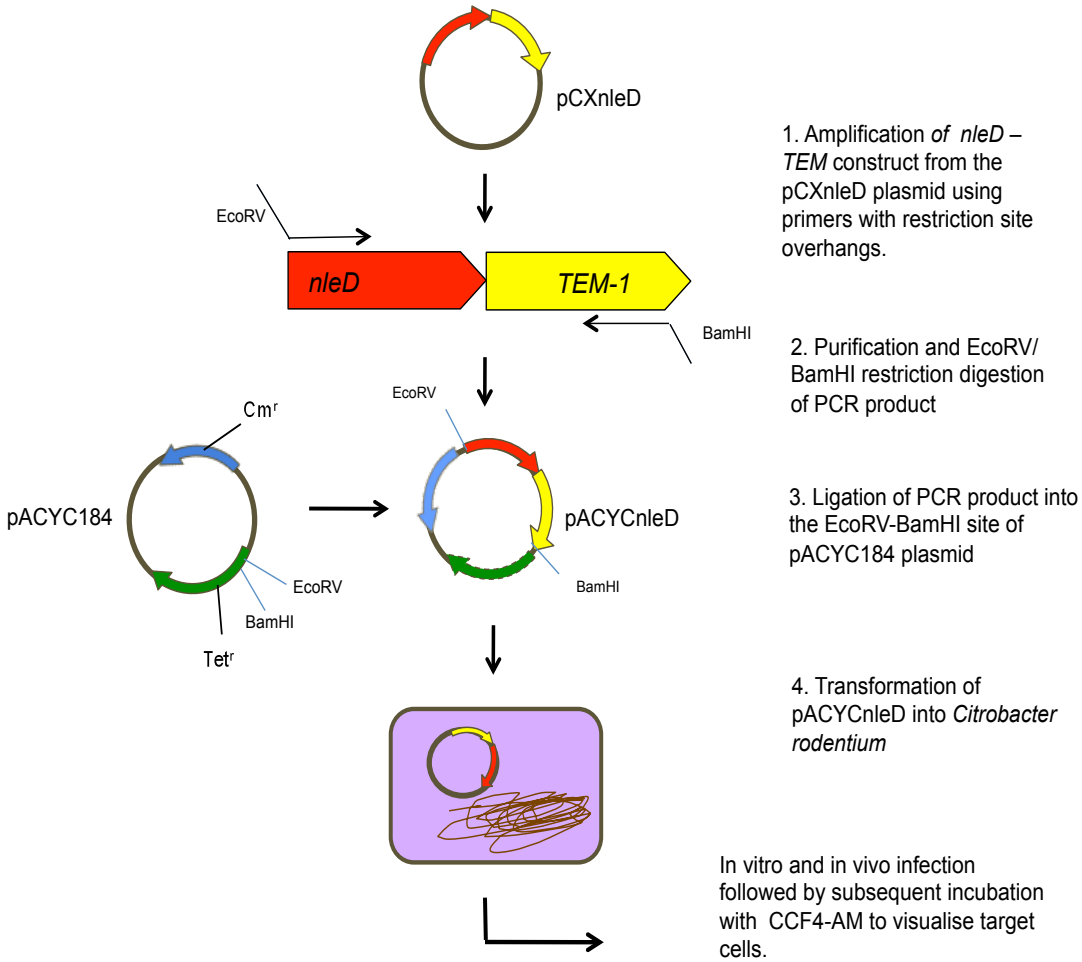

Figure 3.2.23 Overview of the pACYCnleD plasmid construction. To create a plasmid-encoded fusion, the nleDTEM construct was PCR-amplified using primers containing the restriction sites EcoRV and BamHI, and the PCR product was cut and ligated into the EcoRV-BamHI site of the pACYC184 plasmid vector. The resulting pACYCnleD plasmid was transformed into *C. rodentium*, which was subsequently used for *in vivo* and *in vitro* infection studies.

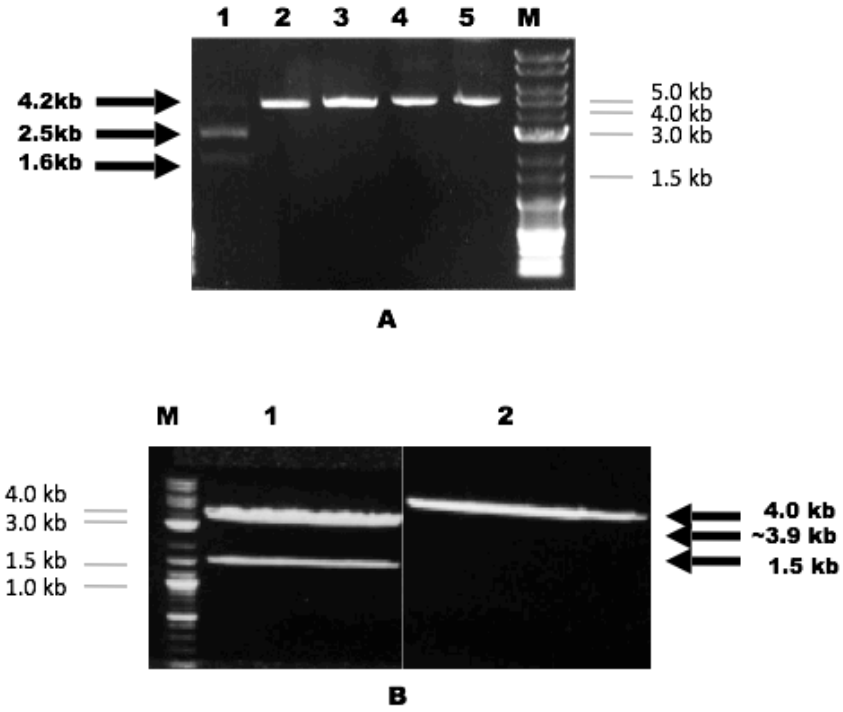

Figure 3.2.24 Construction of plasmid pACYCnleD. (A) Restriction digestion of pACYC184 using EcoRI and EcoRV restriction enzymes (lane 1), EcoRI (lane 2), and EcoRV (lane 3) along with undigested plasmid (lane 4-5). (B) EcoRV and BamHI digestion of pACYC184 (lane 2) and pCR2.1TOPOnleDTEM (lane 1) to generate the vector and insert for ligation.

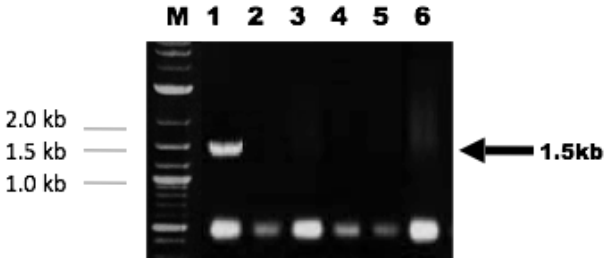

Figure 3.2.25 Verification of plasmid pACYCnleD. Colony PCR of pACYCnleD (lane 1-5) and pACYC184 empty vector (lane 6) using primers NleD-rbs-EcoRV (fw) and BamH1-stop-TEM1 (rv). Positive transformants produced a band at 1.504 kb, confirming the insertion of *nleDTEM* into the pACYCnleD plasmid.

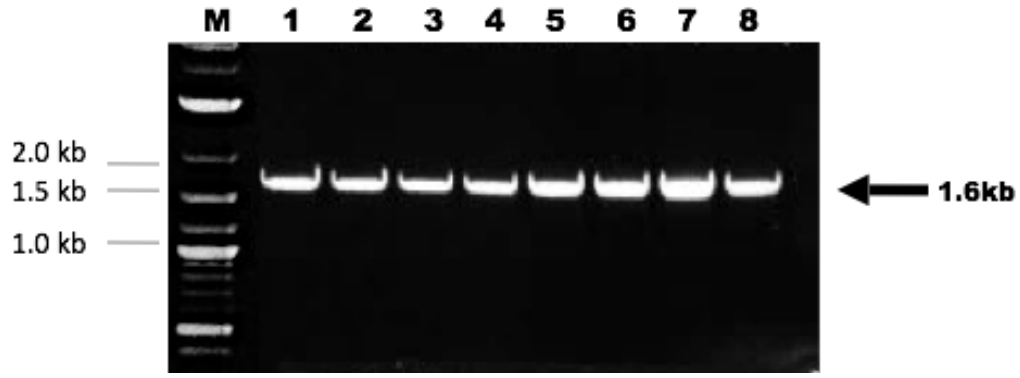

Figure 3.2.26: Verification of the presence of pACYCnleD in the reporter strain and the control mutant strain. PCR product of pACYCnleD using primer pair pACYCtc (fw) and pACYCtc (rv) in various cultures of *Citro* pACYCnleD (1-4) and *Citro* ΔescNpACYCnleD (5-8). These primers are located just outside the *nleDTEM* insert within the pACYCnleD plasmid, such that strains containing the pACYCnleD plasmid produced a DNA fragment of 1680bp.

3.3 Discussion

The aim of this study was to generate a reporter *C. rodentium* expressing the ß-lactamase fusion protein to allow visualisation of *in vivo* effector translocation into immune cells. Having first tried and failed with several methods to create a chromosomally encoded effector fusion, we constructed the gene fusion on a low-copy pACYC184 plasmid. The results of this study confirm that *Citro* pACYCnleD is able to encode the fusion proteins NleDTEM, which is translocated into murine cells in a type 3-dependent manner by *C. rodentium*.

Our inability to generate a chromosomally encoded effector fusion may be associated with the use of the λ Red recombinase system in *C. rodentium*. The λ Red recombinase system, mostly described in *E. coli* (Marches et al, 2003; Garmendia et al, 2004; Nadler et al, 2006; Hemrajani et al, 2008; Jaeger et al, 2004; Umanski et al, 2002; Creuzberg et al, 2005; Dahan et al, 2005; Tu et al, 2003; Baba et al , 2006; Zhang et al, 2004; Kang et al, 2004), where it was originally developed to disrupt and replace chromosomal genes with an antibiotic selection marker (Datsenko and Wanner, 2000), has only rarely been described in *C. rodentium* (Kelly et al, 2006; Angulo et al, 2008; Dong et al, 2009). It is possible that the efficiency of λ Red-mediated homologous recombination, which varies across bacterial species, may be reduced in *C. rodentium* in comparison to *E. coli*. A recent study demonstrated that mutations in the bacterial host replication machinery can reduce the efficiency of λ Red mediated recombination with electroporated DNA species (Poteete, 2013). Although the presence of such mutations has not been reported in *C. rodentium*, the study by Poteete et al. (2013) does suggest the possibility of host interference with λ Red-mediated homologous recombination. However, the use of the λ Red recombinase system to replace the *escN* gene with a kanamycin resistance cassette proved successful for the creation of the *Citro ΔescN* mutant. This indicates that the process of λ Red-mediated homologous recombination in *C. rodentium* is not affected by the host cell machinery, and therefore this does not explain why we were unable to obtain *C. rodentium* colonies that had undergone homologous recombination to produce a chromosomally encoded effector fusion with TEM-1.

In this study, an alternative strategy to create a chromosomally encoded fusion was investigated using the *xylE* locus. A PCR product containing *5' xylE*, a tetracycline promoter, nleDTEM, a chloramphenicol resistance cassette, and *3' xylE* was generated and electroporated into λ Red-expressing *C. rodentium* cells to enable the insertion of an *nleD-TEM* fusion within the chromosomally encoded *xylE* gene. However, as we were unable to obtain any positive transformants, it is possible that homologous recombination of the PCR product occurred with the chromosomal copy of the *nleD* gene rather than with the *xylE* gene. Although the growth of positive transformants in media containing chloroamphenicol and tetracycline should have selected the *C. rodentium* cells, which had recombined at the *xylE* gene and not the *nleD* gene, the lack of colonies observed on the plates containing antibiotics suggests that the *C. rodentium* cells probably did recombine at the *nleD* gene and not the *xylE* gene. The fact that the PCR product contained another *C. rodentium* chromosomal gene (*nleD*) in addition to *xylE* was not discovered until the end of this study. This problem was not encountered by previous studies (Wiles et al, 2004) because the genes used to disrupt the *xylE* locus were not present in the genome of wild type *C. rodentium*. In the future, such factors must be taken into consideration when using similar strategies to integrate DNA at specific locations in bacterial chromosomes.

Regarding the initial strategy to create a chromosomally encoded Effector-TEM fusion, the lack of homologous recombination between the PCR product (containing TEMkn315) and the chromosomal effector may be explained by the size of the insert DNA, which may have reduced the efficiency of the recombineering process by λ Red. According to the Datsenko and Wanner (2000) strategy, λ Red-mediated recombination usually occurs between the chromosome and a small PCR fragment containing a single selectable marker and flanking regions homologous to the sequence of the desired insert site. In our study, however, the PCR fragment contained more than one gene, including a kanamycin resistant marker (*kn315*) and the β-lactamase reporter gene (TEM-1). Perhaps the presence of two genes resulted in a large insert fragment, which may have reduced the efficiency of the homologous recombination. Indeed, a recent study demonstrated a significant decrease in the efficiency of transformation and integration of DNA fragments with increasing size of the insert DNA; the number of successful recombinants obtained from overnight

plates reduced as the size of the insert DNA increased (Kuhlman & Cox, 2010), as shown in Fig. 3.3.1. As a result, no recombinants were obtained from the homologous recombination of insert DNA beyond the size of 2.5kb. In our study, we used an insert size of 1.9kb, which, according to the above study, should produce just over one hundred recombinants, though with very low efficiency of recombination. In comparison, the kanamycin gene (*kn315)* used to disrupt the chromosomal *escN* locus in this study was approximately 0.7kb in size and successfully produced many recombinants, thereby corroborating the finding by Kuhlman & Cox (2010) that success of homologous recombination improves with smaller insert fragments.

Further work is necessary to develop the Datsenko and Wanner (2000) method of λ Red-mediated gene disruption for the chromosomal integration of large DNA constructs. Kuhlman and Cox (2010) demonstrated the use of a 'landing pad' for the insertion of large DNA fragments at specific locations in the bacterial chromosome. The 1.3kb 'landing pad' is a tetracycline resistance gene flanked by I-SceI recognition sites. I-SceI recognition sites do not exist naturally within the bacterial chromosome and are cut by I-SceI homing endonucleases encoded in the yeast mitochondrial DNA. By introducing helper plasmids that express I-SceI endonuclease genes and by inserting I-SceI recognition sites in the desired chromosomal location, it is possible via homologous recombination to insert large DNA fragments in the bacterial chromosome. To use this method, the bacterial cell is first transformed with a helper plasmid carrying the genes encoding λ–Red enzymes and I-SceI endonuclease. Expression of the λ–Red genes facilitate the recombination of the landing pad (tetracycline resistance gene) into the desired chromosomal location. Following tetracycline selection of successful landing pad integrants, the bacterial cell is transformed with a donor plasmid carrying the insert fragment (also flanked by I-SceI recognition sites). The I-SceI recognition sites in both the insert fragment and the landing pad are cleaved and via homologous recombination, the insert DNA is incorporated into the landing pad. After successful chromosomal integration of the insert fragment, the I-SceI recognition sites are eliminated from the landing pad. In this manner, large constructs can be inserted at any desired location in the chromosome, which can be explored for future studies to generate a reporter *C. rodentium* expressing chromosomally encoded fusion proteins.

An alternative strategy to create a chromosomally encoded fusion may utilise a mutant strain of *C. rodentium* carrying a lacZΔM15 deletion to insert TEM-1 in a two-step, λ Red-mediated homologous recombination process. The first step would require the insertion of a *LacZα* gene adjacent to the effector in its native site in the chromosome. This would enable the selection of positive transformants (blue colonies) on agar plates containing x-galactose (x-gal). The second step would involve the disruption of the LacZα gene to insert the TEM-1 adjacent to the effector in its native site. Positive transformants (white colonies) would be selected on agar plates containing x-gal. A chromosomally encoded fusion would thus be constructed between the effector and TEM-1 using a smaller DNA fragment (containing a single gene) without the need of an antibiotic selection marker.

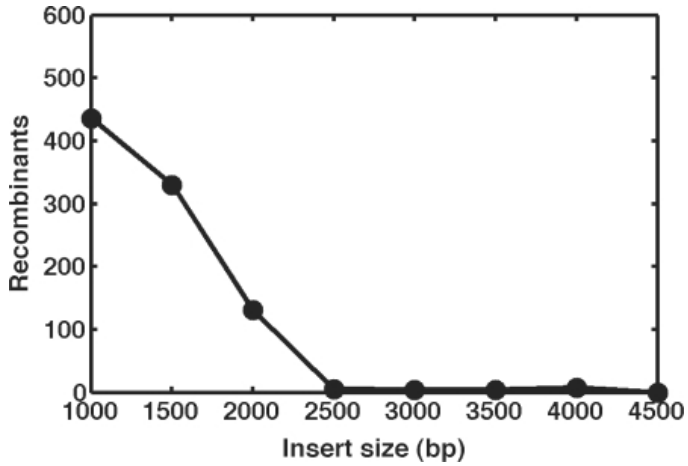

Figure 3.3.1 Representative recombineering efficiency as a function of insert size. Taken from Kuhlman and Cox (2010).

Although the chromosomally encoded reporter fusion is generally more physiologically relevant due to expression of the effectors under its native regulation, the use of a plasmid can also be advantageous for three reasons. First, a plasmid-encoded reporter fusion results in the constitutive expression of the fusion proteins, leading to increased activity of the reporter enzyme and thereby enabling stronger fluorescence to be detected by flow cytometry. Secondly, the dispensable nature of the plasmid allows the manipulation of bacterial genes without compromising host function. For example, a plasmid-encoded fusion would ensure that the chromosomal copy of the effector genes remained intact and would compensate for the loss of function of abnormal or defective effector proteins produced accidentally by genetic

manipulation (such as gene fusion). Thirdly, the use of a low-copy plasmid, such as one with a pACYC origin, would mean that the effector proteins are produced at physiological levels rather than at abnormal levels, as is the case with high copy plasmids where the proteins are over expressed. Moreover, the use of a low-copy plasmid ensures that the plasmid does not impose a metabolic burden on the host and may be more likely to remain stable even in the absence of antibiotic selection.

Indeed, our findings support previous studies wherein the majority of the experiments utilising the ß-lactamase reporter system to monitor effector injection in pathogens containing T3SS employed plasmid-encoded fusions. For example, Marketon et al. (2005) constructed the plasmid pHSG576 to carry the translational fusions of YopM-Bla in *Y. pestis,* while Koberle et al. (2009) used pAYCYC plasmid derivatives to construct YopE-Bla fusion proteins to study *Y. enterocolitica*. More recently, the low-copy vector pHSG576 was used to create translational fusions YopH-Bla, YopN-Bla, and YopJ-Bla in *Y. pestis* (Dewoody et al, 2011), which is similar to the plasmids pYopH-Bla and pYopJ-Bla that were constructed to study *Y. pseudotuberculosis* (Zhang et al, 2011). Similarly, β-lactamase (TEM-1) fusions with effectors NleC, NleD (Marches et al, 2005), and NleE (Vossenkaemper et al, 2010) were constructed on pCX340 plasmid derivatives to study EPEC effectors.

Nevertheless, the use of chromosomally encoded fusions of type 3 effector genes with ß-lactamase has been reported in *E. coli* (Mills et al, 2008). In the study by Mills et al. (2008), the chromosomally encoded fusion was created by first cloning the effectors EspF, EspG, EspH, EspZ, Map, and Tir, along with native promoters, into the pCX340 plasmid containing the TEM-1 gene. The resulting pCX340 plasmid derivatives were propagated in permissive strains and transformed into conjugation-competent permissive strains, where bacterial conjugation enabled the transfer and chromosomal integration of gene fusions to recipient cells when crossed with EPEC strains. Successful transconjugants contained the chromosomally integrated effector-*blaM* fusions placed under native regulation via homologous recombination (Mills et al, 2008). Therefore, for future studies it may be beneficial to explore the use of bacterial conjugation systems to generate a reporter strain of *C. rodentium* expressing chromosomally encoded effector fusions with TEM-1

Chapter 4: *In vitro* visualisation of mouse cells targeted for protein translocation by *C. rodentium*

4. *In vitro* visualisation of mouse cells targeted for protein translocation by *C. rodentium*

4.1 Introduction

The β-lactamase enzyme provides antibiotic resistance against antibiotics containing β-lactam, such as ampicillin, penicillin, and cephalosporin. It is encoded by the TEM-1 gene in many gram-negative bacteria, including *Escherichia coli*. β-lactamases work by catalysing the hydrolysis of the four-atom β-lactam ring, breaking it open and deactivating the antibiotic. The nucleotide sequence of β-lactamase enzyme was first determined by Sutcliffe et al. (1978), who identified a signal sequence made of the first 23 amino acids necessary for the secretion and maturation of the β-lactamase enzyme. Kadonaga (1984) further demonstrated that this enzyme is normally secreted into the periplasmic space, and deletion of the signal sequence prevents the protein secretion across the inner membrane, resulting in accumulation of β-lactamase within the bacterial cytoplasm. Hence, by mutating the signal sequences of the TEM-1 gene, it is possible to retain the β-lactamase enzyme inside the cell where it can carry out its activities against β-lactam antibiotics. Due to the increasing rise of antibiotic resistance across bacterial strains, β-lactamase-mediated cleavage of antibiotics has been studied extensively in the clinical setting.

However, the usefulness of β-lactamase as a reporter system was not appreciated until Zlokarnik et al. (1998) described the design and synthesis of a fluorescent substrate molecule containing a β-lactam ring, known as 7-hydroxycoumarine-3-carboxamide cephalosporin flourescin (CCF2). By linking a donor fluorophore (coumarine) and an acceptor fluorophore (fluorescin) to a cephalosporine bridge, a β-lactamase substrate molecule capable of carrying out efficient Fluorescence Resonance Energy Transfer (FRET) was created. This substrate was further esterified by acetoxymethylation (AM) to form CCF2-AM, which is lipophilic and readily enters the cell without causing any damage to it. Inside the cell, endogenous esterases convert CCF2-AM back to the free acid CCF2, which becomes negatively charged at physiological pH and trapped within the cell cytoplasm. Excitation of coumarine at a wavelength of 408 nm (UV) leads to a FRET between the coumarine and the fluorescin, producing a green fluorescence at 530 nm. However, in the presence of β-lactamase the cephalosporin is cleaved, separating the two fluorophores and allowing

the coumarine to produce a blue fluorescence at 460 nm instead. By measuring the fluorescence signals in the green and blue channels, the presence of β-lactamase in single cells can be detected with fluorescence microscopy and FACS analysis (Zlokarnik 2000).

Additional studies confirmed a lack of toxicity associated with substrate loading into mammalian cells. For example, the viability and proliferation of Jurkat cells remained unaffected after staining with CCF2, and zebrafish embryos were reported to have no developmental abnormalities after microinjection of CCF2 at the single-cell stage (Zlokarnik 1998). Therefore, the β-lactamase reporter system provides a very simple, sensitive, and accurate approach for the detection of gene expression in live systems.

Charpentier and Oswald (2004) were the first to modify and use the β-lactamase reporter system to detect effector injection by bacteria, carried out via the type three secretion system (T3SS). By creating translational fusion proteins between effectors and the β-lactamase gene (TEM-1), the study identified the secretion and translocation domain of an EPEC effector protein known as Cif (Charpentier and Oswald, 2004). The technology became popular and subsequently used to study the effects of protein injection by many T3SS-containing pathogens, including *Yersinia pestis* and its effects on host innate immunity (Marketon et al, 2005); *Yersinia enterocolitica* and its evasion of the host innate and adaptive immune system (Koberle 2009, Autenrieth 2010); and *Salmonella* and *Shigella* and its ability to rupture the host cell membrane for entry into host cytoplasm (Ray, 2010; Nothelfer 2014).

In addition to the study of invasive pathogens, the fluorescent-based reporter system has been useful in the study of type III-mediated secretion by non-invasive pathogens such as *EPEC*, *EHEC*, and *Citrobacter rodentium*. From characterising novel effectors (Marches 2005; Dahan 2005; Li 2006; Echtenkamp 2008) and defining new EPEC strains (Bulgin 2009) to elucidating the role of EPEC effectors in the manipulation of host cellular dynamics (Garmendia, 2004; Whale, 2007) and dampening pro-inflammatory immune responses (Vossenkaemper et al., 2010), the β-lactamase reporter system has proved to be an invaluable tool. In view of this, the aim of this chapter is to determine the usefulness of the β-lactamase reporter system for visualising murine cells targeted for effector injection by *C. rodentium in vitro*.

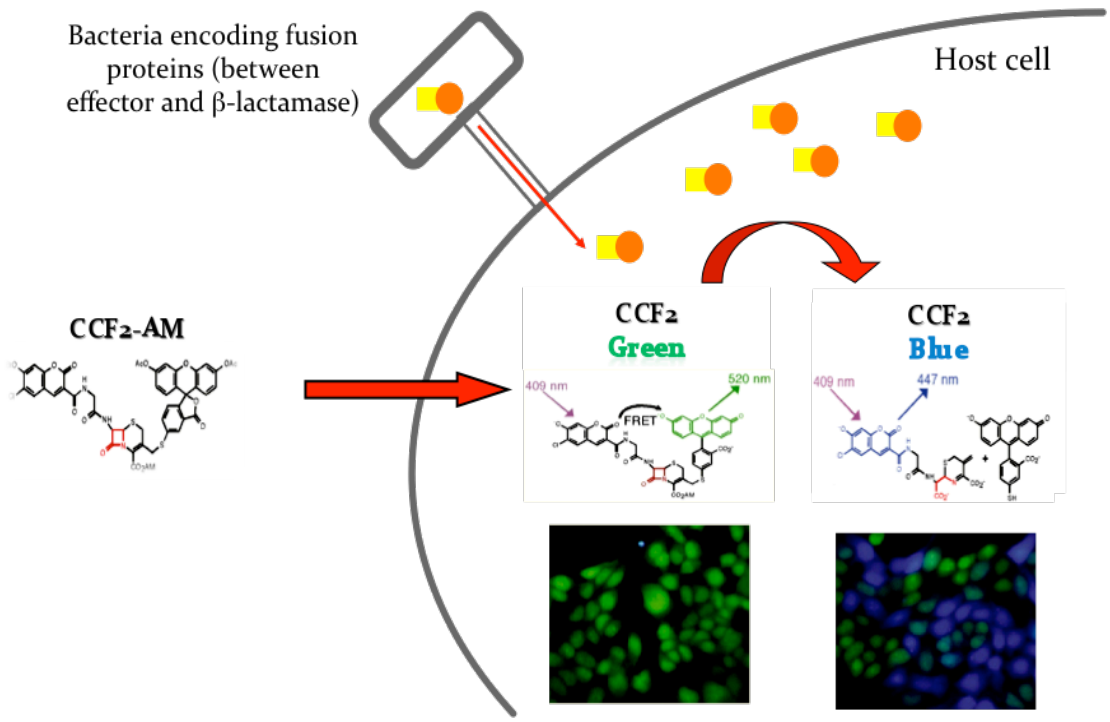

Figure 4.1.1: β-lactamase reporter system. A graphic representation of the β-lactamase reporter system used to visualise effector translocation in host cells by T3SS-containing bacteria. Adapted from Charpentier and Oswald (2004).

4.2 Results

4.2.1 Translocation of NleD-TEM fusion proteins into murine cell lines

Having generated the deletion mutant *Citro* ΔescNpACYCnleD and the reporter strain *Citro* pACYCnleD expressing the NleD-TEM fusion proteins, the usefulness of the β-lactamase system for assaying NleD injection into various host cells was investigated. In the first set of experiments, swiss 3T3 fibroblasts were infected with either the deletion mutant or the reporter strain of *C. rodentium* for 6 hours. This was followed by an hour-long incubation with CCF4-AM and analysis by fluorescence microscopy. In cells infected with the reporter strain, 50% to 70% of cells were blue, indicating that translocation of NleD into the fibroblasts had occurred. In contrast, only green fluorescence was observed in cells infected with the ΔescN mutant, indicating the absence of translocated NleD proteins. These results confirm that translocation of NleD-TEM fusion protiens is type III-dependent and requires a functional T3SS ATPase (Fig. 4.4.1). Similar observations were made in the CMT93 mouse colonic epithelial cell line, where 10% to 15% of cells were blue (Fig. 4.4.2), and in the J774 macrophage cell line, where 20% to 40% of the cells were blue (Fig. 4.4.3).

Although microscopic analysis enabled the visualisation of host cells in which protein translocation had occurred, it was difficult to quantify. As a result, translocation of the NleDTEM fusion proteins into colonic epithelial cells and macrophages was detected by flow cytometry (Figs. 4.4.2 and 4.4.3). However, preparing adherent cells for analysis by flow cytometry proved difficult as the cells formed into clumps following cell detachment, the process of which may have damaged and compromised the physical properties of the cells. In contrast, the mouse thymoma T cell line BW5157, which is grown in suspension, proved more convenient for analysis by flow cytometry.

4.2.2 Detection of NleD translocation into T cell lines by flow cytometry

To detect NleD translocation into T cells, the T cell line was infected with wildtype (WT) *Citrobacter rodentium*, reporter *Citro* pACYCnleD and mutant *Citro* ΔescNpACYCnleD. CCF4 labelled over 95% of the cells. As expected, blue fluorescence was not observed in T cells infected with wildtype strain or the ΔescN mutant strain**.** In contrast, T cells infected with reporter *C. rodentium* strain fluoresced blue in over 40% of the cells (Fig 4.4.4 A-B). The latter experiment was repeated 5 times under identical conditions and the percentage of blue cells ranged from 40% to 65%. To enhance bacterial attachment to the host cells during our experiments, the 12-well plates containing the inoculated cells were centrifuged briefly at the start of the infection.

4.2.3 Effect of time on NleD translocation

To determine whether NleD translocation into host cells increases with time, T cells were infected with *Citro* pACYCnleD (Fig 4.4.5B) and the ΔescN mutant (Fig. 4.4.5C) at various time-points (1, 2, 4, and 6 hours). Cells were incubated with CCF4-AM substrate and analysed by flow cytometry. It is evident from the FACS data that β-lactamase activity increases from 20% to 70% between 4 and 6 hours post infection (Fig. 4.4.6). This shows that effector translocation is time-dependent and the bacteria require sufficient time to interact with and translocate effector proteins into host cells. In contrast, blue fluorescence was detected in 0.3% of the cells at 6 hours after infection with the ΔescN mutant (Fig 4.4.5), confirming that effector delivery into host cells is not possible without a functional T3SS.

4.2.4 Multiplicity of infection (MOI) and NleD translocation

Next, the relationship between NleD translocation and the number of bacteria per target cell—or the multiplicity of infection (MOI)—was investigated. T cells were infected with increasing doses of reporter *C. rodentium*, stained with CCF4, and analysed by flow cytometry (Fig. 4.4.7). Initially, a positive relationship between the percentage of blue cells and the number of bacteria was observed. For instance, at MOI 10^2, approximately 10% of the viable T cells had undergone translocation, which increased to 40% at MOI 10^3 and 75% at MOI 10^4 (Fig. 4.4.8). However, at MOI values beyond 10^5 there was a decline in blue cell numbers and an increase in

cell death (Fig. 4.4.7A). This experiment was repeated using the mutant strain, *Citro* ΔescNpACYCnleD, as a negative control (Fig. 4.4.7B).

4.2.5 Detection of NleD translocation in primary immune cells

Having established the translocation of NleD into cell lines, I aimed to use the β-lacatamase translocation assay to monitor NleD injection into primary immune cells. To do so, single cell suspensions were prepared from the spleen, MLN, and PP of Balb/c mice and infected with either the reporter *C. rodentium* or the ΔescN mutant with a MOI of 10^3 bacteria per cell**.** For FACS analysis, lymphocytes were gated and analysed for green and blue fluorescence (Figs. 4.4.9- 4.4.11).

As seen previously with cells lines, NleD translocation into primary cells also required a functional T3SS. In addition, the highest number of blue cells were observed in the spleen with over 10% of its cells targeted for NleD injection (Fig. 4.4.9), followed by 5% in the MLN (Fig. 4.4.10) and 2.1% in PP cells (Fig. 4.4.11).

4.2.6 Effect of MOI on NleD translocation into primary immune cells

Analogously to the studies using cell lines, I examined the relationship between MOI and NleD translocation into primary cells. After infection of cells isolated from the mouse spleen, MLN, and PP with *Citro* pACYCnleD in varying doses, it was clear that the optimum MOI for primary cells was 10^3 bacteria per cell, an order of magnitude lower than that for T cells (Figs. 4.4.12 and 4.4.13). At this optimum MOI**,** the highest percentage of blue cells observed was 12.5% for the spleen, followed by 8.5% for the MLN and 6.4% for the PP. As with T cells, infection of primary cells with bacteria above the optimum MOI led to an increase in cell toxicity and death.

4.2.7 Concanavalin A (ConA) stimulation of primary immune cells and its effect on NleD injection

To further explore the susceptibility of primary cells to protein injection, the cells were stimulated with Con A**,** a lectin that interacts directly with T cell receptor (TCR) to trigger T lymphocyte activation and stimulation for cytokine synthesis. I hypothesised that stimulation of primary cells with Con A prior to bacterial infection may increase the cell surface area, enabling more bacterial attachment and thereby leading to an increase in NleD translocation.

As described in chapter 2, primary cells from the spleen, MLN, and PP were stimulated with Con A (1µg/ml) for 3 days and subsequently infected with *Citro* pACYCnleD (MOI 10^3) for 6 hours. An increase in the size of lymphocytes in the gated population occurred after stimulation (Figs. 4.4.14-4.4.16). A nearly 3-fold increase was observed in the number of blue cells from 9% in unstimulated splenocytes to 29% in stimulated splenocytes (Fig. 4.4.14). Similarly, there was a 2-fold increase in the percentage of blue cells from before and after stimulation in MLN from 6% to 14% (Fig. 4.4.15) and in PP from 5% to 10% (Fig. 4.4.16). The data were summarized from 5 independent experiments (Fig. 4.4.17).

The results were further confirmed by splenocyte infection with *Citro* pACYCnleD at various MOI for 6 hours following Con A stimulation. The number of blue cells increased significantly for each MOI after stimulation (Figs. 4.4.18 and 4.4.19). This may have been due to the increase in cell size, which may have resulted in a larger surface area for the bacteria to attach and inject its proteins; or it may have been the result of the cells' activated state.

4.2.8 Distribution of NleD injection into splenocyte sub populations *in vitro*

Having established the ability of *Citrobacter* to inject proteins into lymphocytes isolated from the spleen, MLN, and PP, I next examined whether there might be a preferential injection into certain immune cell types. To characterise the splenocyte populations injected with NleD, splenocytes were infected with *Citro* pACYCnleD, then stained with CCF4 and antibodies against CD3, CD19, and CD11c. Flow cytometry analysis determined the composition of spleen cells and confirmed that B and T cells are the most abundant cell sub populations in the spleen (Fig. 4.4.21A). This finding is in agreement with previous studies in *Yersinia* (Marketon et al, 2005; Koberle et al, 2009). In addition, after analysing the cells for various surface expression markers, I found that the highest percentage of blue cells belonged to B cells (6-7%), followed by dendritic cells (5-7%) and then T cells (4-5%) (Figs. 4.4.20B and 4.4.21C). However, this difference is not statistically significant. These findings are representative of 3 independent experiments.

4.2.9 Gating strategies and controls used for flow cytometry

For cell analysis by flow cytometry, the violet laser was used for excitation of the flurochromes at 405nm in the BD FACSCanto II flow cytometer (BD Biosciences). The voltages were set using unstained samples and the forward and side scatter adjusted so that the cell population is clearly delineated. Following the acquisition of cells in the forward and side scatter plots, CCF2-AM stained cells were gated for blue and green fluorescence using the AmyCyan (green) and Pacific blue (blue) filters. Propidium iodide was not used to stain dead cells since CCF2-AM loaded cells that did not fluoresce green were considered dead. Dead cells cannot load with CCF2-AM because retention of the CCF2-AM dye requires active cell processes such as endogenous esterification that convert esterified CCF2-AM in to CCF2-free acid that becomes negatively charged at physiological pH and trapped within the host cell cytoplasm (Zlokarnik et al, 1998). In the absence of active esterification, dead cells are unable to retain CCF2-AM, which readily leaves through the cell membrane. Therefore CCF2-AM staining was sufficient to exclude dead cells from the flow cytometry analysis during this study. Nonetheless, it may have been advisable to confirm this using propidium iodide staining.

For the cell characterisation experiments, the surface markers CD11c, CD19 and CD3e were used to identify dendritic cells, B cells and T cells respectively. Since the emission peaks of the various fluorophors were close together, there was spectral overlap between the channels. Compensation was performed manually based on single antibody staining of splenocytes and unstained samples for all the channels. Although the antibody markers were selected based on their expression on the specific cell types as well as manufacturers recommendations, these antibodies stained more than one cell type. For instance, CD19 is a typical B cell marker but is also expressed by some follicular dendritic cells. In addition, CD11c is expressed mostly on dendritic cells but can also be found on the surface of monocytes, macrophages, neutrophils and some B cells. Similarly, CD3e is expressed on thymocytes, mature T lymphocytes and NK T cells. The overlap of cell surface markers between the different cell types may explain why the total percentage of cells that expressed CD19, CD3 and CD 11c appeared to total to ~150%.

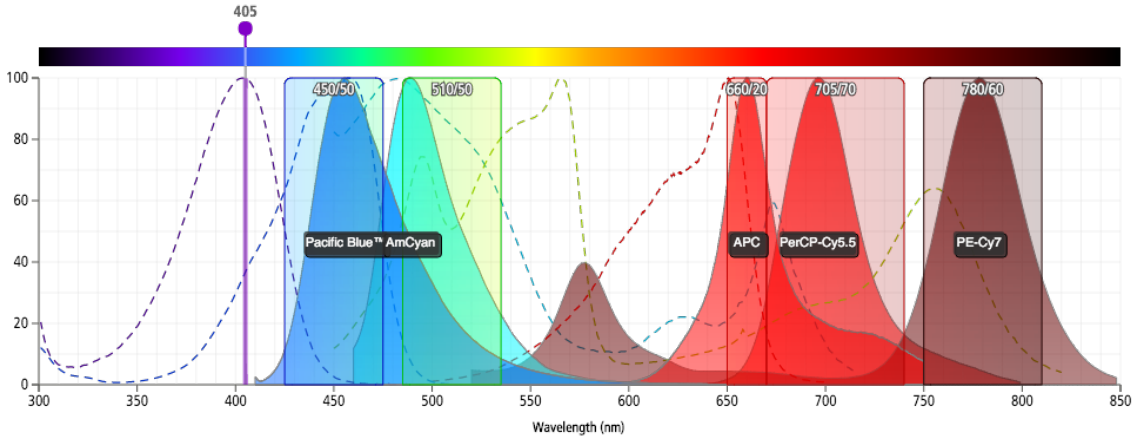

Figure 4.2.1: Fluorescence spectrum showing the excitation (dashed peaks) and emission (filled peaks) wavelengths (nm) of the various flurochromes used in the flow cytometry analysis. Created using BD fluorescence spectrum viewer (http://www.bdbiosciences.com/us/s/spectrumviewer)

4.3 Discussion

The T3SS-mediated delivery of effector proteins into host mammalian cells is an important strategy of enteropathogens to manipulate host cellular processes and immune responses. Although the T3SS and its effectors have been studied extensively in the recent years, very little has been reported on the types of cells targeted for effector injection by attaching effacing (AE) pathogens. In this chapter, the β-lactamase reporter system was applied to *C. rodentium* to investigate its usefulness for visualisation of target cells for effector delivery *in vitro*.

Translocation assays were designed so that the number of blue cells containing the CCF4 hydrolysis product indicated the presence of translocated fusion protiens inside the host cell cytoplasm. In addition, the use of the EscN mutant confirmed that β-lactamase reporter activity is dependant on translocation of the fusion proteins by the bacterial T3SS, as reported in previous studies (Marches et al, 2005; Vossenkaemper et al, 2010). Moreover, green or blue fluorescent signals from the infected cells following the uptake of CCF4-AM dye substrate reflected cell viability, as dead cells were unable to retain the CCF4-AM dye.

This study found that infection of T cell lines with *Citro* pACYCnleD resulted in a time-dependent increase in the percentage of blue cells. An initial lag phase was seen, followed by an exponential increase between 4 and 6 hours with the maximum number of cells turning blue at 6 hours post inoculation. These results are consistent with previous studies wherein real-time analysis of effector translocation in EPEC showed that translocated effectors follow simple Michaelis-Menten enzyme kinetics (Mills et al, 2008; Zlokarnik, 2000). The effector proteins eventually reach a stable steady state at which the rate of accumulation of the CCF2 hydrolysis product becomes constant. The accumulation rate then slows once the enzyme reaches its maximum velocity, thereby indicating the maximum concentration of effectors in the infected host cells (Mills et al, 2008).

These results are further confirmed by studies in *Yersinia enterocolitica* in which over 50% of the host cells reached a steady state after 1 hour of bacterial incubation (Koberle et al, 2009). Similarly, in EPEC most translocated effectors reached a steady state within the first hour of bacterial inoculation, with Tir reaching this state after 40 minutes post-inoculation (Mills et al, 2008). The latter study further

demonstrated that Tir reached its maximum velocity (Vmax) at 60 minutes post-infection, at which point 70-85% of the cells had turned blue. In comparison, according to the translocation assays in our study, 70-80% of the T cells had turned blue at 6 hours post-inoculation, indicating that nleD had reached its maximum velocity at this time-point. These findings suggest that translocation kinetics in *C. rodentium* are slower than in the other T3-containing pathogens, although more studies are required to confirm this. The variation in translocation efficiency between the different pathogens can probably be explained by the species differences, which can influence factors such as the efficiency of bacterial attachment to the host cell, the number of T3SS present per bacterium, effector concentration inside the bacterium, their interaction with chaperon proteins, the coordinated expression of the T3 genes, and the regulation of T3SS assembly.

This study further demonstrated a positive correlation between the percentage of blue cells and the multiplicity of infection (MOI). The percentage of translocated cells increased from 10% to 75% as the MOI increased from 10^2 to 10^4. This supports previous findings in *Yersinia* in which the number of injected cells followed a hyperbolic regression curve with increasing MOI (Koberle et al, 2009). However, our observation of an increase in cell death associated with a very high MOI has not been described previously. It is possible that this increase in cell death was due to effector-induced apoptosis of target cells, which has been widely reported in many T3SS pathogens. For example, *Shigella flexeneri* (Zychlinsky 1994), *Salmonella typhimurium* (Jiang et al, 2004) and *Yersinia pseudotuberculosis* (Zhang et al, 2011) are able to translocate the effectors *Invasin* plasmid antigen B (IpaB), *Salmonella* outer protein D (SopD), and *Yersinia* outer protein J (YopJ), respectively, to induce apoptosis in host macrophages. Similarly, the translocation of effectors EspF, Cif, and EspH by AE pathogens induced apoptosis in epithelial cells and HeLa cells (Wong et al, 2011; Raymond et al, 2013). However, other effectors also belonging to AE pathogens, such as NleH, NleD, NleF, EspZ, and NleB (Hemrajani et al, 2010, Baruch et al, 2011; Shames et al, 2010; Blasche et al, 2013; Pearson et al, 2013), have an anti-apoptotic effect, and hence without further evidence it is difficult to conclude whether the host cell death observed in this study was associated with bacterial effectors.

Another possible explanation for the host cell death observed at high MOI is related to cell toxicity as a result of effector overdose. According to Mills et al (2008), however, this may not be possible due to translocation auto-inhibition, whereby 'early-attaching' EPEC translocated effectors send signals to initiate changes in host cells—for example by inducing modification of the cell membrane—and thereby reducing the capacity of 'late-attaching' EPEC to inject further proteins into the same cells. More recently, studies using typical strains of EPEC showed that the effector EspZ inhibited effector translocation following superinfection of HeLa cells, and this was described as a 'translocation stop' (Berger et al, 2012). Taken together, these findings suggest that host cells are only susceptible to effector translocation during the first wave of infection, which then inhibits effector translocation by the second wave, and hence it is not possible for these cells to receive an effector overdose.

An alternative explanation may be that at high MOI, the buffering capacity of the growth medium becomes exhausted through the consumption of nutrients and build-up of metabolic waste products, resulting in a low (acidic) pH and making it very difficult for cells to survive. Indeed, at high MOI the growth medium was observed to have changed colour from red to yellow, indicating a drop in pH toward the end of the experiment.

The present study, designed to determine the ability of *C. rodentium* to target cells of the immune system, found that *C. rodentium* can indeed inject effectors into immune cells *in vitro*. For example, our results showed that *C. rodentium* can inject effectors into BW5157 T cells, J774 macrophages, and primary lymphocytes harvested from the mouse spleen, MLNs, and PPs. Although the experiments using primary cells isolated from the GALT are physiologically more relevant than those using cell lines, the translocation efficiency—indicated by a high percentage of blue cells—appeared to be greater in the murine cell lines. This may be due to differences in cell size; that is, cells from the cell lines were larger and had a larger surface area than the primary cells.

Due to the many generations of cell passage, cell lines exhibit several alterations in morphology, chromosomal variations, and cell functions relative to the primary cells. For example, when comparing the proteome of a Hepa1-6 cell line with primary hepatocytes, it was found that the former had lost many of its functions, such as complement production and synthesis of the extracellular matrix, and had thereby

switched its resources to other cellular activities associated with proliferation and the maintenance of cell signalling pathways (Pan et al, 2009). This may help to explain the increased susceptibility of cell lines to effector injection in comparison to primary cells observed in our experiments.

To identify factors influencing the translocation efficiency in lymphocytes, cells from the spleen, MLN, and PP were activated with Concanavalin A (Con A) prior to infection with *C. rodentium*. Con A is a mitogen known to stimulate the mouse T cell subset, giving rise to distinct effector T cell populations (Dwyer and Johnson, 1981). According to our data, *C. rodentium* can inject stimulated cells more efficiently than non-stimulated cells. Upon observation by microscopy, these stimulated cells appeared to be larger than non-stimulated cells. The increase in surface area may have facilitated more bacterial attachment.

Moreover, it is possible that the upregulated expression of surface markers on the stimulated cells have led to the increased susceptibility of these cells to effector injection. Indeed, previous studies have described a positive relationship between the expression of cell surface molecules and bacterial invasion of T3SS-containing pathogens. For example, entry by *Shigella* into epithelial cells is facilitated by the interaction of the IpaB effector with host receptor CD44 and α4β1 integrins, which are cell surface molecules upregulated upon lymphocyte activation and recruited to the bacterial entry site, where they localise at the plasma membrane of the cellular protrusions induced by *Shigella* (Watarai 1996; Skoudy 2000; Kinashi 2007). In addition, previous studies demonstrated that activation of T cells resulted in the β1 integrin-mediated adhesion of these cells, while resting T cells displayed limited adhesive activity (Miron et al, 1992), and that *Shigella* invaded activated primary human CD4+T cells rather than inactivated CD4+T cells (Konradt et al, 2011).

Further studies examining the role of surface integrins have revealed that they are involved in the initiation of T3SS-mediated protein transloction. Studies in *Yersinia* have shown that β1 integrins are very important for Yop injection, as these surface molecules mediate adhesion of *Yersinia* and its subsequent internalisation into host cells (Schulte et al, 2000; Eitel & Dersch et al, 2002). β1 integrin-mediated signal transduction is also required for the initiation of Yop effector translocation in *Y. pseudotuberculosis* infection (Mejia et al, 2008). Fibroblasts lacking the expression of β1 integrins displayed lower numbers of adhering *Y.enterocolitica* and a dramatic

reduction in the percentage of blue cells compared to fibroblasts expressing β1 integrins (Koberle et al, 2009). Similarly, intimin, the outer membrane protein in EPEC, was also shown to bind to β1 integrins (α4β1 and α5β1) for adhesion to host cells (Frankel, 1996). Activation of CD4+T cells by PMA also induced β1 integrin-mediated adhesion of these cells to laminin and fibronectin (Frankel, 1996). Taken together, such studies suggest that stimulated cells have increased expression of surface integrins, resulting in greater bacterial adhesion to host cells, which in turn may switch on the assembly of the T3SS and its subsequent translocation of effector proteins.

Finally, the use of β-lactamase translocation assays in this study enabled us to demonstrate NleD injection in all immune cell types characterised from the mouse spleen, including CD19+B cells, CD3e+ T, cells and CD11c+ DCs. Our findings show that splenocytes are composed mostly of B cells and T cells, in agreement with previous studies in which the mouse splenocyte population consisted of 40-60% CD19+ B cells, 30-40% CD3+T cells, and 3-5% CD11c+ dendritic cells (Marketon et al, 2005; Koberle et al, 2009). Despite the abundance of T and B cells in the spleen, NleD-TEM injection seemed to occur more frequently in B cells and dendritic cells and less frequently in T cells. However, since the differences in effector injection between the various immune cells are not statistically significant, it is difficult to conclude whether there is preferential selection of certain immune cells for T3 injection by these bacteria.

On the contrary, previous studies have reported preferential selection of B cells and DCs *in vitro* by *Y. pestis* (Marketon et al, 2005). *In vivo* studies using the same bacterial strain (*Y. pestis*) also demonstrated significant T3 injection in DCs, macrophages, and neutrophils at day 2 after infection, followed by effector injection into all immune cell types, including T and B cells, by day 3. The observation that T and B cells, which constitute the majority of the splenic immune cell population, were not injected on day 2 led the authors to conclude that selection mechanisms must exist for bacterial type III injection of target cells whereby innate immune cells are early targets for injection (Marketon et al, 2005).

Further studies in *Y. enterocolitica* demonstrated that injection of Yops occurs randomly into all immune cells *in vitro* including DCs, granulocytes, NK cells, T cells, and B cells (Koberle et al, 2009). In the same study, Yop-injected cells

comprised, in order of proportion, B cells, dendritic cells, and macrophages *in vivo* upon infection of mice (Koberle et al, 2009). Effector injection into innate immune cells has also been reported for AE pathogens, for which EPEC was shown to inject effectors into DCs (Vossenkamper et al, 2010) and macrophages (Marches et al, 2008). Taken together, these studies support the notion that the pathogens preferentially select certain immune cells for type III injection *in vivo*. Their targeting of innate immune cells in particular suggests that these pathogens use the T3SS to destroy cells that are important for the first line of defence, thereby preventing adaptive responses and causing disease.

To obtain further evidence for this hypothesis, more *in vivo* studies will need to be conducted. For example, analysis of immune cells isolated from mice infected with reporter *C. rodentium* can enable us to determine whether *C. rodentium* preferentially selects certain immune cell types for effector injection *in vivo*. If this were indeed the case, it would be interesting to further investigate the effects of *C. rodentium* injection on immune cell functions, including the proliferation of CD4+ T cells, uptake and presentation of antigen to naïve lymphocytes by DCs, activation and maturation of various immune cells, production of cytokines, and migration of migratory immune cells. Such studies would demonstrate the consequences of protein translocation for host immune cells and provide insight into the immune evasion capabilities of AE pathogens.

4.4 Figures

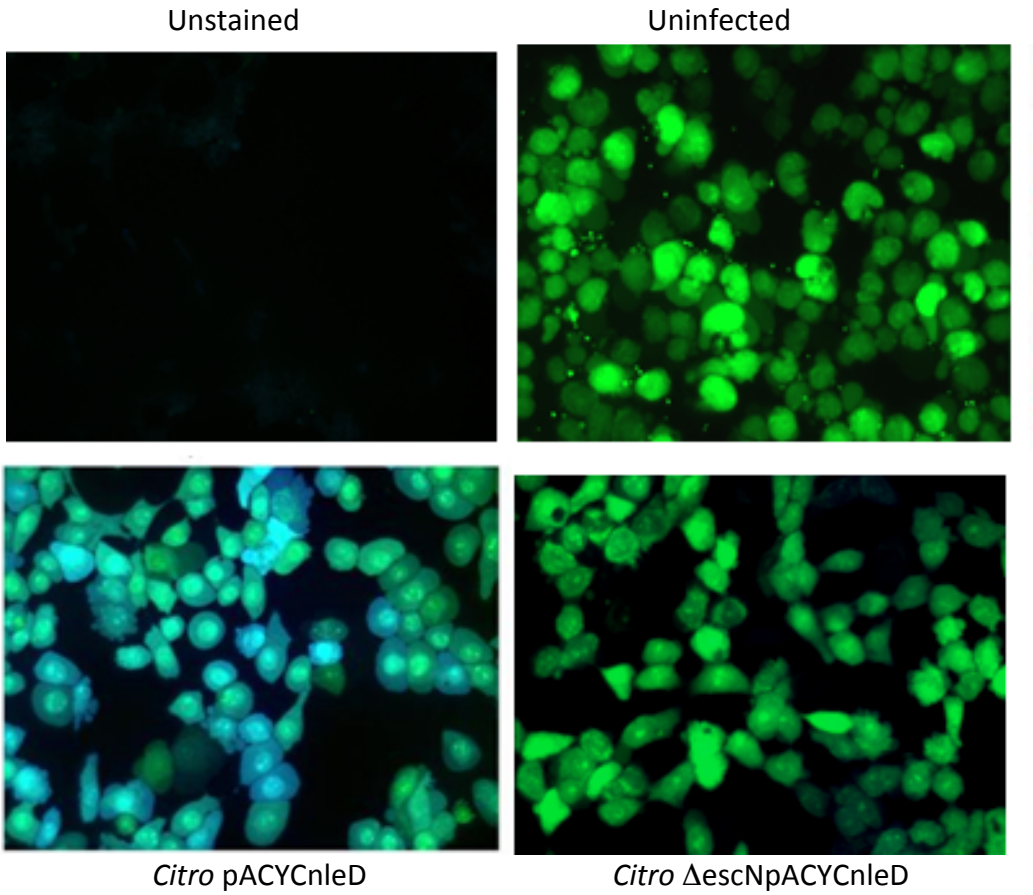

Figure 4.4.1 NleD injection in Swiss fibroblasts (3T3 cell line). Fibroblasts infected with either reporter *Citro* pACYCnleD or *Citro* ΔescNpACYCnleD (mutant strain lacking the T3SS) for 6 hours. The multiplicity of infection (MOI) was 1000. Subsequently, the cells were washed and incubated in CCF4-AM substrate for 1hour. NleD injection was visualised (blue cells) by fluorescence microscopy as described in Materials and Methods. Image is representative of 2 replicates from 5 independent experiments.

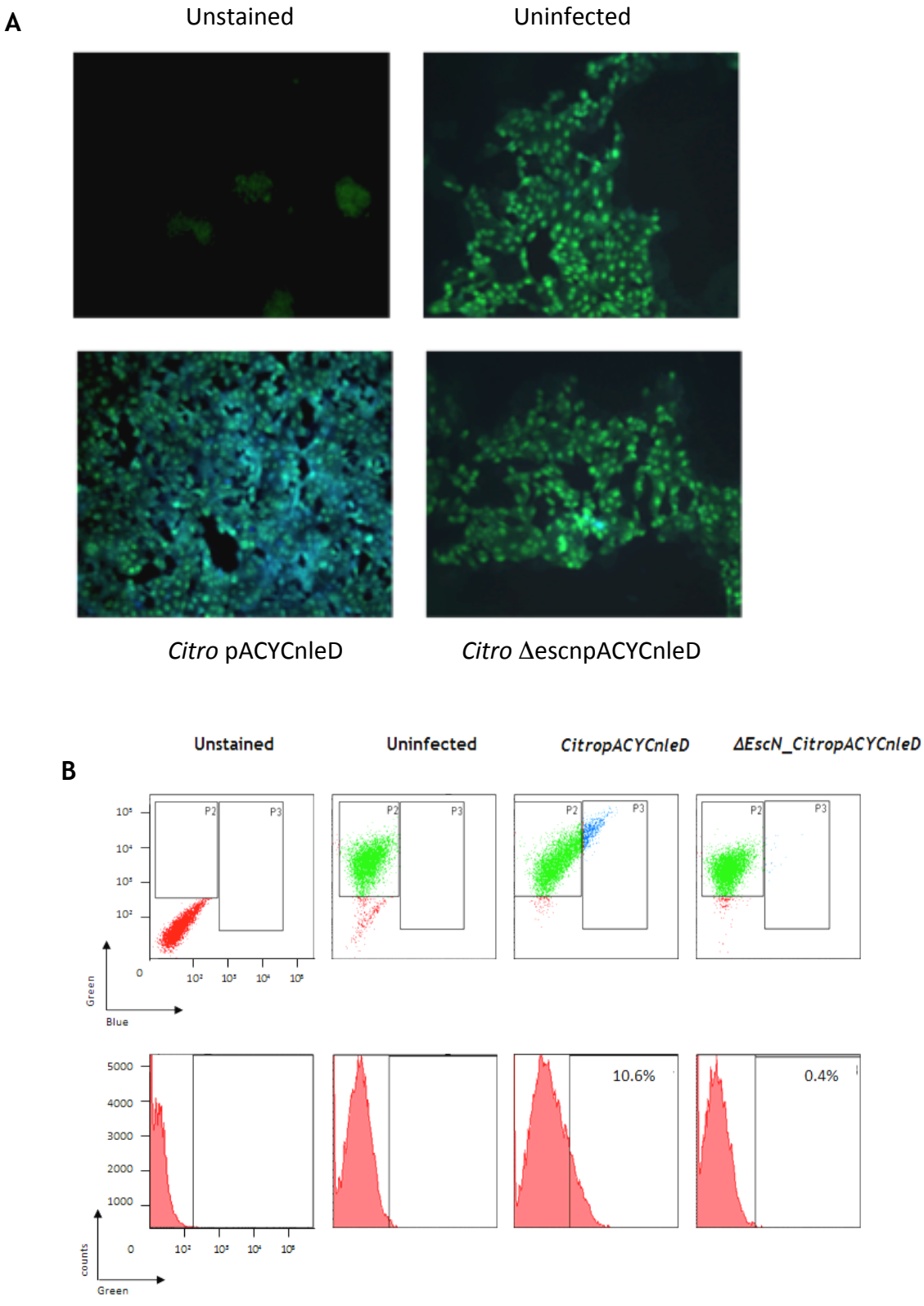

Figure 4.4.2 NleD injection in murine colonic epithelial cells (CMT93 cell line). Epithelial cells infected with either *Citro* pACYCnleD or *Citro* ΔescNpACYCnleD (MOI = 1000) for 6h followed by CCF4-AM substrate incubation. **A)** NleD injection (blue cells) was visualised by fluorescence microscopy and **B)** detected by flow cytometry. Data is representative of 2 replicates from 3 independent experiments.

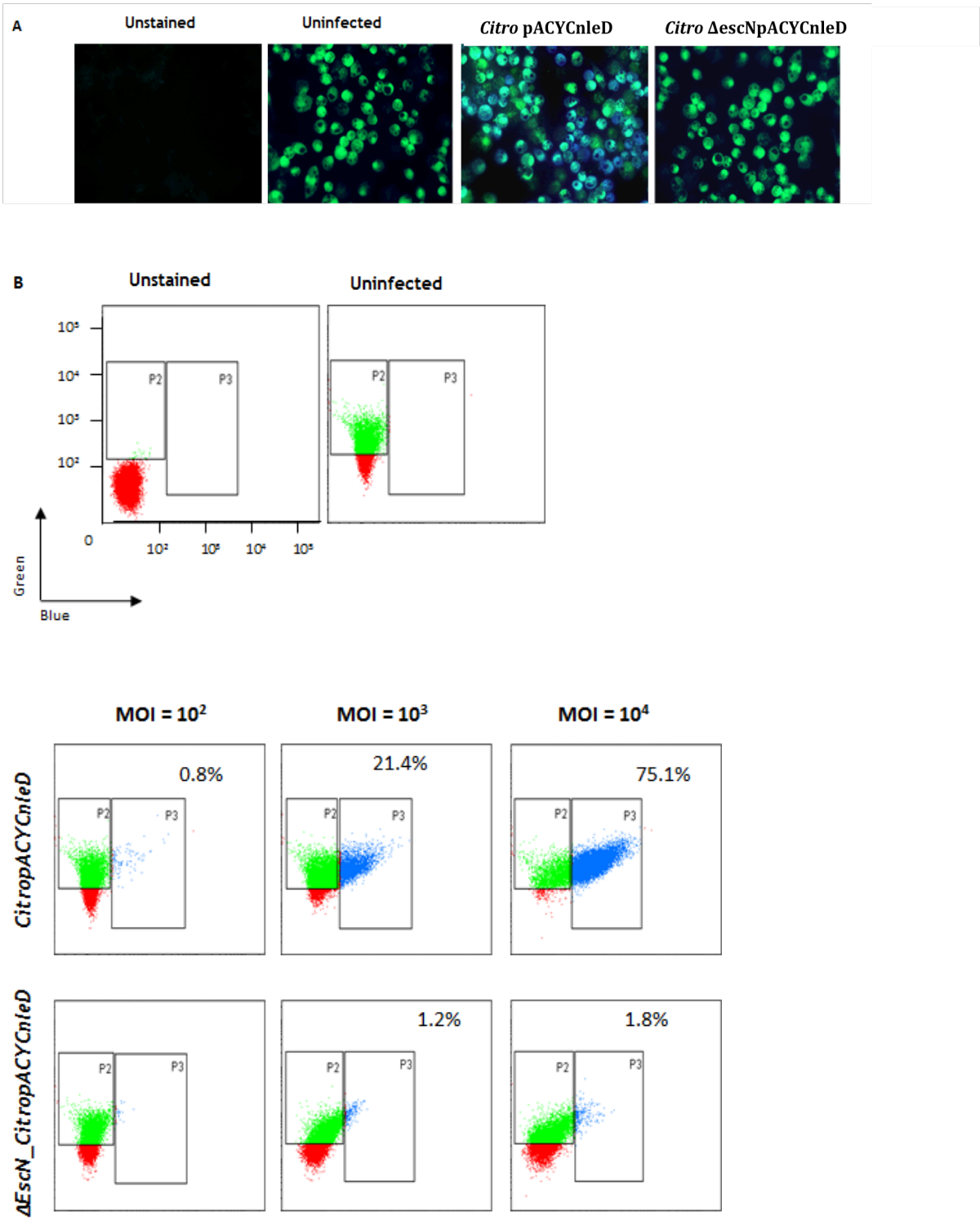

Figure 4.4.3 NleD injection in murine macrophages (J774 cell line). A) Macrophages infected with either *Citro* pACYCnleD or *Citro* ΔescNpACYCnleD (MOI = 1000) for 6h followed by CCF4-AM substrate staining. NleD injection was visualised by fluorescence microscopy. Representative of 5 independent experiments. **B)** The experiments were repeated using different MOI and subsequently analysed by flow cytometry. Representative of 3 independent experiments.

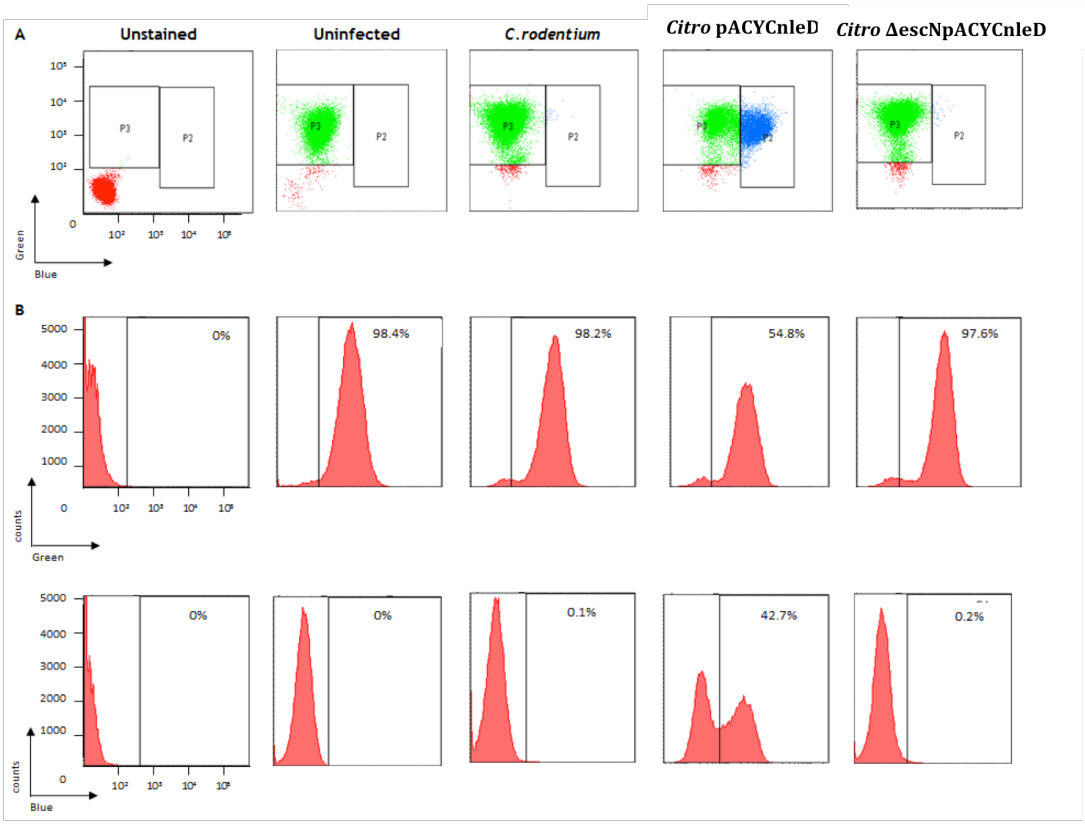

Figure 4.4.4 Detection of NleD injection in T cells *in vitro*. T cells were infected with different strains of *C. rodentium* for 6 hours (MOI=100), incubated with CCF4-AM and analysed by flow cytometry. **A)** FACS plots show the presence of green and blue cells**. B)** The data are depicted as histograms where the upper panel shows uptake of CCF4-AM by cells (green) while the lower panel shows the cleavage of CCF4-AM substrate by cells positive for β-lactamase activity (blue). The vertical bar indicates the gating used to determine the number of cells positive for either intact CCF4-AM substrate or cleaved products of CCF4-AM respectively. Representative data from 5 experiments are shown**.**

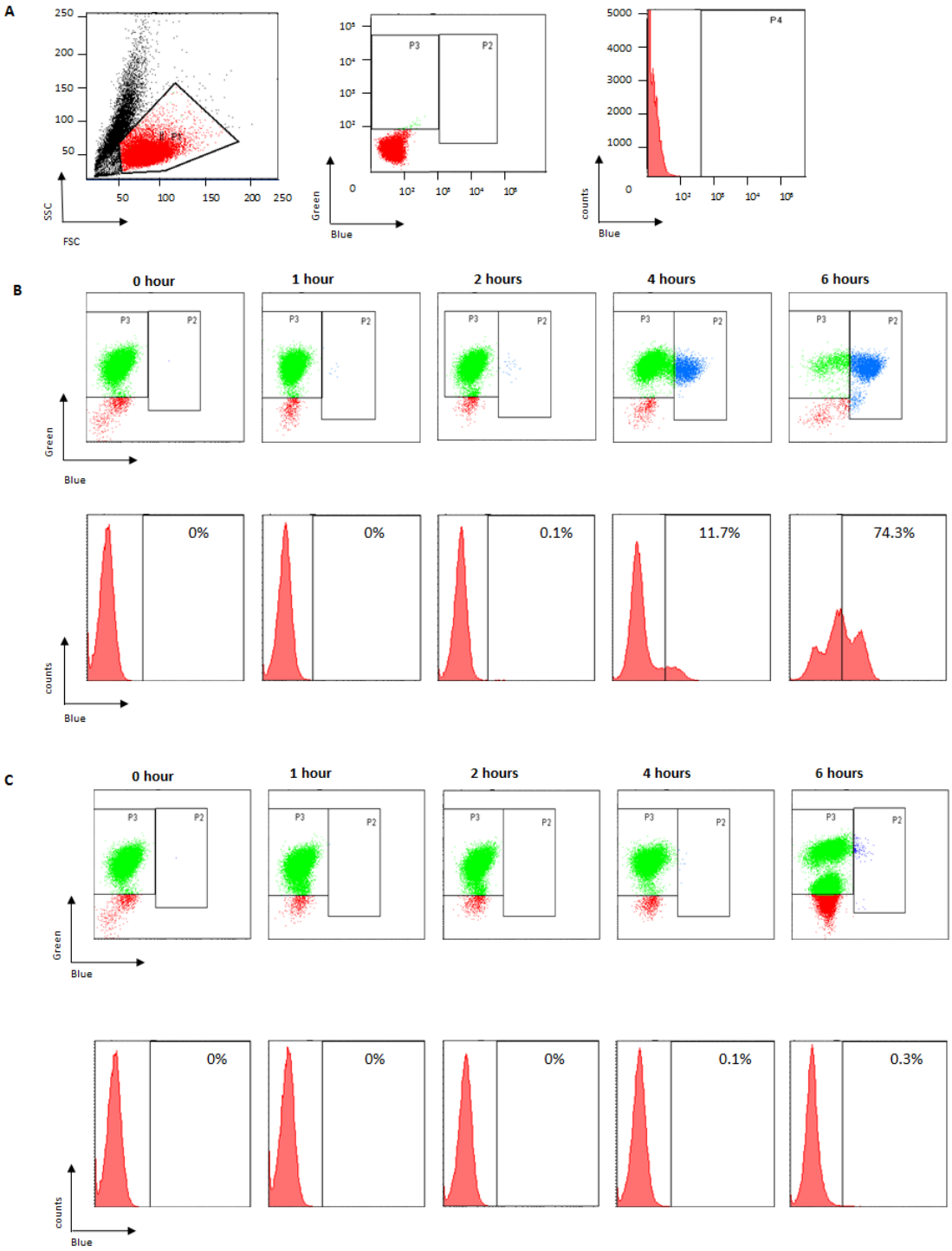

Figure 4.4.5: Timecourse of NleD injection in T cells. **A)** Uninfected T cell control. **B)** T cells infected with *Citro* pACYCnleD for various time durations: 1, 2, 4 and 6 hours (MOI= 1000) followed by CCF4-AM substrate incubation. NleD injection was detected as blue fluorescence by flow cytometry. The data are depicted as histogram where the vertical bar indicates the gating used to show the number of β-lactamase positive cells revealing NleD injection (blue). **C)** The experiment was repeated using the ΔescN mutant strain.

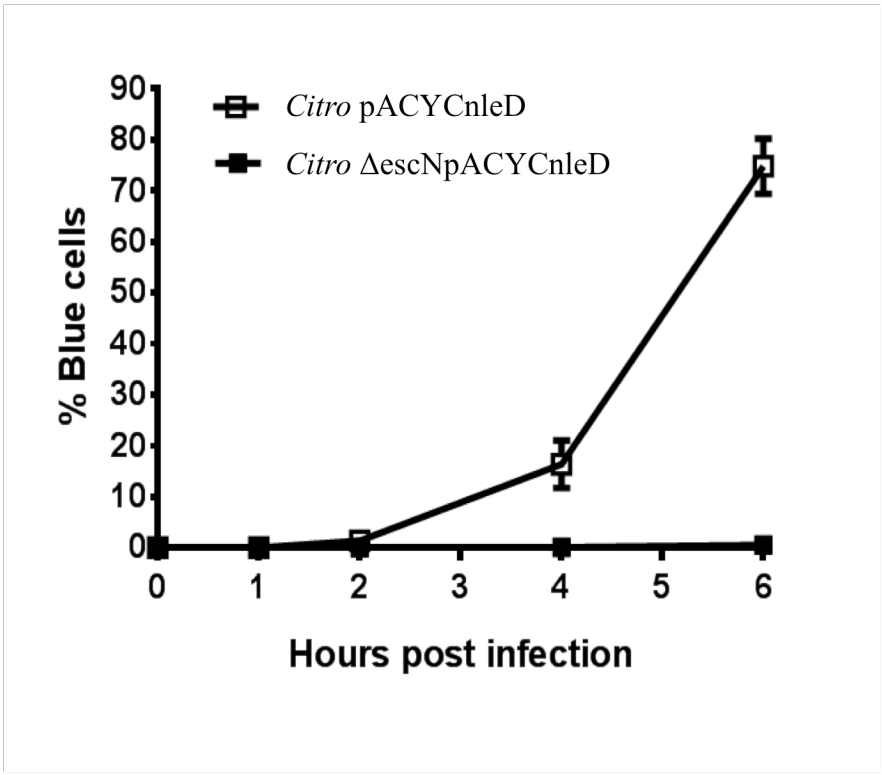

Figure 4.4.6: Timecourse of NleD injection in T cells. T cells were infected with *Citro* pACYCnleD for 1, 2, 4 and 6 hours (MOI= 1000) followed by CCF4-AM substrate staining. NleD injection was detected as blue fluorescence by flow cytometry. The data is summarised as means ± SEM of 5 independent experiments.

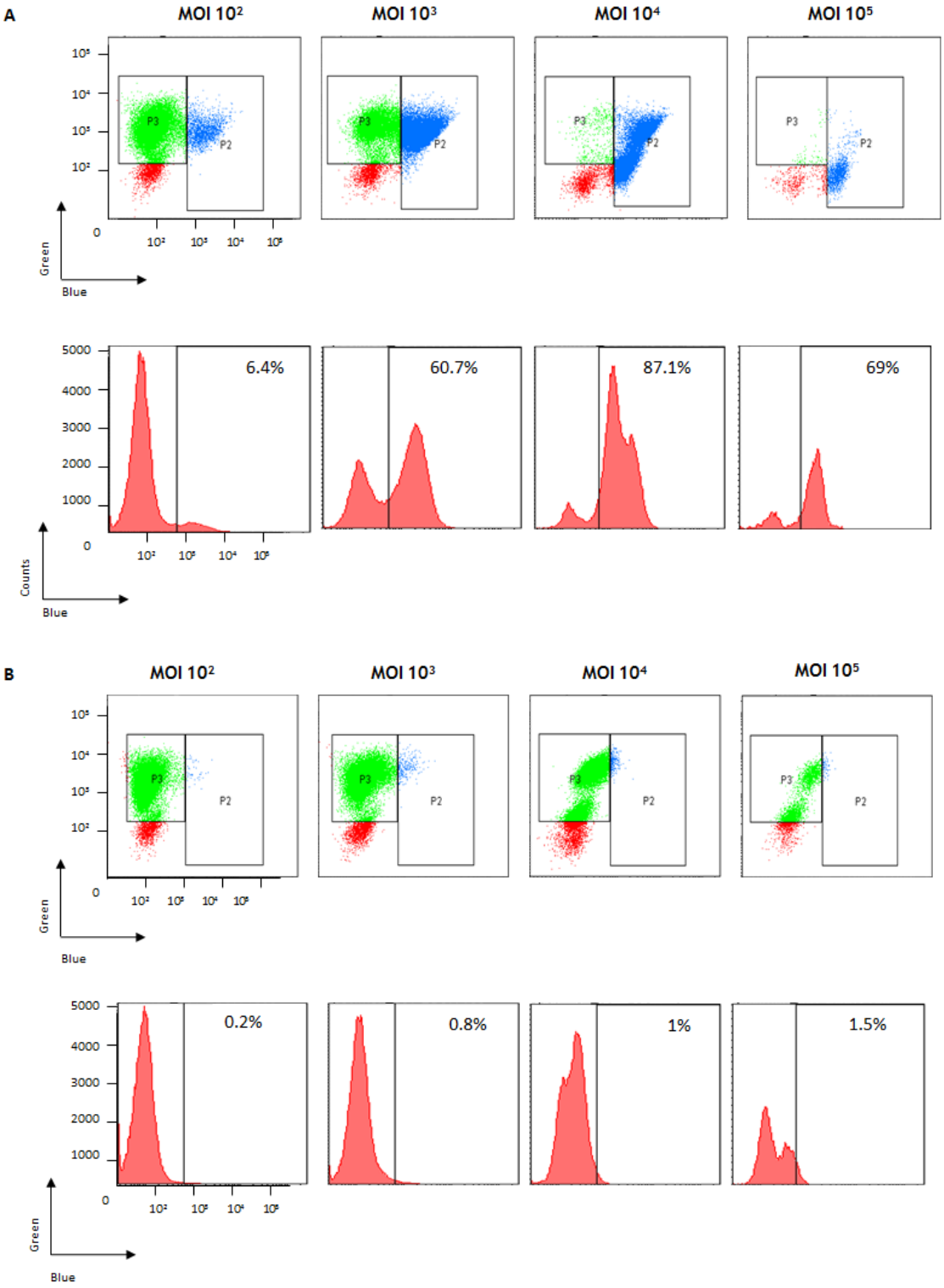

Figure 4.4.7 Detection of NleD injection in T cells with increasing MOI. T cells infected with varying MOI of **A)** *Citro* pACYCnleD or **B)** *Citro* ΔescNpACYCnleD for 6h and subsequently stained with CCF4-AM. NleD injection is indicated by the number of blue cells.

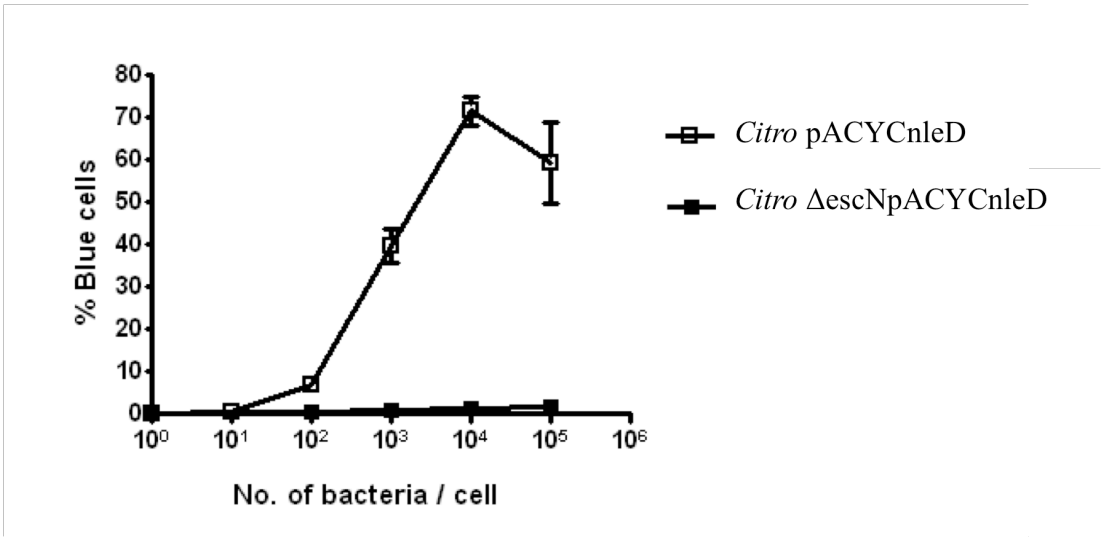

Figure 4.4.8: Detection of NleD injection in T cells with increasing MOI. Summarized data from the previous figure showing mean ±SEM of 12 experiments with *Citro* pACYCnleD (open squares) and 5 experiments with *Citro* ΔescNpACYCnleD (closed squares)

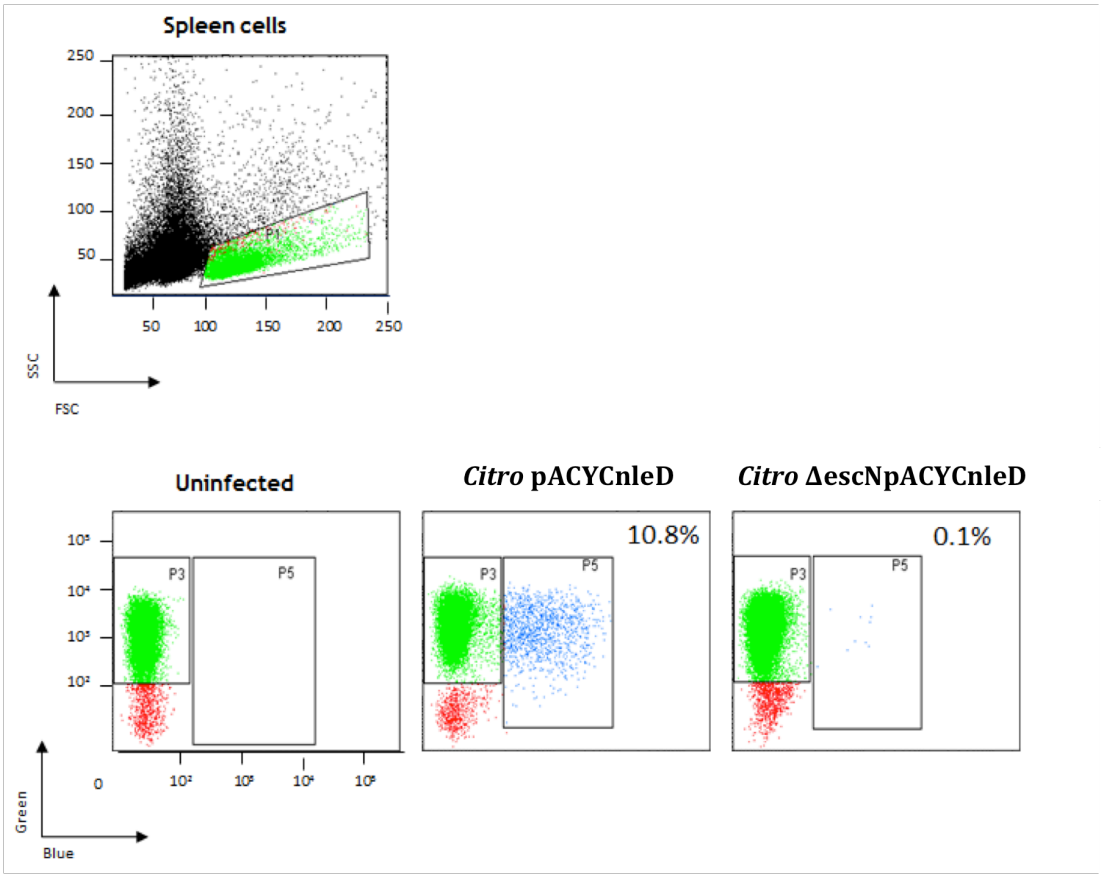

Figure 4.4.9: Detection of NleD injection in primary lymphocytes from the spleen. Single cell suspensions were prepared from the mouse spleen and infected with the reporter *C. rodentium* or the *escN* deletion mutant for 6 hours at MOI 10^3. Cells were subsequently stained with CCF4-AM and analysed by flow cytometry. The lymphocytes were gated as shown. Representative data from 3 experiments are shown.

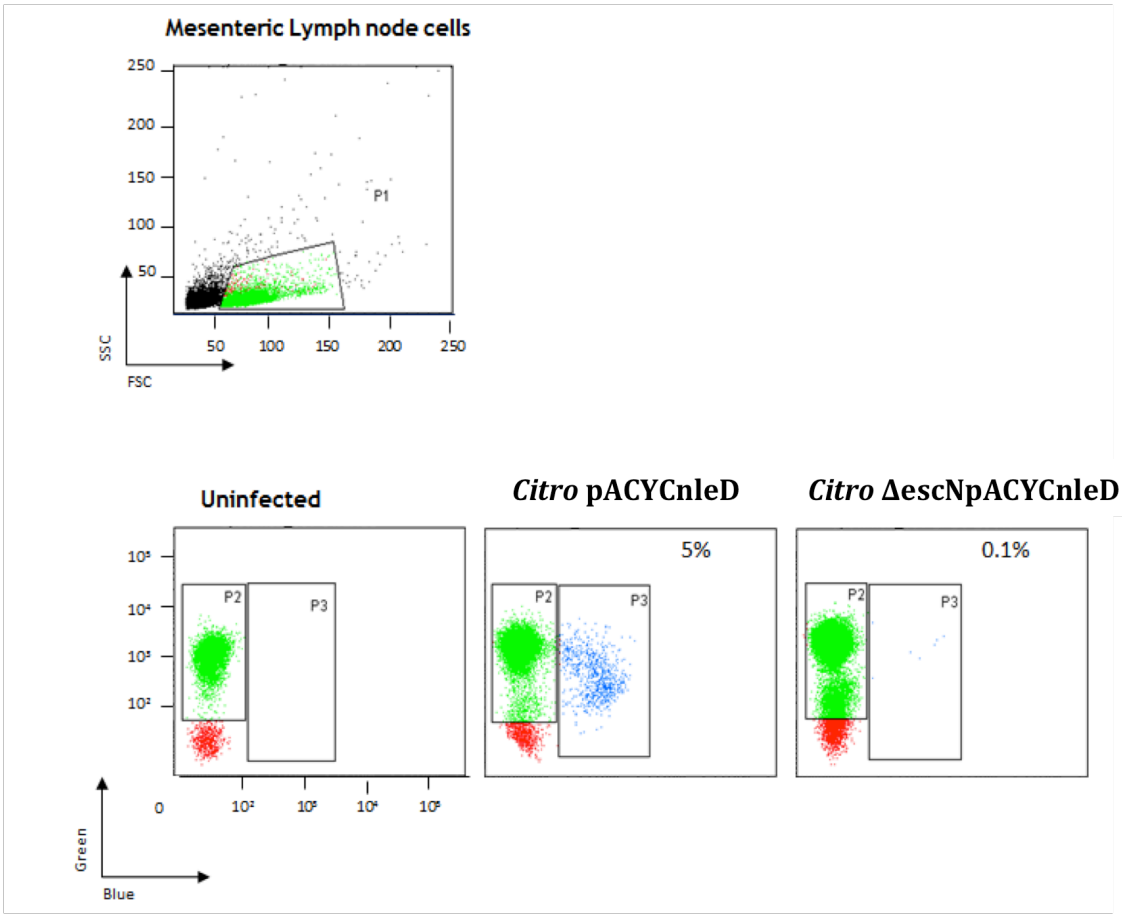

Figure 4.4.10: Detection of NleD injection in primary lymphocytes from the MLN. Single cell suspensions were prepared from the mouse mesenteric lymph nodes and infected with the reporter *C. rodentium* or the *escN* deletion mutant for 6 hours at MOI 10^3. Cells were subsequently stained with CCF4-AM and analysed by flow cytometry. The lymphocytes were gated as shown. Representative data from 3 experiments are shown.

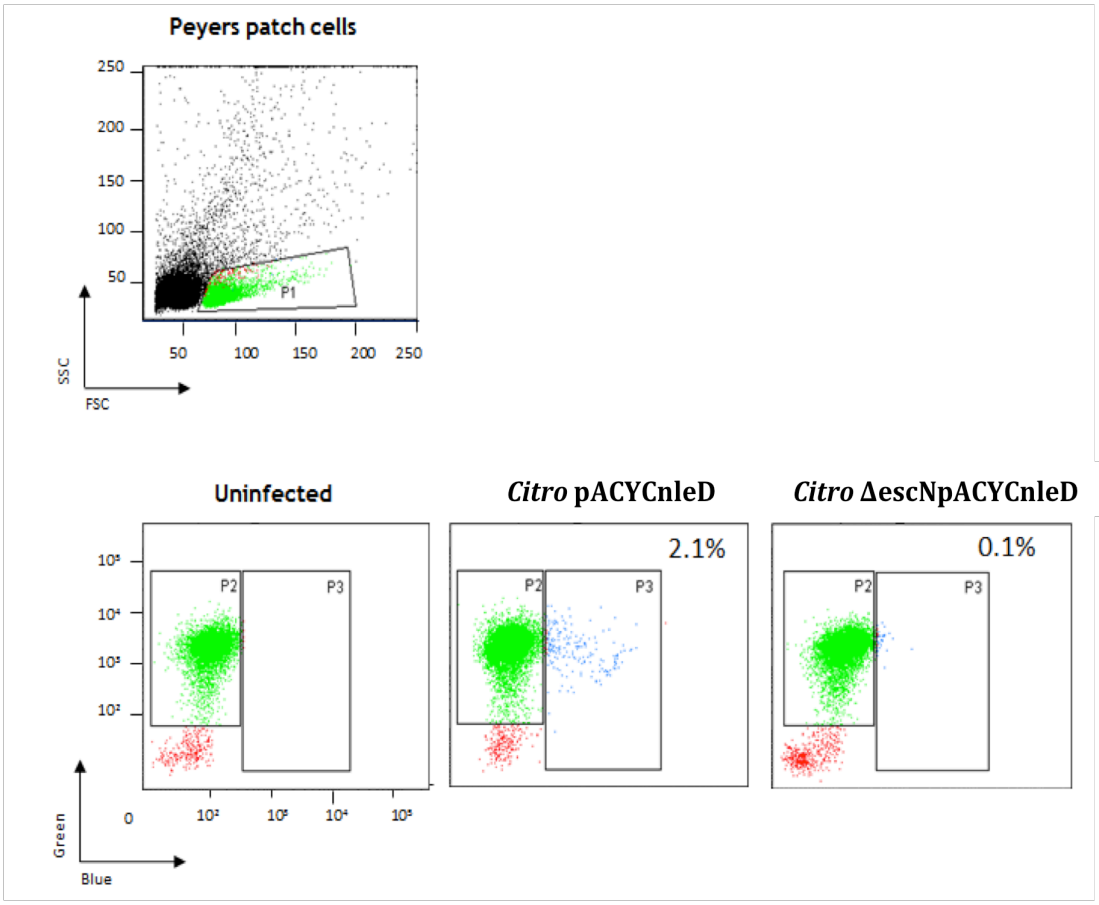

Figure 4.4.11: Detection of NleD injection in primary lymphocytes from the PP. Single cell suspensions were prepared from the mouse Peyer's patches and infected with the reporter *C. rodentium* or the *escN* deletion mutant for 6 hours at MOI 10^3. Cells were subsequently stained with CCF4-AM and analysed by flow cytometry. The lymphocytes were gated as shown. Representative data from 3 experiments are shown.

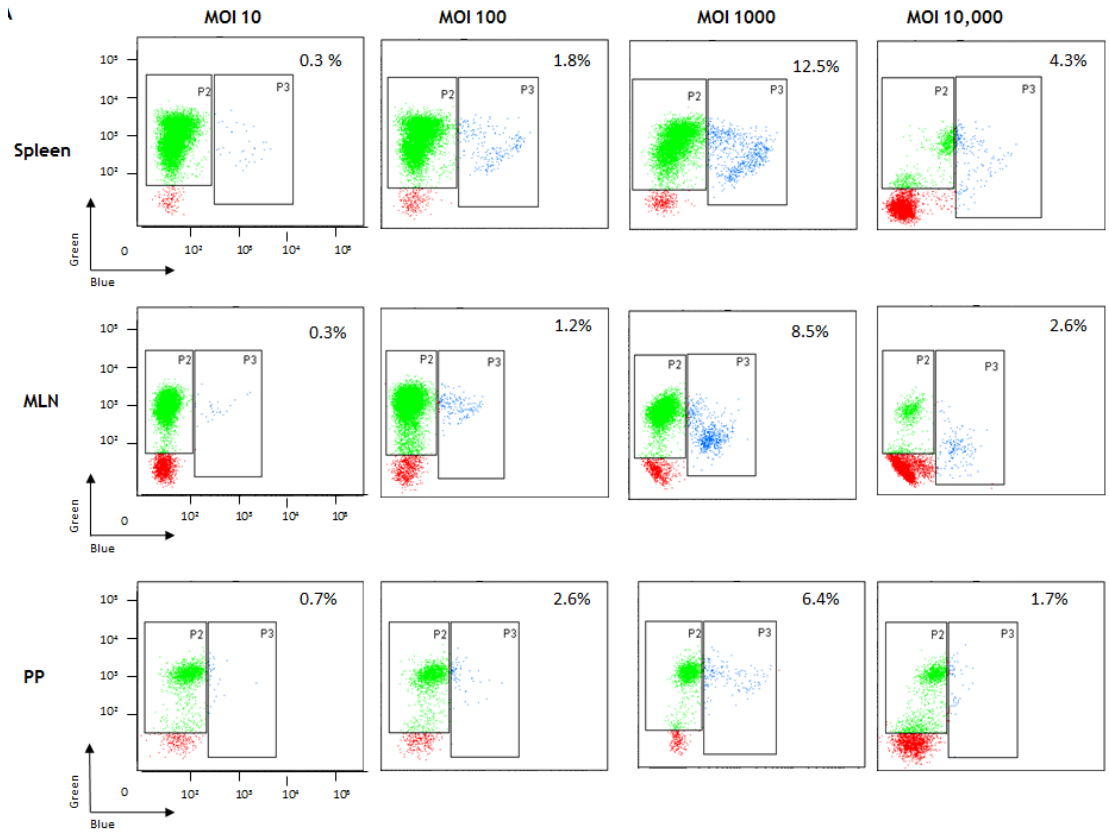

Figure 4.4.12: Detection of NleD injection in primary lymphocytes with varying MOI. Single cell suspensions were prepared from the spleen, MLN and PP and infected with different doses of *Citro* pACYCnleD for 6 hours. Subsequently, cells were stained with CCF4-AM and analysed by flow cytometry. Representative data from 5 experiments are shown.

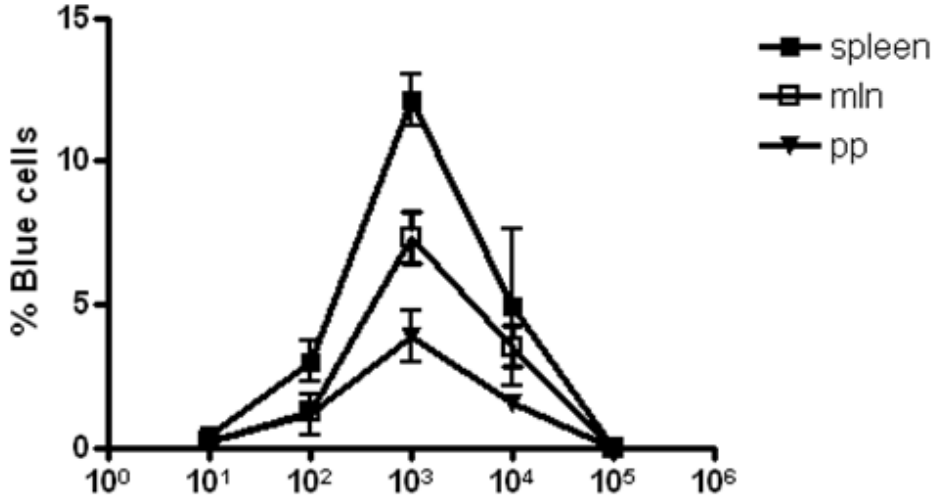

Figure 4.4.13: Detection of NleD injection in primary lymphocytes with varying MOI. Summarized data from the previous figure showing mean ±SEM of 5 independent experiments.

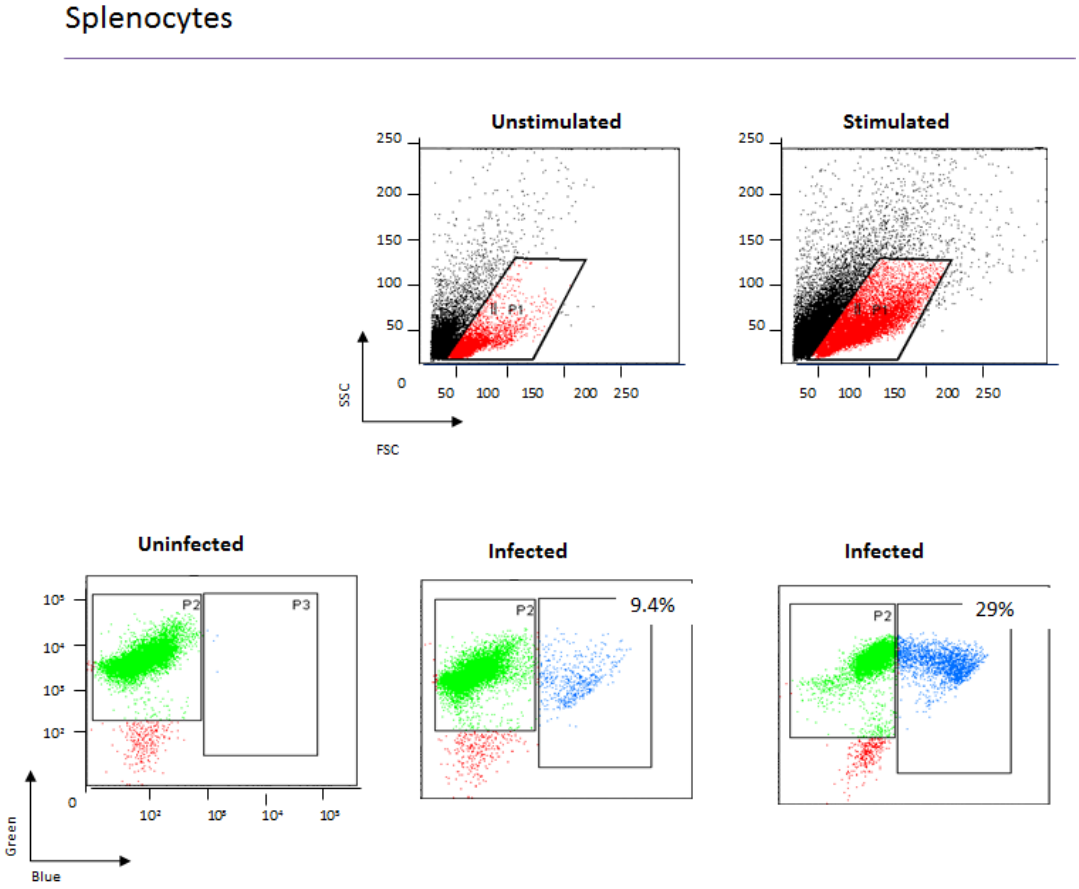

Figure 4.4.14: Detection of NleD injection in splenocytes following ConA stimulation. Single cell suspensions were prepared from the spleen, stimulated with Concanavalin A (1µg/ml) for 3 days and subsequently infected with reporter *C. rodentium* (MOI 10^3) for 6 hours. Cells were stained with CCF4-AM and analysed by flow cytometry. Representative data from 5 experiments are shown.

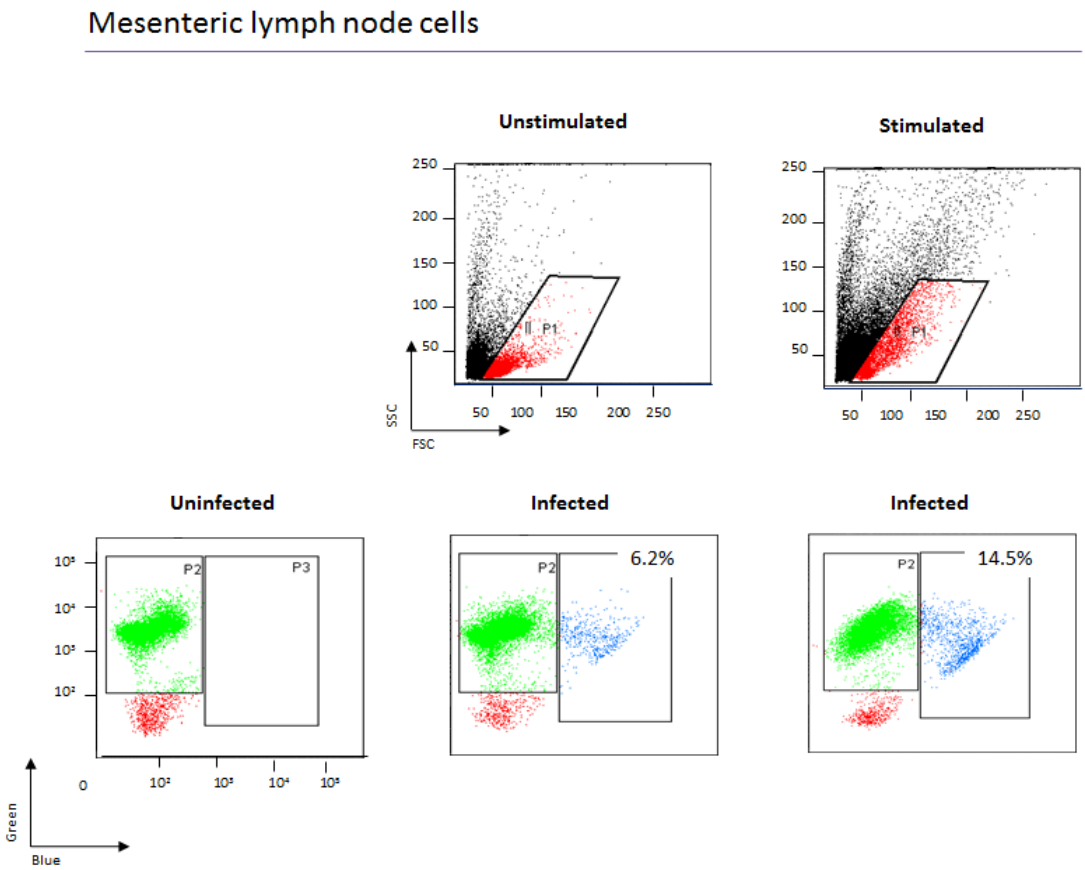

Figure 4.4.15: Detection of NleD injection into MLN cells following ConA stimulation. Single cell suspensions were prepared from the mesenteric lymph nodes, stimulated with Concanavalin A (1µg/ml) for 3 days and subsequently infected with reporter *C. rodentium* (MOI 10^3) for 6 hours. Cells were stained with CCF4-AM and analysed by flow cytometry. Representative data from 5 experiments are shown.

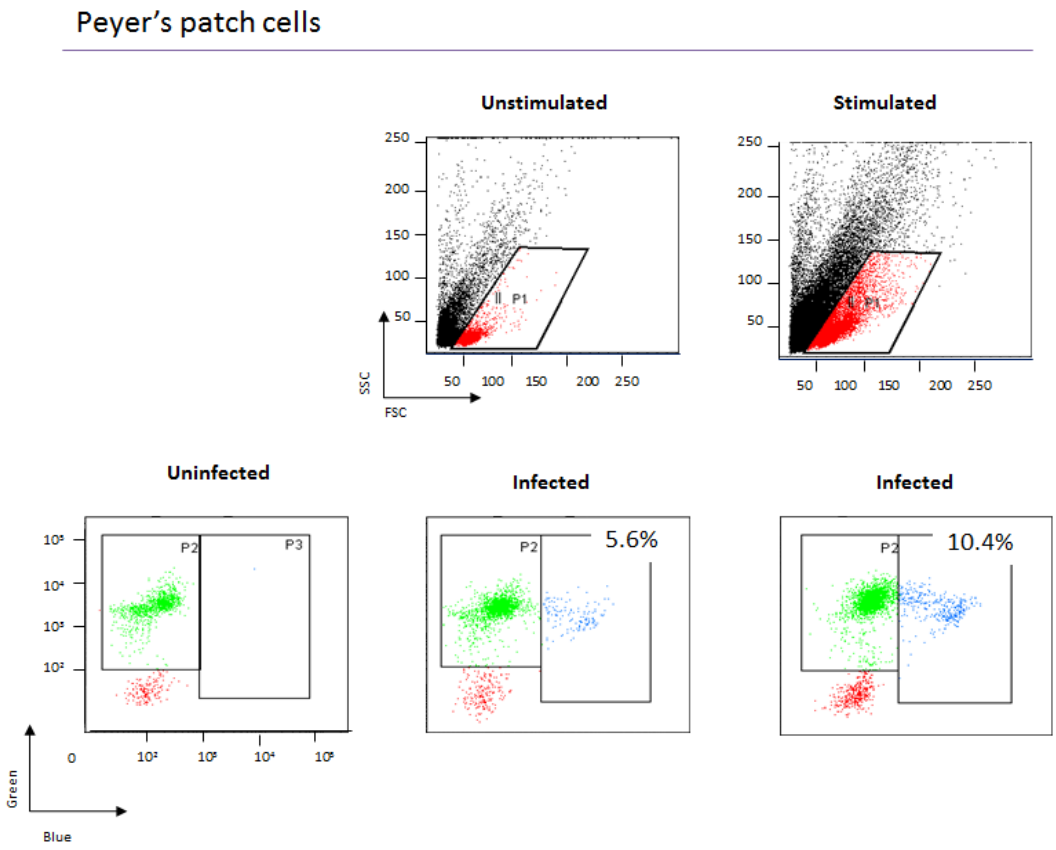

Figure 4.4.16: Detection of NleD injection into PP cells following ConA stimulation. Single cell suspensions were prepared from the Peyer's patches, stimulated with Concanavalin A (1µg/ml) for 3 days and subsequently infected with reporter *C. rodentium* (MOI 10^3) for 6 hours. Cells were stained with CCF4-AM and analysed by flow cytometry. Representative data from 5 experiments are shown.

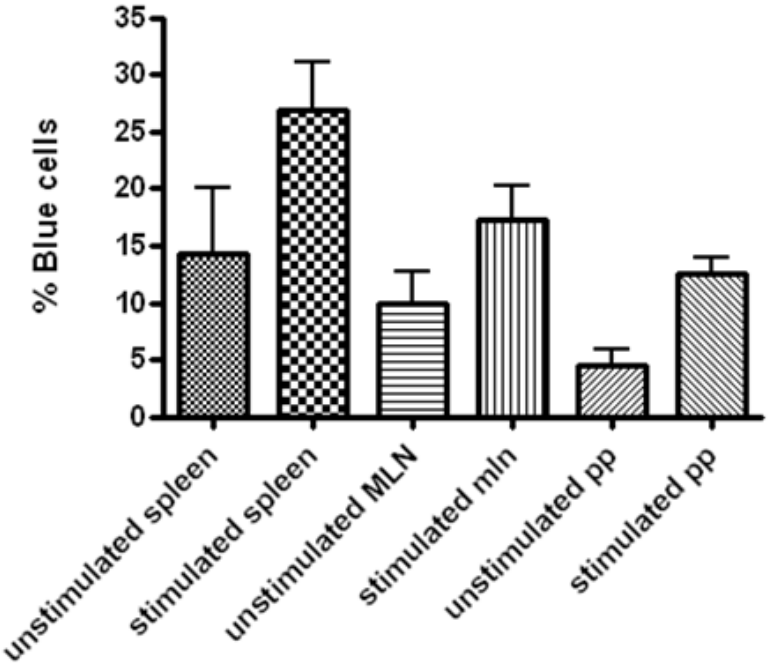

Figure 4.4.17: Comparison of NleD injection into primary lymphocytes before and after conA stimulation. Summarized data from Fig. 4.4.14-16 showing mean ±SEM of 5 independent experiments.

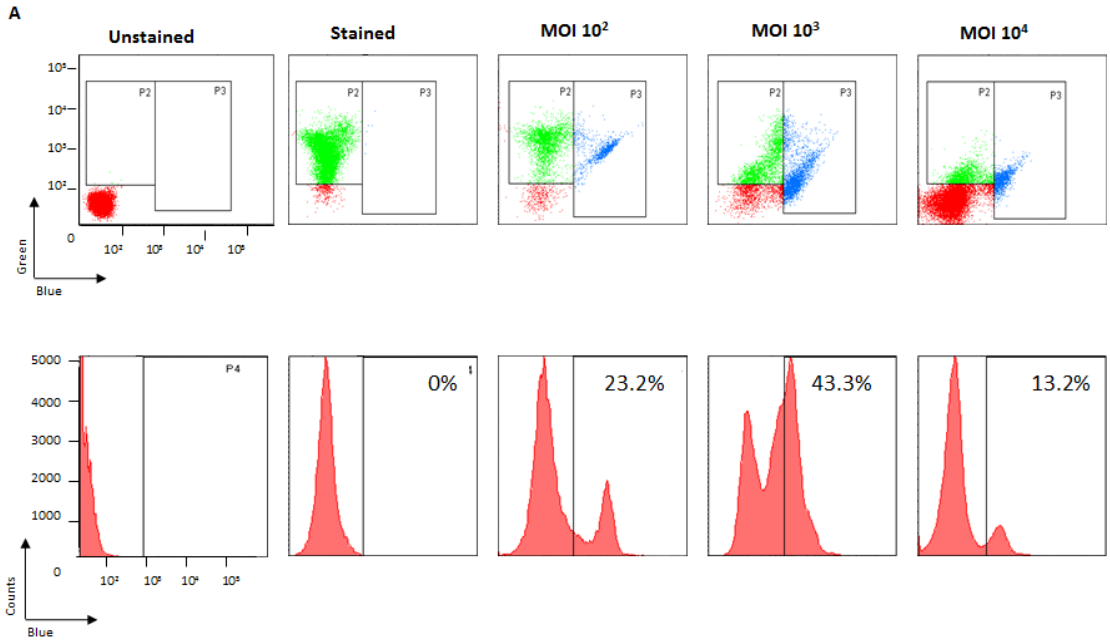

Figure 4.4.18: NleD injection in splenocytes following ConA stimulation under various MOI. Isolated splenocytes were stimulated with ConA (1ug/ml) for 3 days followed by *in vitro* infection with various MOI *of Citro* pACYCnleD for 6 hours. After subsequent CCF4 staining, cells were analysed by flow cytometry. Representative data from 2 experiments are shown.

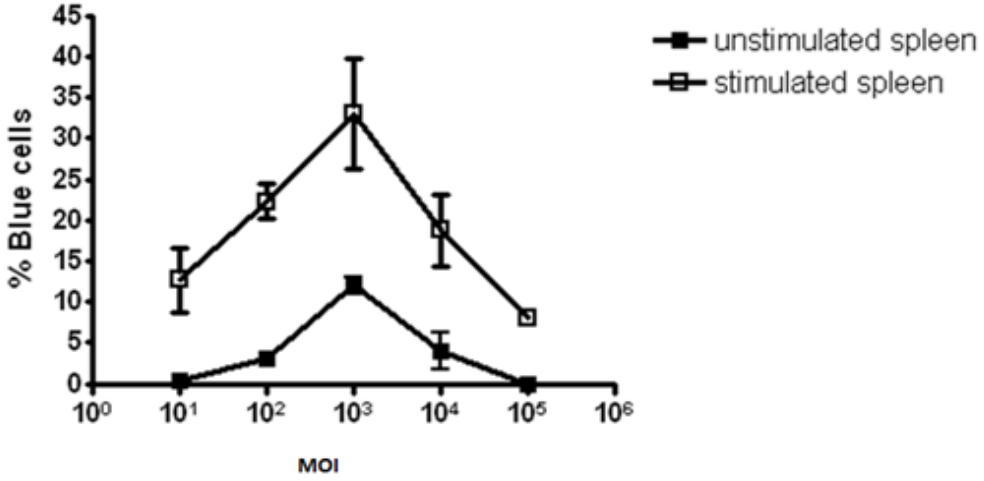

Figure 4.4.19: Comparison of NleD injection in splenocytes before and after ConA stimulation. Mean ±SEM of 5 independent experiments showing percentage of blue cells before stimulation (closed squares) and after stimulation (open squares).

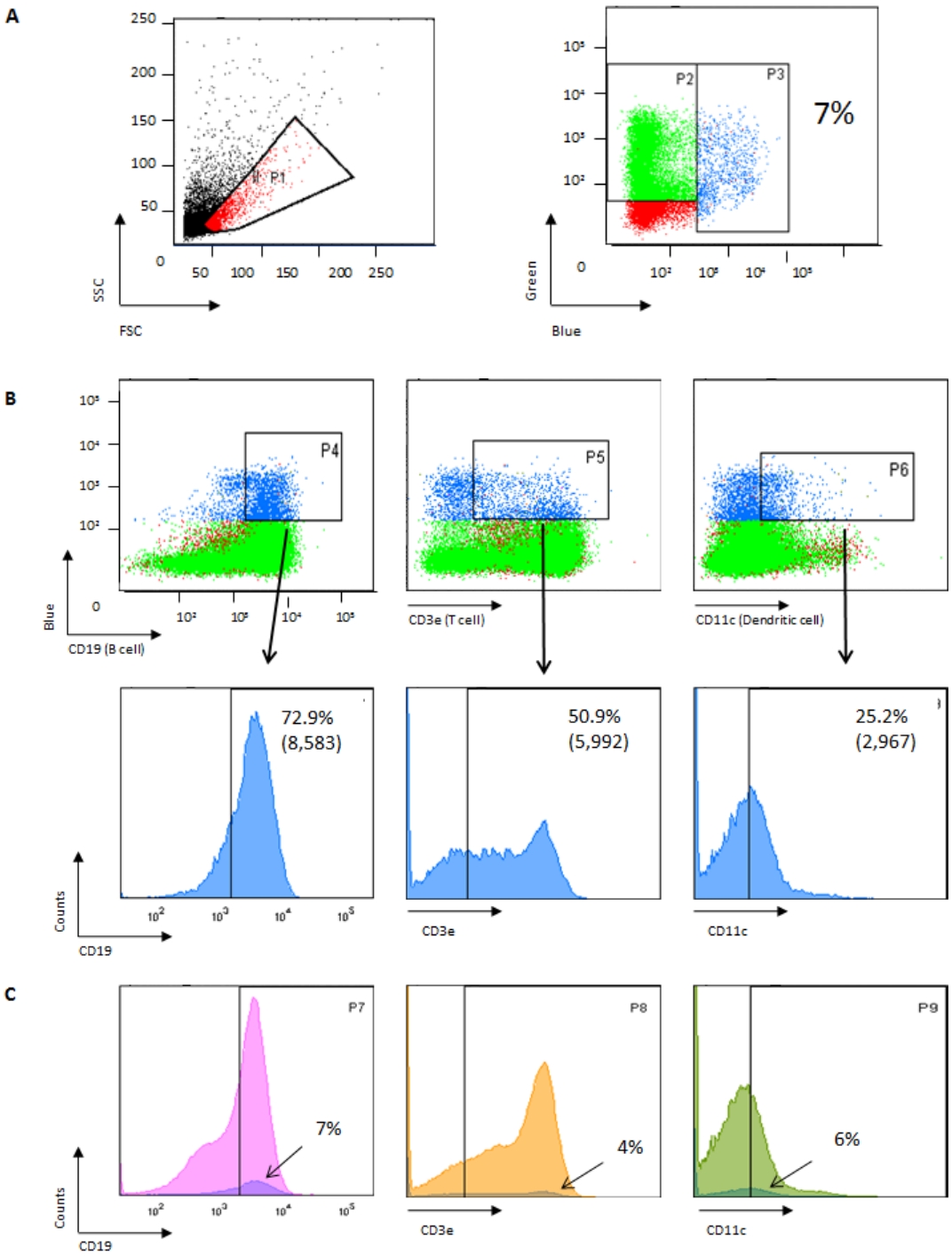

Figure 4.4.20: Distribution of NleD injection in splenocytes *in vitro*. Single cell suspensions from the mouse spleen were infected with *Citro* pACYCnleD (MOI 1000) for 6h. Subsequently cells were analysed by flow cytometry for surface expression of CD3e+ T cells, CD19+ B cells and CD11c+ dendritic cells following staining with CCF4-AM and antibodies**. A)** Gated population of splenocytes containing lymphocytes. **B)** Representative histogram showing percentage of blue cells expressing each surface marker. **C)** Histogram showing percentage blue cells from each subset of splenocytes. Representative data from 3 experiments are shown**.**

A

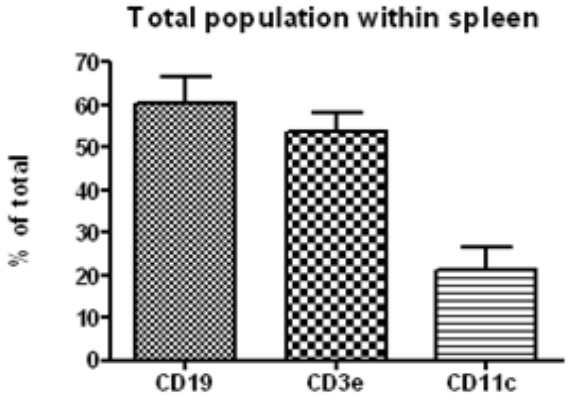

B

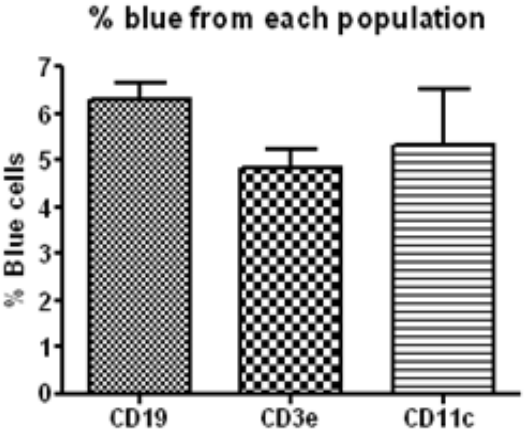

C

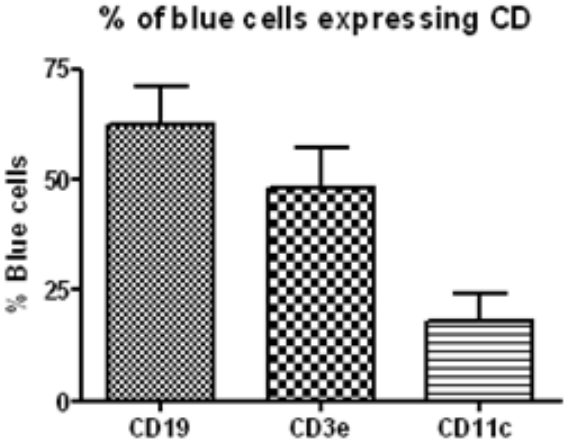

Figure 4.4.21: Distribution of NleD injection in splenocytes *in vitro*. A) Bar chart showing the percentage of splenocytes expressing the indicated surface markers. **B)** Bar chart showing the percentage of blue cells of the indicated subpopulations. **C)** Bar chart showing percentage of blue cells expressing one of the indicated surface markers. Data are summarised as the mean ± SEM of 3 independent experiments.

Chapter 5: *In vivo* visualisation of cells targeted for protein translocation by *C. rodentium*

5. *In vivo* visualisation of cells targeted for protein translocation by *C. rodentium*

5.1 Introduction

The gut-associated lymphoid tissue (GALT) sample antigens directly from mucosal surfaces to initiate protective immune responses in the gastrointestinal tract (described in detail in section 1.1.6). This occurs mainly through M cells present in the follicle-associated epithelium (FAE) of the GALT, where the active uptake and presentation of bacteria and antigens from the gut lumen to the immune cells of the lymphoid follicles helps to generate effective immune responses against enteric pathogens. Many of these enteric pathogens, however, are able to colonise GALT structures and manipulate the host antigen sampling system to gain access to the lymphoid follicles, where they can target immune cells and subvert host immune responses.

5.1.1 Bacterial colonisation of GALT structures

It is becoming increasingly clear that some enteric pathogens containing the T3SS exploit M cells to gain entry into and invade the host epithelium. For example, *Shigella* infects its host by translocating into M cells, where it invades macrophages and DCs residing within the M cell pocket. Inside macrophages, *Shigella* disrupts the vacuolar membranes and replicates within the cytoplasm, which eventually results in macrophage cell death. *Shigella* released from dying macrophages, invade and multiply within the surrounding epithelial cells and subsequently spread from cell to cell, causing shigellosis (Ashida et al., 2011).

Similarly, *Salmonella* preferentially adhere to and enter the epithelium through M cells of the PP (Jones et al., 1994). After crossing the intestinal epithelium in *Salmonella*-containing vacuoles (SCVs), *Salmonella* encounter several different types of phagocytes, such as neutrophils, macrophages, and DCs (Fabrega & Vila, 2013). The migration of these infected phagocytes further facilitate the dissemination of *Salmonella* via the bloodstream to the spleen and liver, where this pathogen preferentially replicates (Worely et al., 2006). Studies show that *Salmonella* from the GALT are able to reach the MLN via DC transportation through the intestinal lymph (Niess & Reinecker, 2006). In addition, DCs can directly take up *Salmonella* from the intestinal lumen by opening tight junctions and sending dendrites into the lumen

(Rescigno et al., 2001). Moreover, infected macrophages accumulate predominantly in the PPs and MLNs of infected mice (Rydstrom & Wick, 2007). Taken together, these studies provide evidence that invasive pathogens can enter the GALT and target immune cells to facilitate bacterial spread into systemic tissue.

Attaching effacing pathogens, despite being non-invasive and colonising the surface of the epithelium, also show tropism for GALT structures. For example, *EHEC* was shown to colonise the follicle-associated epithelium of distal ileal PP (Chong et al., 2007). Similarly, rabbit *EPEC (REPEC)* was observed exclusively in the ileal PP 48 hours after infection and was followed by the formation of an AE lesion in the ileal PP and the proximal colon 3 days after infection (Heczko et al., 2000). In addition, bioluminescent *in vivo* imaging has further demonstrated the localisation of AE pathogens, including *EPEC and EHEC* in the caecum and colon of infected mice (Rhee et al., 2011). These observations were further confirmed in mice infected with *C. rodentium* in which the primary site of bacterial colonisation was the caecum, followed by the distal colon and rectum (Wiles et al., 2004; Wiles et al., 2006). Although AE pathogens colonise GALT structures, they do not promote bacterial entry in to the GALT tissue via M cells. Rather, evidence suggests that AE pathogens may use the T3SS to actively prevent their uptake by M cells (Tahoun et al., 2011).

5.1.2 Targeting immune cells for T3SS-mediated effector translocation

Bacterial pathogens containing T3SS can inject effectors directly into the cytoplasm of host immune cells to alter their function. *Salmonella typhimurium* can inject a multitude of T3SS effectors into macrophages to facilitate intracellular survival and subsequent spread to host tissues. For example, injection of AvrA can dampen the host proinflammatory response inside macrophages (Wu et al., 2012), while translocation of MgtCB can promote the intracellular survival of bacteria (Blanc-Potard et al., 1997) alongside SopD, enabling *Salmonella* to replicate within the *Salmonella*-containing vacuoles of macrophages (Jiang et al., 2004). The translocation of SScI further promotes macrophage motility and accelerates the systemic spread of *Salmonella* (Worley et al., 2006). Eventually, the injection of SipB induces early macrophage pyroptosis and macrophage autophagy (Santos et al., 2001), which enables bacterial systemic dissemination throughout the infected organs (Guiney, 2005).

Similarly, *Yersinia pestis*, another invasive enteric pathogen, was shown to target neutrophils, macrophages, and DCs for injection of T3SS effectors directly into the host cell cytoplasm (Marketon et al., 2005). By injecting YopM, *Y. pestis* was able to deplete the host natural killer cell population (Kerschen et al., 2004). *Y. pestis* was also shown to target DCs for Yop injection, resulting in the inhibition of IL-12 and TNFα production in DCs (Brubaker, 2003). Similarly, *Y. enterocolitica* was shown to inject Yops into neutrophils, macrophages, and DCs but preferentially target follicular B cells, increasing the expression of the cell activation marker CD69 (Koberle et al., 2009). Injection of Yops directly into splenic DCs resulted in the negative regulation of the stimulatory capacity of DCs to induce T cell proliferation by *Y. enterocolitica* (Autenrieth et al., 2010). Moreover, by targeting adaptor molecules of the TCR signalling pathway, injection of YopH and YopP inhibited T cell activation (Gerke et al., 2005) and CD8+T cell priming (Trulzsch et al., 2005), respectively, in a mouse infection model. Similarly, for *Shigella* the injection of IpgD directly into T cells resulted in the inhibition of T cell migration *in vitro* and impaired T cell dynamics *in vivo* (Salgado-Pabon et al., 2014). Collectively, these studies provide strong evidence for the ability of enteric pathogens to target cells of both the adaptive and innate immune system for effector injection and subsequent suppression of the host immune responses, thereby facilitating their own survival.

However, very few studies have reported similar immune-targeting capabilities among non-invasive pathogens. An early study by Inman and Canty (1983) reported that rabbit *EPEC* can adhere to the surfaces of antigen-sampling M cells without forming pedestals or being taken up by these cells. This was later confirmed by subsequent studies in *EPEC* and *EHEC*, where the EspF effector was shown to inhibit *E. coli* translocation through human- and bovine-derived M cells *in vitro* and in co-culture systems (Martinez-Argudo et al., 2007; Tahoun et al., 2011). It is possible that EspF-mediated inhibition of M cell transcytosis allows *E. coli* to prevent its own internalisation early during infection, thereby delaying the initiation of the immune response.

Further studies have reported the ability of *EPEC* to interact with macrophages and inhibit phagocytosis through the T3SS-mediated translocation of EspA, EspB, EspD, EspF, and EspJ into macrophages (Goosney et al., 1999; Quitard et al., 2006; Marches et al., 2008; Tahoun et al., 2011). In particular, the effector EspJ was shown

to block opsono-phagocytosis, including the phagocytosis of C3b- and IgG-opsonised particles mediated through FcyR and CR3, respectively (Marches et al., 2008). These studies suggest that the inhibition of macrophage phagocytosis may allow AE pathogens to prevent their own uptake by host immune cells, thereby bypassing the first line of host defence presented by professional phagocytes and facilitating survival in the gastrointestinal tract.

In a more recent study, Vossenkamper et al. (2010) demonstrated the ability of *EPEC* to translocate effectors directly into DCs by sending dendrites through a model gut epithelium in a transwell system. This was also shown in myeloid DCs isolated from human PP biopsies. Effector translocation into DCs resulted in the inhibition of NFκB activation and the subsequent production of proinflammatory cytokines IL8, TNFα, and IL6. These effects were attributed to the T3-translocated effector NleE. Dendritic cells cultured with *EPEC* in the absence of NleE showed high secretion of IL8, TNFα, and IL6, as well as a strong nuclear translocation of p65 required for NFκB activation. In contrast, cytokine secretion and translocation of p65 were markedly lower in DCs cultured with *EPEC* in the presence of NleE. NleE injection into DCs further resulted in the reduced expression of co-stimulatory molecules CD80 and CD86, impairing the ability of these DCs to activate T cells. T cell activation was indicated by the production of IL2, a marker of lymphocyte activation (Vossenkamper et al., 2010). DCs prime naïve T cells and initiate adaptive immunity against bacteria, and hence by interfering with and suppressing DC function, *EPEC* promotes its own survival. The study by Vossenkamper et al. (2010) was the first of its kind to demonstrate the ability of AE pathogens to inject effectors that have an immunomodulatory role in host immune cells.

Given that *Citrobacter rodentium* is an *in vivo* model of AE pathogens, it is fair to speculate that *C. rodentium* can also target immune cells for effector injection. The finding that subepithelial DCs can extend dendrites into the lumen to sample gut antigens (Rescigno et al., 2001; Niess et al., 2005; Chieppa et al., 2006) and *EPEC* can inject effector proteins into DCs of intact PP as well as cultured DCs (Vossenkamper et al., 2010), strongly suggest that *C. rodentium* also has the capacity to inject effectors into DCs residing in the epithelium and the mouse PP *in vivo*.

Interaction of *C. rodentium* with immune cells can also be facilitated by M cell-mediated entry into the PP during bacterial sampling of the gut lumen. Inside the

subepithelial dome of the PP, *C. rodentium* can interact with naïve DCs, T cells, and B cells to target these cells for effector injection. Immune cells containing the translocated effectors may subsequently drain into the MLN and spleen, where their initiation of mucosal immune responses may be impaired. The impaired functions of immune cells can give pathogens such as *C. rodentium* the advantage of prolonged colonisation in the gut before protective immunity can initiate bacterial clearance. This may explain why AE pathogens show tropism for the follicle-associated epithelium (FAE) overlying the GALT: it contains M cell gateways and a dense population of immune cells, which these pathogens can manipulate to facilitate their own survival.

The aim of this study is to visualise the cells targeted for protein translocation *in vivo* by *C. rodentium*. In previous chapters, we generated a reporter strain of *C. rodentium* containing a plasmid-encoded fusion between the effector protein (NleD) and the β-lactamase reporter enzyme. The reporter strain was subsequently used to infect murine cell lines and primary cells to visualise cells targeted for protein translocation *in vitro*. In this chapter, the reporter strain will be used to infect Balb/c mice to enable the visualisation of effector translocation *in vivo*.

5.2 Results

5.2.1 Colonisation of mice by reporter *Citro* pACYCnleD strain

To investigate the ability of the reporter strain to colonise mice, 5- to 7-week-old female Balb/c mice were orally inoculated with 1-5x10^9 cfu of *Citro* pACYCnleD. A separate group of mice were inoculated with the control strain *Citro* ΔescNpACYCnleD. As described in section 2.8 in chapter 2, the infected mice were monitored over a period of 8-12 days post-inoculation (p.i). Viable counts of *Citrobacter* cfu were recovered from mice faeces at various days p.i.

The results (Fig. 5.4.1) show an initial increase over time in bacterial numbers in mice infected with *Citro* pACYCnleD**.** This peaks to approximately 10^9 cfu per gram of stool by day 6 p.i. In comparison, the number of bacteria in mice inoculated with the EscN mutant strain decreased rapidly until no bacteria were detected by day 6 p.i. This confirms that without the EscN protein, *Citrobacter* is unable to express a functional T3SS and hence cannot colonise mice. During further infection studies comparing the reporter strain with wildtype *C. rodentium,* stool counts showed both strains following similar colonisation dynamics and peaks of infection (Fig. 5.4.2). The transformation of wildtype bacteria with pACYCnleD plasmid thus confers no changes in the ability of *Citrobacter* to colonise the mice gut mucosa.

The hyperplasic responses of mice infected with various strains of *C. rodentium* were also compared (Fig. 5.4.3). Hyperplasia, indicated by an increase in mucosal thickness in the distal colon, was observed in both groups of mice infected with either wildtype *C. rodentium* or the reporter strain, with an average of 220 μm and 240 μm colonic thickness, respectively. The average mucosal thickness in uninfected mice and mice infected with the mutant strain were approximately 150 μm, indicating no hyperplasia. As no changes in other characteristics such as weight (data not shown) or loose stool consistency were seen in the infected mice, bacterial shedding in faeces and mucosal thickness were the only reliable observations for establishing the progression of *Citrobacter* infection in this study.

5.2.2 Plasmid stability of pACYCnleD *in vivo*

Having confirmed the competency of the reporter strain for colonising mice, the stability of the pACYCnleD plasmid *in vivo* was investigated. Mice were infected with the reporter strain as described previously, and bacteria were then isolated from infected mice faeces and grown in antibiotic-containing media to select those that either lost or retained the pACYCnleD plasmid. This was done by growing the bacteria in LB plates containing nalidixic acid and in LB plates containing nalidixic acid combined with chloramphenicol. Resistance to nalidixic acid indicated the presence of all *C. rodentium* strains, while resistance to both nalidixic acid and chromamphenicol indicated strains containing the plasmid only. By quantifying the number of colonies that grew on the plates containing both nalidixic acid and chloroamphenicol and comparing this to the number of colonies that grew on the plates containing only nalidixic acid, we determined the percentage of bacteria that lost or retained the plasmid. The following formula was used:

$$\text{Percentage of bacteria that have lost the plasmid} = \frac{\text{No. of nalidixic acid \& chloramphenicol resistant CFU}}{\text{No. of nalidixic acid resistant CFU}} \times 100$$

The subsequent data (Fig. 5.4.4B) reveal that approximately 45% of bacteria (equivalent to ~50 cfu/g of stool) lost the plasmid by day 9. This confirms that the majority of *Citro* pACYCnleD strains retained the plasmid at least until day 9 p.i. PCR analysis further confirmed the ability of this reporter *C. rodentium* strain to express NleD-TEM fusion proteins in the mouse gut (Fig. 5.4.5).

5.2.3 *In vivo* visualisation of NleD injection into immune cells of *C. rodentium*-infected mice

To determine whether NleD injection can be detected *in vivo*, Balb/c mice were orally gavaged with *Citro* pACYCnleD or *Citro* ΔescNpACYCnleD. The bacterial burden of mice, regularly monitored over the course of infection, confirmed the ability of the reporter strain to successfully colonise the mice gastrointestinal tract (Fig. 5.4.11). Subsequently, after 7 to 11 days, immune cell suspensions were prepared from the spleen, MLN, and Peyer's patch, stained with CCF4-AM for an hour, and subjected to flow cytometry analysis (Figs. 5.4.6-5.4.9). Contrary to our expectations, the flow cytometry data revealed no distinct population of blue cells

from any of the lymphoid organs or tissues. Despite cell analysis at various days including day 7, 8, 9, 10, 11, 12 and 14 post-infection, the results failed to show any blue cells from the infected mice. Representative data for days 7, 9, and 11 are summarised in Figs. 5.4.6-5.4.9.

As a control, epithelial cells were analysed for β- lactamase activity following the above infection protocol. Epithelial cells lining the gut wall are most exposed to bacteria residing in the lumen, and hence if *C. rodentium* injects proteins into host cells, epithelial cells are most likely to be targeted first. Unfortunately, analysis by fluorescence microscopy showed blue cells in both positive and negative controls; that is, in cell preparations infected with wild-type and reporter strains of *C. rodentium*. These blue epithelial cells also appeared to be in clumps (Fig. 5.4.10). The blue fluorescence in wild-type *C. rodentium*-infected cells cannot be attributed to the enzymatic activity of β-lactamase, as these cells do not express β-lactamase fusion proteins. Instead, the CCF4 substrate must somehow have been cleaved in the absence of β-lactamase activity. Enterocytes are filled with digestive enzymes, such as peptidases, sucrase, maltase, lactase, and intestinal lipase, and it is possible that these were cleaving the CCF4 substrate; however, further experiments would be necessary to confirm this. As a result, epithelial cells isolated from the colon of infected mice were not analysed by microscopy.

5.2.4 Ability of immune cells to remain 'injectable' after *in vivo* infection with *Citro* pACYCnleD

To explore whether the lack of β-lactamase activity *in vivo* was due to the gut cells being resistant to NleD injection *in vivo*, immune cell preparations from the spleen, MLN, and PP of infected mice were inoculated with *Citro* pACYCnleD for 6 hours and incubated with CCF4 AM (Figs. 5.4.12-5.414). Flow cytometry analysis confirmed that β-lactamase activity occurred in a dose-dependent manner and mouse cells were not resistant to nleD injection following oral inoculation *in vivo*.

5.2.5 Ability of *Citro* pACYCnleD to inject NleD into host cells after passage through the mouse gut

Next, we investigated the ability of the host-passaged *Citro* pACYCnleD to inject murine cells *in vitro*. *Citro* pACYCnleD was recovered from mouse stool at day 9 post-infection, isolated, grown overnight, and used for subsequent infection of T cells *in vitro*. As expected, normal β-lactamase activity was observed in T cells infected with the host-passaged bacteria (Fig. 5.4.15) In addition, NleD injection increased with increasing MOI of the host-passaged bacteria, confirming that the reporter strain retained its ability to inject murine cells *in vitro*.

5.2.6 *In vivo* infection of mice using hyperinfectious bacteria

In a final attempt to visualise blue cells from the mice gut *in vivo*, infection studies using hyperinfectious bacteria were conducted. Following inoculation of mice with *Citro* PACYCnleD, hyperinfectious bacteria were isolated from the stool at day 6 post-infection, resuspended in sterile PBS, and orally gavaged to a new group of mice. Mice infected with the hyperinfectious bacteria were sacrificed at day 3 p.i and the epithelial cells from the colon and rectum were analysed for blue cells (Fig. 5.4.16). Unfortunately, no β-lactamase activity was observed.

5.3 Discussion

The aim of this study was to visualise host cells targeted for protein translocation by *C. rodentium in vivo.* In previous chapters we generated the reporter strain *Citro* pACYCnleD and demonstrated its ability to inject into murine cell lines and primary cells *in vitro*, and in this chapter we investigated the ability of reporter strain to inject NleD fusion proteins into host cells *in vivo*.

Bacterial shedding in mouse stool throughout the infection period confirmed that *C. rodentium* followed the classical growth curve reported in earlier studies (Wiles et al., 2004; Wiles et al., 2006; Collins et al., 2013). Following an oral gavage, the CFU counts indicated an initial increase in bacterial numbers (~5x10 $^{8-9}$ cfu/g) within 24 hours post-inoculation (p.i) followed by a sudden dip (~5x10$^{6-7}$ cfu/g) in day 2 p.i (data not shown). After day 2, bacterial shedding began to increase again, until day 6 when bacterial numbers peaked to ~5x10 $^{9-10}$ cfu/g. Following the peak, bacterial numbers declined from day 8 until the end of the experiment.

These observations corroborate previous studies in which bioluminescence was used to indicate bacterial colonisation of the mouse GI tract (Wiles et al., 2004; Wiles et al., 2006). Both studies showed that in mice orally gavaged with *C. rodentium*, bacteria reached the caecum and the colon within 1 hour p.i. and began to clear the colon with some remaining in the caecum within 5 hours p.i until the bioluminescent signal was lost due to bacterial numbers falling below 10^3 cfu/g. These studies indicate that the majority of inoculated *C. rodentium* does not colonise the mouse initially but rather passes straight through the gastrointestinal tract, which accounts for the initial increase and subsequent decrease in bacterial shedding within the first 24 hours p.i. According to these studies, only a few bacteria remain in the caecal patch, where they adapt to the gastrointestinal environment and activate virulence genes necessary for subsequent colonisation of the distal colon and rectum. Indeed, the bioluminescent signal was detected again after 24-72 hours p.i when bacteria had increased in number and began to colonise the mouse gastrointestinal tract (Wiles et al., 2004; Wiles et al., 2006).

Although the initial colonisation dynamics observed in previous studies (Wiles et al., 2004; Mundy et al., 2004; Wiles et al., 2006; Girard et al., 2009) are consistent with this study, *C. rodentium* colonisation during the later stages of infection seems to differ slightly. In our study, bacterial numbers reached a peak at day 6 followed by

bacterial clearance from day 8, which is earlier than previous reports in which bacterial numbers peaked from day 8 and started to decline after day 10. The slight difference in bacterial clearance may be due to use of a different strain of mice: we used BALB/c mice, whereas the previous studies used C57Bl/6 mice. Studies comparing mouse strains have suggested that C57Bl/6 mice exhibit increased susceptibility to *C. rodentium*-induced colitis in comparison to BALB/c (Vallance et al., 2003). C57Bl/6J mice infected with *C. rodentium* exhibited a lower survival rate, higher CFU count at day 4 and 6 p.i, and higher colon weight and crypt height at day 6 p.i than infected BALB/c mice (Vallance et al., 2003). Additional studies found that acute colitis induced by dextran sulfate sodium (DSS) progressed to chronicity in C57Bl/6 mice but not in BALB/c mice (Melgar et al., 2005). Such findings suggest that in comparison to C57Bl/6 mice, the BALB/c mice may have reduced susceptibility to *C. rodentium*-mediated colitis, which in turn may help to explain the results observed in this study.

Having established the ability of *C. rodentium* to colonise and infect mice, we monitored the ability of the reporter strain, containing pACYCnleD plasmid, to also establish infection in comparison to the wild-type *C. rodentium* strain. It was assumed that the reporter strain may take longer to colonise, as the presence of a plasmid requires the bacteria to synthesise additional the nucleic acids and proteins necessary to perform plasmid-encoded functions, which may impose an energetic burden on the reporter strain and make it an inferior competitor relative to its wild-type counterpart (DaSilva and Baily, 1986). However, after comparing the viable colony forming untis (CFU) counts and crypt lengths, we found no significant difference in the level of colonisation and colonic hyperplasia between the two strains at any given time. Thus the plasmid pACYCnleD conferred little or no fitness burden on the *C. rodentium* host strain.

Next, the plasmid stability of pACYCnleD within the mouse gut was investigated. The pACYCnleD plasmid was maintained under lab conditions by growing the host strain in LB containing chloramphenicol, due to the presence of the chloramphenicol resistance gene in the plasmid. However, in the absence of antibiotic selection in the mice gut *in vivo*, there was a risk that the reporter strain would revert back to its original plasmid-free form. Without the plasmid, which encodes the reporter enzyme, visualisation of protein translocation would not be possible even if bacterial

colonisation did occur as normal, thus defeating the purpose of this study. Nonetheless, our data confirm that the plasmid-bearing strain was stably maintained in the mouse gut, as the pACYCnleD plasmid was successfully prepared from mouse faecal samples as late as day 10 p.i.

The plasmid vector pACYC184, from which the pACYCnleD was derived, is present at a low copy number in the bacterial cells. Past studies using a pACYC184-transformed strain of *E. coli* grown in antibiotic-free media found that the plasmid-bearing strain was competitively inferior to its plasmid-free counterpart (Bouma and Lenski, 1988). However, when the same strain was propagated for 500 generations (75 days) in media containing chloramphenicol antibiotics, genetic adaptation occurred in the bacterial chromosome such that subsequently the 'evolved' strain was superior to the 'naïve' strain even in the absence of antibiotic selection (Bouma and Lenski, 1988). Not only was the cost of plasmid carriage eliminated, but the plasmid benefitted the bacteria that had evolved with the plasmid present. This may partly explain why the pACYC184 is commercially available and is used routinely as an expression vector for cloning. Evidence from this study, along with findings from previous studies (Mundy et al., 2003; Mundy et al., 2004; Kelly et al., 2006), confirms the stability of the pACYC184 plasmid (and its derivatives) *in vivo* and hence its utility for mouse infection studies.

The current study found that host-adapted reporter *C. rodentium*, isolated from freshly shed stool samples, was able to inject effectors into T cell lines *in vitro*. In other words, the ability of *C. rodentium* to translocate proteins was retained after passage through the mouse gut. This is in line with earlier studies describing the ability of host-adapted *C. rodentium* to efficiently adhere to and trigger actin polymerisation and microcolony formation on cultured epithelial cells (Bishop et al., 2007). In fact, such studies observed a higher expression of LEE genes from the host-adapted bacteria in comparison to bacteria grown in LB broth (Bishop et al., 2007). These findings support the 'hyperinfectious' state of *C. rodentium* first observed by Wiles et al. (2005); these authors reported the enhanced ability of host-adapted *C. rodentium* to infect mice in low doses, which bypassed the initial tropism for the caecum and colonized the colon directly. This is further supported by a recent study that describes the host-adapted bacteria as a 'hypervirulent-host-associated' *Citrobacter rodentium* strain (Smith & Bhagwat, 2013). However, since the

hyperinfectious state of *C. rodentium* is removed with one overnight passage of bacteria in LB broth (Wiles et al., 2005), the host-adapted *C. rodentium* used in this study was not hyperinfectious, as it was grown in LB broth overnight following isolation from mouse stool. Nonetheless, the host-adapted bacteria were able to translocate proteins *in vitro* and their passage through the mouse gut did not reduce the bacteria's ability to subsequently colonise *in vitro*.

Since *C. rodentium* is a non-invasive pathogen that adheres to the epithelial lining of the gut, IECs are the primary targets of *C. rodentium* effector translocation. Upon contact with host epithelium, Tir is translocated through the T3SS, which inserts itself back into the host cell membrane and acts as a receptor for bacterial intimin where Tir-intimin binding causes intimate attachment of *C. rodentium* to its host cell (described in Chapter 1). For this reason, isolated IECs were the first cells to be analysed for effector translocation by *C. rodentium* in this study. Contrary to expectations, IECs prepared from control mice and incubated with CCF4-AM fluoresced blue rather than green. The presence of blue cells in the absence of β-lactamase activity suggests that these epithelial cells were auto-fluorescing, perhaps because of enzyme activity within these cells arising from their role in the digestive system. Indeed, the enterocyte brush border in BALB/c mice is filled with enzymes such as lactase, gamma-glutamyltransferase, alkaline phosphatase, and sucrase (Kozakova et al., 2002). Although further studies are required to confirm cleavage of CCF4 by these enzymes, epithelial cells isolated from the colons of infected mice were excluded from this study.

Since the β- lactamase translocation assay did not appear to work in the isolated epithelial cells due to autofluorescence, further research is necessary to explore alternative methods to isolate IECs in order to minimise/diminish autofluorescence. Alternative isolation procedures may involve (1) mechanical shaking (vortex), (2) enzymatic separation using low trypsin concentration or (3) chelating agents using EDTA. Previous studies show that the microscopic appearance of IECs and the level of brush border enzyme activity changes according to the method of isolation used (Mac Donal et al, 2008). Therefore it is recommended to optimise the IEC isolation procedure to ensure its suitability for the β- lactamase translocation assay, so that visualisation of effector injection into isolated IECs (positive control) is enabled prior to analysis of isolated immune cells during future study.

Less anticipated, however, was our inability to visualise effector translocation *in vivo*. This finding was disappointing given the ability of these reporter bacteria to successfully colonise the mouse gut, express T3SS machinery, express the plasmid encoded reporter fusion, and inject the fusion proteins into mouse gut cells *in vitro*. The fact that the *in vivo* infection studies were carried out several times and always produced the same result, suggests that there may be underlying factors.

One possible explanation is that *C. rodentium* entering the PP was killed by the alternative pathway of the complement system. The alternative pathway of the complement system can be activated by spontaneous hydrolysis of serum C3 into C3b, which binds to bacterial cell wall components of gram-negative bacteria (Goldsby et al., 2003). This initiates the complement cascade, leading to the formation of the membrane attack complex (MAC), which mediates cell lysis of the bacteria. Bacterial phagocytosis can also be enhanced by C3b acting as an opsonin and coating the surfaces of bacteria. Initiation of the complement cascade can additionally produce anaphylatoxins, including C3a, C4a, and C5a, which enhance inflammation by increasing vascular permeability, inducing extravasation and chemotaxis of leukocytes at the site of inflammation, and increasing expression of complement receptors on neutrophils (Goldsby et al., 2003). The increase in inflammation can further contribute to phagocytic killing of *C. rodentium* by complement. Evidence for the presence of complement proteins in the PP is provided by a previous study in which complement components related to the alternative pathway were localised within human lymphoid tissues, including the appendices, PP, and tonsils (Yamakawa & Imai, 1992). Hence, it is possible that the activation of complement by the alternative pathway, which serves as an important innate immune defence against many bacterial pathogens, may have reduced *C. rodentium* numbers in the PP.

Even if some *C. rodentium* in the PP did survive and inject into immune cells, this could have been below the level of detection. It is possible that the number of events in which these bacteria encountered, interacted with, and targeted immune cells for protein translocation was too small to be visualised via the β-lactamase reporter system. Koberle et al. (2009) were unable to detect blue cells following orogastric infection of mice with *Yersinia* because the number of bacteria attached to a single

host cell was too low for detection of the β-lactamase reporter system; however, following tail vein infection the authors detected blue cells in the spleens of the mice.

If effector injection did occur, it is possible that the effector proteins were degraded by proteosome activities inside the host cells. Studies using *Salmonella enterica* have previously reported a difference in the cellular levels of two effectors, SopE and SptP, inside host cells resulting from differential regulation by the host proteosome (Kubori & Galan, 2003). Although both effectors were delivered into host cells in approximately the same amounts, SopE was rapidly degraded by the host proteosome, while SptP exhibited much lower degradation kinetics and remains stable for longer. The half-life of these effector proteins was determined by their secretion and translocation domains (Kubori & Galan, 2003; Buttner 2012). These findings suggest the possibility that following their injection into host cells, NleD fusion proteins may have been subjected to host proteosome degradation. However, this would require the degradation to occur after 6 hours p.i, otherwise visualisation of injected cells *in vitro* would not be possible.

Another factor underlying the lack of blue cells may be a loss of cells during isolation procedures. Although an average of 10^5 to 10^8 live cells were routinely isolated from the spleen, MLN, and PP for analysis in this study, this number does not necessarily reflect their original numbers in the tissue. It is thus possible that our isolation techniques did not pick up the injected cells, which may have been low in number from the outset. Recently, the use of multi-photon confocal microscopy in transgenic mice allowed the visualisation of a dense network of approximately 1 million DCs and macrophages in the small intestinal LP, a number which no current isolation methods can produce (Pabst and Bernhardt, 2010). The use of multi-photon confocal microscopy to visualise cells in transgenic mice following a β-lactamase translocation assay may be an important strategy for future studies.

Koberle et al (2009) found that the efficiency of the ß-lactamase reporter system in *Yersinia* is strain-dependent; the system worked highly efficiently when expressed in the E40(09) strain of *Yersinia* but not the WA-314(08) strain. It may be possible that the ß-lactamase reporter system did not work efficiently in the *C. rodentium* strain used in this study. Future studies should investigate the efficiency of the ß-lactamase reporter system in various strains of *C. rodentium* via transformation of the pACYCnleD plasmid.

Since the reorganization of actin filaments on the surface of IECs are crucial for *C. rodentium* pathogenesis, and this process is dependent on the T3SS mediated translocation of Tir into host cells, it may have been advisable to carry out immunofluorescence staining of Tir-actin in the colonic tissues of infected mice prior to β-lactamase translocation assay. This would ensure that the infecting *C. rodentium* is indeed injecting effectors into host cells. If the actin filaments cannot be visualised, this would indicate that *C. rodentium* is not injecting into host cells and that further studies would be required to optimise mouse infection procedures.

An alternative explanation for the inability to visualise effector injected-host cells may be due to the thick, two layer of mucus present on the surface of epithelium in the mice distal colon, which may have prevented bacterial contact with epithelial cells and the subsequent injection of *C. rodentium* effectors. Having said that, *C. rodentium* colonisation of the distal colon can cause a depletion in goblet cell numbers, which in turn, may reduce the level of mucus present in the colon, thus enabling bacterial contact with the epithelium. In addition, *C. rodentium* mediated inflammation of the mice colon triggers a loss of epithelial barrier integrity, which enables the bacteria to enter the sterile lamina propia, thereby increasing bacterial contact with immune cells. But most importantly, *C. rodentium*, like other attaching effacing pathogens, has the ability to breach the mucosal barrier and bind intimately to IECs in the host epithelium. Future studies should focus on the visualisation of this intimate binding between *C. rodentium* and host IECs, using procedures such as immunolfluorescence staining of Tir-actin (mentioned previously), to confirm that bacterial translocation of effectors into epithelial cells has indeed occurred prior to analysis by β- lactamase translocation assay.

Although isolated immune cells were analysed from the MLN, PP and the spleen, future studies may consider the analysis of immune cells from other lymph nodes. Recently, the caudal lymph node has been described to drain immune cells migrating from the descending colon and the rectum in addition to the MLN, which drains immune cells arriving from the jejunum, ileum, caecum and the ascending colon (Mowat & Agace, 2014). Although the MLN was thought to drain the entire small and large intestine at the time of this study, the possibility of the *C. rodentium* injected immune cells draining into the caudal lymph node should be explored for further study.

Additionally, the thoracic duct is the largest lymphatic vessel of the lymphatic system, collecting most of the lymph in the body, including intestinal immune cells migrating from the MLN, and draining into the systemic blood circulation. Mice, which have undergone the removal of MLN from the lymphatic circulation in a procedure known as mesenteric lymphadenectomy (MLNx), the thoracic duct lymph contains a population of immune cells that are normally present in the MLN (Rhodes, 1985). Another procedure known as thoracic duct cannulation allows the collection of all MLN-bound immune cells in sufficient numbers over a long period of time (Cerovic et al, 2013). The isolation and analysis of such cells for β-lactamase activity following the infection of mice with reporter *C. rodentium* is an important study for future research.

Bacterial shedding during *C. rodentium* infection peaks around day 6-7 p.i, so it is reasonable to assume that effector injection may also peak during this time-point where the highest number of bacteria passes through the colon. However since we were unable to observe bacterial injection during this time, it may be a consideration for future studies to isolate cells during earlier time points. It is known that during the early stages of *C. rodentium* infection, bacteria pass through the colon at day 0-1 p.i. Even though these bacteria do not colonise, there may be a possibility that they may be injecting effectors into the intestinal cells. Bacteria may also be injecting effectors into target cells during early colonisation at days 2-6 p.i when bacterial numbers increase until the peak of infection.

C. rodentium is an extracellular pathogen that colonises the epithelial surface of the caecum, colon, and rectum. As a result, the majority of cells targeted for protein translocation are epithelial cells. However, CX_3CR_1+DCs extend transepithelial processes through the epithelium to sample luminal bacteria (Rescigno et al., 2001; Neiss et al., 2005) and EPEC inject effectors into myeloid-derived DCs to shut down NFκβ; in view of this, we hypothesised that DCs may also be targeted for protein translocation by *C. rodentium.* In addition we hypothesised that target cells containing effectors may migrate to surrounding draining lymph nodes and lymphoid tissue, such as the spleen, MLN, and PP, where the effectors may exert an immunomodulatory effect on the host immune response.

Recently the identity of CX_3CR_1+ cells has come into question. Schulz et al (2009) showed that CX_3CR_1+ cells did not express the chemokine receptor CCR7 required for their migration to the MLNs and were inefficient at priming naïve T cells, which—in addition to the observation that CX_3CR_1+ cells displayed macrophage-like characteristics, including a vacuolar cytoplasm (Bogunovic et al., 2009)—led many researchers to classify these cells as macrophages (Denning et al., 2007; Schulz et al., 2009; Bogunovic et al., 2009; Pabst & Bernhardt, 2010; Farache et al., 2013).

Another population of LP cells associated with the epithelium, CD103+DCs, were recently shown to migrate between the LP and the intraepithelial compartment of the small intestine (Farache et al., 2013). After entering the epithelium, these DCs migrated above the basal membrane, extended thick finger-like projections which could capture luminal *Salmonella*, upregulated the expression of CCR7, migrated back to the LP, and entered draining MLNs. There, they presented antigens to T cells, resulting in the proliferation of antigen-specific CD8 T cells that were later imprinted for gut homing (Farache et al., 2013). Hence, CD103+DCs are considered major players in presenting antigens to T cells and thereby inducing adaptive immunity in the intestine.

Although CX_3CR_1+ cells are more efficient than CD103+ cells at sending dendrites into the lumen and capturing luminal bacteria and/or antigens, the latter express CCR7, migrate to MLN, and are more efficient at presenting antigens to T cells (Farache et al., 2013). A recent study demonstrated a functional cooperation between these two phagocytes to establish oral tolerance (Mazzini et al., 2014). CX_3CR_1+ cells were found to take up soluble fed antigens and transfer them to CD103+DCs by a mechanism that was dependent on the gap junction protein connexin 43. Deletion of connexin 43 prevented CD103+ DCs from acquiring antigens and presenting them to T cells to drive T regulatory cell differentiation and induce oral tolerance (Mazzani et al., 2014).

A slightly different role for CX_3CR_1+ cell-mediated phagocytosis of luminal bacteria has been demonstrated in *C. rodentium* infection (Manta et al., 2013). Upon infection of transgenic CX_3CR_1-GFP mice, *C. rodentium* was associated closely with and within CX_3CR_1+ cells during the peak of infection, suggesting that luminal *C. rodentium* had been phagocytosed by CX_3CR_1+ cells in the colonic LP (Manta et al.,

2013). Phagocytosed *C. rodentium* may provide signals to CX_3CR_1+ cells, which help to facilitate IL22 expression by innate lymphoid cells (ILCs) (Manta et al., 2013); IL22 regulates expression of the antimicrobial molecules RegIIIγ and REGIIIβ as well as increasing epithelial cell proliferation and promoting wound healing. Uptake of *C. rodentium* by CX_3CR_1+ cells and subsequent initiation of the IL22 mediated immune response may thus serve as a host defence mechanism against enteric pathogens (Manta et al., 2013). Although such findings suggest that *C. rodentium* may not actively support its uptake by CX_3CR_1+ cells, experiments using *C. rodentium* lacking the T3SS will need to be conducted in order to clarify this.

For future studies, intravital two-photon microscopy may provide an alternative method to visualise cells targeted for effector translocation by *C. rodentium*. Intravital two-photon microscopy enables live imaging of immune cells deep within lymphoid tissues and organs in real time (Farache et al., 2013). Application of this technology to the β-lactamase reporter system could provide three dimensional information about the identity, location, and motility or migration of live immune cells targeted for effector injection by *C. rodentium* in live mice, generating valuable insight into the modulation of host immune responses by bacterial effectors and advancing our understanding of host-pathogen relationships in the gut.

5.4 Figures

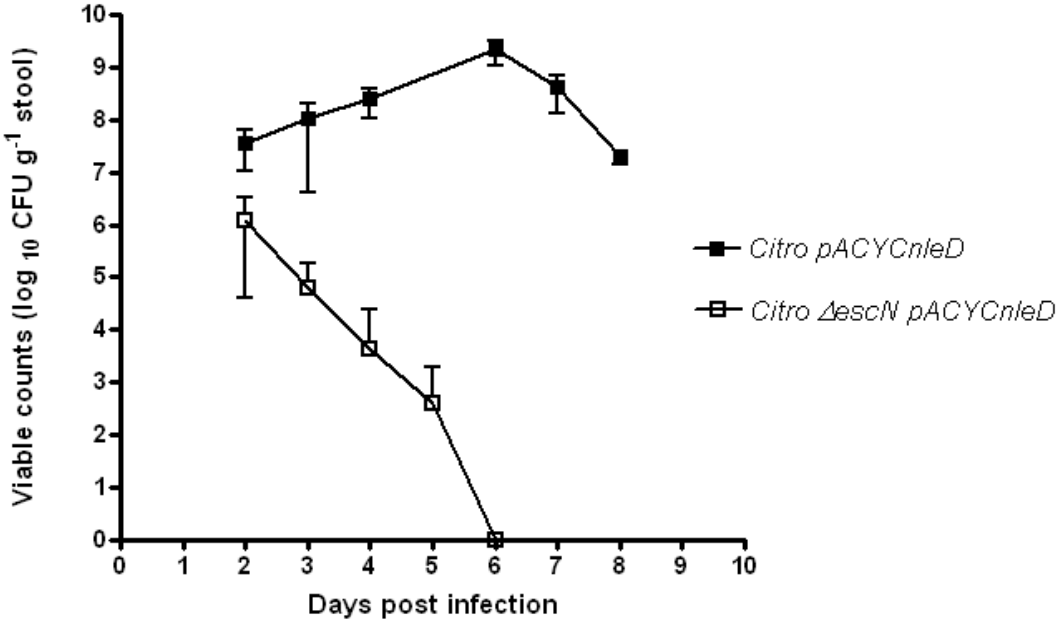

Figure 5.4.1 Bacterial shedding in mice infected with reporter *C. rodentium* or *ΔescN* deletion mutant. Balb/c mice (x12) were orally gavaged with $1x10^9$ colony forming units (CFU) of *Citro pACYCnleD* (closed squares) or *Citro ΔescNpACYCnleD* (open squares) as described in Materials & Methods. Infected mice were monitored for bacterial shedding for 8 days post inoculation (p.i). Viable counts were made by quantification of CFU shed per gram of stool from individual mice. Error bars indicate the mean± SEM of 6 individual mice. Representative data shown from at least 3 independent experiments.

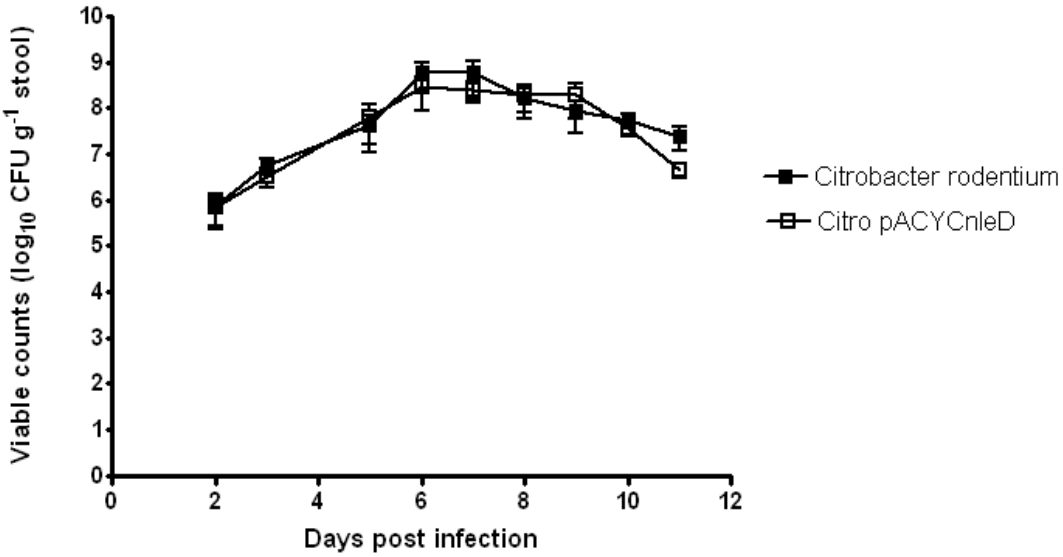

Figure 5.4.2 Bacterial shedding in mice infected with wildtype *C. rodentium* or reporter *C. rodentium*. Mice (x12) were orally gavaged with $1x10^9$ CFU of *Citrobacter rodentium* (closed squares) or *Citro pACYCnleD* (open squares) and monitored for 11 days. Viable counts were made by quantification of CFU shed per gram (G) of stool from individual mice. Error bars indicate the mean±SEM of 6 mice.

A

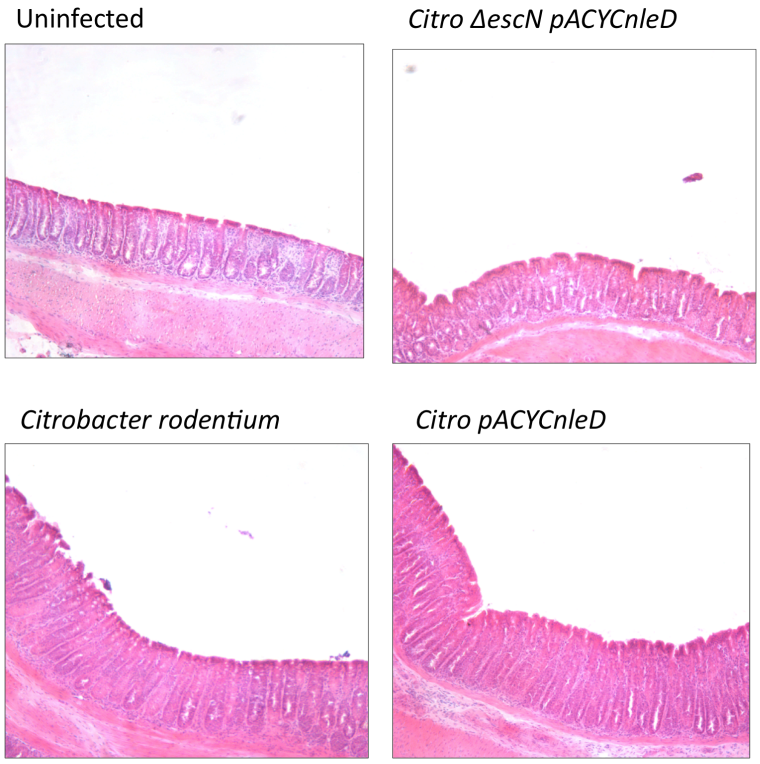

B

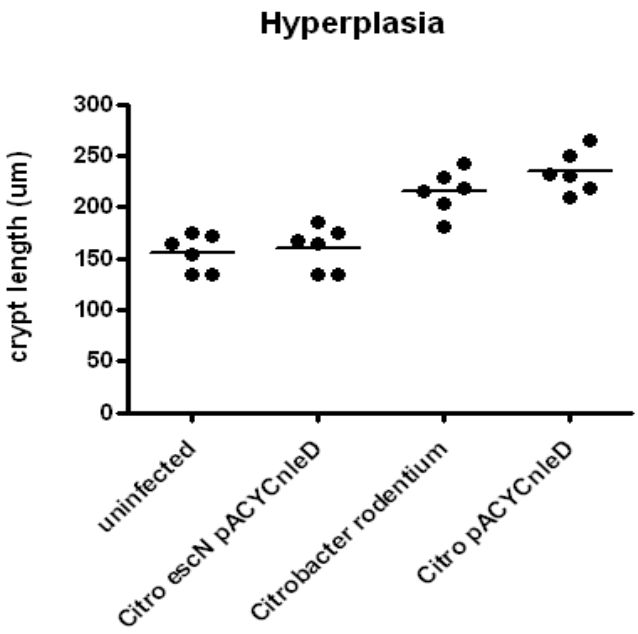

Figure 5.4.3 Comparison of mucosal thickness in mice infected with various strains of *C. rodentium*. Mice infected with *CitroΔescN pACYCnleD, Citrobacter rodentium and CitropACYCnleD* were sacrificed at day 7 p.i and sections of the distal colon were stained with Haematoxylin and Eosin (H&E). **A)** H&E staining of colonic sections showing crypt hyperplasia. **B)** Hyperplasia is indicated by an increase in crypt length (μm) in the distal colon. Data expressed as mean of 6 individual mice. Results are representative of at least 3 independent experiments.

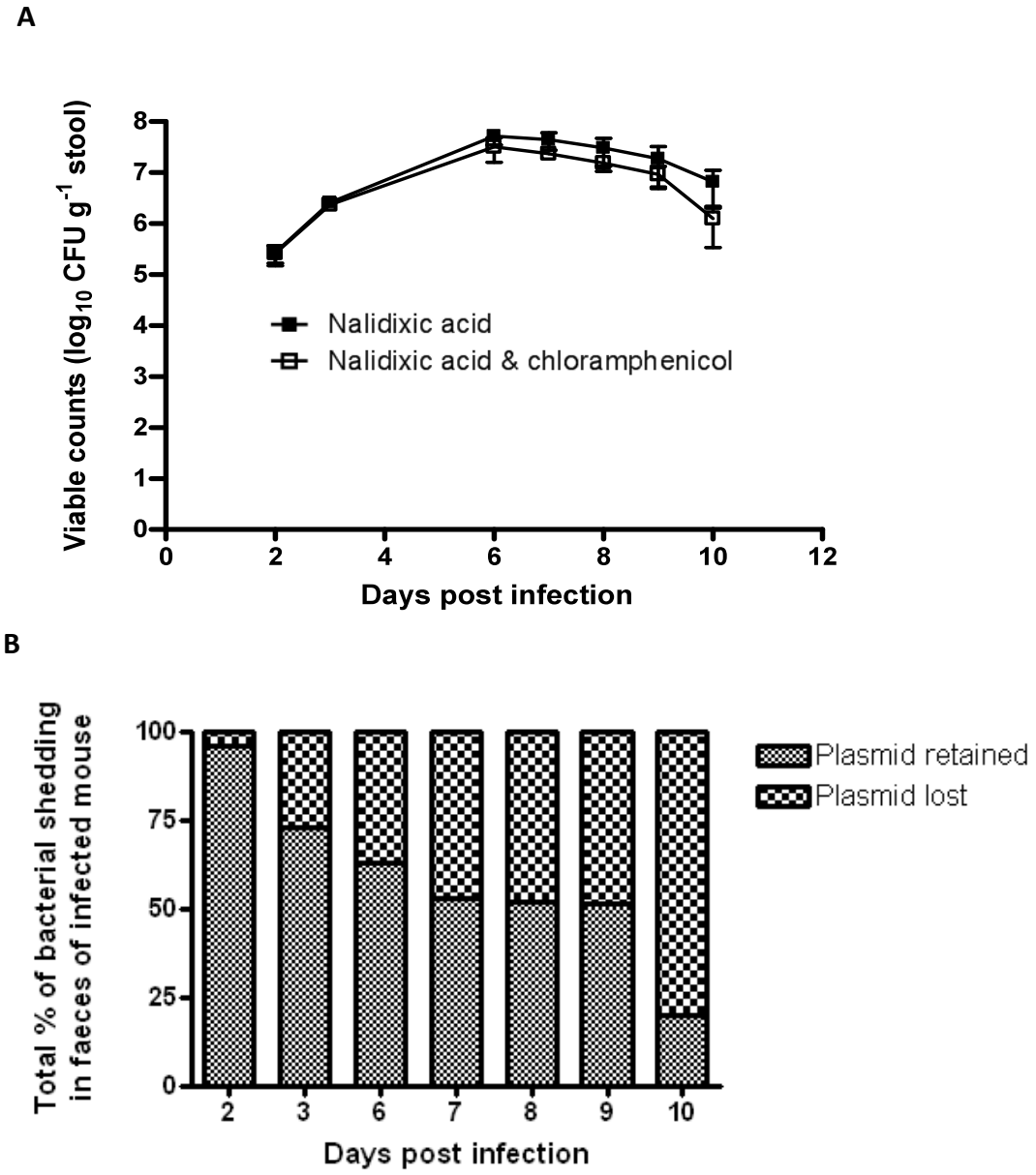

Figure 5.4.4: Plasmid stability in infected mice over time. Mice were infected with *Citro pACYCnleD* and monitored over 10 days. **A)** Viable counts of *Citrobacter* (cfu/G of stool) observed on LB plates containing either nalidixic acid (closed squares) or nalidixic acid with chloramphenicol (open squares). Error bars indicate the mean+ SEM of 7 individual mice. Statistical analysis revealed no significant difference between the datasets Nalidixic acid and Nalidixic acid & chlorampenicol as the P values were all greater than 0.05. **B)** Segmented column chart showing the percentage of bacteria that have either lost or retained the plasmid. Representative data from 4 independent experiments.

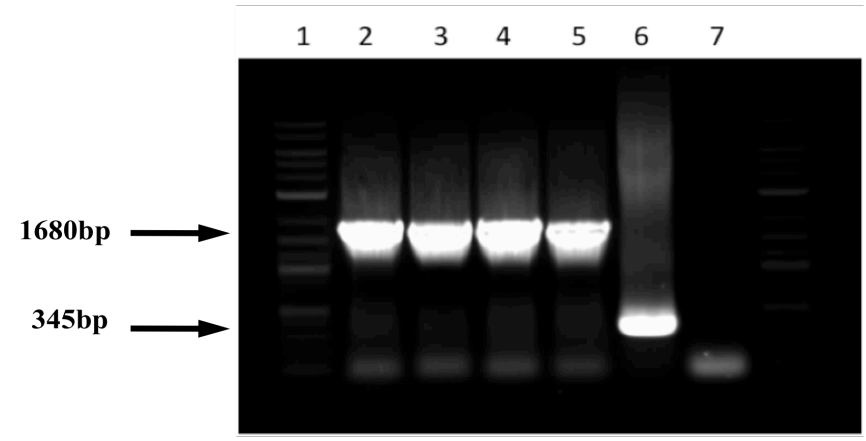

Figure 5.4.5: PCR analysis confirming plasmid stability. PCR was carried out using various preparations of plasmids, which were obtained from bacteria grown from mouse faeces at various days post inoculation (p.i). PCR using primers pACYCtc (fw) and pACYCtc (rv) produced 1680bp and 345bp fragments from plasmid pACYCnleD and pACYC184 respectively. The lanes are labelled as follows (1) DNA ladder (-2 log), (2) pACYCnleD from frozen stock (positive control), (3) pACYCnleD from day 5 p.i, (4) pACYCnleD from day 6 p.i, (5) pACYCnleD from day 7 p.i, (6) pACYC184 from Top 10 (vector without insert) and (7) Water (negative control).

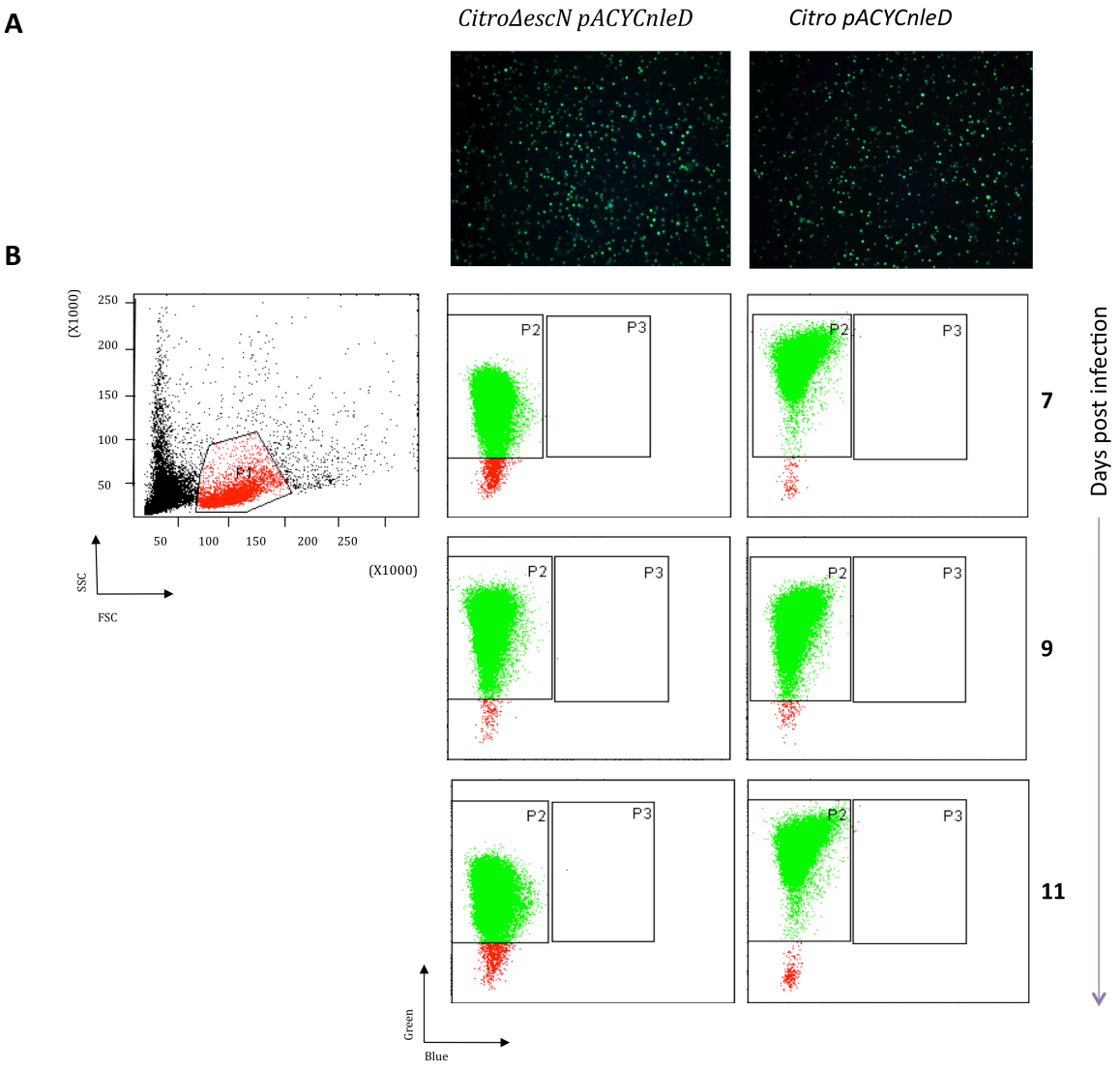

Figure 5.4.6 β-lactamase activity in splenocytes *in vivo*. Splenocytes were isolated from mice infected with either wild type *CitroΔescN pACYCnleD* or *Citro pACYCnleD* and sacrificed at days 7, 9 and 11 p.i. The isolated cells were subsequently stained with CCF4-AM substrate for 1h as described in Materials & Methods. β -lactamase activity was **A)** visualized by fluorescence microscopy (x10 objective) and **B)** detected by flow cytometry. The FACS plots show firstly, the gated live lymphocytes within the total spleen cell population (FSC x SSC), and secondly, the percentage of β-lactamase activity in cells within the gated population (green/blue). Results are representative of approximately 150-210 mice from 15 independent experiments.

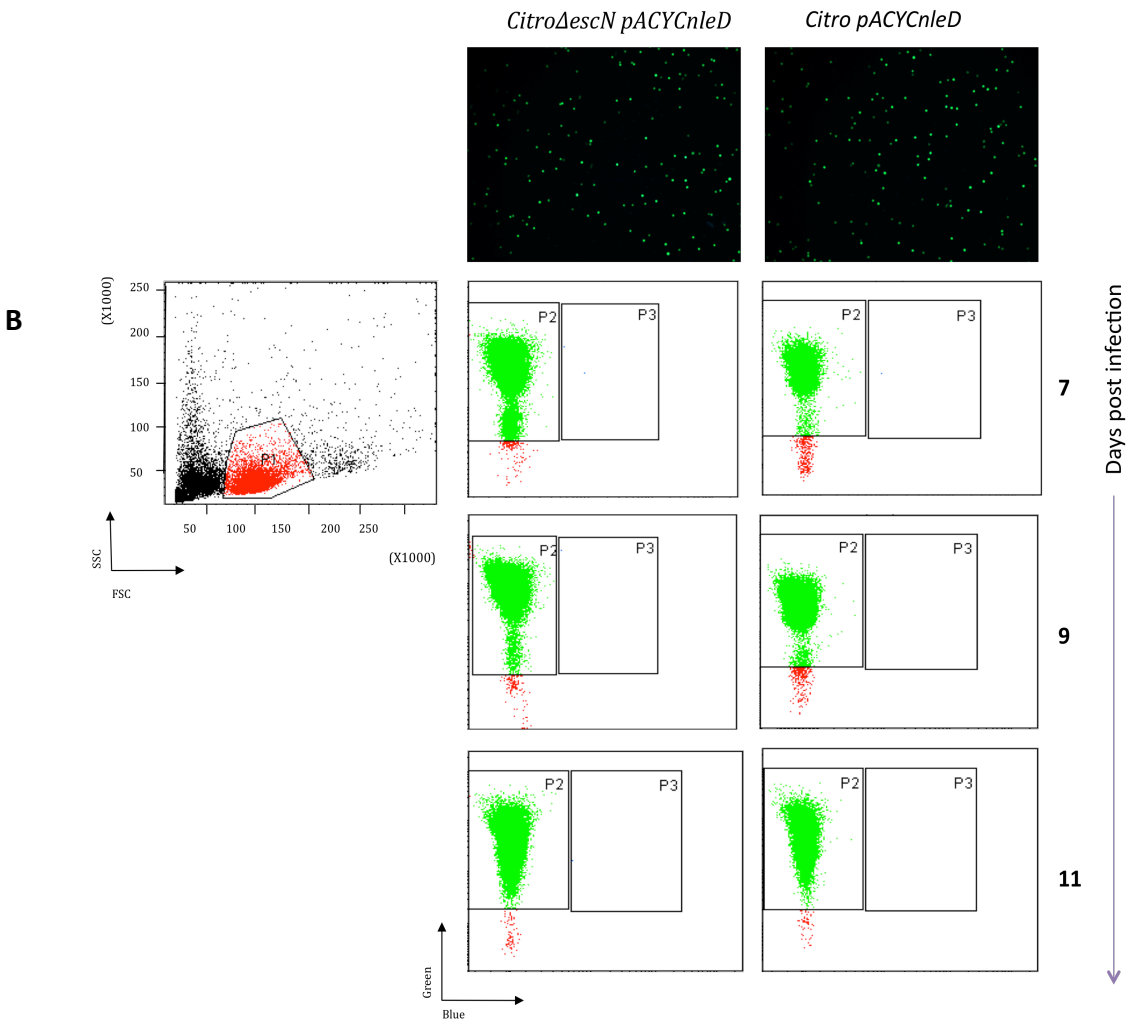

Figure 5.4.7 β-lactamase activity in mesenteric lymph node (MLN) cells *in vivo*
MLN cells were isolated from mice infected with either *CitroΔescN pACYCnleD* or *CitropACYCnleD* at days 7, 9 and 11 p.i and CCF4 stained. β-lactamase activity was **A)** visualized by fluorescence microscopy (x10 objective) and **B)** detected by flow cytometry. The FACS plots show the gated live lymphocytes within the total MLN population (FSC x SSC), and the percentage of green/blue cells. Results are representative of approximately 150-210 mice from 15 independent experiments.

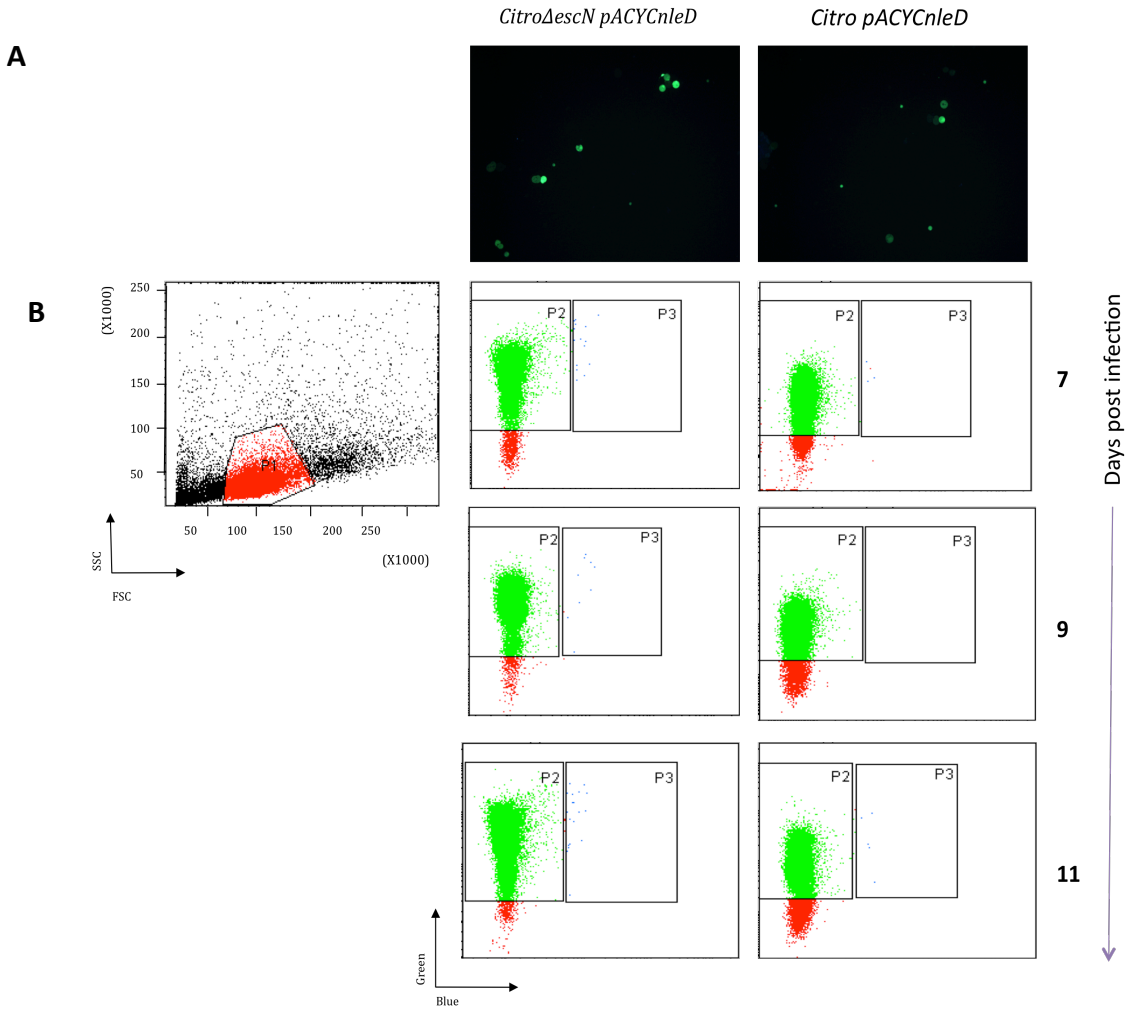

Figure 5.4.8 β-lactamase activity in Peyer's patch (PP) cells *in vivo*. PP cells were isolated from mice and infected with either *CitroΔescN pACYCnleD* or *CitropACYCnleD* at days 7, 9, 11 p.i and CCF4 stained . Protein translocation was **A)** visualized by fluorescence microscopy (x10 objective) and **B)** detected by flow cytometry. The FACS plots show the gated live lymphocytes and the percentage of green/blue cells. Results are representative of approximately 150-210 mice from 15 independent experiments.

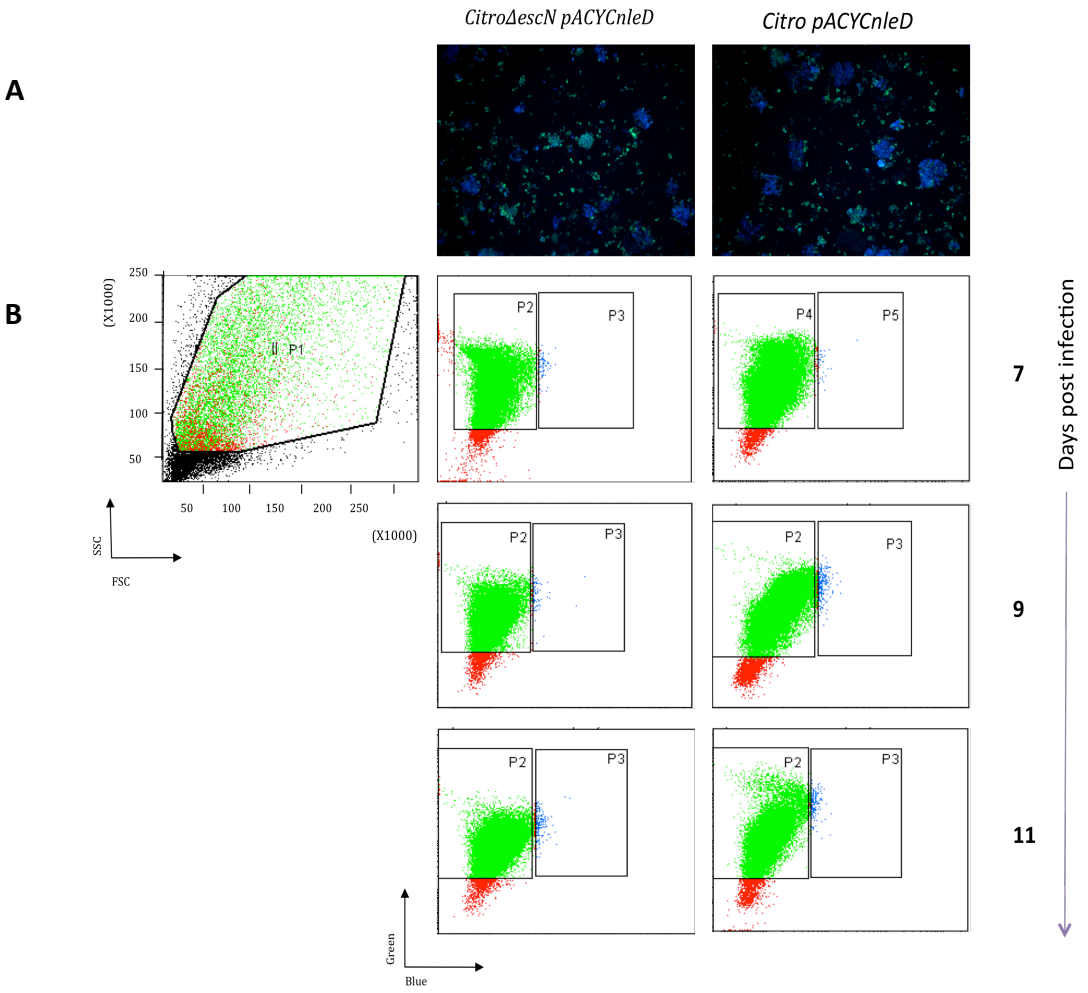

Figure 5.4.9 β-lactamase activity in colonic epithelial cells *in vivo*. Colonic epithelial cells were isolated from individual mice (x12) infected with either *CitroΔescN pACYCnleD* or *Citro pACYCnleD* and incubated with CCF4-AM substrate for 1h. β-lactamase activity was **A)** visualized by fluorescence microscopy (x10 objective) and **B)** detected by flow cytometry. The FACS plots show the gated live epithelial cells and the percentage of green/blue cells. Cell isolates were prepared from mice at days 7, 9 and 11 p.i. Results are representative of at least 5 independent experiments.

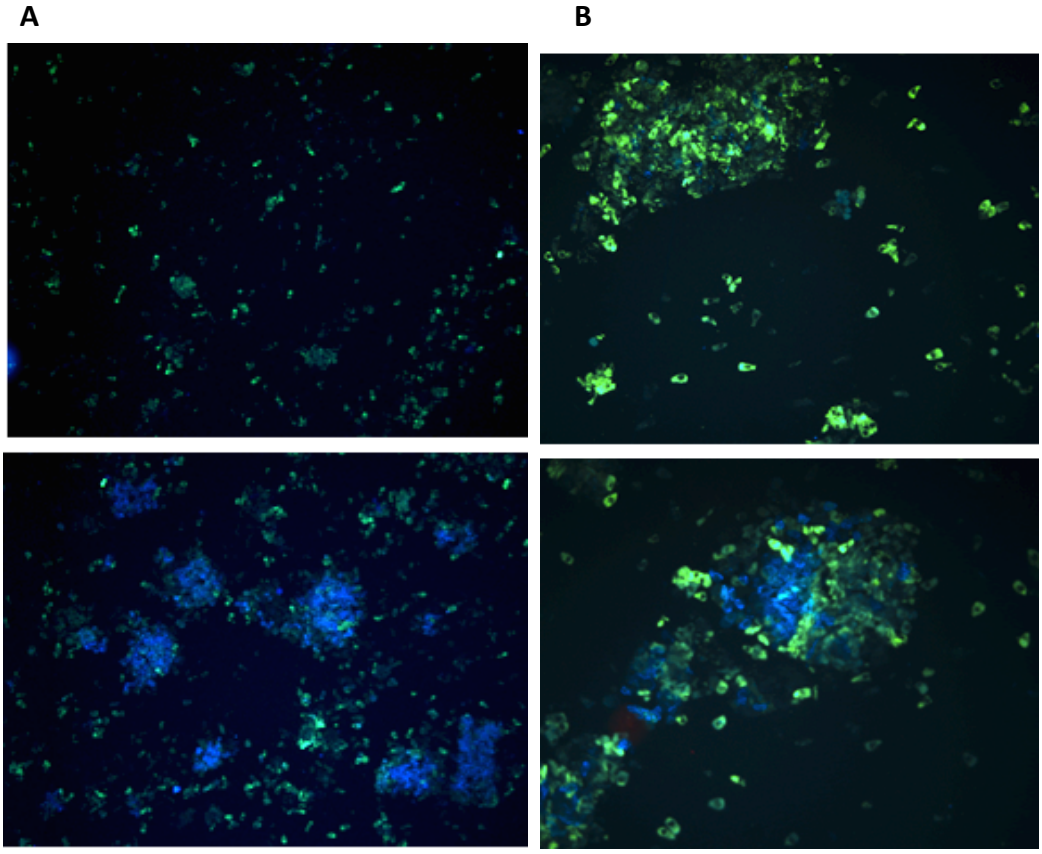

Figure 5.4.10: Autocleavage of CCF4-AM in colonic epithelial cells *in vivo*. Green and blue cells observed in colonic epithelial cells isolated from uninfected mice that have been stained with CCF4-AM and visualized using **A)** x10 objective **B)** x20 objective of fluorescent microscope. These cells are displaying autocleavage of CCF4-AM even in the absence of β-lactamase activity. Images are representative of 5 different mice.

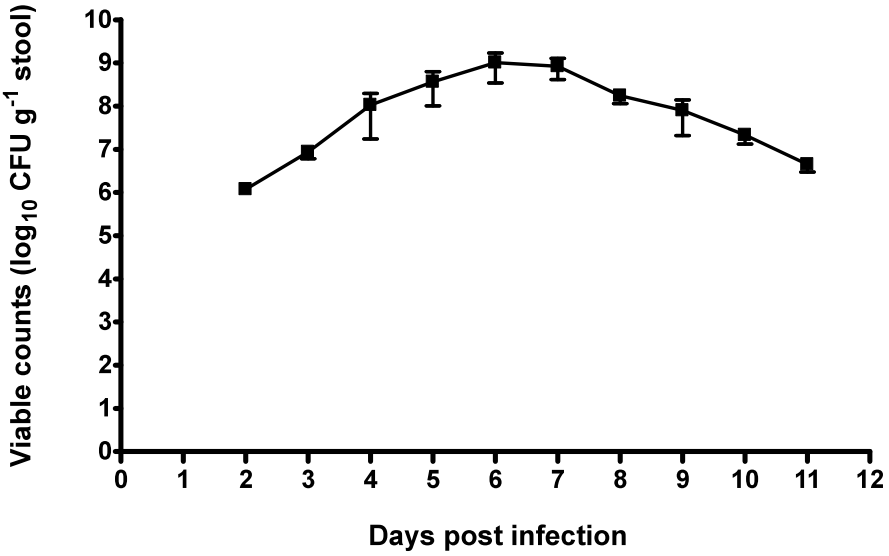

Figure 5.4.11 Bacterial shedding in mouse faeces overtime. Mice were inoculated with *Citro pACYCnleD* and the bacterial burden monitored regularly over the course of infection. Viable counts were made by quantification of CFU per gram of stool from individual mice. Error bars indicate the mean+ SEM of an average of 50 mice pooled from 10 different infection experiments.

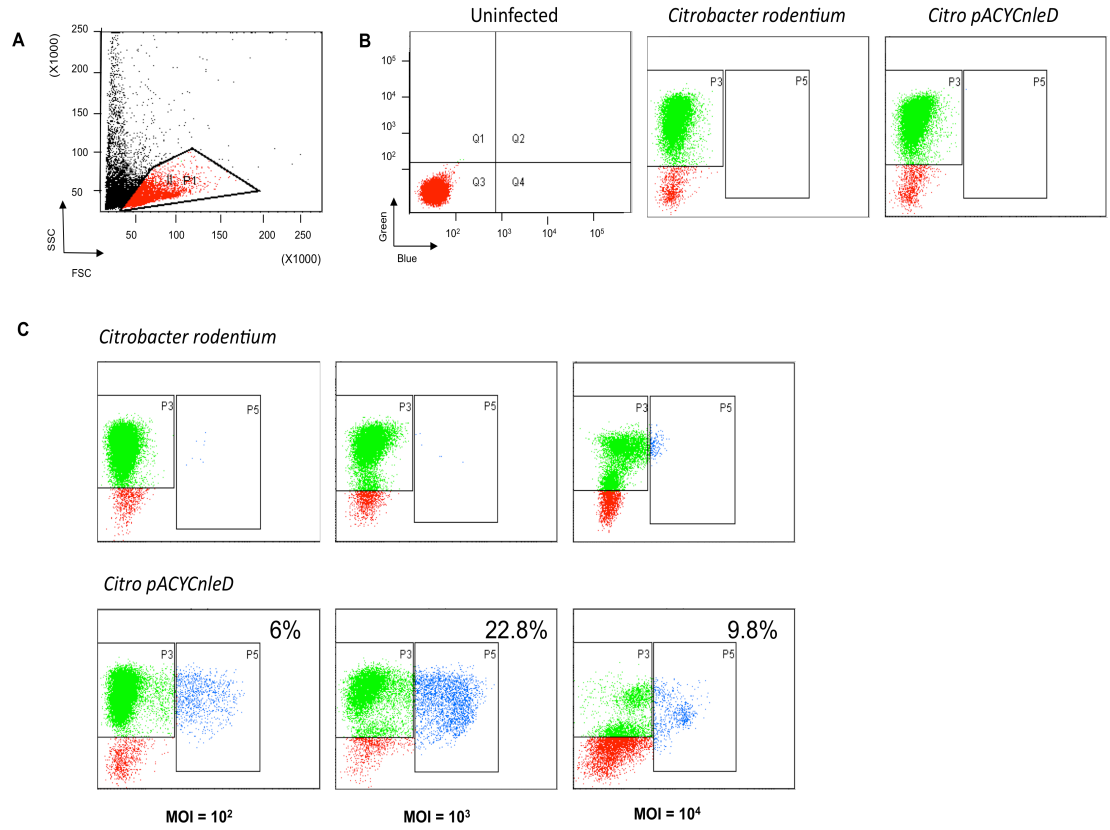

Figure 5.4.12 β-lactamase activity in infected splenocytes isolated from infected mice. Mice (x10) were orally infected with WT *C. rodentium* or *CitropACYCnleD* and monitored regularly until they were sacrificed at day 7 p.i and analysed for β-lactamase activity. **A)** Representative FACS plot showing lymphocyte gate. **B)** Percentage of blue cells after CCF4-AM staining for 1 hour. **C)** The isolated splenocytes were further re-infected with either *Citrobacter rodentium* (control) or *CitropACYCnleD* with increasing MOI for 6 hours in duplicate wells and subsequently analyzed by flow cytometry. **D)** Summarized data from infected mice experiments compared to previous data from uninfected mice. Error bars indicate the mean SEM of 3 experiments.

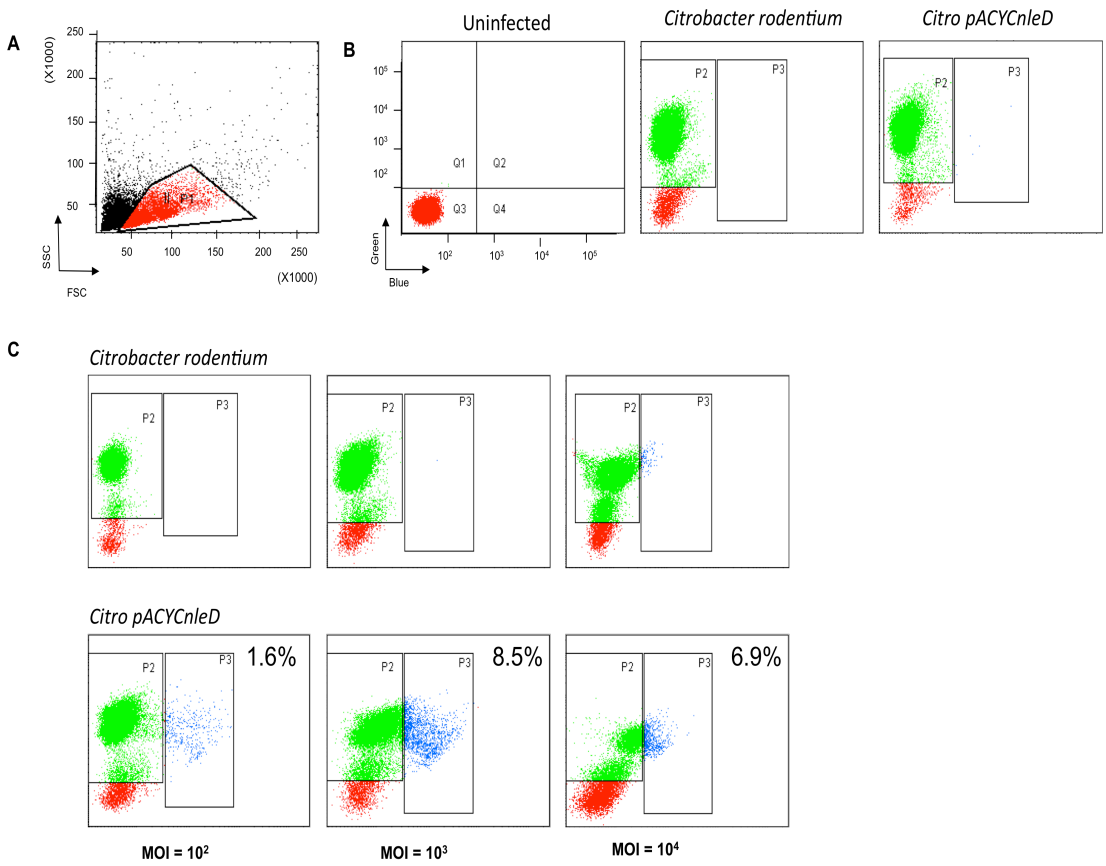

Figure 5.4.13 β-lactamase activity in infected MLN cells isolated from infected mice. A) FACS plot showing lymphocyte gate. **B)** Cells after CCF4-AM staining. **C)** The MLN cells were re-infected with either *Citrobacter rodentium* (control) or *CitropACYCnleD* with increasing MOI for 6 hours in duplicate wells and subsequently analyzed by flow cytometry. **D)** summarized data from infected mice experiments compared to previous data from uninfected mice. Error bars indicate the mean SEM of 3 experiments.

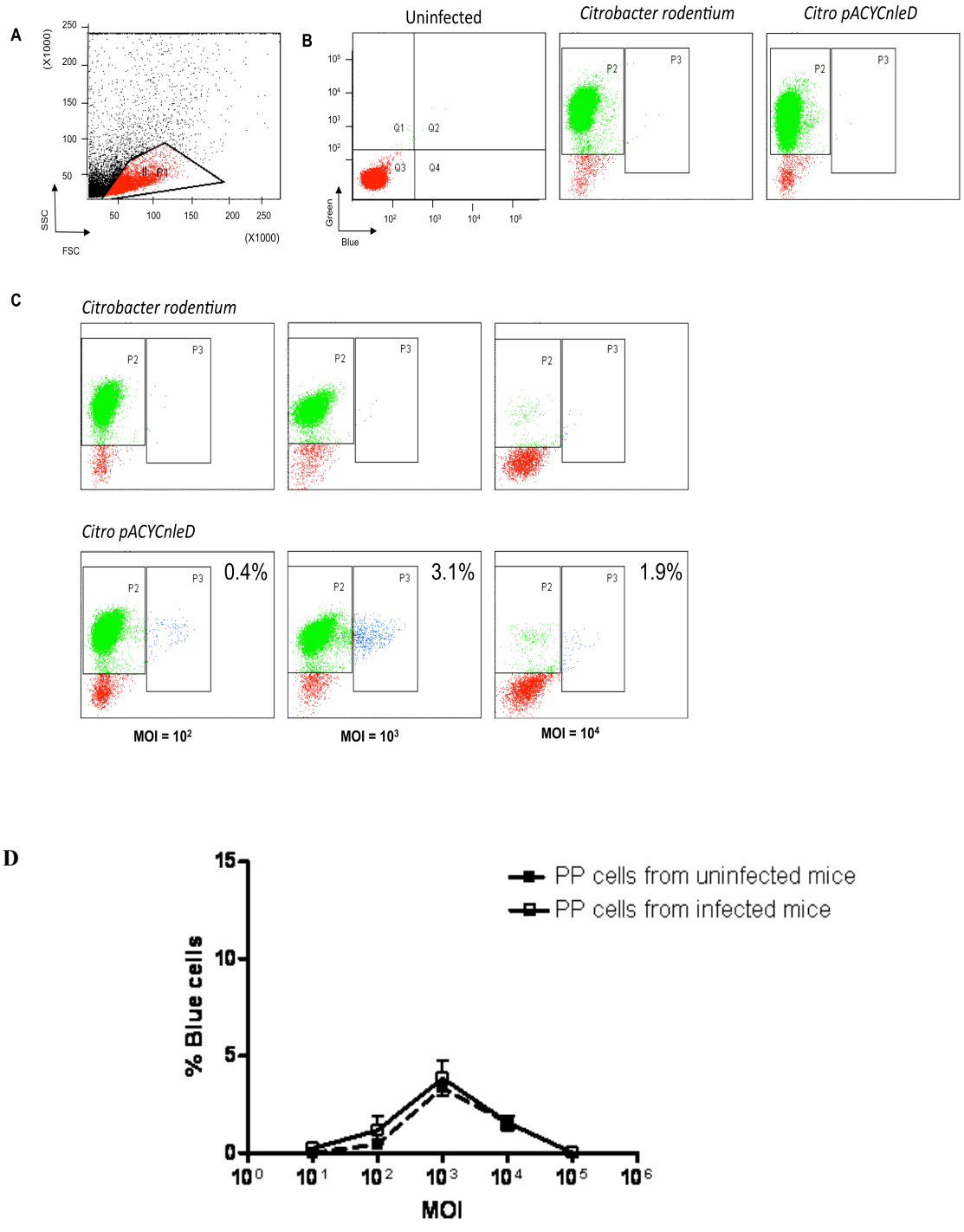

Figure 5.4.14 β-lactamase activity in infected PP cells isolated from infected mice. A) FACS plot showing lymphocyte gate. **B)** Cells after CCF4-AM staining. **C)** The PP cells were re-infected with either Citrobacter rodentium (control) or CitropACYCnleD with increasing MOI for 6 hours in duplicate wells and subsequently analyzed by flow cytometry. **D)** Summarized data from infected mice experiments compared to previous data from uninfected mice. Error bars indicate the mean± SEM of 3 experiments.

A

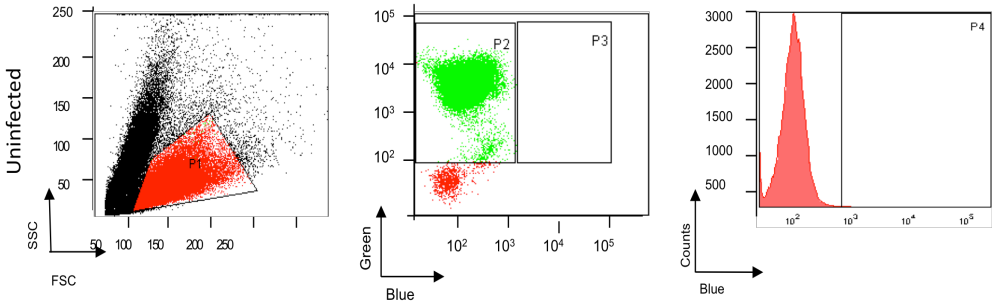

B

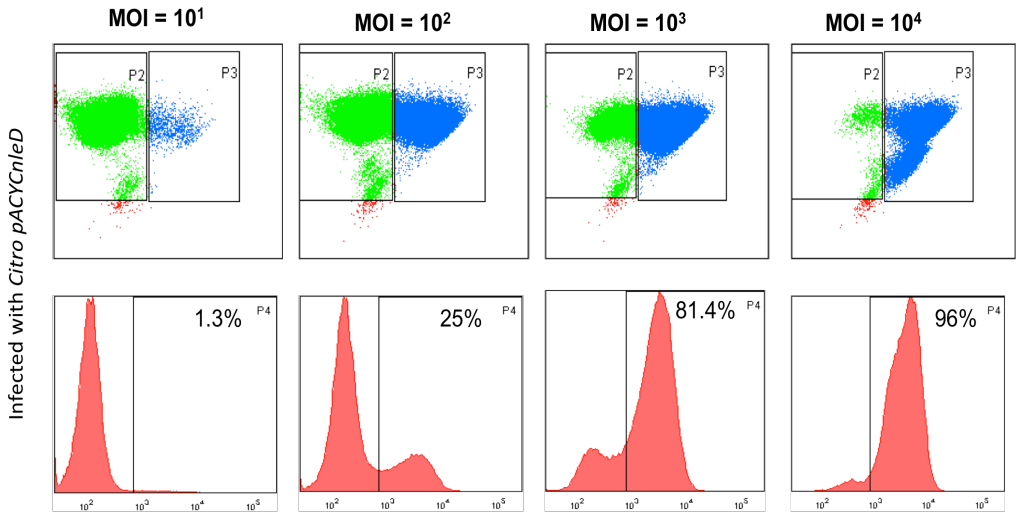

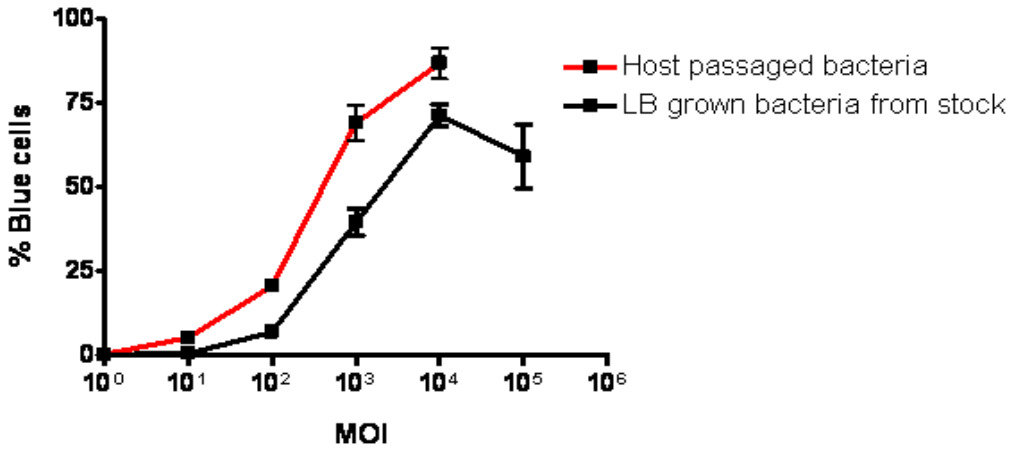

Figure 5.4.15: T cell infection with host-passaged bacteria. T cells infected with varying MOI of *Citro pACYCnleD* recovered from mice stool at day 7 p.i. **A)** Representative FACS plot and histograms of uninfected cells showing the gating of live cells and the percentage of CCF4 labelled cells. **B)** Representative FACS plot of infected T cells**. C)** Data are summarised as the mean SEM of 3 independent experiments, compared with previous data using *Citro pACYCnleD* grown overnight in LB from frozen stock.

A

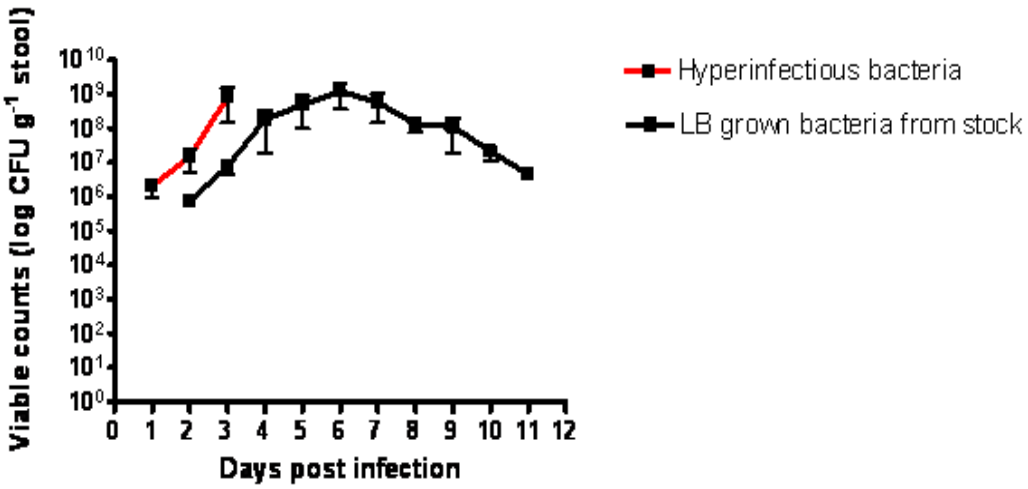

B

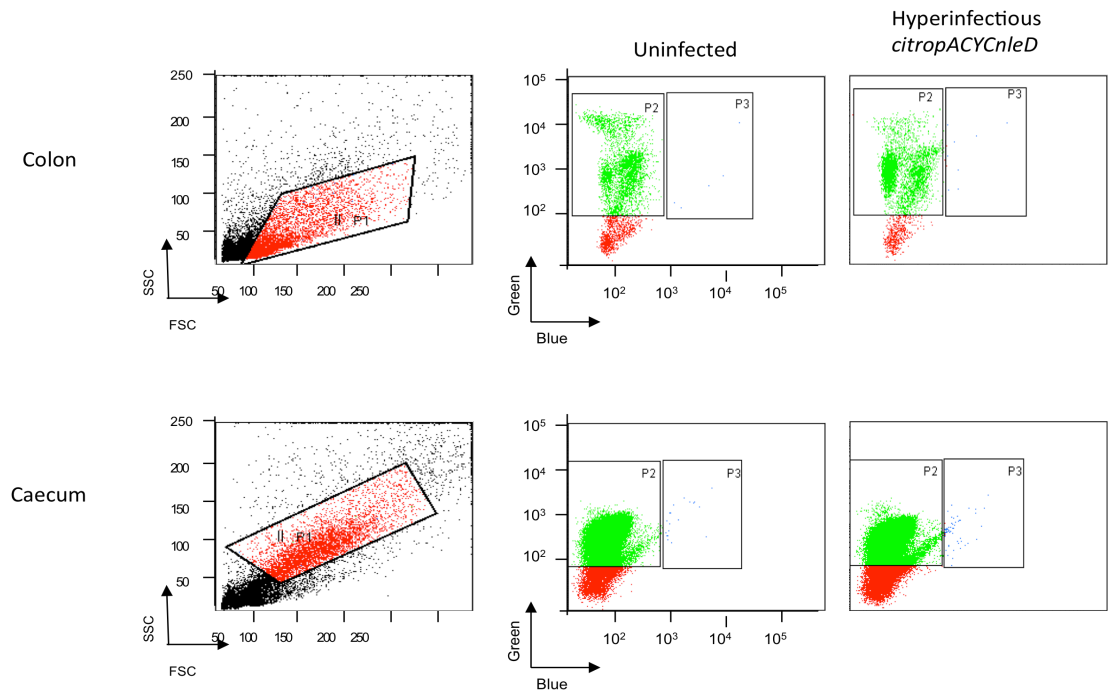

Figure 5.4.16: ***In vivo*** **infection of mice with hyperinfectious bacteria**. Mice were orally gavaged with *CitropACYCnleD* and the infection monitored for 11 days. Bacteria was isolated from mice faeces at day 7 p.i and used to inoculate new mice (x5). **A)** Bacterial load in faeces of mice infected with hyperinfectious bacteria for 3 days, compared with mice infected with non-hyperinfectious bacteria. **B)** Representative FACS plots of isolated and stained epithelial cells from the colon and caecum of the infected mice. Data is representative of 3 independent experiments.

Chapter 6. Final discussion & Future work

In this thesis, *Citrobacter rodentium* infection in mice was used as a model to study host cells targeted for effector translocation by T3SS-containing bacteria. First, we generated a reporter *C. rodentium* expressing ß-lactamase fusion proteins, to allow visualisation of host cells targeted for effector translocation by *C. rodentium*. We determined that the most convenient method for introducing the β-lactamase reporter gene into the *C. rodentium* strain was a pACYC-derived plasmid. Although a chromosomally encoded reporter fusion is physiologically more relevant, due to the expression of the effector in its native context, a plasmid-encoded reporter fusion also has its advantages. Constitutive expression of fusion proteins from the plasmid facilitates the detection of reporter activity inside host cells that have been targeted for protein translocation. In addition, the dispensable nature of the plasmid allows for manipulation of bacterial genes while keeping chromosomal genes intact. Low-copy plasmids, such as those derived from pACYC184, enable the production of fusion proteins at physiological levels, making the experiments physiologically more relevant. Our results demonstrate that the pACYCnleD plasmid remains stable throughout the mouse infection period, thereby confirming its suitability for subsequent infection studies in mice.

In contrast, the λ-Red-mediated homologous recombination in this study was unsuccessful in the integration of β-lactamase into the bacterial chromosome. This may have been due to the large size of the insert DNA (~2kb PCR product), which may have reduced the efficiency of the recombineering process by λ Red. Further work is necessary to explore methods for increasing the efficiency of λ Red-mediated homologous recombination between the β-lactamase reporter gene and the *C. rodentium* chromosome. Alternative methods to integrate the β-lactamase reporter gene into the bacterial chromosome, such as bacterial conjugation or the use of a *LacZ* gene, could be pursued in future studies.

A key part of our research involved using the reporter *C. rodentium* to investigate the utility of a β-lactamase translocation assay *in vitro*. Our results show that *C. rodentium* is capable of injecting effectors into various types of murine cell lines, including Swiss 3T3 fibroblasts, J774 macrophages, CMT93 colonic epithelial cells, and BW715 T cells. In addition, we have observed *C. rodentium*-translocated effectors in primary cells isolated from mouse lymphoid tissues, including the spleen, MLN, and PP. To our

knowledge, we are the first to demonstrate the ability of *C. rodentium* to target cells of the host immune system. Analysis of these cells by flow cytometry has revealed that the cells targeted for effector translocation were B cells, DCs, and T cells. This confirms previous findings in which *E. coli* was shown to inject effectors into macrophages (Marches et al., 2008) and DCs (Vossenkaemper et al., 2010). The findings from our study support the notion that if reporter *C. rodentium* were to encounter immune cells *in vivo*, effector translocation would probably occur.

A natural progression from this work will be to understand the biological significance of the effectors translocated into immune cells *in vitro* by *C. rodentium*. This could be achieved by examining the ability of immune cells injected with bacterial effectors to carry out immune functions, such as presentation of antigens to lymphocytes, production of chemokines and cytokines, and migration to effector sites throughout the lymphatic system. Such studies would provide valuable insight into the consequences of protein translocation for host immune cells and thereby determine to what extent these pathogens can impair host immune responses in a type 3 manner.

In this study, our observation that effector translocation occurs more efficiently in stimulated cells supports previous findings in which stimulated cells exhibited increased expression of surface integrins (Miron et al., 1992; Kinashi et al., 2007). Increased integrin expression facilitates bacterial adhesion to host cells (Frankel et al., 1996; Schulte et al., 2000), which leads to the enhanced translocation of effectors in the stimulated cells (Mejia et al., 2008: Koberle et al., 2009). As the present study has shown that the activated state of a cell can increase the probability of protein translocation, it would be informative to examine conditions that can reduce the likelihood of protein translocation. Additional future work could identify molecules and compounds that inhibit effector translocation by the T3SS for potential treatments against T3SS containing pathogens.

Another key part of this research comprised *in vivo* studies of the reporter *C. rodentium* in mouse models. We infected Balb/c mice with reporter *C. rodentium* and used the escN mutant encoding a non-functional T3SS as a control. Although the mice were successfully colonised by the reporter bacteria, we were unable to detect any reporter activity inside mice cells, despite several attempts. This was unexpected, in view of our success in demonstrating the ability of the reporter strain to express plasmid-encoded fusion proteins throughout the infection period, as indicated by plasmid preparations

from faecal bacteria. We postulate that the reporter *C. rodentium* was destroyed by host innate defences following its entry into the mouse PP, or alternatively that the number of cells injected was below the level of detection by the β-lactamase reporter system.

The success of the β-lactamase reporter technology in visualising bacterial injection *in vivo* may have been limited by the non-invasiveness of *C. rodentium*. Non-invasive bacteria, such as the AE pathogens, only colonise the surface of the epithelium, where the likelihood of having direct contact with an immune cell is rare. Although certain subsets of monocytes and DCs have been shown to associate with the gut epithelium, extend their dendrites into the gut lumen, and be injected with effector proteins by T3SS-containing pathogens, these interactions may simply be too rare for detection by β-lactamase reporter technology. Although small numbers of live bacteria can be recovered from mouse MLNs and the spleen during infection (Goncalves et al., 2001), whether these bacteria are fit enough to inject effectors into host cells at these sites—and whether this is detectable by flow cytometry—is a subject for further study. Non-invasive bacteria cannot survive in intracellular space; instead, upon entry into lymphoid tissues they are subjected to bacterial clearance by the host innate defence mechanisms. These factors may contribute to the lack of reported *in vivo* visualisation of host cells targeted for effector translocation using the β-lactamase translocation assay in AE pathogens to date.

In contrast, invasive pathogens are able to penetrate the epithelial barrier and enter lymphoid tissues and organs, where they encounter various types of immune cells. Invasive pathogens have mechanisms to defend themselves against the host immune response and hence can survive and multiply in the intracellular space. β-lactamase translocation assays carried out on cells isolated from the lymphoid organs of mice infected with such pathogens are likely to reveal more immune cells that have been targeted for protein translocation, in comparison to non-invasive pathogens. This may be why the ability to inject proteins into immune cells and subsequently subvert host immune responses is well-established for invasive pathogens such as *Salmonella, Shigella, and Yerisinia*.

Fukuda et al. (2011) used a PP intestinal loop assay to assess bacterial uptake of fluorescent *Salmonella* by M cells in mice. Based on this method, a future study could employ a ligated intestinal loop assay to evaluate effector translocation by *C. rodentium*

into intestinal immune cells. This would involve ligation of the distal colon while the mouse is anaesthetised, followed by the injection of bacterial suspension containing reporter *C. rodentium* directly into the ligated intestinal loop. After a few hours, the ligated loop would be removed, the mice immediately euthanised, and the intestinal immune cells analysed for effector translocation using the β-lactamase translocation assay. Further research might also explore the use of intravital-2-photon microscopy for live imaging of immune cells within the lymphoid tissues of mice in real time. Analysis with this technology of mice infected with reporter *C. rodentium* would provide three-dimensional information about the phenotype, location, and migration of immune cells targeted for effector translocation by *C. rodentium in vivo*.

Taken as a whole, this study has demonstrated the utility of the β-lactamase translocation assay as a reporter system to monitor effector injection into host cells *in vitro* by *C. rodentium*. To our knowledge, we are the first to show that *C. rodentium* can target immune cells for effector injection *in vitro*. Our findings corroborate previous studies that have characterised the ability of T3SS-containing pathogens to inject effectors into immune cells and subsequently subvert host immune responses. Although further work will be necessary to visualise host cells targeted for effector injection *in vivo*, we conclude that the *Citrobacter rodentium* model of infection is a useful system for studying the host-pathogen relationship in the gut.

References

Abreu, M. T. (2010). Toll-like receptor signalling in the intestinal epithelium: how bacterial recognition shapes intestinal function. *Nat Rev Immunol,* 10**,** 131-44.

Acheson, D. W. & Luccioli, S. (2004). Microbial-gut interactions in health and disease. Mucosal immune responses. *Best Pract Res Clin Gastroenterol,* 18**,** 387-404.

Ahlfors, H., Morrison, P. J., Duarte, J. H., Li, Y., Biro, J., Tolaini, M., Di Meglio, P., Potocnik, A. J. & Stockinger, B. (2014). IL-22 fate reporter reveals origin and control of IL-22 production in homeostasis and infection. *J Immunol,* 193**,** 4602-13.

Ahmed, B., Loos, M., Vanrompay, D. & Cox, E. (2014). Oral immunization with Lactococcus lactis-expressing EspB induces protective immune responses against Escherichia coli O157:H7 in a murine model of colonization. *Vaccine,* 32**,** 3909-16.

Akdis, C. A. & Blaser, K. (2001). Mechanisms of interleukin-10-mediated immune suppression. *Immunology,* 103**,** 131-6.

Allen, I. C., Tekippe, E. M., Woodford, R. M., Uronis, J. M., Holl, E. K., Rogers, A. B., Herfarth, H. H., Jobin, C. & Ting, J. P. (2010). The NLRP3 inflammasome functions as a negative regulator of tumorigenesis during colitis-associated cancer. *J Exp Med,* 207**,** 1045-56.

Amulic, B., Cazalet, C., Hayes, G. L., Metzler, K. D. & Zychlinsky, A. (2012). Neutrophil function: from mechanisms to disease. *Annu Rev Immunol,* 30**,** 459-89.

Andrade, A., Pardo, J. P., Espinosa, N., Perez-Hernandez, G. & Gonzalez-Pedrajo, B. (2007). Enzymatic characterization of the enteropathogenic Escherichia coli type III secretion ATPase EscN. *Arch Biochem Biophys,* 468**,** 121-7.

Apter, F. M., Lencer, W. I., Finkelstein, R. A., Mekalanos, J. J. & Neutra, M. R. ((1993)). Monoclonal immunoglobulin A antibodies directed against cholera toxin prevent the toxin-induced chloride secretory response and block toxin binding to intestinal epithelial cells in vitro. *Infect Immun,* 61**,** 5271-8.

Araki, A., Kanai, T., Ishikura, T., Makita, S., Uraushihara, K., Iiyama, R., Totsuka, T., Takeda, K., Akira, S. & Watanabe, M. (2005). MyD88-deficient mice develop severe intestinal inflammation in dextran sodium sulfate colitis. *J Gastroenterol,* 40**,** 16-23.

Arsenescu, R., Bruno, M. E., Rogier, E. W., Stefka, A. T., Mcmahan, A. E., Wright, T. B., Nasser, M. S., De Villiers, W. J. & Kaetzel, C. S. (2008). Signature biomarkers in Crohn's disease: toward a molecular classification. *Mucosal Immunol,* 1**,** 399-411.

Ashida, H., Ogawa, M., Mimuro, H., Kobayashi, T., Sanada, T. & Sasakawa, C. (2011). Shigella are versatile mucosal pathogens that circumvent the host innate immune system. *Curr Opin Immunol,* 23**,** 448-55.

Asquith, M. J., Boulard, O., Powrie, F. & Maloy, K. J. (2010). Pathogenic and protective roles of MyD88 in leukocytes and epithelial cells in mouse models of inflammatory bowel disease. *Gastroenterology,* 139**,** 519-29, 529 e1-2.

Atarashi, K., Nishimura, J., Shima, T., Umesaki, Y., Yamamoto, M., Onoue, M., Yagita, H., Ishii, N., Evans, R., Honda, K. & Takeda, K. (2008). ATP drives lamina propria T(H)17 cell differentiation. *Nature,* 455**,** 808-12.

Atarashi, K., Tanoue, T., Ando, M., Kamada, N., Nagano, Y., Narushima, S., Suda, W., Imaoka, A., Setoyama, H., Nagamori, T., Ishikawa, E., Shima, T., Hara, T., Kado, S., Jinnohara, T., Ohno, H., Kondo, T., Toyooka, K., Watanabe, E., Yokoyama, S., Tokoro, S., Mori, H., Noguchi, Y., Morita, H., Ivanov, Ii, Sugiyama, T., Nunez, G., Camp, J. G., Hattori, M., Umesaki, Y. & Honda, K. (2015). Th17 Cell Induction by Adhesion of Microbes to Intestinal Epithelial Cells. *Cell,* 163**,** 367-80.

Atarashi, K., Tanoue, T., Shima, T., Imaoka, A., Kuwahara, T., Momose, Y., Cheng, G., Yamasaki, S., Saito, T., Ohba, Y., Taniguchi, T., Takeda, K., Hori, S., Ivanov, Ii, Umesaki, Y., Itoh, K. & Honda, K. (2011). Induction of colonic regulatory T cells by indigenous Clostridium species. *Science,* 331**,** 337-41.

Atuma, C., Strugala, V., Allen, A. & Holm, L. (2001). The adherent gastrointestinal mucus gel layer: thickness and physical state in vivo. *Am J Physiol Gastrointest Liver Physiol,* 280**,** G922-9.

Autenrieth, S. E., Linzer, T. R., Hiller, C., Keller, B., Warnke, P., Koberle, M., Bohn, E., Biedermann, T., Buhring, H. J., Hammerling, G. J., Rammensee, H. G. & Autenrieth, I. B. (2010). Immune evasion by Yersinia enterocolitica: differential targeting of dendritic cell subpopulations in vivo. *PLoS Pathog,* 6**,** e1001212.

Baba, T., Ara, T., Hasegawa, M., Takai, Y., Okumura, Y., Baba, M., Datsenko, K. A., Tomita, M., Wanner, B. L. & Mori, H. (2006). Construction of Escherichia coli K-12 in-frame, single-gene knockout mutants: the Keio collection. *Mol Syst Biol,* 2**,** 2006 0008.

Badea, L., Doughty, S., Nicholls, L., Sloan, J., Robins-Browne, R. M. & Hartland, E. L. (2003). Contribution of Efa1/LifA to the adherence of enteropathogenic Escherichia coli to epithelial cells. *Microb Pathog,* 34**,** 205-15.

Barreau, F., Meinzer, U., Chareyre, F., Berrebi, D., Niwa-Kawakita, M., Dussaillant, M., Foligne, B., Ollendorff, V., Heyman, M., Bonacorsi, S., Lesuffleur, T., Sterkers, G., Giovannini, M. & Hugot, J. P. (2007). CARD15/NOD2 is required for Peyer's patches homeostasis in mice. *PLoS One,* 2**,** e523.

Barthold, S. W. (1980). The microbiology of transmissible murine colonic hyperplasia. *Lab Anim Sci,* 30**,** 167-73.

Barthold, S. W., Coleman, G. L., Bhatt, P. N., Osbaldiston, G. W. & Jonas, A.

M. (1976). The etiology of transmissible murine colonic hyperplasia. *Lab Anim Sci,* 26**,** 889-94.

Barthold, S. W., Coleman, G. L., Jacoby, R. O., Livestone, E. M. & Jonas, A. M. (1978). Transmissible murine colonic hyperplasia. *Vet Pathol,* 15**,** 223-36.

Baruch, K., Gur-Arie, L., Nadler, C., Koby, S., Yerushalmi, G., Ben-Neriah, Y., Yogev, O., Shaulian, E., Guttman, C., Zarivach, R. & Rosenshine, I. (2011). Metalloprotease type III effectors that specifically cleave JNK and NF-kappaB. *EMBO J,* 30**,** 221-31.

Basu, R., O'quinn, D. B., Silberger, D. J., Schoeb, T. R., Fouser, L., Ouyang, W., Hatton, R. D. & Weaver, C. T. (2012). Th22 cells are an important source of IL-22 for host protection against enteropathogenic bacteria. *Immunity,* 37**,** 1061-75.

Battle, S. E., Brady, M. J., Vanaja, S. K., Leong, J. M. & Hecht, G. A. (2014). Actin pedestal formation by enterohemorrhagic Escherichia coli enhances bacterial host cell attachment and concomitant type III translocation. *Infect Immun,* 82**,** 3713-22.

Belzer, C., Liu, Q., Carroll, M. C. & Bry, L. (2011). THE ROLE OF SPECIFIC IgG AND COMPLEMENT IN COMBATING A PRIMARY MUCOSAL INFECTION OF THE GUT EPITHELIUM. *Eur J Microbiol Immunol (Bp),* 1**,** 311-318.

Ben Suleiman, Y., Yoshida, M., Nishiumi, S., Tanaka, H., Mimura, T., Nobutani, K., Yamamoto, K., Takenaka, M., Aoganghua, A., Miki, I., Ota, H., Takahashi, S., Matsui, H., Nakamura, M., Blumberg, R. S. & Azuma, T. (2012). Neonatal Fc receptor for IgG (FcRn) expressed in the gastric epithelium regulates bacterial infection in mice. *Mucosal Immunol,* 5**,** 87-98.

Berger, C. N., Crepin, V. F., Baruch, K., Mousnier, A., Rosenshine, I. & Frankel, G. (2012). EspZ of enteropathogenic and enterohemorrhagic Escherichia coli regulates type III secretion system protein translocation. *MBio,* 3.

Berger, C. N., Crepin, V. F., Jepson, M. A., Arbeloa, A. & Frankel, G. (2009). The mechanisms used by enteropathogenic Escherichia coli to control filopodia dynamics. *Cell Microbiol,* 11**,** 309-22.

Bergstrom, K. S., Sham, H. P., Zarepour, M. & Vallance, B. A. (2012). Innate host responses to enteric bacterial pathogens: a balancing act between resistance and tolerance. *Cell Microbiol,* 14**,** 475-84.

Bhagwat, A. A., Leow, Y. N., Liu, L., Dharne, M. & Kannan, P. (2012). Role of anionic charges of periplasmic glucans of Shigella flexneri in overcoming detergent stress. *Foodborne Pathog Dis,* 9**,** 632-7.

Bhavsar, A. P., Guttman, J. A. & Finlay, B. B. (2007). Manipulation of host-cell pathways by bacterial pathogens. *Nature,* 449**,** 827-34.

Bishop, A. L., Wiles, S., Dougan, G. & Frankel, G. (2007). Cell attachment properties and infectivity of host-adapted and environmentally adapted Citrobacter

rodentium. *Microbes Infect,* 9**,** 1316-24.

Blanc-Potard, A. B. & Groisman, E. A. (1997). The Salmonella selC locus contains a pathogenicity island mediating intramacrophage survival. *EMBO J,* 16**,** 5376-85.

Blasche, S., Mortl, M., Steuber, H., Siszler, G., Nisa, S., Schwarz, F., Lavrik, I., Gronewold, T. M., Maskos, K., Donnenberg, M. S., Ullmann, D., Uetz, P. & Kogl, M. (2013). The E. coli effector protein NleF is a caspase inhibitor. *PLoS One,* 8**,** e58937.

Blocker, A., Komoriya, K. & Aizawa, S. (2003). Type III secretion systems and bacterial flagella: insights into their function from structural similarities. *Proc Natl Acad Sci U S A,* 100**,** 3027-30.

Bogunovic, M., Ginhoux, F., Helft, J., Shang, L., Hashimoto, D., Greter, M., Liu, K., Jakubzick, C., Ingersoll, M. A., Leboeuf, M., Stanley, E. R., Nussenzweig, M., Lira, S. A., Randolph, G. J. & Merad, M. (2009). Origin of the lamina propria dendritic cell network. *Immunity,* 31**,** 513-25.

Bollrath, J. & Powrie, F. M. (2013). Controlling the frontier: regulatory T-cells and intestinal homeostasis. *Semin Immunol,* 25**,** 352-7.

Borghesi, C., Regoli, M., Bertelli, E. & Nicoletti, C. (1996). Modifications of the follicle-associated epithelium by short-term exposure to a non-intestinal bacterium. *J Pathol,* 180**,** 326-32.

Borregaard, N., Sorensen, O. E. & Theilgaard-Monch, K. (2007). Neutrophil granules: a library of innate immunity proteins. *Trends Immunol,* 28**,** 340-5.

Bouma, J. E. & Lenski, R. E. (1988). Evolution of a bacteria/plasmid association. *Nature,* 335**,** 351-2.

Braathen, R., Hohman, V. S., Brandtzaeg, P. & Johansen, F. E. (2007). Secretory antibody formation: conserved binding interactions between J chain and polymeric Ig receptor from humans and amphibians. *J Immunol,* 178**,** 1589-97.

Brandl, K., Plitas, G., Mihu, C. N., Ubeda, C., Jia, T., Fleisher, M., Schnabl, B., Dematteo, R. P. & Pamer, E. G. (2008). Vancomycin-resistant enterococci exploit antibiotic-induced innate immune deficits. *Nature,* 455**,** 804-7.

Brandl, K., Plitas, G., Schnabl, B., Dematteo, R. P. & Pamer, E. G. (2007). MyD88-mediated signals induce the bactericidal lectin RegIII gamma and protect mice against intestinal Listeria monocytogenes infection. *J Exp Med,* 204**,** 1891-900.

Brandtzaeg, P. (2009). Mucosal immunity: induction, dissemination, and effector functions. *Scand J Immunol,* 70**,** 505-15.

Brandtzaeg, P. (2010). Update on mucosal immunoglobulin A in gastrointestinal disease. *Curr Opin Gastroenterol,* 26**,** 554-63.

Brandtzaeg, P. (2011). The gut as communicator between environment and host:

immunological consequences. *Eur J Pharmacol,* 668 Suppl 1**,** S16-32.

Brandtzaeg, P. (2013). Gate-keeper function of the intestinal epithelium. *Benef Microbes,* 4**,** 67-82.

Brinkmann, V., Reichard, U., Goosmann, C., Fauler, B., Uhlemann, Y., Weiss, D. S., Weinrauch, Y. & Zychlinsky, A. (2004). Neutrophil extracellular traps kill bacteria. *Science,* 303**,** 1532-5.

Brubaker, R. R. (2003). Interleukin-10 and inhibition of innate immunity to Yersiniae: roles of Yops and LcrV (V antigen). *Infect Immun,* 71**,** 3673-81.

Bry, L. & Brenner, M. B. (2004). Critical role of T cell-dependent serum antibody, but not the gut-associated lymphoid tissue, for surviving acute mucosal infection with Citrobacter rodentium, an attaching and effacing pathogen. *J Immunol,* 172**,** 433-41.

Bry, L., Brigl, M. & Brenner, M. B. (2006). CD4+-T-cell effector functions and costimulatory requirements essential for surviving mucosal infection with Citrobacter rodentium. *Infect Immun,* 74**,** 673-81.

Bryant, C. & Fitzgerald, K. A. (2009). Molecular mechanisms involved in inflammasome activation. *Trends Cell Biol,* 19**,** 455-64.

Bulgin, R., Arbeloa, A., Goulding, D., Dougan, G., Crepin, V. F., Raymond, B. & Frankel, G. (2009). The T3SS effector EspT defines a new category of invasive enteropathogenic E. coli (EPEC) which form intracellular actin pedestals. *PLoS Pathog,* 5**,** e1000683.

Bulgin, R., Raymond, B., Garnett, J. A., Frankel, G., Crepin, V. F., Berger, C. N. & Arbeloa, A. (2010). Bacterial guanine nucleotide exchange factors SopE-like and WxxxE effectors. *Infect Immun,* 78**,** 1417-25.

Burns, J. W., Siadat-Pajouh, M., Krishnaney, A. A. & Greenberg, H. B. (1996). Protective effect of rotavirus VP6-specific IgA monoclonal antibodies that lack neutralizing activity. *Science,* 272**,** 104-7.

Buttner, D. (2012). Protein export according to schedule: architecture, assembly, and regulation of type III secretion systems from plant- and animal-pathogenic bacteria. *Microbiol Mol Biol Rev,* 76**,** 262-310.

Campellone, K. G., Giese, A., Tipper, D. J. & Leong, J. M. (2002). A tyrosine-phosphorylated 12-amino-acid sequence of enteropathogenic Escherichia coli Tir binds the host adaptor protein Nck and is required for Nck localization to actin pedestals. *Mol Microbiol,* 43**,** 1227-41.

Campellone, K. G., Robbins, D. & Leong, J. M. (2004). EspFU is a translocated EHEC effector that interacts with Tir and N-WASP and promotes Nck-independent actin assembly. *Dev Cell,* 7**,** 217-28.

Campellone, K. G. & Welch, M. D. (2010). A nucleator arms race: cellular control of actin assembly. *Nat Rev Mol Cell Biol,* 11**,** 237-51.

Cario, E., Gerken, G. & Podolsky, D. K. (2004). Toll-like receptor 2 enhances ZO-1-associated intestinal epithelial barrier integrity via protein kinase C. *Gastroenterology,* 127**,** 224-38.

Cario, E., Gerken, G. & Podolsky, D. K. (2007). Toll-like receptor 2 controls mucosal inflammation by regulating epithelial barrier function. *Gastroenterology,* 132**,** 1359-74.

Cassani, B., Villablanca, E. J., De Calisto, J., Wang, S. & Mora, J. R. (2012). Vitamin A and immune regulation: role of retinoic acid in gut-associated dendritic cell education, immune protection and tolerance. *Mol Aspects Med,* 33**,** 63-76.

Castigli, E., Wilson, S. A., Scott, S., Dedeoglu, F., Xu, S., Lam, K. P., Bram, R. J., Jabara, H. & Geha, R. S. (2005). TACI and BAFF-R mediate isotype switching in B cells. *J Exp Med,* 201**,** 35-9.

Castillo, A., Eguiarte, L. E. & Souza, V. (2005). A genomic population genetics analysis of the pathogenic enterocyte effacement island in Escherichia coli: the search for the unit of selection. *Proc Natl Acad Sci U S A,* 102**,** 1542-7.

Castro-Sanchez, P. & Martin-Villa, J. M. (2013). Gut immune system and oral tolerance. *Br J Nutr,* 109 Suppl 2**,** S3-11.

Cazac, B. B. & Roes, J. (2000). TGF-beta receptor controls B cell responsiveness and induction of IgA in vivo. *Immunity,* 13**,** 443-51.

Cerutti, A. (2008). The regulation of IgA class switching. *Nat Rev Immunol,* 8**,** 421-34.

Cerutti, A., Puga, I. & Cols, M. (2011). Innate control of B cell responses. *Trends Immunol,* 32**,** 202-11.

Cerutti, A. & Rescigno, M. (2008). The biology of intestinal immunoglobulin A responses. *Immunity,* 28**,** 740-50.

Chamaillard, M., Hashimoto, M., Horie, Y., Masumoto, J., Qiu, S., Saab, L., Ogura, Y., Kawasaki, A., Fukase, K., Kusumoto, S., Valvano, M. A., Foster, S. J., Mak, T. W., Nunez, G. & Inohara, N. (2003). An essential role for NOD1 in host recognition of bacterial peptidoglycan containing diaminopimelic acid. *Nat Immunol,* 4**,** 702-7.

Chan, J. M., Bhinder, G., Sham, H. P., Ryz, N., Huang, T., Bergstrom, K. S. & Vallance, B. A. (2013). CD4+ T cells drive goblet cell depletion during Citrobacter rodentium infection. *Infect Immun,* 81**,** 4649-58.

Charpentier, X. & Oswald, E. (2004). Identification of the secretion and translocation domain of the enteropathogenic and enterohemorrhagic Escherichia coli effector Cif, using TEM-1 beta-lactamase as a new fluorescence-based reporter. *J Bacteriol,* 186**,** 5486-95.

Chen, G., Chan, A. J., Chung, J. I., Jang, J. C., Osborne, L. C. & Nair, M. G. (2014). Polarizing the T helper 17 response in Citrobacter rodentium infection via

expression of resistin-like molecule alpha. *Gut Microbes,* 5**,** 363-8.

Chieppa, M., Rescigno, M., Huang, A. Y. & Germain, R. N. (2006). Dynamic imaging of dendritic cell extension into the small bowel lumen in response to epithelial cell TLR engagement. *J Exp Med,* 203**,** 2841-52.

Chong, Y., Fitzhenry, R., Heuschkel, R., Torrente, F., Frankel, G. & Phillips, A. D. (2007). Human intestinal tissue tropism in Escherichia coli O157 : H7--initial colonization of terminal ileum and Peyer's patches and minimal colonic adhesion ex vivo. *Microbiology,* 153**,** 794-802.

Chorny, A., Puga, I. & Cerutti, A. (2012). Regulation of frontline antibody responses by innate immune signals. *Immunol Res,* 54**,** 4-13.

Clements, A., Smollett, K., Lee, S. F., Hartland, E. L., Lowe, M. & Frankel, G. (2011). EspG of enteropathogenic and enterohemorrhagic E. coli binds the Golgi matrix protein GM130 and disrupts the Golgi structure and function. *Cell Microbiol,* 13**,** 1429-39.

Clements, A., Stoneham, C. A., Furniss, R. C. & Frankel, G. (2014). Enterohaemorrhagic Escherichia coli inhibits recycling endosome function and trafficking of surface receptors. *Cell Microbiol,* 16**,** 1693-705.

Coburn, B., Sekirov, I. & Finlay, B. B. (2007). Type III secretion systems and disease. *Clin Microbiol Rev,* 20**,** 535-49.

Collins, J. W., Keeney, K. M., Crepin, V. F., Rathinam, V. A., Fitzgerald, K. A., Finlay, B. B. & Frankel, G. (2014). Citrobacter rodentium: infection, inflammation and the microbiota. *Nat Rev Microbiol,* 12**,** 612-23.

Collins, J. W., Meganck, J. A., Kuo, C., Francis, K. P. & Frankel, G. (2013). 4D multimodality imaging of Citrobacter rodentium infections in mice. *J Vis Exp*.

Constantinovits, M., Sipos, F., Molnar, B., Tulassay, Z. & Muzes, G. (2012). Organizer and regulatory role of colonic isolated lymphoid follicles in inflammation. *Acta Physiol Hung,* 99**,** 344-52.

Cornelis, G. R. (2006). The type III secretion injectisome. *Nat Rev Microbiol,* 4**,** 811-25.

Cornelis, G. R. (2010). The type III secretion injectisome, a complex nanomachine for intracellular 'toxin' delivery. *Biol Chem,* 391**,** 745-51.

Corthesy, B. (2013). Multi-faceted functions of secretory IgA at mucosal surfaces. *Front Immunol,* 4**,** 185.

Cox, D., Berg, J. S., Cammer, M., Chinegwundoh, J. O., Dale, B. M., Cheney, R. E. & Greenberg, S. (2002). Myosin X is a downstream effector of PI(3)K during phagocytosis. *Nat Cell Biol,* 4**,** 469-77.

Creuzburg, K., Kohler, B., Hempel, H., Schreier, P., Jacobs, E. & Schmidt, H. (2005). Genetic structure and chromosomal integration site of the cryptic prophage CP-1639 encoding Shiga toxin 1. *Microbiology,* 151**,** 941-50.

Creuzburg, K., Kohler, B., Hempel, H., Schreier, P., Jacobs, E. & Schmidt, H. (2005). Genetic structure and chromosomal integration site of the cryptic prophage CP-1639 encoding Shiga toxin 1. *Microbiology,* 151**,** 941-50.

Croxen, M. A., Law, R. J., Scholz, R., Keeney, K. M., Wlodarska, M. & Finlay, B. B. (2013). Recent advances in understanding enteric pathogenic Escherichia coli. *Clin Microbiol Rev,* 26**,** 822-80.

Czinn, S. J., Cai, A. & Nedrud, J. G. (1993). Protection of germ-free mice from infection by Helicobacter felis after active oral or passive IgA immunization. *Vaccine,* 11**,** 637-42.

Da Silva, N. A. & Bailey, J. E. (1986). Theoretical growth yield estimates for recombinant cells. *Biotechnol Bioeng,* 28**,** 741-6.

Dabert, P. & Smith, G. R. (1997). Gene replacement with linear DNA fragments in wild-type Escherichia coli: enhancement by Chi sites. *Genetics,* 145**,** 877-89.

Dahan, S., Wiles, S., La Ragione, R. M., Best, A., Woodward, M. J., Stevens, M. P., Shaw, R. K., Chong, Y., Knutton, S., Phillips, A. & Frankel, G. (2005). EspJ is a prophage-carried type III effector protein of attaching and effacing pathogens that modulates infection dynamics. *Infect Immun,* 73**,** 679-86.

Dahan, S., Wiles, S., La Ragione, R. M., Best, A., Woodward, M. J., Stevens, M. P., Shaw, R. K., Chong, Y., Knutton, S., Phillips, A. & Frankel, G. (2005). EspJ is a prophage-carried type III effector protein of attaching and effacing pathogens that modulates infection dynamics. *Infect Immun,* 73**,** 679-86.

Datsenko, K. A. & Wanner, B. L. (2000). One-step inactivation of chromosomal genes in Escherichia coli K-12 using PCR products. *Proc Natl Acad Sci U S A,* 97**,** 6640-5.

Dautin, N., Karimova, G. & Ladant, D. (2002). Bordetella pertussis adenylate cyclase toxin: a versatile screening tool. *Toxicon,* 40**,** 1383-7.

Day, J. B., Ferracci, F. & Plano, G. V. (2003). Translocation of YopE and YopN into eukaryotic cells by Yersinia pestis yopN, tyeA, sycN, yscB and lcrG deletion mutants measured using a phosphorylatable peptide tag and phosphospecific antibodies. *Mol Microbiol,* 47**,** 807-23.

Dean, P. (2011). Functional domains and motifs of bacterial type III effector proteins and their roles in infection. *FEMS Microbiol Rev,* 35**,** 1100-25.

Dean, P. & Kenny, B. (2009). The effector repertoire of enteropathogenic E. coli: ganging up on the host cell. *Curr Opin Microbiol,* 12**,** 101-9.

Deane, J. E., Abrusci, P., Johnson, S. & Lea, S. M. (2010). Timing is everything: the regulation of type III secretion. *Cell Mol Life Sci,* 67**,** 1065-75.

Deng, W., De Hoog, C. L., Yu, H. B., Li, Y., Croxen, M. A., Thomas, N. A., Puente, J. L., Foster, L. J. & Finlay, B. B. (2010). A comprehensive proteomic analysis of the type III secretome of Citrobacter rodentium. *J Biol Chem,* 285**,**

6790-800.

Deng, W., Li, Y., Vallance, B. A. & Finlay, B. B. (2001). Locus of enterocyte effacement from Citrobacter rodentium: sequence analysis and evidence for horizontal transfer among attaching and effacing pathogens. *Infect Immun,* 69**,** 6323-35.

Deng, W., Puente, J. L., Gruenheid, S., Li, Y., Vallance, B. A., Vazquez, A., Barba, J., Ibarra, J. A., O'donnell, P., Metalnikov, P., Ashman, K., Lee, S., Goode, D., Pawson, T. & Finlay, B. B. (2004). Dissecting virulence: systematic and functional analyses of a pathogenicity island. *Proc Natl Acad Sci U S A,* 101**,** 3597-602.

Deng, W., Vallance, B. A., Li, Y., Puente, J. L. & Finlay, B. B. (2003). Citrobacter rodentium translocated intimin receptor (Tir) is an essential virulence factor needed for actin condensation, intestinal colonization and colonic hyperplasia in mice. *Mol Microbiol,* 48**,** 95-115.

Denning, T. L., Wang, Y. C., Patel, S. R., Williams, I. R. & Pulendran, B. (2007). Lamina propria macrophages and dendritic cells differentially induce regulatory and interleukin 17-producing T cell responses. *Nat Immunol,* 8**,** 1086-94.

Derbise, A., Lesic, B., Dacheux, D., Ghigo, J. M. & Carniel, E. (2003). A rapid and simple method for inactivating chromosomal genes in Yersinia. *FEMS Immunol Med Microbiol,* 38**,** 113-6.

Dessein, R., Gironella, M., Vignal, C., Peyrin-Biroulet, L., Sokol, H., Secher, T., Lacas-Gervais, S., Gratadoux, J. J., Lafont, F., Dagorn, J. C., Ryffel, B., Akira, S., Langella, P., Nunez, G., Sirard, J. C., Iovanna, J., Simonet, M. & Chamaillard, M. (2009). Toll-like receptor 2 is critical for induction of Reg3 beta expression and intestinal clearance of Yersinia pseudotuberculosis. *Gut,* 58**,** 771-6.

Devinney, R., Gauthier, A., Abe, A. & Finlay, B. B. (1999). Enteropathogenic Escherichia coli: a pathogen that inserts its own receptor into host cells. *Cell Mol Life Sci,* 55**,** 961-76.

Dewoody, R., Merritt, P. M., Houppert, A. S. & Marketon, M. M. (2011). YopK regulates the Yersinia pestis type III secretion system from within host cells. *Mol Microbiol,* 79**,** 1445-61.

Dewoody, R. S., Merritt, P. M. & Marketon, M. M. (2013). Regulation of the Yersinia type III secretion system: traffic control. *Front Cell Infect Microbiol,* 3**,** 4.

Diepold, A., Amstutz, M., Abel, S., Sorg, I., Jenal, U. & Cornelis, G. R. (2010). Deciphering the assembly of the Yersinia type III secretion injectisome. *EMBO J,* 29**,** 1928-40.

Dong, N., Liu, L. & Shao, F. (2010). A bacterial effector targets host DH-PH domain RhoGEFs and antagonizes macrophage phagocytosis. *EMBO J,* 29**,** 1363-76.

Donnenberg, M. S., Yu, J. & Kaper, J. B. (1993). A second chromosomal gene necessary for intimate attachment of enteropathogenic Escherichia coli to epithelial cells. *J Bacteriol,* 175**,** 4670-80.

Dwyer, J. M. & Johnson, C. (1981). The use of concanavalin A to study the immunoregulation of human T cells. *Clin Exp Immunol,* 46**,** 237-49.

Dziva, F., Van Diemen, P. M., Stevens, M. P., Smith, A. J. & Wallis, T. S. (2004). Identification of Escherichia coli O157 : H7 genes influencing colonization of the bovine gastrointestinal tract using signature-tagged mutagenesis. *Microbiology,* 150**,** 3631-45.

Eberl, G. (2007). From induced to programmed lymphoid tissues: the long road to preempt pathogens. *Trends Immunol,* 28**,** 423-8.

Eberl, G. & Littman, D. R. (2003). The role of the nuclear hormone receptor RORgammat in the development of lymph nodes and Peyer's patches. *Immunol Rev,* 195**,** 81-90.

Eberl, G., Marmon, S., Sunshine, M. J., Rennert, P. D., Choi, Y. & Littman, D. R. (2004). An essential function for the nuclear receptor RORgamma(t) in the generation of fetal lymphoid tissue inducer cells. *Nat Immunol,* 5**,** 64-73.

Eberl, G. & Sawa, S. (2010). Opening the crypt: current facts and hypotheses on the function of cryptopatches. *Trends Immunol,* 31**,** 50-5.

Echtenkamp, F., Deng, W., Wickham, M. E., Vazquez, A., Puente, J. L., Thanabalasuriar, A., Gruenheid, S., Finlay, B. B. & Hardwidge, P. R. (2008). Characterization of the NleF effector protein from attaching and effacing bacterial pathogens. *FEMS Microbiol Lett,* 281**,** 98-107.

Eichelberg, K., Ginocchio, C. C. & Galan, J. E. (1994). Molecular and functional characterization of the Salmonella typhimurium invasion genes invB and invC: homology of InvC to the F0F1 ATPase family of proteins. *J Bacteriol,* 176**,** 4501-10.

Eitel, J. & Dersch, P. (2002). The YadA protein of Yersinia pseudotuberculosis mediates high-efficiency uptake into human cells under environmental conditions in which invasin is repressed. *Infect Immun,* 70**,** 4880-91.

Elliott, S. J., Krejany, E. O., Mellies, J. L., Robins-Browne, R. M., Sasakawa, C. & Kaper, J. B. (2001). EspG, a novel type III system-secreted protein from enteropathogenic Escherichia coli with similarities to VirA of Shigella flexneri. *Infect Immun,* 69**,** 4027-33.

Erdem, A. L., Avelino, F., Xicohtencatl-Cortes, J. & Giron, J. A. (2007). Host protein binding and adhesive properties of H6 and H7 flagella of attaching and effacing Escherichia coli. *J Bacteriol,* 189**,** 7426-35.

Erhardt, M., Namba, K. & Hughes, K. T. (2010). Bacterial nanomachines: the flagellum and type III injectisome. *Cold Spring Harb Perspect Biol,* 2**,** a000299.

Fabrega, A. & Vila, J. (2013). Salmonella enterica serovar Typhimurium skills to

succeed in the host: virulence and regulation. *Clin Microbiol Rev,* 26**,** 308-41.

Fagarasan, S., Kawamoto, S., Kanagawa, O. & Suzuki, K. (2010). Adaptive immune regulation in the gut: T cell-dependent and T cell-independent IgA synthesis. *Annu Rev Immunol,* 28**,** 243-73.

Fagarasan, S., Kinoshita, K., Muramatsu, M., Ikuta, K. & Honjo, T. (2001). In situ class switching and differentiation to IgA-producing cells in the gut lamina propria. *Nature,* 413**,** 639-43.

Fan, F. & Macnab, R. M. (1996). Enzymatic characterization of FliI. An ATPase involved in flagellar assembly in Salmonella typhimurium. *J Biol Chem,* 271**,** 31981-8.

Farache, J., Zigmond, E., Shakhar, G. & Jung, S. (2013). Contributions of dendritic cells and macrophages to intestinal homeostasis and immune defense. *Immunol Cell Biol,* 91**,** 232-9.

Favre, L., Spertini, F. & Corthesy, B. (2005). Secretory IgA possesses intrinsic modulatory properties stimulating mucosal and systemic immune responses. *J Immunol,* 175**,** 2793-800.

Feuerbacher, L. A. & Hardwidge, P. R. (2014). Influence of NleH effector expression, host genetics, and inflammation on Citrobacter rodentium colonization of mice. *Microbes Infect,* 16**,** 429-33.

Fiorentino, D. F., Zlotnik, A., Vieira, P., Mosmann, T. R., Howard, M., Moore, K. W. & O'garra, A. (1991). IL-10 acts on the antigen-presenting cell to inhibit cytokine production by Th1 cells. *J Immunol,* 146**,** 3444-51.

Flavell, R. A., Sanjabi, S., Wrzesinski, S. H. & Licona-Limon, P. (2010). The polarization of immune cells in the tumour environment by TGFbeta. *Nat Rev Immunol,* 10**,** 554-67.

Forsberg, A., Viitanen, A. M., Skurnik, M. & Wolf-Watz, H. (1991). The surface-located YopN protein is involved in calcium signal transduction in Yersinia pseudotuberculosis. *Mol Microbiol,* 5**,** 977-86.

Fournier, B. M. & Parkos, C. A. (2012). The role of neutrophils during intestinal inflammation. *Mucosal Immunol,* 5**,** 354-66.

Franchi, L., Mcdonald, C., Kanneganti, T. D., Amer, A. & Nunez, G. (2006). Nucleotide-binding oligomerization domain-like receptors: intracellular pattern recognition molecules for pathogen detection and host defense. *J Immunol,* 177**,** 3507-13.

Franchimont, D., Vermeire, S., El Housni, H., Pierik, M., Van Steen, K., Gustot, T., Quertinmont, E., Abramowicz, M., Van Gossum, A., Deviere, J. & Rutgeerts, P. (2004). Deficient host-bacteria interactions in inflammatory bowel disease? The toll-like receptor (TLR)-4 Asp299gly polymorphism is associated with Crohn's disease and ulcerative colitis. *Gut,* 53**,** 987-92.

Frankel, G., Lider, O., Hershkoviz, R., Mould, A. P., Kachalsky, S. G., Candy, D. C., Cahalon, L., Humphries, M. J. & Dougan, G. (1996). The cell-binding domain of intimin from enteropathogenic Escherichia coli binds to beta1 integrins. *J Biol Chem,* 271**,** 20359-64.

Frankel, G., Phillips, A. D., Trabulsi, L. R., Knutton, S., Dougan, G. & Matthews, S. (2001). Intimin and the host cell--is it bound to end in Tir(s)? *Trends Microbiol,* 9**,** 214-8.

Fuchs, T. A., Abed, U., Goosmann, C., Hurwitz, R., Schulze, I., Wahn, V., Weinrauch, Y., Brinkmann, V. & Zychlinsky, A. (2007). Novel cell death program leads to neutrophil extracellular traps. *J Cell Biol,* 176**,** 231-41.

Fukata, M. & Abreu, M. T. (2007). TLR4 signalling in the intestine in health and disease. *Biochem Soc Trans,* 35**,** 1473-8.

Fukata, M., Hernandez, Y., Conduah, D., Cohen, J., Chen, A., Breglio, K., Goo, T., Hsu, D., Xu, R. & Abreu, M. T. (2009). Innate immune signaling by Toll-like receptor-4 (TLR4) shapes the inflammatory microenvironment in colitis-associated tumors. *Inflamm Bowel Dis,* 15**,** 997-1006.

Fukata, M., Michelsen, K. S., Eri, R., Thomas, L. S., Hu, B., Lukasek, K., Nast, C. C., Lechago, J., Xu, R., Naiki, Y., Soliman, A., Arditi, M. & Abreu, M. T. (2005). Toll-like receptor-4 is required for intestinal response to epithelial injury and limiting bacterial translocation in a murine model of acute colitis. *Am J Physiol Gastrointest Liver Physiol,* 288**,** G1055-65.

Fukuda, S., Hase, K. & Ohno, H. (2011). Application of a mouse ligated Peyer's patch intestinal loop assay to evaluate bacterial uptake by M cells. *J Vis Exp*.

Gal-Mor, O. & Finlay, B. B. (2006). Pathogenicity islands: a molecular toolbox for bacterial virulence. *Cell Microbiol,* 8**,** 1707-19.

Galan, J. E. & Collmer, A. (1999). Type III secretion machines: bacterial devices for protein delivery into host cells. *Science,* 284**,** 1322-8.

Gallo, R. L. & Hooper, L. V. (2012). Epithelial antimicrobial defence of the skin and intestine. *Nat Rev Immunol,* 12**,** 503-16.

Galluzzi, L., Bravo-San Pedro, J. M. & Kroemer, G. (2014). Organelle-specific initiation of cell death. *Nat Cell Biol,* 16**,** 728-36.

Gao, X., Wan, F., Mateo, K., Callegari, E., Wang, D., Deng, W., Puente, J., Li, F., Chaussee, M. S., Finlay, B. B., Lenardo, M. J. & Hardwidge, P. R. (2009). Bacterial effector binding to ribosomal protein s3 subverts NF-kappaB function. *PLoS Pathog,* 5**,** e1000708.

Gao, X., Wang, X., Pham, T. H., Feuerbacher, L. A., Lubos, M. L., Huang, M., Olsen, R., Mushegian, A., Slawson, C. & Hardwidge, P. R. (2013). NleB, a bacterial effector with glycosyltransferase activity, targets GAPDH function to inhibit NF-kappaB activation. *Cell Host Microbe,* 13**,** 87-99.

Garcia-Angulo, V. A., Deng, W., Thomas, N. A., Finlay, B. B. & Puente, J. L. (2008). Regulation of expression and secretion of NleH, a new non-locus of enterocyte effacement-encoded effector in Citrobacter rodentium. *J Bacteriol,* 190**,** 2388-99.

Garmendia, J., Phillips, A. D., Carlier, M. F., Chong, Y., Schuller, S., Marches, O., Dahan, S., Oswald, E., Shaw, R. K., Knutton, S. & Frankel, G. (2004). TccP is an enterohaemorrhagic Escherichia coli O157:H7 type III effector protein that couples Tir to the actin-cytoskeleton. *Cell Microbiol,* 6**,** 1167-83.

Gauthier, A. & Finlay, B. B. (2003). Translocated intimin receptor and its chaperone interact with ATPase of the type III secretion apparatus of enteropathogenic Escherichia coli. *J Bacteriol,* 185**,** 6747-55.

Gauthier, A., Puente, J. L. & Finlay, B. B. (2003). Secretin of the enteropathogenic Escherichia coli type III secretion system requires components of the type III apparatus for assembly and localization. *Infect Immun,* 71**,** 3310-9.

Gavilanes-Parra, S., Mendoza-Hernandez, G., Chavez-Berrocal, M. E., Giron, J. A., Orozco-Hoyuela, G. & Manjarrez-Hernandez, A. (2013). Identification of secretory immunoglobulin A antibody targets from human milk in cultured cells infected with enteropathogenic Escherichia coli (EPEC). *Microb Pathog,* 64**,** 48-56.

Gebert, A. & Bartels, H. (1995). Ultrastructure and protein transport of M cells in the rabbit cecal patch. *Anat Rec,* 241**,** 487-95.

Geddes, K., Rubino, S. J., Magalhaes, J. G., Streutker, C., Le Bourhis, L., Cho, J. H., Robertson, S. J., Kim, C. J., Kaul, R., Philpott, D. J. & Girardin, S. E. (2011). Identification of an innate T helper type 17 response to intestinal bacterial pathogens. *Nat Med,* 17**,** 837-44.

Gerke, C., Falkow, S. & Chien, Y. H. (2005). The adaptor molecules LAT and SLP-76 are specifically targeted by Yersinia to inhibit T cell activation. *J Exp Med,* 201**,** 361-71.

Gibson, A., Futter, C. E., Maxwell, S., Allchin, E. H., Shipman, M., Kraehenbuhl, J. P., Domingo, D., Odorizzi, G., Trowbridge, I. S. & Hopkins, C. R. (1998). Sorting mechanisms regulating membrane protein traffic in the apical transcytotic pathway of polarized MDCK cells. *J Cell Biol,* 143**,** 81-94.

Gibson, D. L., Ma, C., Bergstrom, K. S., Huang, J. T., Man, C. & Vallance, B. A. (2008). MyD88 signalling plays a critical role in host defence by controlling pathogen burden and promoting epithelial cell homeostasis during Citrobacter rodentium-induced colitis. *Cell Microbiol,* 10**,** 618-31.

Gibson, D. L., Ma, C., Rosenberger, C. M., Bergstrom, K. S., Valdez, Y., Huang, J. T., Khan, M. A. & Vallance, B. A. (2008). Toll-like receptor 2 plays a critical role in maintaining mucosal integrity during Citrobacter rodentium-induced colitis. *Cell Microbiol,* 10**,** 388-403.

Gibson, D. L., Montero, M., Ropeleski, M. J., Bergstrom, K. S., Ma, C., Ghosh,

S., Merkens, H., Huang, J., Mansson, L. E., Sham, H. P., Mcnagny, K. M. & Vallance, B. A. (2010). Interleukin-11 reduces TLR4-induced colitis in TLR2-deficient mice and restores intestinal STAT3 signaling. *Gastroenterology,* 139**,** 1277-88.

Girard, F., Crepin, V. F. & Frankel, G. (2009). Modelling of infection by enteropathogenic Escherichia coli strains in lineages 2 and 4 ex vivo and in vivo by using Citrobacter rodentium expressing TccP. *Infect Immun,* 77**,** 1304-14.

Girardin, S. E., Boneca, I. G., Carneiro, L. A., Antignac, A., Jehanno, M., Viala, J., Tedin, K., Taha, M. K., Labigne, A., Zahringer, U., Coyle, A. J., Distefano, P. S., Bertin, J., Sansonetti, P. J. & Philpott, D. J. (2003). Nod1 detects a unique muropeptide from gram-negative bacterial peptidoglycan. *Science,* 300**,** 1584-7.

Giron, J. A., Ho, A. S. & Schoolnik, G. K. (1991). An inducible bundle-forming pilus of enteropathogenic Escherichia coli. *Science,* 254**,** 710-3.

Glocker, E. O., Kotlarz, D., Boztug, K., Gertz, E. M., Schaffer, A. A., Noyan, F., Perro, M., Diestelhorst, J., Allroth, A., Murugan, D., Hatscher, N., Pfeifer, D., Sykora, K. W., Sauer, M., Kreipe, H., Lacher, M., Nustede, R., Woellner, C., Baumann, U., Salzer, U., Koletzko, S., Shah, N., Segal, A. W., Sauerbrey, A., Buderus, S., Snapper, S. B., Grimbacher, B. & Klein, C. (2009). Inflammatory bowel disease and mutations affecting the interleukin-10 receptor. *N Engl J Med,* 361**,** 2033-45.

Glotfelty, L. G., Zahs, A., Hodges, K., Shan, K., Alto, N. M. & Hecht, G. A. (2014). Enteropathogenic E. coli effectors EspG1/G2 disrupt microtubules, contribute to tight junction perturbation and inhibit restoration. *Cell Microbiol,* 16**,** 1767-83.

Gobert, A. P., Wilson, K. T. & Martin, C. (2005). Cellular responses to attaching and effacing bacteria: activation and implication of the innate immune system. *Arch Immunol Ther Exp (Warsz),* 53**,** 234-44.

Goncalves, N. S., Ghaem-Maghami, M., Monteleone, G., Frankel, G., Dougan, G., Lewis, D. J., Simmons, C. P. & Macdonald, T. T. (2001). Critical role for tumor necrosis factor alpha in controlling the number of lumenal pathogenic bacteria and immunopathology in infectious colitis. *Infect Immun,* 69**,** 6651-9.

Goosney, D. L., Celli, J., Kenny, B. & Finlay, B. B. (1999). Enteropathogenic Escherichia coli inhibits phagocytosis. *Infect Immun,* 67**,** 490-5.

Gophna, U., Ron, E. Z. & Graur, D. (2003). Bacterial type III secretion systems are ancient and evolved by multiple horizontal-transfer events. *Gene,* 312**,** 151-63.

Grimm, M. C. & Pavli, P. (2004). NOD2 mutations and Crohn's disease: are Paneth cells and their antimicrobial peptides the link? *Gut,* 53**,** 1558-60.

Grishin, A. M., Cherney, M., Anderson, D. H., Phanse, S., Babu, M. & Cygler, M. (2014). NleH defines a new family of bacterial effector kinases. *Structure,* 22**,** 250-9.

Gruenheid, S., Devinney, R., Bladt, F., Goosney, D., Gelkop, S., Gish, G. D., Pawson, T. & Finlay, B. B. (2001). Enteropathogenic E. coli Tir binds Nck to initiate actin pedestal formation in host cells. *Nat Cell Biol,* 3**,** 856-9.

Gruenheid, S., Sekirov, I., Thomas, N. A., Deng, W., O'donnell, P., Goode, D., Li, Y., Frey, E. A., Brown, N. F., Metalnikov, P., Pawson, T., Ashman, K. & Finlay, B. B. (2004). Identification and characterization of NleA, a non-LEE-encoded type III translocated virulence factor of enterohaemorrhagic Escherichia coli O157:H7. *Mol Microbiol,* 51**,** 1233-49.

Gueguen, E. & Cascales, E. (2013). Promoter swapping unveils the role of the Citrobacter rodentium CTS1 type VI secretion system in interbacterial competition. *Appl Environ Microbiol,* 79**,** 32-8.

Guiney, D. G. (2005). The role of host cell death in Salmonella infections. *Curr Top Microbiol Immunol,* 289**,** 131-50.

Halavaty, A. S., Anderson, S. M., Wawrzak, Z., Kudritska, M., Skarina, T., Anderson, W. F. & Savchenko, A. (2014). Type III effector NleH2 from Escherichia coli O157:H7 str. Sakai features an atypical protein kinase domain. *Biochemistry,* 53**,** 2433-5.

Hall, J. A., Cannons, J. L., Grainger, J. R., Dos Santos, L. M., Hand, T. W., Naik, S., Wohlfert, E. A., Chou, D. B., Oldenhove, G., Robinson, M., Grigg, M. E., Kastenmayer, R., Schwartzberg, P. L. & Belkaid, Y. (2011). Essential role for retinoic acid in the promotion of CD4(+) T cell effector responses via retinoic acid receptor alpha. *Immunity,* 34**,** 435-47.

Hamada, D., Hamaguchi, M., Suzuki, K. N., Sakata, I. & Yanagihara, I. (2010). Cytoskeleton-modulating effectors of enteropathogenic and enterohemorrhagic Escherichia coli: a case for EspB as an intrinsically less-ordered effector. *FEBS J,* 277**,** 2409-15.

Hamada, H., Hiroi, T., Nishiyama, Y., Takahashi, H., Masunaga, Y., Hachimura, S., Kaminogawa, S., Takahashi-Iwanaga, H., Iwanaga, T., Kiyono, H., Yamamoto, H. & Ishikawa, H. (2002). Identification of multiple isolated lymphoid follicles on the antimesenteric wall of the mouse small intestine. *J Immunol,* 168**,** 57-64.

Hamaguchi, M., Kamikubo, H., Suzuki, K. N., Hagihara, Y., Yanagihara, I., Sakata, I., Kataoka, M. & Hamada, D. (2013). Structural basis of alpha-catenin recognition by EspB from enterohaemorrhagic E. coli based on hybrid strategy using low-resolution structural and protein dissection. *PLoS One,* 8**,** e71618.

Hansson, G. C. & Johansson, M. E. (2010). The inner of the two Muc2 mucin-dependent mucus layers in colon is devoid of bacteria. *Gut Microbes,* 1**,** 51-54.

Harrison, O. J. & Powrie, F. M. (2013). Regulatory T cells and immune tolerance in the intestine. *Cold Spring Harb Perspect Biol,* 5.

He, B., Xu, W., Santini, P. A., Polydorides, A. D., Chiu, A., Estrella, J., Shan, M., Chadburn, A., Villanacci, V., Plebani, A., Knowles, D. M., Rescigno, M. & Cerutti, A. (2007). Intestinal bacteria trigger T cell-independent immunoglobulin A(2) class switching by inducing epithelial-cell secretion of the cytokine APRIL. *Immunity,* 26**,** 812-26.

Heazlewood, C. K., Cook, M. C., Eri, R., Price, G. R., Tauro, S. B., Taupin, D., Thornton, D. J., Png, C. W., Crockford, T. L., Cornall, R. J., Adams, R., Kato, M., Nelms, K. A., Hong, N. A., Florin, T. H., Goodnow, C. C. & Mcguckin, M. A. (2008). Aberrant mucin assembly in mice causes endoplasmic reticulum stress and spontaneous inflammation resembling ulcerative colitis. *PLoS Med,* 5**,** e54.

Heczko, U., Abe, A. & Finlay, B. B. (2000). In vivo interactions of rabbit enteropathogenic Escherichia coli O103 with its host: an electron microscopic and histopathologic study. *Microbes Infect,* 2**,** 5-16.

Hemrajani, C., Berger, C. N., Robinson, K. S., Marches, O., Mousnier, A. & Frankel, G. (2010). NleH effectors interact with Bax inhibitor-1 to block apoptosis during enteropathogenic Escherichia coli infection. *Proc Natl Acad Sci U S A,* 107**,** 3129-34.

Hemrajani, C., Marches, O., Wiles, S., Girard, F., Dennis, A., Dziva, F., Best, A., Phillips, A. D., Berger, C. N., Mousnier, A., Crepin, V. F., Kruidenier, L., Woodward, M. J., Stevens, M. P., La Ragione, R. M., Macdonald, T. T. & Frankel, G. (2008). Role of NleH, a type III secreted effector from attaching and effacing pathogens, in colonization of the bovine, ovine, and murine gut. *Infect Immun,* 76**,** 4804-13.

Herbert, D. R., Yang, J. Q., Hogan, S. P., Groschwitz, K., Khodoun, M., Munitz, A., Orekov, T., Perkins, C., Wang, Q., Brombacher, F., Urban, J. F., Jr., Rothenberg, M. E. & Finkelman, F. D. (2009). Intestinal epithelial cell secretion of RELM-beta protects against gastrointestinal worm infection. *J Exp Med,* 206**,** 2947-57.

Hermiston, M. L. & Gordon, J. I. (1995). In vivo analysis of cadherin function in the mouse intestinal epithelium: essential roles in adhesion, maintenance of differentiation, and regulation of programmed cell death. *J Cell Biol,* 129**,** 489-506.

Hicks, S. W. & Galan, J. E. (2013). Exploitation of eukaryotic subcellular targeting mechanisms by bacterial effectors. *Nat Rev Microbiol,* 11**,** 316-26.

Higgins, L. M., Frankel, G., Douce, G., Dougan, G. & Macdonald, T. T. (1999). Citrobacter rodentium infection in mice elicits a mucosal Th1 cytokine response and lesions similar to those in murine inflammatory bowel disease. *Infect Immun,* 67**,** 3031-9.

Hisamatsu, T., Suzuki, M., Reinecker, H. C., Nadeau, W. J., Mccormick, B. A. & Podolsky, D. K. (2003). CARD15/NOD2 functions as an antibacterial factor in human intestinal epithelial cells. *Gastroenterology,* 124**,** 993-1000.

Holmes, A., Lindestam Arlehamn, C. S., Wang, D., Mitchell, T. J., Evans, T. J. & Roe, A. J. (2012). Expression and regulation of the Escherichia coli O157:H7 effector proteins NleH1 and NleH2. *PLoS One,* 7**,** e33408.

Hueck, C. J. (1998). Type III protein secretion systems in bacterial pathogens of animals and plants. *Microbiol Mol Biol Rev,* 62**,** 379-433.

Husseiny, M. I. & Hensel, M. (2005). Rapid method for the construction of Salmonella enterica Serovar Typhimurium vaccine carrier strains. *Infect Immun,* 73**,** 1598-605.

Hyland, R. M., Sun, J., Griener, T. P., Mulvey, G. L., Klassen, J. S., Donnenberg, M. S. & Armstrong, G. D. (2008). The bundlin pilin protein of enteropathogenic Escherichia coli is an N-acetyllactosamine-specific lectin. *Cell Microbiol,* 10**,** 177-87.

Iguchi, A., Thomson, N. R., Ogura, Y., Saunders, D., Ooka, T., Henderson, I. R., Harris, D., Asadulghani, M., Kurokawa, K., Dean, P., Kenny, B., Quail, M. A., Thurston, S., Dougan, G., Hayashi, T., Parkhill, J. & Frankel, G. (2009). Complete genome sequence and comparative genome analysis of enteropathogenic Escherichia coli O127:H6 strain E2348/69. *J Bacteriol,* 191**,** 347-54.

Iizumi, Y., Sagara, H., Kabe, Y., Azuma, M., Kume, K., Ogawa, M., Nagai, T., Gillespie, P. G., Sasakawa, C. & Handa, H. (2007). The enteropathogenic E. coli effector EspB facilitates microvillus effacing and antiphagocytosis by inhibiting myosin function. *Cell Host Microbe,* 2**,** 383-92.

Inman, L. R. & Cantey, J. R. (1983). Specific adherence of Escherichia coli (strain RDEC-1) to membranous (M) cells of the Peyer's patch in Escherichia coli diarrhea in the rabbit. *J Clin Invest,* 71**,** 1-8.

Inohara, N., Koseki, T., Del Peso, L., Hu, Y., Yee, C., Chen, S., Carrio, R., Merino, J., Liu, D., Ni, J. & Nunez, G. (1999). Nod1, an Apaf-1-like activator of caspase-9 and nuclear factor-kappaB. *J Biol Chem,* 274**,** 14560-7.

Inohara, N., Ogura, Y., Fontalba, A., Gutierrez, O., Pons, F., Crespo, J., Fukase, K., Inamura, S., Kusumoto, S., Hashimoto, M., Foster, S. J., Moran, A. P., Fernandez-Luna, J. L. & Nunez, G. (2003). Host recognition of bacterial muramyl dipeptide mediated through NOD2. Implications for Crohn's disease. *J Biol Chem,* 278**,** 5509-12.

Ivanov, Ii, Atarashi, K., Manel, N., Brodie, E. L., Shima, T., Karaoz, U., Wei, D., Goldfarb, K. C., Santee, C. A., Lynch, S. V., Tanoue, T., Imaoka, A., Itoh, K., Takeda, K., Umesaki, Y., Honda, K. & Littman, D. R. (2009). Induction of intestinal Th17 cells by segmented filamentous bacteria. *Cell,* 139**,** 485-98.

Ivanov, Ii, Frutos Rde, L., Manel, N., Yoshinaga, K., Rifkin, D. B., Sartor, R. B., Finlay, B. B. & Littman, D. R. (2008). Specific microbiota direct the differentiation of IL-17-producing T-helper cells in the mucosa of the small intestine. *Cell Host*

Microbe, 4**,** 337-49.

Ivanov, Ii & Littman, D. R. (2010). Segmented filamentous bacteria take the stage. *Mucosal Immunol,* 3**,** 209-12.

Iwata, M., Hirakiyama, A., Eshima, Y., Kagechika, H., Kato, C. & Song, S. Y. (2004). Retinoic acid imprints gut-homing specificity on T cells. *Immunity,* 21**,** 527-38.

Jaeger, A. S., P. Sidsworth, R. Tint, N. (2004). initial stages in creating a lacI knockout in Escherichia coli C29 using the lambda red recombinase system. *Journal of Experimental Microbiology and I mmunology (JEMI),* 5:65-71.

Jaensson, E., Uronen-Hansson, H., Pabst, O., Eksteen, B., Tian, J., Coombes, J. L., Berg, P. L., Davidsson, T., Powrie, F., Johansson-Lindbom, B. & Agace, W. W. (2008). Small intestinal CD103+ dendritic cells display unique functional properties that are conserved between mice and humans. *J Exp Med,* 205**,** 2139-49.

Jepson, M. A., Pellegrin, S., Peto, L., Banbury, D. N., Leard, A. D., Mellor, H. & Kenny, B. (2003). Synergistic roles for the Map and Tir effector molecules in mediating uptake of enteropathogenic Escherichia coli (EPEC) into non-phagocytic cells. *Cell Microbiol,* 5**,** 773-83.

Jiang, X., Rossanese, O. W., Brown, N. F., Kujat-Choy, S., Galan, J. E., Finlay, B. B. & Brumell, J. H. (2004). The related effector proteins SopD and SopD2 from Salmonella enterica serovar Typhimurium contribute to virulence during systemic infection of mice. *Mol Microbiol,* 54**,** 1186-98.

Johansen, F. E., Pekna, M., Norderhaug, I. N., Haneberg, B., Hietala, M. A., Krajci, P., Betsholtz, C. & Brandtzaeg, P. (1999). Absence of epithelial immunoglobulin A transport, with increased mucosal leakiness, in polymeric immunoglobulin receptor/secretory component-deficient mice. *J Exp Med,* 190**,** 915-22.

Johansson, M. E., Ambort, D., Pelaseyed, T., Schutte, A., Gustafsson, J. K., Ermund, A., Subramani, D. B., Holmen-Larsson, J. M., Thomsson, K. A., Bergstrom, J. H., Van Der Post, S., Rodriguez-Pineiro, A. M., Sjovall, H., Backstrom, M. & Hansson, G. C. (2011). Composition and functional role of the mucus layers in the intestine. *Cell Mol Life Sci,* 68**,** 3635-41.

Jones, B. D., Ghori, N. & Falkow, S. (1994). Salmonella typhimurium initiates murine infection by penetrating and destroying the specialized epithelial M cells of the Peyer's patches. *J Exp Med,* 180**,** 15-23.

Josefowicz, S. Z., Lu, L. F. & Rudensky, A. Y. (2012). Regulatory T cells: mechanisms of differentiation and function. *Annu Rev Immunol,* 30**,** 531-64.

Journet, L., Agrain, C., Broz, P. & Cornelis, G. R. (2003). The needle length of bacterial injectisomes is determined by a molecular ruler. *Science,* 302**,** 1757-60.

Jung, C., Hugot, J. P. & Barreau, F. (2010). Peyer's Patches: The Immune Sensors of the Intestine. *Int J Inflam,* 2010**,** 823710.

Kadonaga, J. T., Gautier, A. E., Straus, D. R., Charles, A. D., Edge, M. D. & Knowles, J. R. (1984). The role of the beta-lactamase signal sequence in the secretion of proteins by Escherichia coli. *J Biol Chem,* 259**,** 2149-54.

Kaetzel, C. S., Robinson, J. K., Chintalacharuvu, K. R., Vaerman, J. P. & Lamm, M. E. (1991). The polymeric immunoglobulin receptor (secretory component) mediates transport of immune complexes across epithelial cells: a local defense function for IgA. *Proc Natl Acad Sci U S A,* 88**,** 8796-800.

Kanack, K. J., Crawford, J. A., Tatsuno, I., Karmali, M. A. & Kaper, J. B. (2005). SepZ/EspZ is secreted and translocated into HeLa cells by the enteropathogenic Escherichia coli type III secretion system. *Infect Immun,* 73**,** 4327-37.

Kang, S. G., Lim, H. W., Andrisani, O. M., Broxmeyer, H. E. & Kim, C. H. (2007). Vitamin A metabolites induce gut-homing FoxP3+ regulatory T cells. *J Immunol,* 179**,** 3724-33.

Kang, Y., Durfee, T., Glasner, J. D., Qiu, Y., Frisch, D., Winterberg, K. M. & Blattner, F. R. (2004). Systematic mutagenesis of the Escherichia coli genome. *J Bacteriol,* 186**,** 4921-30.

Kato, C., Ohmiya, R. & Mizuno, T. (1998). A rapid method for disrupting genes in the Escherichia coli genome. *Biosci Biotechnol Biochem,* 62**,** 1826-9.

Kawai, T. & Akira, S. (2011). Toll-like receptors and their crosstalk with other innate receptors in infection and immunity. *Immunity,* 34**,** 637-50.

Kayama, H. & Takeda, K. (2012). Regulation of intestinal homeostasis by innate and adaptive immunity. *Int Immunol,* 24**,** 673-80.

Keestra, A. M., Godinez, I., Xavier, M. N., Winter, M. G., Winter, S. E., Tsolis, R. M. & Baumler, A. J. (2011). Early MyD88-dependent induction of interleukin-17A expression during Salmonella colitis. *Infect Immun,* 79**,** 3131-40.

Kelly, M., Hart, E., Mundy, R., Marches, O., Wiles, S., Badea, L., Luck, S., Tauschek, M., Frankel, G., Robins-Browne, R. M. & Hartland, E. L. (2006). Essential role of the type III secretion system effector NleB in colonization of mice by Citrobacter rodentium. *Infect Immun,* 74**,** 2328-37.

Kenny, B., Devinney, R., Stein, M., Reinscheid, D. J., Frey, E. A. & Finlay, B. B. (1997). Enteropathogenic E. coli (EPEC) transfers its receptor for intimate adherence into mammalian cells. *Cell,* 91**,** 511-20.

Kenny, B., Ellis, S., Leard, A. D., Warawa, J., Mellor, H. & Jepson, M. A. (2002). Co-ordinate regulation of distinct host cell signalling pathways by multifunctional enteropathogenic Escherichia coli effector molecules. *Mol Microbiol,* 44**,** 1095-1107.

Kenny, B. & Jepson, M. (2000). Targeting of an enteropathogenic Escherichia coli

(EPEC) effector protein to host mitochondria. *Cell Microbiol,* 2**,** 579-90.

Kenny, B., Lai, L. C., Finlay, B. B. & Donnenberg, M. S. (1996). EspA, a protein secreted by enteropathogenic Escherichia coli, is required to induce signals in epithelial cells. *Mol Microbiol,* 20**,** 313-23.

Kerschen, E. J., Cohen, D. A., Kaplan, A. M. & Straley, S. C. (2004). The plague virulence protein YopM targets the innate immune response by causing a global depletion of NK cells. *Infect Immun,* 72**,** 4589-602.

Khan, M. A., Ma, C., Knodler, L. A., Valdez, Y., Rosenberger, C. M., Deng, W., Finlay, B. B. & Vallance, B. A. (2006). Toll-like receptor 4 contributes to colitis development but not to host defense during Citrobacter rodentium infection in mice. *Infect Immun,* 74**,** 2522-36.

Khounlotham, M., Kim, W., Peatman, E., Nava, P., Medina-Contreras, O., Addis, C., Koch, S., Fournier, B., Nusrat, A., Denning, T. L. & Parkos, C. A. (2012). Compromised intestinal epithelial barrier induces adaptive immune compensation that protects from colitis. *Immunity,* 37**,** 563-73.

Kim, D., Mebius, R. E., Macmicking, J. D., Jung, S., Cupedo, T., Castellanos, Y., Rho, J., Wong, B. R., Josien, R., Kim, N., Rennert, P. D. & Choi, Y. (2000). Regulation of peripheral lymph node genesis by the tumor necrosis factor family member TRANCE. *J Exp Med,* 192**,** 1467-78.

Kim, M., Ogawa, M., Fujita, Y., Yoshikawa, Y., Nagai, T., Koyama, T., Nagai, S., Lange, A., Fassler, R. & Sasakawa, C. (2009). Bacteria hijack integrin-linked kinase to stabilize focal adhesions and block cell detachment. *Nature,* 459**,** 578-82.

Kim, S. H. & Jang, Y. S. (2014). Antigen targeting to M cells for enhancing the efficacy of mucosal vaccines. *Exp Mol Med,* 46**,** e85.

Kim, Y. G., Kamada, N., Shaw, M. H., Warner, N., Chen, G. Y., Franchi, L. & Nunez, G. (2011). The Nod2 sensor promotes intestinal pathogen eradication via the chemokine CCL2-dependent recruitment of inflammatory monocytes. *Immunity,* 34**,** 769-80.

Kinashi, T. (2007). Integrin regulation of lymphocyte trafficking: lessons from structural and signaling studies. *Adv Immunol,* 93**,** 185-227.

Kindon, H., Pothoulakis, C., Thim, L., Lynch-Devaney, K. & Podolsky, D. K. (1995). Trefoil peptide protection of intestinal epithelial barrier function: cooperative interaction with mucin glycoprotein. *Gastroenterology,* 109**,** 516-23.

Klapproth, J. M., Sasaki, M., Sherman, M., Babbin, B., Donnenberg, M. S., Fernandes, P. J., Scaletsky, I. C., Kalman, D., Nusrat, A. & Williams, I. R. (2005). Citrobacter rodentium lifA/efa1 is essential for colonic colonization and crypt cell hyperplasia in vivo. *Infect Immun,* 73**,** 1441-51.

Knoop, K. A., Butler, B. R., Kumar, N., Newberry, R. D. & Williams, I. R. (2011). Distinct developmental requirements for isolated lymphoid follicle formation in the

small and large intestine: RANKL is essential only in the small intestine. *Am J Pathol,* 179**,** 1861-71.

Knutton, S., Adu-Bobie, J., Bain, C., Phillips, A. D., Dougan, G. & Frankel, G. (1997). Down regulation of intimin expression during attaching and effacing enteropathogenic Escherichia coli adhesion. *Infect Immun,* 65**,** 1644-52.

Knutton, S., Rosenshine, I., Pallen, M. J., Nisan, I., Neves, B. C., Bain, C., Wolff, C., Dougan, G. & Frankel, G. (1998). A novel EspA-associated surface organelle of enteropathogenic Escherichia coli involved in protein translocation into epithelial cells. *EMBO J,* 17**,** 2166-76.

Kobayashi, K. S., Chamaillard, M., Ogura, Y., Henegariu, O., Inohara, N., Nunez, G. & Flavell, R. A. (2005). Nod2-dependent regulation of innate and adaptive immunity in the intestinal tract. *Science,* 307**,** 731-4.

Koberle, M., Klein-Gunther, A., Schutz, M., Fritz, M., Berchtold, S., Tolosa, E., Autenrieth, I. B. & Bohn, E. (2009). Yersinia enterocolitica targets cells of the innate and adaptive immune system by injection of Yops in a mouse infection model. *PLoS Pathog,* 5**,** e1000551.

Konradt, C., Frigimelica, E., Nothelfer, K., Puhar, A., Salgado-Pabon, W., Di Bartolo, V., Scott-Algara, D., Rodrigues, C. D., Sansonetti, P. J. & Phalipon, A. (2011). The Shigella flexneri type three secretion system effector IpgD inhibits T cell migration by manipulating host phosphoinositide metabolism. *Cell Host Microbe,* 9**,** 263-72.

Kozakova, H., Mlckova, P., Kolinska, J., Cechova, D., Stepankova, R., Rehakova, Z. & Prokesova, L. (2002). Differential effect of Bacillus firmus on immune response and enterocyte brush-border enzyme levels in BALB/c and B10.BR mice. *Folia Microbiol (Praha),* 47**,** 759-65.

Kraehenbuhl, J. P. & Neutra, M. R. (2000). Epithelial M cells: differentiation and function. *Annu Rev Cell Dev Biol,* 16**,** 301-32.

Kubori, T. & Galan, J. E. (2003). Temporal regulation of salmonella virulence effector function by proteasome-dependent protein degradation. *Cell,* 115**,** 333-42.

Kuhl, A. A., Kakirman, H., Janotta, M., Dreher, S., Cremer, P., Pawlowski, N. N., Loddenkemper, C., Heimesaat, M. M., Grollich, K., Zeitz, M., Farkas, S. & Hoffmann, J. C. (2007). Aggravation of different types of experimental colitis by depletion or adhesion blockade of neutrophils. *Gastroenterology,* 133**,** 1882-92.

Kuhlman, T. E. & Cox, E. C. (2010). Site-specific chromosomal integration of large synthetic constructs. *Nucleic Acids Res,* 38**,** e92.

Kuhn, R., Lohler, J., Rennick, D., Rajewsky, K. & Muller, W. (1993). Interleukin-10-deficient mice develop chronic enterocolitis. *Cell,* 75**,** 263-74.

Kumar, H., Kawai, T. & Akira, S. (2009). Pathogen recognition in the innate immune response. *Biochem J,* 420**,** 1-16.

Kumar, H., Kawai, T. & Akira, S. (2011). Pathogen recognition by the innate immune system. *Int Rev Immunol,* 30**,** 16-34.

Kurushima, J., Nagai, T., Nagamatsu, K. & Abe, A. (2010). EspJ effector in enterohemorrhagic E. coli translocates into host mitochondria via an atypical mitochondrial targeting signal. *Microbiol Immunol,* 54**,** 371-9.

Lai, Y., Rosenshine, I., Leong, J. M. & Frankel, G. (2013). Intimate host attachment: enteropathogenic and enterohaemorrhagic Escherichia coli. *Cell Microbiol,* 15**,** 1796-808.

Lanzavecchia, A. & Sallusto, F. (2001). Antigen decoding by T lymphocytes: from synapses to fate determination. *Nat Immunol,* 2**,** 487-92.

Lavelle, E. C., Murphy, C., O'neill, L. A. & Creagh, E. M. (2010). The role of TLRs, NLRs, and RLRs in mucosal innate immunity and homeostasis. *Mucosal Immunol,* 3**,** 17-28.

Law, R. J., Gur-Arie, L., Rosenshine, I. & Finlay, B. B. (2013). In vitro and in vivo model systems for studying enteropathogenic Escherichia coli infections. *Cold Spring Harb Perspect Med,* 3**,** a009977.

Lebeis, S. L., Bommarius, B., Parkos, C. A., Sherman, M. A. & Kalman, D. (2007). TLR signaling mediated by MyD88 is required for a protective innate immune response by neutrophils to Citrobacter rodentium. *J Immunol,* 179**,** 566-77.

Lee, D. J., Bingle, L. E., Heurlier, K., Pallen, M. J., Penn, C. W., Busby, S. J. & Hobman, J. L. (2009). Gene doctoring: a method for recombineering in laboratory and pathogenic Escherichia coli strains. *BMC Microbiol,* 9**,** 252.

Lee, J., Mo, J. H., Katakura, K., Alkalay, I., Rucker, A. N., Liu, Y. T., Lee, H. K., Shen, C., Cojocaru, G., Shenouda, S., Kagnoff, M., Eckmann, L., Ben-Neriah, Y. & Raz, E. (2006). Maintenance of colonic homeostasis by distinctive apical TLR9 signalling in intestinal epithelial cells. *Nat Cell Biol,* 8**,** 1327-36.

Lee, J., Tattoli, I., Wojtal, K. A., Vavricka, S. R., Philpott, D. J. & Girardin, S. E. (2009). pH-dependent internalization of muramyl peptides from early endosomes enables Nod1 and Nod2 signaling. *J Biol Chem,* 284**,** 23818-29.

Lee, V. T., Anderson, D. M. & Schneewind, O. (1998). Targeting of Yersinia Yop proteins into the cytosol of HeLa cells: one-step translocation of YopE across bacterial and eukaryotic membranes is dependent on SycE chaperone. *Mol Microbiol,* 28**,** 593-601.

Lenski, R. E. (1998). Bacterial evolution and the cost of antibiotic resistance. *Int Microbiol,* 1**,** 265-70.

Li, L., Shi, Q. G., Lin, F., Liang, Y. G., Sun, L. J., Mu, J. S., Wang, Y. G., Su, H. B., Xu, B., Ji, C. C., Huang, H. H., Li, K. & Wang, H. F. (2014). Cytokine IL-6 is required in Citrobacter rodentium infection-induced intestinal Th17 responses and promotes IL-22 expression in inflammatory bowel disease. *Mol Med Rep,* 9**,** 831-6.

Li, M., Rosenshine, I., Yu, H. B., Nadler, C., Mills, E., Hew, C. L. & Leung, K. Y. (2006). Identification and characterization of NleI, a new non-LEE-encoded effector of enteropathogenic Escherichia coli (EPEC). *Microbes Infect,* 8**,** 2890-8.

Li, M. O., Wan, Y. Y., Sanjabi, S., Robertson, A. K. & Flavell, R. A. (2006). Transforming growth factor-beta regulation of immune responses. *Annu Rev Immunol,* 24**,** 99-146.

Li, W., Liu, Y., Sheng, X., Yin, P., Hu, F., Liu, Y., Chen, C., Li, Q., Yan, C. & Wang, J. (2014). Structure and mechanism of a type III secretion protease, NleC. *Acta Crystallogr D Biol Crystallogr,* 70**,** 40-7.

Long, T. M., Nisa, S., Donnenberg, M. S. & Hassel, B. A. (2014). Enteropathogenic Escherichia coli inhibits type I interferon- and RNase L-mediated host defense to disrupt intestinal epithelial cell barrier function. *Infect Immun,* 82**,** 2802-14.

Lorenz, M. G. & Wackernagel, W. (1994). Bacterial gene transfer by natural genetic transformation in the environment. *Microbiol Rev,* 58**,** 563-602.

Lucas, P. J., Kim, S. J., Melby, S. J. & Gress, R. E. (2000). Disruption of T cell homeostasis in mice expressing a T cell-specific dominant negative transforming growth factor beta II receptor. *J Exp Med,* 191**,** 1187-96.

Lugering, A. & Kucharzik, T. (2006). Induction of intestinal lymphoid tissue: the role of cryptopatches. *Ann N Y Acad Sci,* 1072**,** 210-7.

Luo, Y., Frey, E. A., Pfuetzner, R. A., Creagh, A. L., Knoechel, D. G., Haynes, C. A., Finlay, B. B. & Strynadka, N. C. (2000). Crystal structure of enteropathogenic Escherichia coli intimin-receptor complex. *Nature,* 405**,** 1073-7.

Luperchio, S. A., Newman, J. V., Dangler, C. A., Schrenzel, M. D., Brenner, D. J., Steigerwalt, A. G. & Schauer, D. B. (2000). Citrobacter rodentium, the causative agent of transmissible murine colonic hyperplasia, exhibits clonality: synonymy of C. rodentium and mouse-pathogenic Escherichia coli. *J Clin Microbiol,* 38**,** 4343-50.

Luperchio, S. A. & Schauer, D. B. (2001). Molecular pathogenesis of Citrobacter rodentium and transmissible murine colonic hyperplasia. *Microbes Infect,* 3**,** 333-40.

Lupp, C., Robertson, M. L., Wickham, M. E., Sekirov, I., Champion, O. L., Gaynor, E. C. & Finlay, B. B. (2007). Host-mediated inflammation disrupts the intestinal microbiota and promotes the overgrowth of Enterobacteriaceae. *Cell Host Microbe,* 2**,** 119-29.

Lycke, N., Erlandsson, L., Ekman, L., Schon, K. & Leanderson, T. (1999). Lack of J chain inhibits the transport of gut IgA and abrogates the development of intestinal antitoxic protection. *J Immunol,* 163**,** 913-9.

Maaser, C., Housley, M. P., Iimura, M., Smith, J. R., Vallance, B. A., Finlay, B.

B., Schreiber, J. R., Varki, N. M., Kagnoff, M. F. & Eckmann, L. (2004). Clearance of Citrobacter rodentium requires B cells but not secretory immunoglobulin A (IgA) or IgM antibodies. *Infect Immun,* 72**,** 3315-24.

Mabbott, N. A., Donaldson, D. S., Ohno, H., Williams, I. R. & Mahajan, A. (2013). Microfold (M) cells: important immunosurveillance posts in the intestinal epithelium. *Mucosal Immunol,* 6**,** 666-77.

Macdonald, T. T., Monteleone, I., Fantini, M. C. & Monteleone, G. (2011). Regulation of homeostasis and inflammation in the intestine. *Gastroenterology,* 140**,** 1768-75.

Macnab, R. M. (2004). Type III flagellar protein export and flagellar assembly. *Biochim Biophys Acta,* 1694**,** 207-17.

Maddocks, O. D., Scanlon, K. M. & Donnenberg, M. S. (2013). An Escherichia coli effector protein promotes host mutation via depletion of DNA mismatch repair proteins. *MBio,* 4**,** e00152-13.

Madyagol, M., Al-Alami, H., Levarski, Z., Drahovska, H., Turna, J. & Stuchlik, S. (2011). Gene replacement techniques for Escherichia coli genome modification. *Folia Microbiol (Praha),* 56**,** 253-63.

Maeda, S., Hsu, L. C., Liu, H., Bankston, L. A., Iimura, M., Kagnoff, M. F., Eckmann, L. & Karin, M. (2005). Nod2 mutation in Crohn's disease potentiates NF-kappaB activity and IL-1beta processing. *Science,* 307**,** 734-8.

Mangan, P. R., Harrington, L. E., O'quinn, D. B., Helms, W. S., Bullard, D. C., Elson, C. O., Hatton, R. D., Wahl, S. M., Schoeb, T. R. & Weaver, C. T. (2006). Transforming growth factor-beta induces development of the T(H)17 lineage. *Nature,* 441**,** 231-4.

Manta, C., Heupel, E., Radulovic, K., Rossini, V., Garbi, N., Riedel, C. U. & Niess, J. H. (2013). CX(3)CR1(+) macrophages support IL-22 production by innate lymphoid cells during infection with Citrobacter rodentium. *Mucosal Immunol,* 6**,** 177-88.

Marches, O., Covarelli, V., Dahan, S., Cougoule, C., Bhatta, P., Frankel, G. & Caron, E. (2008). EspJ of enteropathogenic and enterohaemorrhagic Escherichia coli inhibits opsono-phagocytosis. *Cell Microbiol,* 10**,** 1104-15.

Marches, O., Ledger, T. N., Boury, M., Ohara, M., Tu, X., Goffaux, F., Mainil, J., Rosenshine, I., Sugai, M., De Rycke, J. & Oswald, E. (2003). Enteropathogenic and enterohaemorrhagic Escherichia coli deliver a novel effector called Cif, which blocks cell cycle G2/M transition. *Mol Microbiol,* 50**,** 1553-67.

Marches, O., Nougayrede, J. P., Boullier, S., Mainil, J., Charlier, G., Raymond, I., Pohl, P., Boury, M., De Rycke, J., Milon, A. & Oswald, E. (2000). Role of tir and intimin in the virulence of rabbit enteropathogenic Escherichia coli serotype O103:H2. *Infect Immun,* 68**,** 2171-82.

Marches, O., Wiles, S., Dziva, F., La Ragione, R. M., Schuller, S., Best, A., Phillips, A. D., Hartland, E. L., Woodward, M. J., Stevens, M. P. & Frankel, G. (2005). Characterization of two non-locus of enterocyte effacement-encoded type III-translocated effectors, NleC and NleD, in attaching and effacing pathogens. *Infect Immun,* 73**,** 8411-7.

Marketon, M. M., Depaolo, R. W., Debord, K. L., Jabri, B. & Schneewind, O. (2005). Plague bacteria target immune cells during infection. *Science,* 309**,** 1739-41.

Martinez, E., Schroeder, G. N., Berger, C. N., Lee, S. F., Robinson, K. S., Badea, L., Simpson, N., Hall, R. A., Hartland, E. L., Crepin, V. F. & Frankel, G. (2010). Binding to Na(+) /H(+) exchanger regulatory factor 2 (NHERF2) affects trafficking and function of the enteropathogenic Escherichia coli type III secretion system effectors Map, EspI and NleH. *Cell Microbiol,* 12**,** 1718-31.

Martinez-Argudo, I., Sands, C. & Jepson, M. A. (2007). Translocation of enteropathogenic Escherichia coli across an in vitro M cell model is regulated by its type III secretion system. *Cell Microbiol,* 9**,** 1538-46.

Masahata, K., Umemoto, E., Kayama, H., Kotani, M., Nakamura, S., Kurakawa, T., Kikuta, J., Gotoh, K., Motooka, D., Sato, S., Higuchi, T., Baba, Y., Kurosaki, T., Kinoshita, M., Shimada, Y., Kimura, T., Okumura, R., Takeda, A., Tajima, M., Yoshie, O., Fukuzawa, M., Kiyono, H., Fagarasan, S., Iida, T., Ishii, M. & Takeda, K. (2014). Generation of colonic IgA-secreting cells in the caecal patch. *Nat Commun,* 5**,** 3704.

Mashimo, H., Wu, D. C., Podolsky, D. K. & Fishman, M. C. (1996). Impaired defense of intestinal mucosa in mice lacking intestinal trefoil factor. *Science,* 274**,** 262-5.

Mazzini, E., Massimiliano, L., Penna, G. & Rescigno, M. (2014). Oral tolerance can be established via gap junction transfer of fed antigens from CX3CR1(+) macrophages to CD103(+) dendritic cells. *Immunity,* 40**,** 248-61.

Mcauley, J. L., Linden, S. K., Png, C. W., King, R. M., Pennington, H. L., Gendler, S. J., Florin, T. H., Hill, G. R., Korolik, V. & Mcguckin, M. A. (2007). MUC1 cell surface mucin is a critical element of the mucosal barrier to infection. *J Clin Invest,* 117**,** 2313-24.

Mccormick, B. A., Parkos, C. A., Colgan, S. P., Carnes, D. K. & Madara, J. L. (1998). Apical secretion of a pathogen-elicited epithelial chemoattractant activity in response to surface colonization of intestinal epithelia by Salmonella typhimurium. *J Immunol,* 160**,** 455-66.

Mcdaniel, T. K., Jarvis, K. G., Donnenberg, M. S. & Kaper, J. B. (1995). A genetic locus of enterocyte effacement conserved among diverse enterobacterial pathogens. *Proc Natl Acad Sci U S A,* 92**,** 1664-8.

Mcdaniel, T. K. & Kaper, J. B. (1997). A cloned pathogenicity island from

enteropathogenic Escherichia coli confers the attaching and effacing phenotype on E. coli K-12. *Mol Microbiol,* 23**,** 399-407.

Mcdole, J. R., Wheeler, L. W., Mcdonald, K. G., Wang, B., Konjufca, V., Knoop, K. A., Newberry, R. D. & Miller, M. J. (2012). Goblet cells deliver luminal antigen to CD103+ dendritic cells in the small intestine. *Nature,* 483**,** 345-9.

Mcghee, J. R. & Fujihashi, K. (2012). Inside the mucosal immune system. *PLoS Biol,* 10**,** e1001397.

Mcgourty, K., Thurston, T. L., Matthews, S. A., Pinaud, L., Mota, L. J. & Holden, D. W. (2012). Salmonella inhibits retrograde trafficking of mannose-6-phosphate receptors and lysosome function. *Science,* 338**,** 963-7.

Mcguckin, M. A., Every, A. L., Skene, C. D., Linden, S. K., Chionh, Y. T., Swierczak, A., Mcauley, J., Harbour, S., Kaparakis, M., Ferrero, R. & Sutton, P. (2007). Muc1 mucin limits both Helicobacter pylori colonization of the murine gastric mucosa and associated gastritis. *Gastroenterology,* 133**,** 1210-8.

Mcguckin, M. A., Linden, S. K., Sutton, P. & Florin, T. H. (2011). Mucin dynamics and enteric pathogens. *Nat Rev Microbiol,* 9**,** 265-78.

Mcnamara, B. P. & Donnenberg, M. S. (1998). A novel proline-rich protein, EspF, is secreted from enteropathogenic Escherichia coli via the type III export pathway. *FEMS Microbiol Lett,* 166**,** 71-8.

Mebius, R. E., Miyamoto, T., Christensen, J., Domen, J., Cupedo, T., Weissman, I. L. & Akashi, K. (2001). The fetal liver counterpart of adult common lymphoid progenitors gives rise to all lymphoid lineages, CD45+CD4+CD3- cells, as well as macrophages. *J Immunol,* 166**,** 6593-601.

Mejia, E., Bliska, J. B. & Viboud, G. I. (2008). Yersinia controls type III effector delivery into host cells by modulating Rho activity. *PLoS Pathog,* 4**,** e3.

Melgar, S., Karlsson, A. & Michaelsson, E. (2005). Acute colitis induced by dextran sulfate sodium progresses to chronicity in C57BL/6 but not in BALB/c mice: correlation between symptoms and inflammation. *Am J Physiol Gastrointest Liver Physiol,* 288**,** G1328-38.

Metcalf, W. W., Jiang, W., Daniels, L. L., Kim, S. K., Haldimann, A. & Wanner, B. L. (1996). Conditionally replicative and conjugative plasmids carrying lacZ alpha for cloning, mutagenesis, and allele replacement in bacteria. *Plasmid,* 35**,** 1-13.

Michetti, P., Porta, N., Mahan, M. J., Slauch, J. M., Mekalanos, J. J., Blum, A. L., Kraehenbuhl, J. P. & Neutra, M. R. (1994). Monoclonal immunoglobulin A prevents adherence and invasion of polarized epithelial cell monolayers by Salmonella typhimurium. *Gastroenterology,* 107**,** 915-23.

Miki, H. & Takenawa, T. (2003). Regulation of actin dynamics by WASP family proteins. *J Biochem,* 134**,** 309-13.

Mills, E., Baruch, K., Charpentier, X., Kobi, S. & Rosenshine, I. (2008).

Real-time analysis of effector translocation by the type III secretion system of enteropathogenic Escherichia coli. *Cell Host Microbe,* 3**,** 104-13.

Minamino, T. & Pugsley, A. P. (2005). Measure for measure in the control of type III secretion hook and needle length. *Mol Microbiol,* 56**,** 303-8.

Miron, S., Hershkoviz, R., Tirosh, I., Schechter, Y., Yayun, A. & Lider, O. (1992). Involvement of a protein kinase C and protein phosphatases in adhesion of CD4+ T cells to and detachment from extracellular matrix proteins. *Cell Immunol,* 144**,** 182-9.

Molloy, S. (2012). Cellular microbiology: EPEC puts actin on the Map. *Nat Rev Microbiol,* 10**,** 236.

Monjaras Feria, J., Garcia-Gomez, E., Espinosa, N., Minamino, T., Namba, K. & Gonzalez-Pedrajo, B. (2012). Role of EscP (Orf16) in injectisome biogenesis and regulation of type III protein secretion in enteropathogenic Escherichia coli. *J Bacteriol,* 194**,** 6029-45.

Mora, J. R. (2008). Homing imprinting and immunomodulation in the gut: role of dendritic cells and retinoids. *Inflamm Bowel Dis,* 14**,** 275-89.

Mora, J. R., Iwata, M., Eksteen, B., Song, S. Y., Junt, T., Senman, B., Otipoby, K. L., Yokota, A., Takeuchi, H., Ricciardi-Castagnoli, P., Rajewsky, K., Adams, D. H. & Von Andrian, U. H. (2006). Generation of gut-homing IgA-secreting B cells by intestinal dendritic cells. *Science,* 314**,** 1157-60.

Moraes, T. F., Spreter, T. & Strynadka, N. C. (2008). Piecing together the type III injectisome of bacterial pathogens. *Curr Opin Struct Biol,* 18**,** 258-66.

Mowat, A. M. & Agace, W. W. (2014). Regional specialization within the intestinal immune system. *Nat Rev Immunol,* 14**,** 667-85.

Mueller, T., Terada, T., Rosenberg, I. M., Shibolet, O. & Podolsky, D. K. (2006). Th2 cytokines down-regulate TLR expression and function in human intestinal epithelial cells. *J Immunol,* 176**,** 5805-14.

Mukherjee, S., Zheng, H., Derebe, M. G., Callenberg, K. M., Partch, C. L., Rollins, D., Propheter, D. C., Rizo, J., Grabe, M., Jiang, Q. X. & Hooper, L. V. (2014). Antibacterial membrane attack by a pore-forming intestinal C-type lectin. *Nature,* 505**,** 103-7.

Muller, D., Benz, I., Liebchen, A., Gallitz, I., Karch, H. & Schmidt, M. A. (2009). Comparative analysis of the locus of enterocyte effacement and its flanking regions. *Infect Immun,* 77**,** 3501-13.

Mundy, R., Jenkins, C., Yu, J., Smith, H. & Frankel, G. (2004). Distribution of espI among clinical enterohaemorrhagic and enteropathogenic Escherichia coli isolates. *J Med Microbiol,* 53**,** 1145-9.

Mundy, R., Macdonald, T. T., Dougan, G., Frankel, G. & Wiles, S. (2005). Citrobacter rodentium of mice and man. *Cell Microbiol,* 7**,** 1697-706.

Mundy, R., Pickard, D., Wilson, R. K., Simmons, C. P., Dougan, G. & Frankel, G. (2003). Identification of a novel type IV pilus gene cluster required for gastrointestinal colonization of Citrobacter rodentium. *Mol Microbiol,* 48**,** 795-809.

Munera, D., Crepin, V. F., Marches, O. & Frankel, G. (2010). N-terminal type III secretion signal of enteropathogenic Escherichia coli translocator proteins. *J Bacteriol,* 192**,** 3534-9.

Murai, M., Turovskaya, O., Kim, G., Madan, R., Karp, C. L., Cheroutre, H. & Kronenberg, M. (2009). Interleukin 10 acts on regulatory T cells to maintain expression of the transcription factor Foxp3 and suppressive function in mice with colitis. *Nat Immunol,* 10**,** 1178-84.

Muramatsu, M., Kinoshita, K., Fagarasan, S., Yamada, S., Shinkai, Y. & Honjo, T. (2000). Class switch recombination and hypermutation require activation-induced cytidine deaminase (AID), a potential RNA editing enzyme. *Cell,* 102**,** 553-63.

Murphy, K. C. (1998). Use of bacteriophage lambda recombination functions to promote gene replacement in Escherichia coli. *J Bacteriol,* 180**,** 2063-71.

Murphy, K. C. (2000). Bacteriophage P22 Abc2 protein binds to RecC increases the 5' strand nicking activity of RecBCD and together with lambda bet, promotes Chi-independent recombination. *J Mol Biol,* 296**,** 385-401.

Murphy, K. C. & Campellone, K. G. (2003). Lambda Red-mediated recombinogenic engineering of enterohemorrhagic and enteropathogenic E. coli. *BMC Mol Biol,* 4**,** 11.

Murthy, A. K., Dubose, C. N., Banas, J. A., Coalson, J. J. & Arulanandam, B. P. (2006). Contribution of polymeric immunoglobulin receptor to regulation of intestinal inflammation in dextran sulfate sodium-induced colitis. *J Gastroenterol Hepatol,* 21**,** 1372-80.

Nadler, C., Baruch, K., Kobi, S., Mills, E., Haviv, G., Farago, M., Alkalay, I., Bartfeld, S., Meyer, T. F., Ben-Neriah, Y. & Rosenshine, I. (2010). The type III secretion effector NleE inhibits NF-kappaB activation. *PLoS Pathog,* 6**,** e1000743.

Nadler, C., Shifrin, Y., Nov, S., Kobi, S. & Rosenshine, I. (2006). Characterization of enteropathogenic Escherichia coli mutants that fail to disrupt host cell spreading and attachment to substratum. *Infect Immun,* 74**,** 839-49.

Nataro, J. P. & Kaper, J. B. (1998). Diarrheagenic Escherichia coli. *Clin Microbiol Rev,* 11**,** 142-201.

Nenci, A., Becker, C., Wullaert, A., Gareus, R., Van Loo, G., Danese, S., Huth, M., Nikolaev, A., Neufert, C., Madison, B., Gumucio, D., Neurath, M. F. & Pasparakis, M. (2007). Epithelial NEMO links innate immunity to chronic intestinal inflammation. *Nature,* 446**,** 557-61.

Netea, M. G., Azam, T., Ferwerda, G., Girardin, S. E., Walsh, M., Park, J. S.,

Abraham, E., Kim, J. M., Yoon, D. Y., Dinarello, C. A. & Kim, S. H. (2005). IL-32 synergizes with nucleotide oligomerization domain (NOD) 1 and NOD2 ligands for IL-1beta and IL-6 production through a caspase 1-dependent mechanism. *Proc Natl Acad Sci U S A,* 102**,** 16309-14.

Neutra, M. R., Frey, A. & Kraehenbuhl, J. P. (1996). Epithelial M cells: gateways for mucosal infection and immunization. *Cell,* 86**,** 345-8.

Neutra, M. R., Mantis, N. J. & Kraehenbuhl, J. P. (2001). Collaboration of epithelial cells with organized mucosal lymphoid tissues. *Nat Immunol,* 2**,** 1004-9.

Newton, H. J., Pearson, J. S., Badea, L., Kelly, M., Lucas, M., Holloway, G., Wagstaff, K. M., Dunstone, M. A., Sloan, J., Whisstock, J. C., Kaper, J. B., Robins-Browne, R. M., Jans, D. A., Frankel, G., Phillips, A. D., Coulson, B. S. & Hartland, E. L. (2010). The type III effectors NleE and NleB from enteropathogenic E. coli and OspZ from Shigella block nuclear translocation of NF-kappaB p65. *PLoS Pathog,* 6**,** e1000898.

Newton, K. & Dixit, V. M. (2012). Signaling in innate immunity and inflammation. *Cold Spring Harb Perspect Biol,* 4.

Ng, S. C., Kamm, M. A., Stagg, A. J. & Knight, S. C. (2010). Intestinal dendritic cells: their role in bacterial recognition, lymphocyte homing, and intestinal inflammation. *Inflamm Bowel Dis,* 16**,** 1787-807.

Nguyen, M., Rizvi, J. & Hecht, G. (2015). Expression of enteropathogenic Escherichia coli map is significantly different than that of other type III secreted effectors in vivo. *Infect Immun,* 83**,** 130-7.

Niess, J. H. & Adler, G. (2010). Enteric flora expands gut lamina propria CX3CR1+ dendritic cells supporting inflammatory immune responses under normal and inflammatory conditions. *J Immunol,* 184**,** 2026-37.

Niess, J. H., Brand, S., Gu, X., Landsman, L., Jung, S., Mccormick, B. A., Vyas, J. M., Boes, M., Ploegh, H. L., Fox, J. G., Littman, D. R. & Reinecker, H. C. (2005). CX3CR1-mediated dendritic cell access to the intestinal lumen and bacterial clearance. *Science,* 307**,** 254-8.

Niess, J. H. & Reinecker, H. C. (2006). Dendritic cells in the recognition of intestinal microbiota. *Cell Microbiol,* 8**,** 558-64.

Nieto-Pelegrin, E., Kenny, B. & Martinez-Quiles, N. (2014). Nck adaptors, besides promoting N-WASP mediated actin-nucleation activity at pedestals, influence the cellular levels of enteropathogenic Escherichia coli Tir effector. *Cell Adh Migr,* 8**,** 404-17.

Nochi, T., Denton, P. W., Wahl, A. & Garcia, J. V. (2013). Cryptopatches are essential for the development of human GALT. *Cell Rep,* 3**,** 1874-84.

Nothelfer, K., Arena, E. T., Pinaud, L., Neunlist, M., Mozeleski, B., Belotserkovsky, I., Parsot, C., Dinadayala, P., Burger-Kentischer, A., Raqib,

R., Sansonetti, P. J. & Phalipon, A. (2014). B lymphocytes undergo TLR2-dependent apoptosis upon Shigella infection. *J Exp Med,* 211**,** 1215-29.

Nougayrede, J. P. & Donnenberg, M. S. (2004). Enteropathogenic Escherichia coli EspF is targeted to mitochondria and is required to initiate the mitochondrial death pathway. *Cell Microbiol,* 6**,** 1097-111.

O'byrne, S. M., Wongsiriroj, N., Libien, J., Vogel, S., Goldberg, I. J., Baehr, W., Palczewski, K. & Blaner, W. S. (2005). Retinoid absorption and storage is impaired in mice lacking lecithin:retinol acyltransferase (LRAT). *J Biol Chem,* 280**,** 35647-57.

Oft, M. (2014). IL-10: master switch from tumor-promoting inflammation to antitumor immunity. *Cancer Immunol Res,* 2**,** 194-9.

Ogura, Y., Bonen, D. K., Inohara, N., Nicolae, D. L., Chen, F. F., Ramos, R., Britton, H., Moran, T., Karaliuskas, R., Duerr, R. H., Achkar, J. P., Brant, S. R., Bayless, T. M., Kirschner, B. S., Hanauer, S. B., Nunez, G. & Cho, J. H. (2001). A frameshift mutation in NOD2 associated with susceptibility to Crohn's disease. *Nature,* 411**,** 603-6.

Olsen, R. L., Echtenkamp, F., Cheranova, D., Deng, W., Finlay, B. B. & Hardwidge, P. R. (2013). The enterohemorrhagic Escherichia coli effector protein NleF binds mammalian Tmp21. *Vet Microbiol,* 164**,** 164-70.

Owen, R. L., Piazza, A. J. & Ermak, T. H. (1991). Ultrastructural and cytoarchitectural features of lymphoreticular organs in the colon and rectum of adult BALB/c mice. *Am J Anat,* 190**,** 10-8.

Pabst, O. (2012). New concepts in the generation and functions of IgA. *Nat Rev Immunol,* 12**,** 821-32.

Pabst, O. (2013). Trafficking of regulatory T cells in the intestinal immune system. *Int Immunol,* 25**,** 139-43.

Pabst, O. & Bernhardt, G. (2010). The puzzle of intestinal lamina propria dendritic cells and macrophages. *Eur J Immunol,* 40**,** 2107-11.

Pabst, O., Herbrand, H., Friedrichsen, M., Velaga, S., Dorsch, M., Berhardt, G., Worbs, T., Macpherson, A. J. & Forster, R. (2006). Adaptation of solitary intestinal lymphoid tissue in response to microbiota and chemokine receptor CCR7 signaling. *J Immunol,* 177**,** 6824-32.

Pallen, M. J., Beatson, S. A. & Bailey, C. M. (2005). Bioinformatics, genomics and evolution of non-flagellar type-III secretion systems: a Darwinian perspective. *FEMS Microbiol Rev,* 29**,** 201-29.

Pallett, M. A., Berger, C. N., Pearson, J. S., Hartland, E. L. & Frankel, G. (2014). The type III secretion effector NleF of enteropathogenic Escherichia coli activates NF-kappaB early during infection. *Infect Immun,* 82**,** 4878-88.

Pan, C., Kumar, C., Bohl, S., Klingmueller, U. & Mann, M. (2009). Comparative

proteomic phenotyping of cell lines and primary cells to assess preservation of cell type-specific functions. *Mol Cell Proteomics,* 8**,** 443-50.

Papatheodorou, P., Domanska, G., Oxle, M., Mathieu, J., Selchow, O., Kenny, B. & Rassow, J. (2006). The enteropathogenic Escherichia coli (EPEC) Map effector is imported into the mitochondrial matrix by the TOM/Hsp70 system and alters organelle morphology. *Cell Microbiol,* 8**,** 677-89.

Papayannopoulos, V. & Zychlinsky, A. (2009). NETs: a new strategy for using old weapons. *Trends Immunol,* 30**,** 513-21.

Pearson, C., Uhlig, H. H. & Powrie, F. (2012). Lymphoid microenvironments and innate lymphoid cells in the gut. *Trends Immunol,* 33**,** 289-96.

Pearson, J. S., Giogha, C., Ong, S. Y., Kennedy, C. L., Kelly, M., Robinson, K. S., Lung, T. W., Mansell, A., Riedmaier, P., Oates, C. V., Zaid, A., Muhlen, S., Crepin, V. F., Marches, O., Ang, C. S., Williamson, N. A., O'reilly, L. A., Bankovacki, A., Nachbur, U., Infusini, G., Webb, A. I., Silke, J., Strasser, A., Frankel, G. & Hartland, E. L. (2013). A type III effector antagonizes death receptor signalling during bacterial gut infection. *Nature,* 501**,** 247-51.

Pearson, J. S., Riedmaier, P., Marches, O., Frankel, G. & Hartland, E. L. (2011). A type III effector protease NleC from enteropathogenic Escherichia coli targets NF-kappaB for degradation. *Mol Microbiol,* 80**,** 219-30.

Peterson, L. W. & Artis, D. (2014). Intestinal epithelial cells: regulators of barrier function and immune homeostasis. *Nat Rev Immunol,* 14**,** 141-53.

Petrilli, V., Dostert, C., Muruve, D. A. & Tschopp, J. (2007). The inflammasome: a danger sensing complex triggering innate immunity. *Curr Opin Immunol,* 19**,** 615-22.

Phalipon, A., Michetti, P., Kaufmann, M., Cavaillon, J. M., Huerre, M., Kraehenbuhl, J. P. & Sansonetti, P. J. (1994). Protection against invasion of the mouse pulmonary epithelium by a monoclonal IgA directed against Shigella flexneri lipopolysaccharide. *Ann N Y Acad Sci,* 730**,** 356-8.

Phalipon, A. & Sansonetti, P. J. (2007). Shigella's ways of manipulating the host intestinal innate and adaptive immune system: a tool box for survival? *Immunol Cell Biol,* 85**,** 119-29.

Pham, T. H., Gao, X., Tsai, K., Olsen, R., Wan, F. & Hardwidge, P. R. (2012). Functional differences and interactions between the Escherichia coli type III secretion system effectors NleH1 and NleH2. *Infect Immun,* 80**,** 2133-40.

Pickert, G., Neufert, C., Leppkes, M., Zheng, Y., Wittkopf, N., Warntjen, M., Lehr, H. A., Hirth, S., Weigmann, B., Wirtz, S., Ouyang, W., Neurath, M. F. & Becker, C. (2009). STAT3 links IL-22 signaling in intestinal epithelial cells to mucosal wound healing. *J Exp Med,* 206**,** 1465-72.

Podolsky, D. K., Gerken, G., Eyking, A. & Cario, E. (2009). Colitis-associated

variant of TLR2 causes impaired mucosal repair because of TFF3 deficiency. *Gastroenterology,* 137**,** 209-20.

Poteete, A. R. (2001). What makes the bacteriophage lambda Red system useful for genetic engineering: molecular mechanism and biological function. *FEMS Microbiol Lett,* 201**,** 9-14.

Poteete, A. R. (2013). Involvement of DNA Replication Proteins in Phage Lambda Red-Mediated Homologous Recombination. *PLoS One,* 8**,** e67440.

Poteete, A. R., Rosadini, C. & St Pierre, C. (2006). Gentamicin and other cassettes for chromosomal gene replacement in Escherichia coli. *Biotechniques,* 41**,** 261-2, 264.

Potten, C. S., Booth, C. & Pritchard, D. M. (1997). The intestinal epithelial stem cell: the mucosal governor. *Int J Exp Pathol,* 78**,** 219-43.

Pugsley, A. P. (1993). The complete general secretory pathway in gram-negative bacteria. *Microbiol Rev,* 57**,** 50-108.

Quitard, S., Dean, P., Maresca, M. & Kenny, B. (2006). The enteropathogenic Escherichia coli EspF effector molecule inhibits PI-3 kinase-mediated uptake independently of mitochondrial targeting. *Cell Microbiol,* 8**,** 972-81.

Rachmilewitz, D., Katakura, K., Karmeli, F., Hayashi, T., Reinus, C., Rudensky, B., Akira, S., Takeda, K., Lee, J., Takabayashi, K. & Raz, E. (2004). Toll-like receptor 9 signaling mediates the anti-inflammatory effects of probiotics in murine experimental colitis. *Gastroenterology,* 126**,** 520-8.

Rakoff-Nahoum, S., Paglino, J., Eslami-Varzaneh, F., Edberg, S. & Medzhitov, R. (2004). Recognition of commensal microflora by toll-like receptors is required for intestinal homeostasis. *Cell,* 118**,** 229-41.

Ramalingam, R., Larmonier, C. B., Thurston, R. D., Midura-Kiela, M. T., Zheng, S. G., Ghishan, F. K. & Kiela, P. R. (2012). Dendritic cell-specific disruption of TGF-beta receptor II leads to altered regulatory T cell phenotype and spontaneous multiorgan autoimmunity. *J Immunol,* 189**,** 3878-93.

Ranallo, R. T., Barnoy, S., Thakkar, S., Urick, T. & Venkatesan, M. M. (2006). Developing live Shigella vaccines using lambda Red recombineering. *FEMS Immunol Med Microbiol,* 47**,** 462-9.

Ray, K., Bobard, A., Danckaert, A., Paz-Haftel, I., Clair, C., Ehsani, S., Tang, C., Sansonetti, P., Tran, G. V. & Enninga, J. (2010). Tracking the dynamic interplay between bacterial and host factors during pathogen-induced vacuole rupture in real time. *Cell Microbiol,* 12**,** 545-56.

Raymond, B., Crepin, V. F., Collins, J. W. & Frankel, G. (2011). The WxxxE effector EspT triggers expression of immune mediators in an Erk/JNK and NF-kappaB-dependent manner. *Cell Microbiol,* 13**,** 1881-93.

Raymond, B., Young, J. C., Pallett, M., Endres, R. G., Clements, A. & Frankel,

G. (2013). Subversion of trafficking, apoptosis, and innate immunity by type III secretion system effectors. *Trends Microbiol,* 21**,** 430-41.

Reis, R. S. & Horn, F. (2010). Enteropathogenic Escherichia coli, Samonella, Shigella and Yersinia: cellular aspects of host-bacteria interactions in enteric diseases. *Gut Pathog,* 2**,** 8.

Rendon, M. A., Saldana, Z., Erdem, A. L., Monteiro-Neto, V., Vazquez, A., Kaper, J. B., Puente, J. L. & Giron, J. A. (2007). Commensal and pathogenic Escherichia coli use a common pilus adherence factor for epithelial cell colonization. *Proc Natl Acad Sci U S A,* 104**,** 10637-42.

Rescigno, M. (2010). Intestinal dendritic cells. *Adv Immunol,* 107**,** 109-38.

Rescigno, M. (2011). Dendritic cells in bacteria handling in the gut. *J Leukoc Biol,* 90**,** 669-72.

Rescigno, M. (2011). The intestinal epithelial barrier in the control of homeostasis and immunity. *Trends Immunol,* 32**,** 256-64.

Rescigno, M. (2013). Mucosal immunology and bacterial handling in the intestine. *Best Pract Res Clin Gastroenterol,* 27**,** 17-24.

Rescigno, M., Urbano, M., Valzasina, B., Francolini, M., Rotta, G., Bonasio, R., Granucci, F., Kraehenbuhl, J. P. & Ricciardi-Castagnoli, P. (2001). Dendritic cells express tight junction proteins and penetrate gut epithelial monolayers to sample bacteria. *Nat Immunol,* 2**,** 361-7.

Rhee, K. J., Cheng, H., Harris, A., Morin, C., Kaper, J. B. & Hecht, G. (2011). Determination of spatial and temporal colonization of enteropathogenic E. coli and enterohemorrhagic E. coli in mice using bioluminescent in vivo imaging. *Gut Microbes,* 2**,** 34-41.

Ritchie, J. M. & Waldor, M. K. (2005). The locus of enterocyte effacement-encoded effector proteins all promote enterohemorrhagic Escherichia coli pathogenicity in infant rabbits. *Infect Immun,* 73**,** 1466-74.

Rosenshine, I., Ruschkowski, S., Stein, M., Reinscheid, D. J., Mills, S. D. & Finlay, B. B. (1996). A pathogenic bacterium triggers epithelial signals to form a functional bacterial receptor that mediates actin pseudopod formation. *EMBO J,* 15**,** 2613-24.

Rosenstiel, P., Fantini, M., Brautigam, K., Kuhbacher, T., Waetzig, G. H., Seegert, D. & Schreiber, S. (2003). TNF-alpha and IFN-gamma regulate the expression of the NOD2 (CARD15) gene in human intestinal epithelial cells. *Gastroenterology,* 124**,** 1001-9.

Rosenzweig, J. A., Weltman, G., Plano, G. V. & Schesser, K. (2005). Modulation of yersinia type three secretion system by the S1 domain of polynucleotide phosphorylase. *J Biol Chem,* 280**,** 156-63.

Ross, N. T. & Miller, B. L. (2007). Characterization of the binding surface of the

translocated intimin receptor, an essential protein for EPEC and EHEC cell adhesion. *Protein Sci,* 16**,** 2677-83.

Rothstein, R. (1991). Targeting, disruption, replacement, and allele rescue: integrative DNA transformation in yeast. *Methods Enzymol,* 194**,** 281-301.

Round, J. L., Lee, S. M., Li, J., Tran, G., Jabri, B., Chatila, T. A. & Mazmanian, S. K. (2011). The Toll-like receptor 2 pathway establishes colonization by a commensal of the human microbiota. *Science,* 332**,** 974-7.

Roxas, J. L., Ryan, K., Vedantam, G. & Viswanathan, V. K. (2014). Enteropathogenic Escherichia coli dynamically regulates EGFR signaling in intestinal epithelial cells. *Am J Physiol Gastrointest Liver Physiol,* 307**,** G374-80.

Roxas, J. L., Wilbur, J. S., Zhang, X., Martinez, G., Vedantam, G. & Viswanathan, V. K. (2012). The enteropathogenic Escherichia coli-secreted protein EspZ inhibits host cell apoptosis. *Infect Immun,* 80**,** 3850-7.

Royan, S. V., Jones, R. M., Koutsouris, A., Roxas, J. L., Falzari, K., Weflen, A. W., Kim, A., Bellmeyer, A., Turner, J. R., Neish, A. S., Rhee, K. J., Viswanathan, V. K. & Hecht, G. A. (2010). Enteropathogenic E. coli non-LEE encoded effectors NleH1 and NleH2 attenuate NF-kappaB activation. *Mol Microbiol,* 78**,** 1232-45.

Ruchaud-Sparagano, M. H., Muhlen, S., Dean, P. & Kenny, B. (2011). The enteropathogenic E. coli (EPEC) Tir effector inhibits NF-kappaB activity by targeting TNFalpha receptor-associated factors. *PLoS Pathog,* 7**,** e1002414.

Rydstrom, A. & Wick, M. J. (2007). Monocyte recruitment, activation, and function in the gut-associated lymphoid tissue during oral Salmonella infection. *J Immunol,* 178**,** 5789-801.

Sal-Man, N., Biemans-Oldehinkel, E., Sharon, D., Croxen, M. A., Scholz, R., Foster, L. J. & Finlay, B. B. (2012). EscA is a crucial component of the type III secretion system of enteropathogenic Escherichia coli. *J Bacteriol,* 194**,** 2819-28.

Sal-Man, N., Deng, W. & Finlay, B. B. (2012). EscI: a crucial component of the type III secretion system forms the inner rod structure in enteropathogenic Escherichia coli. *Biochem J,* 442**,** 119-25.

Saldana, Z., Erdem, A. L., Schuller, S., Okeke, I. N., Lucas, M., Sivananthan, A., Phillips, A. D., Kaper, J. B., Puente, J. L. & Giron, J. A. (2009). The Escherichia coli common pilus and the bundle-forming pilus act in concert during the formation of localized adherence by enteropathogenic E. coli. *J Bacteriol,* 191**,** 3451-61.

Salgado-Pabon, W., Konradt, C., Sansonetti, P. J. & Phalipon, A. (2014). New insights into the crosstalk between Shigella and T lymphocytes. *Trends Microbiol,* 22**,** 192-8.

Salzman, N. H. (2010). Paneth cell defensins and the regulation of the

microbiome: detente at mucosal surfaces. *Gut Microbes,* 1**,** 401-6.

Salzman, N. H., Ghosh, D., Huttner, K. M., Paterson, Y. & Bevins, C. L. (2003). Protection against enteric salmonellosis in transgenic mice expressing a human intestinal defensin. *Nature,* 422**,** 522-6.

Samba-Louaka, A., Taieb, F., Nougayrede, J. P. & Oswald, E. (2009). Cif type III effector protein: a smart hijacker of the host cell cycle. *Future Microbiol,* 4**,** 867-77.

Sansonetti, P. J. (2004). War and peace at mucosal surfaces. *Nat Rev Immunol,* 4**,** 953-64.

Sansonetti, P. J. & Di Santo, J. P. (2007). Debugging how bacteria manipulate the immune response. *Immunity,* 26**,** 149-61.

Santos, R. L., Tsolis, R. M., Baumler, A. J., Smith, R., 3rd & Adams, L. G. (2001). Salmonella enterica serovar typhimurium induces cell death in bovine monocyte-derived macrophages by early sipB-dependent and delayed sipB-independent mechanisms. *Infect Immun,* 69**,** 2293-301.

Saraiva, M. & O'garra, A. (2010). The regulation of IL-10 production by immune cells. *Nat Rev Immunol,* 10**,** 170-81.

Savage, P. J., Leong, J. M. & Murphy, K. C. (2006). Rapid allelic exchange in enterohemorrhagic Escherichia coli (EHEC) and other E. coli using lambda red recombination. *Curr Protoc Microbiol,* Chapter 5**,** Unit5A 2.

Schauer, D. B. & Falkow, S. (1993). Attaching and effacing locus of a Citrobacter freundii biotype that causes transmissible murine colonic hyperplasia. *Infect Immun,* 61**,** 2486-92.

Schmidt, M. A. (2010). LEEways: tales of EPEC, ATEC and EHEC. *Cell Microbiol,* 12**,** 1544-52.

Schuller, S., Chong, Y., Lewin, J., Kenny, B., Frankel, G. & Phillips, A. D. (2007). Tir phosphorylation and Nck/N-WASP recruitment by enteropathogenic and enterohaemorrhagic Escherichia coli during ex vivo colonization of human intestinal mucosa is different to cell culture models. *Cell Microbiol,* 9**,** 1352-64.

Schuller, S., Lucas, M., Kaper, J. B., Giron, J. A. & Phillips, A. D. (2009). The ex vivo response of human intestinal mucosa to enteropathogenic Escherichia coli infection. *Cell Microbiol,* 11**,** 521-30.

Schulte, R., Kerneis, S., Klinke, S., Bartels, H., Preger, S., Kraehenbuhl, J. P., Pringault, E. & Autenrieth, I. B. (2000). Translocation of Yersinia entrocolitica across reconstituted intestinal epithelial monolayers is triggered by Yersinia invasin binding to beta1 integrins apically expressed on M-like cells. *Cell Microbiol,* 2**,** 173-85.

Schulz, O., Jaensson, E., Persson, E. K., Liu, X., Worbs, T., Agace, W. W. & Pabst, O. (2009). Intestinal CD103+, but not CX3CR1+, antigen sampling cells

migrate in lymph and serve classical dendritic cell functions. *J Exp Med,* 206**,** 3101-14.

Schulz, O. & Pabst, O. (2013). Antigen sampling in the small intestine. *Trends Immunol,* 34**,** 155-61.

Sekiya, K., Ohishi, M., Ogino, T., Tamano, K., Sasakawa, C. & Abe, A. (2001). Supermolecular structure of the enteropathogenic Escherichia coli type III secretion system and its direct interaction with the EspA-sheath-like structure. *Proc Natl Acad Sci U S A,* 98**,** 11638-43.

Selyunin, A. S. & Alto, N. M. (2011). Activation of PAK by a bacterial type III effector EspG reveals alternative mechanisms of GTPase pathway regulation. *Small GTPases,* 2**,** 217-221.

Sham, H. P., Shames, S. R., Croxen, M. A., Ma, C., Chan, J. M., Khan, M. A., Wickham, M. E., Deng, W., Finlay, B. B. & Vallance, B. A. (2011). Attaching and effacing bacterial effector NleC suppresses epithelial inflammatory responses by inhibiting NF-kappaB and p38 mitogen-activated protein kinase activation. *Infect Immun,* 79**,** 3552-62.

Shames, S. R., Croxen, M. A., Deng, W. & Finlay, B. B. (2011). The type III system-secreted effector EspZ localizes to host mitochondria and interacts with the translocase of inner mitochondrial membrane 17b. *Infect Immun,* 79**,** 4784-90.

Shames, S. R., Deng, W., Guttman, J. A., De Hoog, C. L., Li, Y., Hardwidge, P. R., Sham, H. P., Vallance, B. A., Foster, L. J. & Finlay, B. B. (2010). The pathogenic E. coli type III effector EspZ interacts with host CD98 and facilitates host cell prosurvival signalling. *Cell Microbiol,* 12**,** 1322-39.

Shang, L., Fukata, M., Thirunarayanan, N., Martin, A. P., Arnaboldi, P., Maussang, D., Berin, C., Unkeless, J. C., Mayer, L., Abreu, M. T. & Lira, S. A. (2008). Toll-like receptor signaling in small intestinal epithelium promotes B-cell recruitment and IgA production in lamina propria. *Gastroenterology,* 135**,** 529-38.

Sharp, F. A., Ruane, D., Claass, B., Creagh, E., Harris, J., Malyala, P., Singh, M., O'hagan, D. T., Petrilli, V., Tschopp, J., O'neill, L. A. & Lavelle, E. C. (2009). Uptake of particulate vaccine adjuvants by dendritic cells activates the NALP3 inflammasome. *Proc Natl Acad Sci U S A,* 106**,** 870-5.

Shevach, E. M. (2009). Mechanisms of foxp3+ T regulatory cell-mediated suppression. *Immunity,* 30**,** 636-45.

Shroff, K. E., Meslin, K. & Cebra, J. J. (1995). Commensal enteric bacteria engender a self-limiting humoral mucosal immune response while permanently colonizing the gut. *Infect Immun,* 63**,** 3904-13.

Simmons, C. P., Clare, S., Ghaem-Maghami, M., Uren, T. K., Rankin, J., Huett, A., Goldin, R., Lewis, D. J., Macdonald, T. T., Strugnell, R. A., Frankel, G. & Dougan, G. (2003). Central role for B lymphocytes and CD4+ T cells in immunity to infection by the attaching and effacing pathogen Citrobacter rodentium. *Infect*

Immun, 71**,** 5077-86.

Skoudy, A., Mounier, J., Aruffo, A., Ohayon, H., Gounon, P., Sansonetti, P. & Tran Van Nhieu, G. (2000). CD44 binds to the Shigella IpaB protein and participates in bacterial invasion of epithelial cells. *Cell Microbiol,* 2**,** 19-33.

Slack, E., Hapfelmeier, S., Stecher, B., Velykoredko, Y., Stoel, M., Lawson, M. A., Geuking, M. B., Beutler, B., Tedder, T. F., Hardt, W. D., Bercik, P., Verdu, E. F., Mccoy, K. D. & Macpherson, A. J. (2009). Innate and adaptive immunity cooperate flexibly to maintain host-microbiota mutualism. *Science,* 325**,** 617-20.

Smith, A. & Bhagwat, A. A. (2013). Hypervirulent-host-associated Citrobacter rodentium cells have poor acid tolerance. *Curr Microbiol,* 66**,** 522-6.

Smith, B. A., Daugherty-Clarke, K., Goode, B. L. & Gelles, J. (2013). Pathway of actin filament branch formation by Arp2/3 complex revealed by single-molecule imaging. *Proc Natl Acad Sci U S A,* 110**,** 1285-90.

Smythies, L. E., Sellers, M., Clements, R. H., Mosteller-Barnum, M., Meng, G., Benjamin, W. H., Orenstein, J. M. & Smith, P. D. (2005). Human intestinal macrophages display profound inflammatory anergy despite avid phagocytic and bacteriocidal activity. *J Clin Invest,* 115**,** 66-75.

Song, X., Zhu, S., Shi, P., Liu, Y., Shi, Y., Levin, S. D. & Qian, Y. (2011). IL-17RE is the functional receptor for IL-17C and mediates mucosal immunity to infection with intestinal pathogens. *Nat Immunol,* 12**,** 1151-8.

Sory, M. P. & Cornelis, G. R. (1994). Translocation of a hybrid YopE-adenylate cyclase from Yersinia enterocolitica into HeLa cells. *Mol Microbiol,* 14**,** 583-94.

Spehlmann, M. E., Dann, S. M., Hruz, P., Hanson, E., Mccole, D. F. & Eckmann, L. (2009). CXCR2-dependent mucosal neutrophil influx protects against colitis-associated diarrhea caused by an attaching/effacing lesion-forming bacterial pathogen. *J Immunol,* 183**,** 3332-43.

Spiekermann, G. M., Finn, P. W., Ward, E. S., Dumont, J., Dickinson, B. L., Blumberg, R. S. & Lencer, W. I. (2002). Receptor-mediated immunoglobulin G transport across mucosal barriers in adult life: functional expression of FcRn in the mammalian lung. *J Exp Med,* 196**,** 303-10.

Stavrinides, J., Mccann, H. C. & Guttman, D. S. (2008). Host-pathogen interplay and the evolution of bacterial effectors. *Cell Microbiol,* 10**,** 285-92.

Stevens, M. P. & Frankel, G. M. (2014). The Locus of Enterocyte Effacement and Associated Virulence Factors of Enterohemorrhagic Escherichia coli. *Microbiol Spectr,* 2**,** EHEC-0007-2013.

Strugnell, R. A. & Wijburg, O. L. (2010). The role of secretory antibodies in infection immunity. *Nat Rev Microbiol,* 8**,** 656-67.

Sun, W., Wang, S. & Curtiss, R., 3rd (2008). Highly efficient method for introducing successive multiple scarless gene deletions and markerless gene

insertions into the Yersinia pestis chromosome. *Appl Environ Microbiol,* 74**,** 4241-5.

Sung, J. L., Lin, J. T. & Gorham, J. D. (2003). CD28 co-stimulation regulates the effect of transforming growth factor-beta1 on the proliferation of naive CD4+ T cells. *Int Immunopharmacol,* 3**,** 233-45.

Sutcliffe, J. G. (1978). Nucleotide sequence of the ampicillin resistance gene of Escherichia coli plasmid pBR322. *Proc Natl Acad Sci U S A,* 75**,** 3737-41.

Suzuki, M., Hisamatsu, T. & Podolsky, D. K. (2003). Gamma interferon augments the intracellular pathway for lipopolysaccharide (LPS) recognition in human intestinal epithelial cells through coordinated up-regulation of LPS uptake and expression of the intracellular Toll-like receptor 4-MD-2 complex. *Infect Immun,* 71**,** 3503-11.

Swennes, A. G., Buckley, E. M., Parry, N. M., Madden, C. M., Garcia, A., Morgan, P. B., Astrofsky, K. M. & Fox, J. G. (2012). Enzootic enteropathogenic Escherichia coli infection in laboratory rabbits. *J Clin Microbiol,* 50**,** 2353-8.

Swindle, E. J. & Metcalfe, D. D. (2007). The role of reactive oxygen species and nitric oxide in mast cell-dependent inflammatory processes. *Immunol Rev,* 217**,** 186-205.

Tahoun, A., Siszler, G., Spears, K., Mcateer, S., Tree, J., Paxton, E., Gillespie, T. L., Martinez-Argudo, I., Jepson, M. A., Shaw, D. J., Koegl, M., Haas, J., Gally, D. L. & Mahajan, A. (2011). Comparative analysis of EspF variants in inhibition of Escherichia coli phagocytosis by macrophages and inhibition of E. coli translocation through human- and bovine-derived M cells. *Infect Immun,* 79**,** 4716-29.

Taylor, R. T. & Williams, I. R. (2005). Lymphoid organogenesis in the intestine. *Immunol Res,* 33**,** 167-81.

Tezuka, H., Abe, Y., Iwata, M., Takeuchi, H., Ishikawa, H., Matsushita, M., Shiohara, T., Akira, S. & Ohteki, T. (2007). Regulation of IgA production by naturally occurring TNF/iNOS-producing dendritic cells. *Nature,* 448**,** 929-33.

Thanabalasuriar, A., Koutsouris, A., Weflen, A., Mimee, M., Hecht, G. & Gruenheid, S. (2010). The bacterial virulence factor NleA is required for the disruption of intestinal tight junctions by enteropathogenic Escherichia coli. *Cell Microbiol,* 12**,** 31-41.

Thomassin, J. L., He, X. & Thomas, N. A. (2011). Role of EscU auto-cleavage in promoting type III effector translocation into host cells by enteropathogenic Escherichia coli. *BMC Microbiol,* 11**,** 205.

Ting, J. P., Willingham, S. B. & Bergstralh, D. T. (2008). NLRs at the intersection of cell death and immunity. *Nat Rev Immunol,* 8**,** 372-9.

Tobe, T., Beatson, S. A., Taniguchi, H., Abe, H., Bailey, C. M., Fivian, A., Younis, R., Matthews, S., Marches, O., Frankel, G., Hayashi, T. & Pallen, M. J.

(2006). An extensive repertoire of type III secretion effectors in Escherichia coli O157 and the role of lambdoid phages in their dissemination. *Proc Natl Acad Sci U S A,* 103**,** 14941-6.

Torchinsky, M. B., Garaude, J., Martin, A. P. & Blander, J. M. (2009). Innate immune recognition of infected apoptotic cells directs T(H)17 cell differentiation. *Nature,* 458**,** 78-82.

Toro, C. S., Mora, G. C. & Figueroa-Bossi, N. (1998). Gene transfer between related bacteria by electrotransformation: mapping Salmonella typhi genes in Salmonella typhimurium. *J Bacteriol,* 180**,** 4750-2.

Trabulsi, L. R., Keller, R. & Tardelli Gomes, T. A. (2002). Typical and atypical enteropathogenic Escherichia coli. *Emerg Infect Dis,* 8**,** 508-13.

Travis, M. A. & Sheppard, D. (2014). TGF-beta activation and function in immunity. *Annu Rev Immunol,* 32**,** 51-82.

Trulzsch, K., Geginat, G., Sporleder, T., Ruckdeschel, K., Hoffmann, R., Heesemann, J. & Russmann, H. (2005). Yersinia outer protein P inhibits CD8 T cell priming in the mouse infection model. *J Immunol,* 174**,** 4244-51.

Tu, X., Nisan, I., Yona, C., Hanski, E. & Rosenshine, I. (2003). EspH, a new cytoskeleton-modulating effector of enterohaemorrhagic and enteropathogenic Escherichia coli. *Mol Microbiol,* 47**,** 595-606.

Tumanov, A. V., Koroleva, E. P., Guo, X., Wang, Y., Kruglov, A., Nedospasov, S. & Fu, Y. X. (2011). Lymphotoxin controls the IL-22 protection pathway in gut innate lymphoid cells during mucosal pathogen challenge. *Cell Host Microbe,* 10**,** 44-53.

Turco, M. M. & Sousa, M. C. (2014). The structure and specificity of the type III secretion system effector NleC suggest a DNA mimicry mechanism of substrate recognition. *Biochemistry,* 53**,** 5131-9.

Turner, J. R. (2009). Intestinal mucosal barrier function in health and disease. *Nat Rev Immunol,* 9**,** 799-809.

Umanski, T., Rosenshine, I. & Friedberg, D. (2002). Thermoregulated expression of virulence genes in enteropathogenic Escherichia coli. *Microbiology,* 148**,** 2735-44.

Underhill, D. M. & Goodridge, H. S. (2012). Information processing during phagocytosis. *Nat Rev Immunol,* 12**,** 492-502.

Uren, T. K., Johansen, F. E., Wijburg, O. L., Koentgen, F., Brandtzaeg, P. & Strugnell, R. A. (2003). Role of the polymeric Ig receptor in mucosal B cell homeostasis. *J Immunol,* 170**,** 2531-9.

Uren, T. K., Wijburg, O. L., Simmons, C., Johansen, F. E., Brandtzaeg, P. & Strugnell, R. A. (2005). Vaccine-induced protection against gastrointestinal bacterial infections in the absence of secretory antibodies. *Eur J Immunol,* 35**,**

180-8.

Uzzau, S., Figueroa-Bossi, N., Rubino, S. & Bossi, L. (2001). Epitope tagging of chromosomal genes in Salmonella. *Proc Natl Acad Sci U S A,* 98**,** 15264-9.

Vallance, B. A., Deng, W., Jacobson, K. & Finlay, B. B. (2003). Host susceptibility to the attaching and effacing bacterial pathogen Citrobacter rodentium. *Infect Immun,* 71**,** 3443-53.

Vallance, B. A., Deng, W., Knodler, L. A. & Finlay, B. B. (2002). Mice lacking T and B lymphocytes develop transient colitis and crypt hyperplasia yet suffer impaired bacterial clearance during Citrobacter rodentium infection. *Infect Immun,* 70**,** 2070-81.

Vallance, B. A., Dijkstra, G., Qiu, B., Van Der Waaij, L. A., Van Goor, H., Jansen, P. L., Mashimo, H. & Collins, S. M. (2004). Relative contributions of NOS isoforms during experimental colitis: endothelial-derived NOS maintains mucosal integrity. *Am J Physiol Gastrointest Liver Physiol,* 287**,** G865-74.

Vallon-Eberhard, A., Landsman, L., Yogev, N., Verrier, B. & Jung, S. (2006). Transepithelial pathogen uptake into the small intestinal lamina propria. *J Immunol,* 176**,** 2465-9.

Vamadevan, A. S., Fukata, M., Arnold, E. T., Thomas, L. S., Hsu, D. & Abreu, M. T. (2010). Regulation of Toll-like receptor 4-associated MD-2 in intestinal epithelial cells: a comprehensive analysis. *Innate Immun,* 16**,** 93-103.

Van De Pavert, S. A. & Mebius, R. E. (2010). New insights into the development of lymphoid tissues. *Nat Rev Immunol,* 10**,** 664-74.

Van De Pavert, S. A., Olivier, B. J., Goverse, G., Vondenhoff, M. F., Greuter, M., Beke, P., Kusser, K., Hopken, U. E., Lipp, M., Niederreither, K., Blomhoff, R., Sitnik, K., Agace, W. W., Randall, T. D., De Jonge, W. J. & Mebius, R. E. (2009). Chemokine CXCL13 is essential for lymph node initiation and is induced by retinoic acid and neuronal stimulation. *Nat Immunol,* 10**,** 1193-9.

Van Der Sluis, M., De Koning, B. A., De Bruijn, A. C., Velcich, A., Meijerink, J. P., Van Goudoever, J. B., Buller, H. A., Dekker, J., Van Seuningen, I., Renes, I. B. & Einerhand, A. W. (2006). Muc2-deficient mice spontaneously develop colitis, indicating that MUC2 is critical for colonic protection. *Gastroenterology,* 131**,** 117-29.

Veiga-Fernandes, H., Coles, M. C., Foster, K. E., Patel, A., Williams, A., Natarajan, D., Barlow, A., Pachnis, V. & Kioussis, D. (2007). Tyrosine kinase receptor RET is a key regulator of Peyer's patch organogenesis. *Nature,* 446**,** 547-51.

Velcich, A., Yang, W., Heyer, J., Fragale, A., Nicholas, C., Viani, S., Kucherlapati, R., Lipkin, M., Yang, K. & Augenlicht, L. (2002). Colorectal cancer in mice genetically deficient in the mucin Muc2. *Science,* 295**,** 1726-9.

Veltman, D. M. & Insall, R. H. (2010). WASP family proteins: their evolution and its physiological implications. *Mol Biol Cell,* 21**,** 2880-93.

Viala, J., Chaput, C., Boneca, I. G., Cardona, A., Girardin, S. E., Moran, A. P., Athman, R., Memet, S., Huerre, M. R., Coyle, A. J., Distefano, P. S., Sansonetti, P. J., Labigne, A., Bertin, J., Philpott, D. J. & Ferrero, R. L. (2004). Nod1 responds to peptidoglycan delivered by the Helicobacter pylori cag pathogenicity island. *Nat Immunol,* 5**,** 1166-74.

Viala, J., Chaput, C., Boneca, I. G., Cardona, A., Girardin, S. E., Moran, A. P., Athman, R., Memet, S., Huerre, M. R., Coyle, A. J., Distefano, P. S., Sansonetti, P. J., Labigne, A., Bertin, J., Philpott, D. J. & Ferrero, R. L. (2004). Nod1 responds to peptidoglycan delivered by the Helicobacter pylori cag pathogenicity island. *Nat Immunol,* 5**,** 1166-74.

Vieira, M. A., Salvador, F. A., Silva, R. M., Irino, K., Vaz, T. M., Rockstroh, A. C., Guth, B. E. & Gomes, T. A. (2010). Prevalence and characteristics of the O122 pathogenicity island in typical and atypical enteropathogenic Escherichia coli strains. *J Clin Microbiol,* 48**,** 1452-5.

Vijay-Kumar, M., Aitken, J. D. & Gewirtz, A. T. (2008). Toll like receptor-5: protecting the gut from enteric microbes. *Semin Immunopathol,* 30**,** 11-21.

Vijay-Kumar, M., Sanders, C. J., Taylor, R. T., Kumar, A., Aitken, J. D., Sitaraman, S. V., Neish, A. S., Uematsu, S., Akira, S., Williams, I. R. & Gewirtz, A. T. (2007). Deletion of TLR5 results in spontaneous colitis in mice. *J Clin Invest,* 117**,** 3909-21.

Vijay-Kumar, M., Wu, H., Aitken, J., Kolachala, V. L., Neish, A. S., Sitaraman, S. V. & Gewirtz, A. T. (2007). Activation of toll-like receptor 3 protects against DSS-induced acute colitis. *Inflamm Bowel Dis,* 13**,** 856-64.

Vingadassalom, D., Kazlauskas, A., Skehan, B., Cheng, H. C., Magoun, L., Robbins, D., Rosen, M. K., Saksela, K. & Leong, J. M. (2009). Insulin receptor tyrosine kinase substrate links the E. coli O157:H7 actin assembly effectors Tir and EspF(U) during pedestal formation. *Proc Natl Acad Sci U S A,* 106**,** 6754-9.

Vlisidou, I., Dziva, F., La Ragione, R. M., Best, A., Garmendia, J., Hawes, P., Monaghan, P., Cawthraw, S. A., Frankel, G., Woodward, M. J. & Stevens, M. P. (2006). Role of intimin-tir interactions and the tir-cytoskeleton coupling protein in the colonization of calves and lambs by Escherichia coli O157:H7. *Infect Immun,* 74**,** 758-64.

Vossenkamper, A., Blair, P. A., Safinia, N., Fraser, L. D., Das, L., Sanders, T. J., Stagg, A. J., Sanderson, J. D., Taylor, K., Chang, F., Choong, L. M., D'cruz, D. P., Macdonald, T. T., Lombardi, G. & Spencer, J. (2013). A role for gut-associated lymphoid tissue in shaping the human B cell repertoire. *J Exp Med,* 210**,** 1665-74.

Vossenkamper, A., Macdonald, T. T. & Marches, O. (2011). Always one step

ahead: How pathogenic bacteria use the type III secretion system to manipulate the intestinal mucosal immune system. *J Inflamm (Lond),* 8**,** 11.

Vossenkamper, A., Marches, O., Fairclough, P. D., Warnes, G., Stagg, A. J., Lindsay, J. O., Evans, P. C., Luong Le, A., Croft, N. M., Naik, S., Frankel, G. & Macdonald, T. T. (2010). Inhibition of NF-kappaB signaling in human dendritic cells by the enteropathogenic Escherichia coli effector protein NleE. *J Immunol,* 185**,** 4118-27.

Wagner, S., Stenta, M., Metzger, L. C., Dal Peraro, M. & Cornelis, G. R. (2010). Length control of the injectisome needle requires only one molecule of Yop secretion protein P (YscP). *Proc Natl Acad Sci U S A,* 107**,** 13860-5.

Wales, A. D., Woodward, M. J. & Pearson, G. R. (2005). Attaching-effacing bacteria in animals. *J Comp Pathol,* 132**,** 1-26.

Wan, F., Weaver, A., Gao, X., Bern, M., Hardwidge, P. R. & Lenardo, M. J. (2011). IKKbeta phosphorylation regulates RPS3 nuclear translocation and NF-kappaB function during infection with Escherichia coli strain O157:H7. *Nat Immunol,* 12**,** 335-43.

Wan, Y. Y. & Flavell, R. A. (2007). 'Yin-Yang' functions of transforming growth factor-beta and T regulatory cells in immune regulation. *Immunol Rev,* 220**,** 199-213.

Wang, R., Song, L., Han, G., Wang, J., Chen, G., Xu, R., Yu, M., Qian, J., Shen, B. & Li, Y. (2007). Mechanisms of regulatory T-cell induction by antigen-IgG-transduced splenocytes. *Scand J Immunol,* 66**,** 515-22.

Wang, Y., Koroleva, E. P., Kruglov, A. A., Kuprash, D. V., Nedospasov, S. A., Fu, Y. X. & Tumanov, A. V. (2010). Lymphotoxin beta receptor signaling in intestinal epithelial cells orchestrates innate immune responses against mucosal bacterial infection. *Immunity,* 32**,** 403-13.

Wang, Z., Friedrich, C., Hagemann, S. C., Korte, W. H., Goharani, N., Cording, S., Eberl, G., Sparwasser, T. & Lochner, M. (2014). Regulatory T cells promote a protective Th17-associated immune response to intestinal bacterial infection with C. rodentium. *Mucosal Immunol,* 7**,** 1290-301.

Watarai, M., Funato, S. & Sasakawa, C. (1996). Interaction of Ipa proteins of Shigella flexneri with alpha5beta1 integrin promotes entry of the bacteria into mammalian cells. *J Exp Med,* 183**,** 991-9.

Wehkamp, J., Salzman, N. H., Porter, E., Nuding, S., Weichenthal, M., Petras, R. E., Shen, B., Schaeffeler, E., Schwab, M., Linzmeier, R., Feathers, R. W., Chu, H., Lima, H., Jr., Fellermann, K., Ganz, T., Stange, E. F. & Bevins, C. L. (2005). Reduced Paneth cell alpha-defensins in ileal Crohn's disease. *Proc Natl Acad Sci U S A,* 102**,** 18129-34.

Weiss, A., Kortemeier, D. & Brockmeyer, J. (2014). Biochemical characterization of the SPATE members EspPalpha and EspI. *Toxins (Basel),* 6**,**

2719-31.

Weiss, S. M., Ladwein, M., Schmidt, D., Ehinger, J., Lommel, S., Stading, K., Beutling, U., Disanza, A., Frank, R., Jansch, L., Scita, G., Gunzer, F., Rottner, K. & Stradal, T. E. (2009). IRSp53 links the enterohemorrhagic E. coli effectors Tir and EspFU for actin pedestal formation. *Cell Host Microbe,* 5**,** 244-58.

Whale, A. D., Hernandes, R. T., Ooka, T., Beutin, L., Schuller, S., Garmendia, J., Crowther, L., Vieira, M. A., Ogura, Y., Krause, G., Phillips, A. D., Gomes, T. A., Hayashi, T. & Frankel, G. (2007). TccP2-mediated subversion of actin dynamics by EPEC 2 - a distinct evolutionary lineage of enteropathogenic Escherichia coli. *Microbiology,* 153**,** 1743-55.

Wickham, M. E., Lupp, C., Vazquez, A., Mascarenhas, M., Coburn, B., Coombes, B. K., Karmali, M. A., Puente, J. L., Deng, W. & Finlay, B. B. (2007). Citrobacter rodentium virulence in mice associates with bacterial load and the type III effector NleE. *Microbes Infect,* 9**,** 400-7.

Wiles, S., Clare, S., Harker, J., Huett, A., Young, D., Dougan, G. & Frankel, G. (2004). Organ specificity, colonization and clearance dynamics in vivo following oral challenges with the murine pathogen Citrobacter rodentium. *Cell Microbiol,* 6**,** 963-72.

Wiles, S., Dougan, G. & Frankel, G. (2005). Emergence of a 'hyperinfectious' bacterial state after passage of Citrobacter rodentium through the host gastrointestinal tract. *Cell Microbiol,* 7**,** 1163-72.

Wiles, S., Pickard, K. M., Peng, K., Macdonald, T. T. & Frankel, G. (2006). In vivo bioluminescence imaging of the murine pathogen Citrobacter rodentium. *Infect Immun,* 74**,** 5391-6.

Willingham, S. B., Bergstralh, D. T., O'connor, W., Morrison, A. C., Taxman, D. J., Duncan, J. A., Barnoy, S., Venkatesan, M. M., Flavell, R. A., Deshmukh, M., Hoffman, H. M. & Ting, J. P. (2007). Microbial pathogen-induced necrotic cell death mediated by the inflammasome components CIAS1/cryopyrin/NLRP3 and ASC. *Cell Host Microbe,* 2**,** 147-59.

Wilson, C. L., Ouellette, A. J., Satchell, D. P., Ayabe, T., Lopez-Boado, Y. S., Stratman, J. L., Hultgren, S. J., Matrisian, L. M. & Parks, W. C. (1999). Regulation of intestinal alpha-defensin activation by the metalloproteinase matrilysin in innate host defense. *Science,* 286**,** 113-7.

Wilson, R. K., Shaw, R. K., Daniell, S., Knutton, S. & Frankel, G. (2001). Role of EscF, a putative needle complex protein, in the type III protein translocation system of enteropathogenic Escherichia coli. *Cell Microbiol,* 3**,** 753-62.

Woestyn, S., Allaoui, A., Wattiau, P. & Cornelis, G. R. (1994). YscN, the putative energizer of the Yersinia Yop secretion machinery. *J Bacteriol,* 176**,** 1561-9.

Wong, A. R., Clements, A., Raymond, B., Crepin, V. F. & Frankel, G. (2012). The interplay between the Escherichia coli Rho guanine nucleotide exchange

factor effectors and the mammalian RhoGEF inhibitor EspH. *MBio,* 3.

Wong, A. R., Pearson, J. S., Bright, M. D., Munera, D., Robinson, K. S., Lee, S. F., Frankel, G. & Hartland, E. L. (2011). Enteropathogenic and enterohaemorrhagic Escherichia coli: even more subversive elements. *Mol Microbiol,* 80**,** 1420-38.

Wong, A. R., Raymond, B., Collins, J. W., Crepin, V. F. & Frankel, G. (2012). The enteropathogenic E. coli effector EspH promotes actin pedestal formation and elongation via WASP-interacting protein (WIP). *Cell Microbiol,* 14**,** 1051-70.

Worley, M. J., Nieman, G. S., Geddes, K. & Heffron, F. (2006). Salmonella typhimurium disseminates within its host by manipulating the motility of infected cells. *Proc Natl Acad Sci U S A,* 103**,** 17915-20.

Wright, A., Lamm, M. E. & Huang, Y. T. (2008). Excretion of human immunodeficiency virus type 1 through polarized epithelium by immunoglobulin A. *J Virol,* 82**,** 11526-35.

Wright, N. A., Hoffmann, W., Otto, W. R., Rio, M. C. & Thim, L. (1997). Rolling in the clover: trefoil factor family (TFF)-domain peptides, cell migration and cancer. *FEBS Lett,* 408**,** 121-3.

Wu, B., Skarina, T., Yee, A., Jobin, M. C., Dileo, R., Semesi, A., Fares, C., Lemak, A., Coombes, B. K., Arrowsmith, C. H., Singer, A. U. & Savchenko, A. (2010). NleG Type 3 effectors from enterohaemorrhagic Escherichia coli are U-Box E3 ubiquitin ligases. *PLoS Pathog,* 6**,** e1000960.

Wu, H., Jones, R. M. & Neish, A. S. (2012). The Salmonella effector AvrA mediates bacterial intracellular survival during infection in vivo. *Cell Microbiol,* 14**,** 28-39.

Xicohtencatl-Cortes, J., Monteiro-Neto, V., Saldana, Z., Ledesma, M. A., Puente, J. L. & Giron, J. A. (2009). The type 4 pili of enterohemorrhagic Escherichia coli O157:H7 are multipurpose structures with pathogenic attributes. *J Bacteriol,* 191**,** 411-21.

Yamakawa, M. & Imai, Y. (1992). Complement activation in the follicular light zone of human lymphoid tissues. *Immunology,* 76**,** 378-84.

Yamazaki, K., Shimada, S., Kato-Nagaoka, N., Soga, H., Itoh, T. & Nanno, M. (2005). Accumulation of intestinal intraepithelial lymphocytes in association with lack of polymeric immunoglobulin receptor. *Eur J Immunol,* 35**,** 1211-9.

Yan, D., Wang, X., Luo, L., Cao, X. & Ge, B. (2012). Inhibition of TLR signaling by a bacterial protein containing immunoreceptor tyrosine-based inhibitory motifs. *Nat Immunol,* 13**,** 1063-71.

Yan, H., Lamm, M. E., Bjorling, E. & Huang, Y. T. (2002). Multiple functions of immunoglobulin A in mucosal defense against viruses: an in vitro measles virus model. *J Virol,* 76**,** 10972-9.

Yao, Q., Zhang, L., Wan, X., Chen, J., Hu, L., Ding, X., Li, L., Karar, J., Peng, H., Chen, S., Huang, N., Rauscher, F. J., 3rd & Shao, F. (2014). Structure and specificity of the bacterial cysteine methyltransferase effector NleE suggests a novel substrate in human DNA repair pathway. *PLoS Pathog,* 10**,** e1004522.

Yen, T. H. & Wright, N. A. (2006). The gastrointestinal tract stem cell niche. *Stem Cell Rev,* 2**,** 203-12.

Yipp, B. G. & Kubes, P. (2013). NETosis: how vital is it? *Blood,* 122**,** 2784-94.

Yoshida, H., Naito, A., Inoue, J., Satoh, M., Santee-Cooper, S. M., Ware, C. F., Togawa, A., Nishikawa, S. & Nishikawa, S. (2002). Different cytokines induce surface lymphotoxin-alphabeta on IL-7 receptor-alpha cells that differentially engender lymph nodes and Peyer's patches. *Immunity,* 17**,** 823-33.

Yoshida, M., Claypool, S. M., Wagner, J. S., Mizoguchi, E., Mizoguchi, A., Roopenian, D. C., Lencer, W. I. & Blumberg, R. S. (2004). Human neonatal Fc receptor mediates transport of IgG into luminal secretions for delivery of antigens to mucosal dendritic cells. *Immunity,* 20**,** 769-83.

Yoshida, M., Kobayashi, K., Kuo, T. T., Bry, L., Glickman, J. N., Claypool, S. M., Kaser, A., Nagaishi, T., Higgins, D. E., Mizoguchi, E., Wakatsuki, Y., Roopenian, D. C., Mizoguchi, A., Lencer, W. I. & Blumberg, R. S. (2006). Neonatal Fc receptor for IgG regulates mucosal immune responses to luminal bacteria. *J Clin Invest,* 116**,** 2142-2151.

Yu, B., Yang, M., Wong, H. Y., Watt, R. M., Song, E., Zheng, B. J., Yuen, K. Y. & Huang, J. D. (2011). A method to generate recombinant Salmonella typhi Ty21a strains expressing multiple heterologous genes using an improved recombineering strategy. *Appl Microbiol Biotechnol,* 91**,** 177-88.

Yu, D., Ellis, H. M., Lee, E. C., Jenkins, N. A., Copeland, N. G. & Court, D. L. (2000). An efficient recombination system for chromosome engineering in Escherichia coli. *Proc Natl Acad Sci U S A,* 97**,** 5978-83.

Zaki, M. H., Vogel, P., Body-Malapel, M., Lamkanfi, M. & Kanneganti, T. D. (2010). IL-18 production downstream of the Nlrp3 inflammasome confers protection against colorectal tumor formation. *J Immunol,* 185**,** 4912-20.

Zarivach, R., Vuckovic, M., Deng, W., Finlay, B. B. & Strynadka, N. C. (2007). Structural analysis of a prototypical ATPase from the type III secretion system. *Nat Struct Mol Biol,* 14**,** 131-7.

Zhang, Y., Romanov, G. & Bliska, J. B. (2011). Type III secretion system-dependent translocation of ectopically expressed Yop effectors into macrophages by intracellular Yersinia pseudotuberculosis. *Infect Immun,* 79**,** 4322-31.

Zhao, S., Zhou, Y., Wang, C., Yang, Y., Wu, X., Wei, Y., Zhu, L., Zhao, W., Zhang, Q. & Wan, C. (2013). The N-terminal domain of EspF induces host cell apoptosis after infection with enterohaemorrhagic Escherichia coli O157:H7. *PLoS*

One, 8**,** e55164.

Zheng, Y., Lilo, S., Brodsky, I. E., Zhang, Y., Medzhitov, R., Marcu, K. B. & Bliska, J. B. (2011). A Yersinia effector with enhanced inhibitory activity on the NF-kappaB pathway activates the NLRP3/ASC/caspase-1 inflammasome in macrophages. *PLoS Pathog,* 7**,** e1002026.

Zheng, Y., Valdez, P. A., Danilenko, D. M., Hu, Y., Sa, S. M., Gong, Q., Abbas, A. R., Modrusan, Z., Ghilardi, N., De Sauvage, F. J. & Ouyang, W. (2008). Interleukin-22 mediates early host defense against attaching and effacing bacterial pathogens. *Nat Med,* 14**,** 282-9.

Zhou, W., Cao, Q., Peng, Y., Zhang, Q. J., Castrillon, D. H., Depinho, R. A. & Liu, Z. P. (2009). FoxO4 inhibits NF-kappaB and protects mice against colonic injury and inflammation. *Gastroenterology,* 137**,** 1403-14.

Ziegler, S. F. (2006). FOXP3: of mice and men. *Annu Rev Immunol,* 24**,** 209-26.

Zlokarnik, G. (2000). Fusions to beta-lactamase as a reporter for gene expression in live mammalian cells. *Methods Enzymol,* 326**,** 221-44.

Zlokarnik, G., Negulescu, P. A., Knapp, T. E., Mere, L., Burres, N., Feng, L., Whitney, M., Roemer, K. & Tsien, R. Y. (1998). Quantitation of transcription and clonal selection of single living cells with beta-lactamase as reporter. *Science,* 279**,** 84-8.

Zychlinsky, A., Kenny, B., Menard, R., Prevost, M. C., Holland, I. B. & Sansonetti, P. J. (1994). IpaB mediates macrophage apoptosis induced by Shigella flexneri. *Mol Microbiol,* 11**,** 619-27.

Appendix A: Cells and molecules of the host immune system that facilitate bacterial clearance in *C. rodentium* infection of mice

Immune cell/molecule	Role in *C.rodentium* infection	References
	Innate immune response	
MyD88	Key adaptor molecule in immune signaling downstream of TLR and ILIR. MYD88 signaling controls infection by recruiting neutrophils, DC and macrophages to the mucosa, expressing iNOS and triggering the proliferation of epithelial cells (colonic hyperplasia).	Vallance et al, 2004 Gibson et al, 2008 Lebeis et al, 2007 Bhinder et al, 2014
TLR	TLR2 and TLR4 are activated infection, which induces the up-regulation of iNOS and the production of proinflammatory cytokines KC, TNF and IL6. TLR2 signaling in stromal cells induces tissue protective responses, which are especially required in the presence of TLR 4 signaling. TLR2 mediated signaling limits tissue damage which is associated with the production of cytoprotective cytokines IL-11 by subepithelial mesenchymal cells. IL-11 is essential for STAT 3 phosphorylation in colonic crypt epithelial cells, which promote epithelial cell health and proliferation. This may also protect against TLR 4 driven damage. TLR4 expressing hematopoietic cells drive infection induced mucosal damage and may facilitate *C.rodentium* colonization by helping to remove competing commensals.	Lupp et al, 2007 Gibson et al, 2008 Khan et al, 2006
NOD	NOD1 and NOD2 signaling are activated by *C.rodentium*, which protects against pathogen induced damage by limiting bacterial translocation and promoting mucosal integrity. This occurs through the production of IL17A by ILC3 cells which are responsible for early IL17A mediated production of IL22 and RegIIIy. NOD2 signaling also leads to the recruitment of cd11c+ inflammatory monocytes to the site of infection, which also promote pathogen killing.	Geddes et al, 2011 Kim et al, 2011
Caspase	Caspase I mediated mucosal responses are crucial for host resistance to *C.rodentium*. Caspase 1 proteolytically cleaves the precursor forms of IL1b and IL18 into active mature peptides. Caspase 11 is required for *C.rodentium* mediated NLRP3 dependent caspase 1 maturation and IL-1 responses. Caspase 11 is regulated by TRIF (an adaptor molecule downstream of TLR 4). Caspase 12 is a negative regulator of caspase 1 and inflammasome function. Caspase 12 directly interferes with NOD signaling required for NF-κB activation and the production of the NOD regulated B-defensin-2. By doing so, caspase 12 dampens NF-κB activation thus inhibiting NOD activation and the resulting antimicrobial peptide production.	Liu et al, 2012 Kayagaki et al, 2011 LeBlanc et al, 2008

Inflammasome	Macromolecular scaffolds in the cytosol of immune cells that are responsible for the proteolytic maturation of caspase 1 and the IL-1 family of cytokines including IL1b and IL18.	Kayagaki et al, 2011 Gurung et al, 2012 Liu et al, 2012 Alipour et al, 2013
ILC3	ILC3 are an important source of IL22 and IL17 in the early stage of *C.rodentium* infection. ILC3 are induced early in the caecum and is dependent on NOD1 and NOD2 signaling as well as imprinting by the intestinal microbiota.	O'Quinn et al, 2008 Torchinsky et al, 2009 Song et al, 2011 Collins et al, 2014 Liu et al, 2009
Complement	Compliment protein C3b and complement fixing IgG enter the gut lumen during infection and bind to adhering *C.rodentium*. Opsonization of *C.rodentium* leads to increased phagocytosis, neutralization of bacterial adhesins and bacterial lysis.	Belzer et 2011
Reactive nitrogen species	Reactive nitrogen species are generated by Inducible nitric oxide synthase (iNOS) in neutrophils, macrophages and epithelial cells. Infection results in a strong expression of iNOS by epithelial cells and thus increased nitric oxide (NO) in the lumen of the gut. NO is bacteriostatic against *C.rodentium* but seems to play a minor role in host defense against *C.rodentium*.	Simmons et al, 2002 Gobert et al, 2004
Mononuclear phagocytes	CX(3)CR1(+) mononuclear phagocytes produce IL23 and IL-1beta which support IL22 production by ILC3s in response to infection. IL22 production induces the expression of the antimicrobial peptides RegIIIb and RegIIIy.	Longman et al, 2014 Manta et al, 2014
NK cells	During infection, NK cells are recruited to the mucosal tissue where they express a diverse array of immunomodulatory factors such as TNFa and IFNγ, which provide protection against *C.rodentium*. NK cells reduce *C.rodentium* burden in the colon, modulate infiltration and cytokine (such as IL17) profiles of MLN immune cells (such as neutrophils), recruit colonic effector cells (T and B cells), prevent extracolonic dissemination of *C.rodentium* (by stimulating macrophages and neutrophils to produce ROS) and are directly cytotoxic (by producing a-defensins) to *C.rodentium*.	Hall et al, 2013
Antimicrobial peptides	Murine B defensins (mBD1 and mBD3) are upregulated in colonic tissue of infected mice. Defensins have antimicrobial activity against *C.rodentium* by disrupting bacterial membrane and causing cell death. Murine cathelicidin-related antimicrobial peptide (mCRAMP) also play a role in limiting *C.rodentium* colonization early during infection. RegIIIy and RegIIIb expression are induced by the production of IL22 and have antimicrobial activity against C.rodentium.	Simmons et al, 2002 Limura et al, 2005 Manta et al, 2013

Adaptive immune response

T cells	CD4+T cells elicit a Th1 cell response that is characterized by the production of IFNγ and TNFa. CD4+T cell dependent IgG response is required to overcome *C.rodentium* infection. CD8 T cells increase in the submucosa of infected tissue but do not have a major role in the resolution of infection. Th22 cells are an important source of IL22 which induce the production of Reg III antimicrobial peptides and promote epithelial barrier integrity. Development of Th22 cells is dependent on IL6 and the transcription factor T bet and Ahr. Th17 are an important source of IL17 which increases chemokine and cytokine production in various tissues to recruit monocytes and neutrophils to the local site of infection. Foxp3+ T regulatory cells induce a strong Th17 response in the colon which helps to clear the pathogen. Th17 cell response also induces inflammation associated pathology in the gut.	Simmons et al, 2003 Bry & Brenner 2004 Zheng et al, 2008 Basu et al, 2012 Li et al, 2014 Wang et al, 2014 Symonds et al, 2009
B cells	The functions of B cells are mainly mediated by serum IgG, which is crucial for the resolution of *C.rodentium* infection. B cells also play an important role in the development and formation of intestinal lymphoid tissue. B cells are potent APC and facilitate the development of effective T cell responses. B cells can also secrete chemotactic cytokines which are important for immune cell recruitment.	Simmons et al, 2003 Maaser et al, 2004 Bry & Brenner 2004 Uren et al, 2005 Belzer et al, 2011
	Cytokine response	
IL12	IL-12 plays an important role in limiting bacterial infection of the colonic epithelium.	Simmons et al, 2002
IFNγ	IFNγ enhances macrophage phagocytic activity against *C.rodentium* and induces the activation of antigen specific T cells. Drive goblet cell depletion and IEC proliferation. IFNγ produced by antigen specific CD4+Tcells play an important role in defense against *C.rodentium*.	Shiomi et al, 2010 Chan et al, 2013
TNFa	TNFa downregulates mucosal pathology and Th1 immune responses by dampening down IL12 and IFNγ. TNFa might limit intestinal colonization through enhancing innate immune responses through neutrophil recruitment and defensin production. Thus, TNFa has a role in controlling bacterial burden and limiting mucosal immune mediated pathology but does not contribute to pathogen clearance.	Goncalves et al, 2001

IL17	Produced by ILC3s and CD4 Th17 cells. ILC3 responses occur mainly in the caecum and is dependent on NOD1 and NOD2 signaling, imprinting by the intestinal microbiota, IL6 induction and is associated with *C.rodentium* induced apoptosis of IECs. The phagocytosis of infected apoptotic cells by DCs can induce the simultaneous production of IL6 and TGFb which lead to the polarization of Th17 cells. Blocking apoptosis during infection, impairs the Th17 cell response in the lamina propia. IL17 increases chemokine and cytokine production in infected tissue to recruit innate cells including monocytes and neutrophils to the site of infection.	O'Quinn et al, 2008 Torchinsky et al, 2009 Song et al, 2011 Brereton & Blander 2011 Liu et al, 2009 Li et al, 2014
IL22	Produced by Th17cells, Th22 cells and ILC3s. DC derived IL23 and macrophage derived IL1b facilitates IL22 production by ILCs. IL22 induces the production of Reg III antimicrobial peptide and promote epithelial barrier integrity. IL22 also facilitate host responses by modulating the expression of various chemokines including CXCL1, CXCL5 and CXCL9. STAT 3 is required for IL22 production in both innate and adaptive immune cells.	Zheng et al, 2008 Basu et al, 2012 Manta et al, 2013 Guo et al, 2014
IL-1b & IL-18	Produced by *C.rodentium* mediated activation of Nlrp3 inflammasome. IL-1b and IL-18 play a critical role in host defense against enteric infection. IL1b controls the production of IL22 by RORgt+ILC cells.	Lebeis et al, 2009 Liu et al, 2012 Alipour et al, 2013
IL6	Inflammatory cytokine required for the differentiation and activation of Th17 cells in PP as well as promoting IL22 expression.	Li et al, 2014
IL10	Infection induced macrophage and DC production of IL10 is associated with diminished anti bacterial host defenses.	Dann et al, 2014

Appendix B: Response of various knockout mice to *C. rodentium* infection

PRR signaling			
Knockout mice	**Immune phenotype**	**Response to infection**	**Reference**
MyD88-/-	Impaired signaling of TLR and IL-1	Mice suffer from bacteremia, gangrenous mucosal necrosis, severe colitis and death.	Lebeis et al, 2007
	Delayed inflammatory cell recruitment, reduced iNOS and abrogated production of TNFa and IL6 from macrophages and colons. Unable to promote epithelial cell turnover and repair.	Mice develop lethal colitis with colonic mucosal ulcerations and bleeding associated with high bacterial burden, bacterial invasion of colonic crypts and intestinal barrier dysfunction.	Gibson et al, 2008
P50-/-	Non-functional NF-κB heterodimer	Mice are unable to clear infection, exhibit reduced influx of immune cells into infected colonic tissue and increased levels of mucosal hyperplasia, IFNγ and TNFa. Also show higher levels of anti *C.rodentium* IgG and IgM.	Dennis et al, 2008
P38a deletion in IECs.	Impaired chemokine expression in IECs.	Mice suffer from a sustained bacterial burden and fail to recruit CD4 T cells into colonic mucosal lesions due to impaired chemokines expression in IECs.	Kang et al, 2010
Nlrp3-/-	Defective protoelytic maturation of caspase 1 required for the production of IL1b and IL18	Compared to Casp1-/-, there was a delayed onset of body weight loss and increase in bacterial burden.	Liu et al, 2012
		Infected mice developed severe colitis. Treatment of infected mice with IL-1B reduced bacterial colonization, abrogated bacterial translocation to mesenteric lymph nodes and protected epithelial integrity.	Alipour et al, 2013

Casp1-/-	Defective production of IL-1 family of cytokines (IL1b and IL18)	Mice were highly susceptible to *C.rodentium* infection. There was significant loss of body weight, increased colon inflammation, increased inflammatory cytokine production and higher bacterial burden.	Liu et al, 2012
NOD2-/-	Reduced CCL2 chemokine production by stromal cells, inflammatory monocyte recruitment and Th1 cell responses.	Impaired clearance of *C. rodentium*, due to reduced CCL2 chemokine production (by colonic stromal cells or CD11b+ phagocytic cells in a NOD2-dependent manner), reduced inflammatory monocytes recruitment (which produces IL12 required for inducing adaptive immunity) and a reduced TH1 cell response in the intestine.	Kim et al, 2011
Pellino3-/-	Loss of function of NOD2 and reduced activation NF-kB and MAPKs.	Less induction of cytokines after engagement of NOD2 and had exacerbated disease in *C.rodentium* colitis.	Yang et al, 2013

Innate immunity			
Knockout mice	**Immune phenotype**	**Response to infection**	**Reference**
Mtg16-/- (Myeloid translocation gene 16)	Increase in innate cells Gr1(+), F4/80(+), CD11c(+) and MHCII(+); CD11c(+) and Th1 adaptive (CD4) immune cells	Severe colitis and greater bacterial colonisation. MTG16 is a transcriptional corepressor that regulates inflammatory recruitment and is critical for colonocyte survival and regeneration	Williams et al, 2013
ASK-/- (Activator of S phase kinase)	Inability of macrophages to kill bacteria	Increased susceptibility to colonic inflammation by *C.rodentium* in vivo. In vitro, ASK-/- macrophages are impaired in their ability to kill bacteria and had increased susceptibility to bacteria-induced apoptosis. Ant apoptotic genes were greatly reduced in ASK-/- macrophages.	Hayakawa et al, 2010
PSGL-1-/- (P-Selectin glycoprotein ligand)	Inability to recruit innate immune cells such as neutrophils and macrophages to site of inflammation.	More pronounced morbidity associated with higher bacterial load, elevated IL-12p70, TNF-a, IFNγ, MCP-1 and IL-6 production, more severe inflammation and higher leucocyte infiltration in the guts.	Kum et al, 2010

CX3CR1-/-	Lack CX3CR1+ macrophages and DCs	Delayed clearance of *C.rodentium*, associated with reduced IL-22 expression. Without CX3CR1, there is reduction of IL22 production by lymphoid tissue inducer (Lti) cells. This also correlates with the decreased expression of antimicrobial peptides RegIIIβ and RegIIIy.	Manta et al, 2013
GM-CSF-/- (Granulocyte-macrophage colony-stimulating factor)	Decreased CD11c+DC recruitment and survival in the mucosa due to failure of epithelial cells to upregulate production of DC attractant CCL22.	Had fewer mucosal CD11c (+) DCs, greater bacterial burden, increased mucosal inflammation and systemic spread of infection, decreased antibody responses, and delayed pathogen clearance.	Hirata et al, 2010
Nfil3-/-	Impaired development of Peyer's patches and ILC2 and ILC3 subsets.	Highly susceptible to infection due to reduced PP formation and impaired recruitment and distribution of lymphocytes within the patches. In Nfil3 defecient mice, ILC3s including LTi cells are severly diminished in number and function.	Seillet et al, 2014 Geiger et al, 2014
Ahr-/- (Aryl hydrocarbon receptor)	There is increased apoptosis of RORgammat(+) ILCs and less production of IL-22.	Infected mice succumb to *C.rodentium* infection. Without Ahr, RORγt(+) ILCs have increased apoptosis and less production of IL-22 which mediates innate gut immunity.	Qiu et al, 2012
Ltbr-/-	Impaired development of secondary lymphoid tissues. Also defective LTbr signaling in gut epithelial cells fail to produce CXCL chemokines that recruit LT producing neutrophils and RORgt+ innate cells	Mice lost weight and died of overwhelming infection within two weeks post infection. There were multiple defects in the development and maintenance of secondary lymphoid tissue and sever epithelial cell damage with edema, ulceration and bacterial abscesses in the colon.	Wang et al, 2010
LTβR-/-		NCR22 cells in gut cryptopatches function through IL22 mediated production of antibacterial peptides after infection with *C.rodentium*, same as wild type.	Satoh-Takayama et al, 2011
Atg7-/- (Autophagy)	Inability of infected, damaged cells to undergo autophagy.	Greater clinical evidence of disease and higher expression levels of pro-inflammatory cytokine mRNA in the large intestine and reduced bacterial clearance.	Inoue et al, 2012
NK1.1 cell depletions	Loss of NK cells resulting in lower colonic IFNγ, TNFa and IL-12, and a delay in homing of IFNγ+CD4+ T cells to the gut, resulting in a reduced IgG response.	Higher bacterial load, intestinal pathology and crypt hyperplasia at the peak of infection due to a reduced IgG response against *C.rodentium*.	Reid-Yu et al, 2013 Hall et al, 2013

iNOS-/- (inducible nitric oxide synthase)	Present in neutrophils, macrophages and epithelial cells which generate reactive nitrogen species.	Significant induction of IFNγ, IL-1 and TNFa mRNA expression in colitis tissue	Gobert et al, 2004
Cnpl-/- (Cathelicidin)	Deficient in cathelicidin (mCRAMP), an important antimicrobial peptide.	Increased bacterial colonization, epithelial damage and systemic dissemination	Limura et al, 2005
Core3-/-	Defective in mucin secretion.	Mice exhibited significant colitis in response to *C.rodentium*. Restoring signaling via the Notch and Wnt/B-catenin pathways promoted crypt regeneration and replenished the mucus layer leading to amelioration of bacterial colitis.	Ahmed et al, 2012
NKp46-/-	Impaired IL22 production	Mice show increased susceptibility to *C. rodentium.*	Satoh-Takayama et al, 2008
C3-/-	No complement protein		Belzer et al, 2011

Adaptive immunity			
Knockout mice	**Immune phenotype**	**Response to infection**	**Reference**
RAG-/-	RAG -/- knockout (KO) mice have undergone a targeted deletion in the recombination-activating gene and are unable to perform V(D)J recombination of the immunoglobulin and T cell receptor genes. As a result, these mice lack both mature T and B lymphocytes and thus are deficient in developing acquired immunity.	Mice develop severe pathology in colon and internal organs and deteriorate rapidly during acute infection.	Bry & Brenner 2004
RAG 1-/-		Mice do not display a reduction in the number of goblet cells or in mediators (Muc2 and tff3) expression as observed in infected wild type.	Bergstrom et al, 2008
RAG1-/-		Mice gradually lost weight and eventually died around 3–4 weeks post infection	Wang et al , 2010
RAG-/-		Heavily infected with high bacterial load which are often fatal. Surviving mice display reduced tissue pathology and disease.	Vallance et al, 2002
RAG-/-		Infected mice suffer high mortality rates but do not display goblet cell depletion. Reconstitution of RAG-/-mice with CD8(+) T cells, leads to colonic ulcers but not goblet cell depletion. RAG-/- mice receiving CD4(+) T cells show goblet cell depletion as well as exaggerated IEC proliferation.	Chan et al, 2013

Adaptive immunity: T cells			
Knockout mice	**Immune phenotype**	**Response to infection**	**Reference**
TCR-/-	Non functional T cells		
CD4-/-	Defecient in CD4+T cells, unable to activate B cells for antibody production	Mice are highly susceptible to infection and develop severe colitis. Reduced IgG and IgA response to EspA and Intimin.	Simmons et al, 2003
CD8alpha-/-	Defecient in CD8+T cells	Same as wild type	Bry and Brenner 2004
TCR delta-/-	Defecient in gammadelta T cells.	Same as wild type	Bry and Brenner 2004
CD28-/-	Costimulatory molecules on the surface of naïve CD4 T cells, essential for activating B cell antibody responses	Mice succumbed to acute infection	Bry, Brigl, Brenner 2006
CD40L-/-	Costimulatory molecules on the surface of activated CD4 T cells that bind to APC, necessary for B cell antibody response.	Over 50% mice failed to clear infection resulting in progressive mucosal destruction, polymicrobial sepsis and death	Bry, Brigl, Brenner 2006

Adaptive immunity: B cells & Antibody response			
Knockout mice	**Immune phenotype**	**Response to infection**	**Reference**
B cell-/-	B cell defecient	Severe epithelial hyperplasia with ulcerations and mucosal inflammation later on in infection	Maaser et al, 2004
MuMT-/-	B cell defecient	Highly susceptible to *C.rodentium* infection. Systemic immunity can be restored by adoptive transfer of convalescent immune sera and immune B cells to infected UMT mice.	Simmons et al, 2003
MuMT-/-	B cell defecient	Mice develop severe pathology in colon and internal organs and deteriorate rapidly during acute infection.	Bry and Brenner 2004
IgA-/-	IgA defecient	Same as wild type	Maaser et al, 2004
SIgM-/-	Secretory IgM defecient	Same as wild type	Maaser et al, 2004
pIgR (Polymeric Ig receptor)	Defecient in secretory IgA and IgM in the mucosa.	Same as wild type	Maaser et al, 2004

pIgR	Defecient in secretory IgA and IgM in the mucosa.	Lack secretory antibodies, Clear infection in the same way as WT mice although higher bacterial load initially.	Uren et al, 2005
J chain-/-	Defecient in secretory IgA and IgM in the mucosa.	Same as wild type	Maaser et al, 2004
TNF-a and iNOS deletions in B cells	B cells unable to produce TNFa and iNOS	Reduction in IgA production, altered gut microbiota, and poor clearance of *C.rodentium*.	Fritz et al, 2011
MicroRNA (miR)-155-/-	Impaired germinal center formation and humoral immune responses.	Infected mice exhibit prolonged colonization with *C.rodentium*, associated with higher bacterial burden in the gastrointestinal tissue and spread into systemic tissues. Germinal center formation and humoral immune responses are severely impaired.	Clare et al, 2013

Cytokine response			
Knockout mice	**Immune phenotype**	**Response to infection**	**Reference**
IL-1ß-/-	impaired IL1 signalling via MyD88 adaptor resulting in a reduced proinflammatory response	Increased bacterial burden and exacerbated histopathology	Liu et al, 2012
IL-18-/-	Impaired IL1 signalling via MyD88 adaptor resulting in a reduced proinflammatory response	Increased bacterial burden and exacerbated histopathology	Liu et al, 2012
IL1R-/-	Impaired IL1 signalling via MyD88 adaptor resulting in a reduced proinflammatory response	Exhibit increased mortality and severe colitis characterized by intramural colonic bleeding and intestinal damage including gangrenous mucosal necrosis similar to MyD88-/- mice. Mice also have increased predisposition to intestinal damage caused by *C.rodentium*.	Lebeis et al, 2009
TNFa p55-/-	Deficient in TNFa	Higher colonic bacterial burden although bacterial clearance was the same as WT. Markedly enhanced pathology with increased mucosal weight and thickness, increased T cell infiltrate and a greater Th1response	Goncalves et al, 2001
IL12 p40-/-	Deficient in IL12 and IL23 cytokine	Significantly more susceptible to *C.rodentium* with a proportion of mice dying. Gut mucosa of infected mice displayed an influx of CD(+) T cells and a local IFNγ response. Infected mouse mounted IgA response and expressed iNOS. Expression of the mouse beta defensin (mBD-3) was attenuated.	Simmons et al, 2002
IFNy-/-	Deficient in IFNγ	Mice are more susceptible to *C.rodentium* infection and mounted IgA responses,	Simmons et al, 2002

		expressed iNOS and the expression of mBD-3 was attenuated.	
IFNy-/-	Deficient in IFNγ	70% of infected mice survived	Bry, Brigl, Brenner 2006
IL4-/-	Induces differentiation of naïve CD4+T cells in to Th2 cells and B cell class switching to IgE	Same as wildtype	Bry, Brigl, Brenner 2006
Blocking IL6 signalling	Impaired development of IL-22-producing CD4(+) T cells	Mice are more susceptible to C.rodentium	Li et al, 2014
IL23-/-	Impaired IL22 production by ILCs.	Mice exhibit elevated bacterial loads and succumb to infection at high doses (10^9 CFU). At low doses (10^7 CFU) however, mice are able to recover from infection.	Mangan et al, 2006
IL23-/-		Very high bacterial load from the beginning and all mice succumbed day 8-12 p.i. Severe multifocal ulcerations of the descending colon with translocation of dense colonies of bacteria as well as multifocal transmural inflammation. IL-6 was attenuated which led to defective IL-22 production, may be due to the significant reductions in IL-1B, TNFa, IFNγ.	Basu et al, 2012
IL22-/-	Defective RegIII production by epithelial cells	Increased intestinal epithelial damage, systemic bacterial burden and mortality associated with inability to induce the Reg family of antimicrobial proteins in colonic epithelial cells.	Zheng et al, 2008
IL17RE-/-	Lower levels of innate antibacterial molecules.	Receptor for IL17C, without which there is lower expression of genes encoding antibacterial molecules, greater bacterial burden and early mortality during infection.	Song et al, 2011
IL10-/-	Increased antibacterial host defences, downregulation of proinflammatory pathways, increased expression of anti-inflammatory IL27 which suppresses differentiation of Th1 and Th17 cells.	Infected mice had less acute infection associated colitis and resolved it more rapidly than WT. IL10 defeciency is associated with downregulation of proinflammatory pathways and increased expression of anti inflammatory ctokine IL27 which suppresses Th17 and Th1 differentiation.	Dann et al, 2014
IL22-/- **&** **IL6-/-**		High bacterial load and majority succumbed by day 14. Significant increase in epithelial injury and ulceration associated with greater numbers of invasive bacterial colonies. Normal production of IL-1B and TNFa.	Basu et al, 2012

Other			
Knockout mice	**Immune phenotype**	**Response to infection**	**Reference**
Cx43+/-	Gap junction hemichannells contribute to water release during diarrheal disease.	Infected mice do not suffer from diarrheal disease.	Guttman et al, 2010
OPN-/-	Osteopontin contributes to pedestal formation, colonization, and colonic epithelial cell hyperplasia in response to bacterial infection	Reduced colonic epithelial cell hyperplasia, bacterial colonization and colonic epithelial cell hyperplasia.	Wine et al, 2010
ILK (integrin-linked kinase)	Reduced CCL2 expression and pro-inflammatory cytokines.	Reduced weight loss, crypt proliferation, histological inflammatory scores, CCL2 and proinflammatory cytokines. This was due to an altered pattern of bacterial migration associated with attenuated fibronectin expression. .	Assi et al, 2013
FOXO3-/-	FOXO3 is a negative regulator of and acts downstream of epidermal growth factor receptor (EGFR) required for colonocyte proliferation.	Increased proliferation of colonocytes during infection due to the elevated levels of EGFR.	Qi et al, 2010
Klf5-/- (Kruppel-like factor 5)	A key mediator for crypt cell proliferation	Mice display an attenuated induction of Klf5 expression and a reduced hyperproliferative response of crypt cells to C. rodentium compared to Wild type.	McConnell et al, 2008
MMP9-/-	Elevated levels of protective segmented filamentous bacteria and IL-17		
VDR-/-	Increased IL22 producing ILCs and antibacterial peptides.	Mice had fewer *C.rodentium* in the feces, kinetics of clearance was faster, there were more IL22 producing ILCs and more antibacterial peptides than WT mice.	Chen et al, 2014
MMP3-/-	Impaired migration of CD4+ T lymphocytes to the intestinal mucosa during tissue injury and repair.	Delayed clearance of bacteria associated with delayed appearance of CD4 T cells in the lamina propria.	Li et al, 2004
GPR41-/- GPR43-/- (G-protein-coupled receptors)	epithelial cells are impaired in their ability to induce the production of chemokines and cytokines required for the recruitment of leukocytes and activation of effector T cells in the intestine. This resulted in reduced inflammatory responses and slower immune responses.	Slower immune response to bacterial infection and delayed bacterial clearance. This is associated with inability to recruit leukocytes and activated effector T cells in the gut following activation of epithelial cells by SCFA to produce chemokines and cytokines.	Kim MH et al 2013
(IDO) -/- (Indoleamine 2.3-dioxygenase)	IDO inhibits tryptophan catabolism which suppresses T cell activation.	Mice are more resistant to intestinal colonization by Citrobacter, develop lower levels of serum IgM and IgG antibodies and significantly attenuated Citrobacter induced colitis.	Harrington et al, 2008
GPR15-/-	Inability to control homing of FOXP3(+) regulatory T cells (Tregs) to the large intestine lamina propria	More prone to develop severe large intestine inflammation due to the absence of FOXP3(+) Tregs homing to the large intestine lamina propria. This was rescued by the transfer of GPR15-suffiecient T regs.	Kim SV et al, 2013
RAC2-/-	Increased mononuclear cell infiltration characterized by higher numbers of CD3(+) T cells. Increased	Severe clinical symptoms, unresolved crypt hyperplasia and marked mononuclear cell infiltration	Fattouh et al, 2013

	levels of IFNg and IL-17 in the spleen.	characterized by higher numbers of T (CD3+) cells.	
RELMa-/-	Decreased CD4(+) T cell expression of the proinflammatory cytokine IL-17A and reduced levels of serum IL-23p19 due to macrophages deficient in IL-23p19 induction.	Infected mice exhibited reduced infection-induced intestinal inflammation, characterized by decreased leukocyte recruitment to the colons and reduced immune cell activation. Suggests that immune stimulatory effects of RELMa were pathologic rather than host protective.	Osborne et al, 2013